15243

NATIONAL LIBRARY
OTTAWA

BIBLIOTHÈQUE NATIONALE
OTTAWA

CANADA

NAME OF AUTHOR...A.V. GOPALAKRISHNAYYA...........

TITLE OF THESIS....ANALYSIS...OF...CRACKING...OF

....EARTH DAMS.......................

....

UNIVERSITY.......UNIVERSITY....OF...ALBERTA.....

DEGREE FOR WHICH THESIS WAS PRESENTED.....Ph.D............

YEAR THIS DEGREE GRANTED.......1973.......................

(Signed)....A.V.G. Krishnayya

PERMANENT ADDRESS:

.NEAR. BUDAMERU. BRIDGE

.....P.O.: VIJAYAWADA-3 (A.P)

..........INDIA..........

DATED...Dec. 4.........1972

NL-91 (10-68)

THE UNIVERSITY OF ALBERTA

ANALYSIS OF CRACKING OF EARTH DAMS

by

© ADDANKI VENKATA GOPALAKRISHNAYYA

A THESIS

SUBMITTED TO THE FACULTY OF GRADUATE STUDIES AND RESEARCH

IN PARTIAL FULFILMENT OF THE REQUIREMENTS FOR THE DEGREE

OF DOCTOR OF PHILOSOPHY

DEPARTMENT OF CIVIL ENGINEERING

EDMONTON, ALBERTA

SPRING, 1973

THE UNIVERSITY OF ALBERTA

FACULTY OF GRADUATE STUDIES AND RESEARCH

The undersigned certify that they have read, and recommend to the Faculty of Graduate Studies and Research for acceptance, a thesis entitled "ANALYSIS OF CRACKING OF EARTH DAMS" submitted by Addanki Venkata Gopalakrishnayya in partial fulfilment of the requirements for the degree of Doctor of Philosophy.

....
Dr. Z. Eisenstein - Supervisor

....
Dr. A. Craggs

....
Dr. N.R. Morgenstern

....
Dr. S. Thomson

....
Dr. J.M. Duncan - External Examiner

Date........November 27, 1972........

ABSTRACT

This dissertation deals with the finite element analysis of cracking of earth dams. The principal objectives of this investigation are (1) to contribute to an understanding of the tensile behaviour of a low-plastic core soil which has a high susceptibility to tensile cracking, (2) to study the relative importance of the factors that influence the analysis of cracking of earth dams, and (3) to develop analytical procedures for prediction and control of tensile cracks that are likely to develop during and at the end of the construction period.

The indirect tension test (Brazilian test) was used to conduct laboratory tensile studies on Mica Till. A procedure was developed to determine the tensile stress-strain relationship based on the results of the biaxial, indirect tension test.

The laboratory studies showed that a core material of low plasticity has a very low tensile strength which, for the purpose of analysis of cracking of earth dams, can be ignored. A rapid increase in flexibility of soil in tension was accompanied by a rapid decrease in tensile strength when water content was increased beyond the standard Proctor optimum. However, with the addition of a small percentage of bentonite to till it was possible to increase the flexibility of the mixture without an appreciable reduction of its tensile strength. An increase in the compactive effort increased the

tensile strength of till and decreased its flexibility, for water contents well below the Proctor optimum. For water contents above optimum, the tensile strength and the stiffness of soil were slightly decreased with the increase of compactive effort. The rate of tensile loading had a considerable influence on the tensile characteristics of till. Rates of loading mobilizing the minimum tensile strength and tensile failure strain were observed.

From the finite element analysis conducted with two and three dimensional modelling of earth dams, it has been observed that the construction step sequence, the non-linear stress-strain relationships of soil, and the boundary conditions associated with the three dimensionality of a dam are the most important factors to be properly simulated in the analysis for reasonable predictions of cracking of earth dams. Such simulation procedures were developed and their usefulness in practice was tested by analyzing a case study of cracking at Duncan Dam. The predicted location of cracks and sequence of their occurrence showed reasonable agreement with the field observations.

The analytical procedure developed can also be used as a design tool to study the influence of different factors on control of cracking of earth dams. A method is indicated for controlling tensile cracks in an earth dam, built in a narrow valley with rigid abutments and on incompressible foundations. The method consists of performing analyses with non-homogeneous modelling of the core material of the dam to specify the placement conditions of core material for an effective control on the development of tensile cracks.

ACKNOWLEDGEMENTS

The work reported in this thesis was carried out in the Department of Civil Engineering, University of Alberta, under the supervision of Dr. Z. Eisenstein.

The author expresses his sincere gratitude to Dr. Eisenstein for his guidance, help, and encouragement throughout the period of this study.

The author's sincerest thanks are due to Professor N.R. Morgenstern and Professor D.W. Murray with whom he had many stimulating and highly rewarding discussions. The suggestions given by Professor S. Thomson on the form of presentation of the thesis are highly appreciated.

The author is grateful to Dr. R.M. Hardy for providing access to the detailed field observations at Duncan Dam and to both the Montreal Engineering Co. Ltd. and the British Columbia Hydro Power Authority for permission to use these data in this study.

The assistance received from Messrs. O. Wood, G. Cyre, A. Muir and R.F. Howells of the Department of Civil Engineering in the experimental and the computational work is gratefully acknowledged.

The author expresses his sincere thanks to Mr. L.M. Chizawsky of the Alberta Research Council, Highways Division, for his helpful suggestions in building the tensile clip gauges used in the experiments.

The author is highly grateful to the University of

Alberta and the National Research Council of Canada for providing him financial support throughout the period of the study.

All the research work reported in this thesis has been carried out with the assistance of grants from the National Research Council of Canada.

Acknowledgements are due to Miss Susan Schultz for typing of the thesis.

The author wishes to express his sincerest gratitude to his wife, Leela, for her encouragement throughout the period of this work.

TABLE OF CONTENTS

Page

Page

Page

Page

Page

LIST OF TABLES

LIST OF FIGURES

CHAPTER I

INTRODUCTION

1.1 Scope

In this chapter the problem of cracking of earth and rockfill dams is introduced, the past work done on the topic is reviewed, and the purpose of the present work and its scope are presented.

1.2 Importance of the Problem of Cracking of Earth and Rockfill Dams

Cracking of the core of an earth or rockfill dam has been a subject of considerable importance to the designers of dams for a number of years. Cracking of several earth and rockfill dams and in some cases, subsequent failures caused by erosion of soil through the cracks have been reported in the literature (Marsal and Ramirez, 1967; Patrick, 1967; Pope, 1967; Schober, 1967; Kjaernsli and Torblaa, 1968; Gordon and Duguid, 1970; Vaughan *et al.*, 1970). The cracking phenomenon is a matter of considerable concern because, most of these dams in which this distress occurred were built with the best available construction practices developed over recent years. The ASCE Committee on Earth and Rockfill Dams (1967) stressed the importance of research concerning cracking of the core of earth and rockfill dams. It is necessary to evolve suitable design and construction procedures for earth and rockfill dams to resist cracking. This necessity has been strengthened further by the increasing need to utilize heterogeneous compressible foundations, irregular steep valley walls, declining quality of embankment materials at many sites, and fills of ever increasing height.

1.3 General Information on Cracking of Earth and Rockfill Dams

Covarrubias (1969) and Lowe (1970) have noted several factors that contribute to the cracking of earth and rockfill dams, the different types of cracks, and their relative importance with respect to the safety of the structure. For completeness some general information on cracking of earth and rockfill dams is discussed in the following sections.

1.3.1 Factors Contributing to the Formation of Cracks

Stress states favouring the formation of cracks in earth and rockfill dams are generally caused by any one or a combination of the factors listed below:

(a) Excessive differential settlements caused by non-homogeneous compressible material in the foundation.

(b) Steepness and/or irregular shape of valley walls or abutments.

(c) Differential deformations caused within the dam due to:

  (i) the presence of rigid structures such as conduits, concrete cut offs, etc. within the body of the dam,

  (ii) the softening of certain materials of the dam due to saturation, and

(iii) the large difference in stress-strain properties of materials in adjacent zones or layers within the dam.

(d) Large rates of strain caused in the upstream shell by the rapid filling of reservoir, especially during the first filling.

(e) Large transient stresses caused by earthquakes and other dynamic loads.

(f) Shrinkage effects caused by excessive drying of the core of the dam for long periods either during construction or operation of reservoir.

1.3.2 Types of Cracks

The cracks occurring in earth and rockfill dams are classified in different ways. Three well-known classifications are:

(a) Classification by the orientation of the crack (Fig. 1.1):

(i) Transverse cracks: are those that are perpendicular to the longitudinal axis of the dam. These could be horizontal, vertical, inclined or skewed. They provide a free path for the passage of water from the upstream to the downstream side and are considered to be the most dangerous in causing failures due to erosion in dams.

(ii) Longitudinal cracks: are those running in a direction, approximately parallel to the length of dam. Though these cracks do not create a free passage of water from the upstream to downstream faces, they may however aggravate a piping failure in a dam by connecting the transverse cracks.

(b) Visible classification of the cracks (Fig. 1.1):

(i) Interior cracks are those not visible from outside.

(ii) Exterior cracks are those which are formed at the surface (e.g., transverse or longitudinal cracks at the crest). Interior transverse cracks are the worst type of cracks which could cause unexpected failures due to erosion in dams.

(c) Classification according to the mode of formation (Fig. 1.2):

(i) Tensile cracks are those caused by tensile stresses.

(ii) Shear cracks are those caused by sliding failures.

(iii) Tearing cracks are those caused by torsional (rotational) shear failures.

(iv) Shrinkage cracks are tension cracks formed due to shrinkage effects.

In the investigation that forms the basis of this thesis only tension cracks have been considered. Therefore, in the remainder of this report, the term 'cracking' is implied to mean 'tensile cracking'.

1.4 Usefulness of an Analysis for the Prediction of Cracking of Dams

An analysis that can reasonably predict the extent of tensile zones that are likely to develop in a dam structure during critical periods will be useful in designing and instrumenting the structure in a rational manner. From the performance of the structure as revealed by field observations, the analysis could be checked and causes for any discrepancies be ascertained. It is hoped that such endeavours, as the one made in this thesis, will lead to a better understanding and control of cracking of earth and rockfill dams.

1.5 Brief Review of Past Work on Cracking of Dams

A comprehensive review of investigations of the cracking of earth and rockfill dams has been made by Covarrubias (1969). These investigations, which were described in detail by Covarrubias, are mentioned only in brief here. The investigations carried out by Covarrubias (1969) and later workers have been considered in some detail for the purpose of justifying the need for the present work.

Terzaghi (1943, p. 431) observed that tensile cracks would be caused by the tensile stresses prevailing at some distance behind the face of a vertical cut in clay overlying a rigid base. The distance at which maximum tensile stress occurs and the resulting maximum depth of tension zone were estimated to be about one-half the height of the cut.

Casagrande (1950) recognized the possibilities of piping failures that could be caused by cracks in earth and rockfill dams. He suggested that enough provisions should be made in the design of dams to make the cracks self healing.

Sherard (1952), after a comprehensive study on the performance of several earth dams, some of which cracked, arrived at criteria to classify the soils that are susceptible to cracking. These criteria were based on the grain size and consistency limits. A similar classification was also made by Tamez and Springhall (1960). From these studies it was concluded that, in general, silty soils with uniform gradation and low plasticity index are highly susceptible to cracking. Even though these criteria help to classify soils with regard to their susceptibility to cracking, they are of very limited use in the overall evaluation of the cracking potential of an earth structure.

Nonveiller and Anagnosti (1961) proposed a limit analysis for investigating horizontal cracks in a narrow vertical clay core supported by less compressible rockshells. This analysis disregards the elastic strains which by themselves could produce cracks.

Narain (1962) tried to compare the tensile strains at failure obtained by the laboratory beam tests on soils with the tensile strains computed for a number of dams which were idealized as homogeneous isotropic linearly elastic beams of uniform cross section. He concluded that when the computed tensile strains exceeded the laboratory failure tensile strains, cracks would occur in the real structure. Even though some correlations with observed cracking were made, the analysis recommended by him is not applicable for all classes of problems involving irregular valley profiles and non-homogeneous materials because of his over-simplified idealization of the real structure.

Lee and Shen (1968) analyzed the longitudinal section of dams using a finite element method to compute the horizontal stresses and strains. Results of such computations made on El Infiernillo Dam agreed well with the field observations. The analysis was performed in a single step under plane strain conditions with the appropriate linear stress-strain relationships.

Covarrubias (1969) analyzed a number of longitudinal and transverse sections representing different simple geometrical shapes of earth dams. In all cases a finite element method was used and the analyses were performed in a single step using the assumption of linear stress-strain relationships and plane strain conditions. The purpose of these analyses was to evaluate the effect of the shape of valley and compressibility of different materials in dams and foundations on the development of tensile zones. Similar analyses were conducted on the longitudinal sections of existing dams to predict transverse cracking. Reasonable correlations were obtained even though the tensile stresses and strains were over-estimated due to the single step linear elastic analysis used.

Dolezalova (1970) considered the effect of steepness of a triangular valley on the formation of tension zones to predict transverse tensile cracking. A finite difference method was used to perform a linear elastic analysis in a single step and in a number of steps under plane strain conditions. These analyses have the same disadvantages mentioned before in addition to the lesser adaptability of the finite difference technique to more complex problems.

Strohm and Johnson (1971) included the construction step sequence and non-linear material behaviour in the finite element analyses they have conducted for different valley profiles under plane strain conditions. These studies revealed, that by introducing the realistic non-linear material properties and the construction step sequence, the extent of tensile zones computed was very much smaller than that obtained by a single step linear analysis. In addition the principal stress ratios computed by the incremental non-linear analysis are closer to reality than the ones obtained by a single step linear analysis.

1.6 Requirements of an Analysis for Predicting Cracks

For a successful prediction of cracking of an earth structure particular attention has to be paid to the following:

(1) The idealization of the structure for the analysis has to be such that the geometry of the structure, the boundary and body forces, the boundary displacement conditions, and the construction sequence are represented as close to the prototype as possible.

(2) The material properties and the stress-strain relationships used in the analysis should be such that they lead to the proper simulation of the deformational behaviour of the structure.

(3) The tensile behaviour of the materials of the structure

should be known so that the results of analysis are interpreted properly for the prediction of cracking.

1.7 Objectives of the Present Investigation

Since a procedure satisfying the requirements stated in Section 1.6 is not available yet to deal with the problem of cracking of earth dams, the present investigation was undertaken with the following objectives:

(1) To conduct laboratory studies that contribute to an understanding of the tensile behaviour of soils,

(2) to conduct analytical studies that contribute to an understanding of the influence of certain factors on cracking phenomena and to the development of a procedure for a reasonable prediction of the cracking of earth dams, and

(3) to suggest a design procedure that contributes to the minimization of the possibilities of cracking of earth dams.

1.8 Scope of the Present Work

(1) Laboratory studies on tensile behaviour of soils are restricted to a mountain till that represents a typical core material generally used for the dams constructed in western Canada. The influence of the most important factors, namely the water content at failure, the compactive effort, the rate of loading, and the addition of bentonite to till, on the tensile characteristics of

soil has been investigated. The laboratory studies are described in Chapter II.

(2) Suitable simulation procedures for linear and non-linear finite element analyses for two and three dimensional conditions have been developed. These procedures are described in Chapter III.

(3) Parametric studies to investigate the influence of construction sequence, non-linear stress-strain relationships of materials, and three dimensional effects on the development of tensile cracks during or at the end-of-construction period have been conducted. Studies on the first two factors namely, the construction sequence and non-linear material properties are extensions of the work done by Strohm and Johnson (1971). The other critical states, such as the first filling of reservoir, or an earthquake, have not been investigated. All the studies in this work are restricted to tensile cracking. Cracking due to shrinkage effects and shear is not considered. All the parametric studies are described in Chapter IV.

(4) A design procedure that takes into account the redistribution of stresses due to non-homogeneity of the materials of the dam, has been suggested to minimize the transverse tensile cracks near the abutments. This procedure has been described in Chapter IV.

(5) The simulation procedure that utilizes the analytical tools developed in Chapter III has been applied to a case study for verifying its usefulness in practice.

This case study is presented in Chapter V.

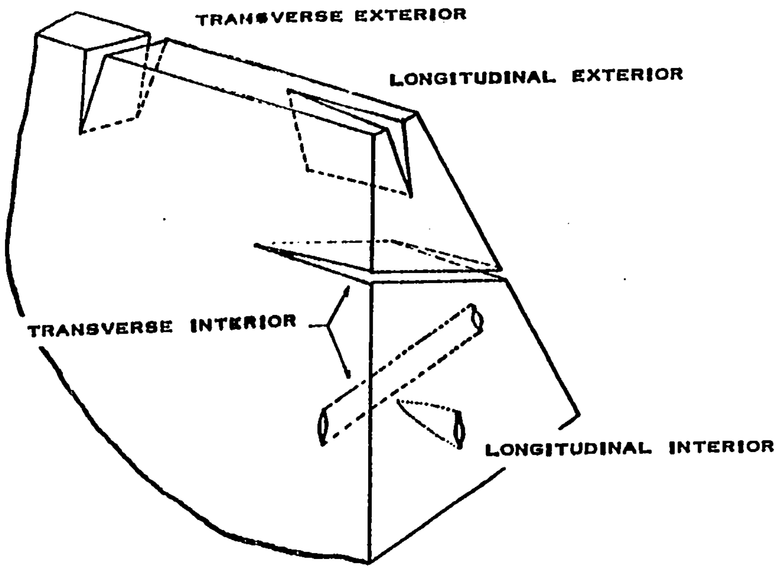

FIG. I.1 CLASSIFICATION OF CRACKS IN THE CORE OF A DAM [AFTER COVARRUBIAS, 1969]

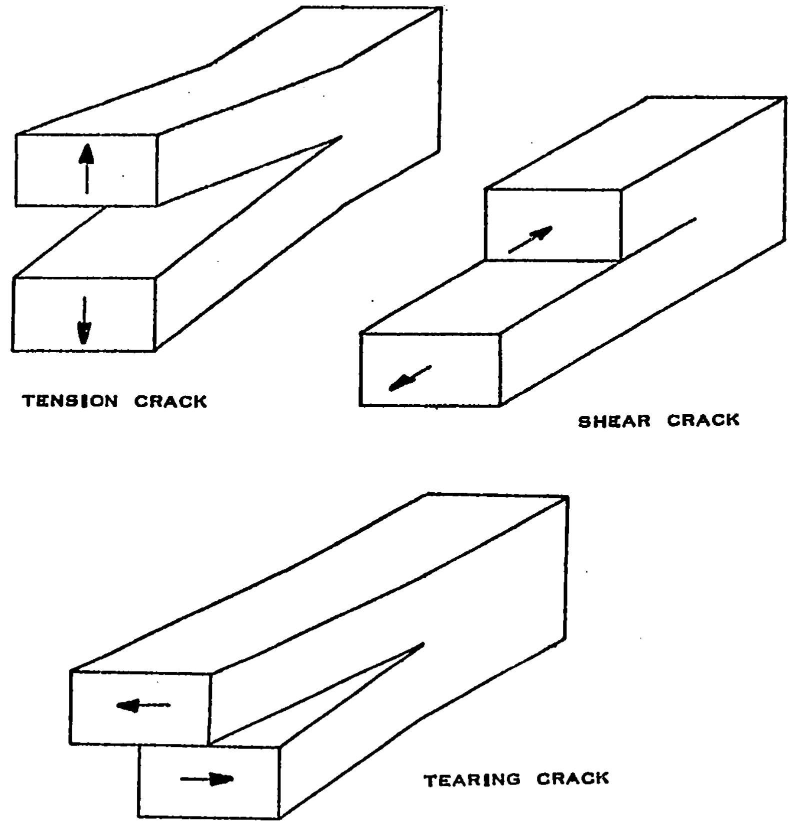

FIG. I.2 BASIC MODES OF CRACK-SURFACE DISPLACEMENTS [AFTER COVARRUBIAS, 1969]

CHAPTER II

LABORATORY STUDIES ON THE TENSILE BEHAVIOUR OF SOILS

2.1 Scope

This chapter discusses the usefulness of the laboratory studies on the tensile behaviour of soils for the analysis of cracking of earth dams. Laboratory tensile studies on soils by the previous investigators are briefly reviewed. Different tensile test methods applicable to soils are examined and the indirect tension test procedure used in the present work is described. Tests performed to evaluate the influence of different factors on the tensile behaviour of a typical core material are described and the results discussed.

2.2 Introduction

When compared to the extent of work done on the shear strength and the deformational behaviour of soils, the amount of research directed towards an understanding of the tensile behaviour of soils is very meagre. This is mainly due to the generally low tensile strength of soils. Although it is reasonable to assume zero tensile strength for soils in the analysis and design of earth dams, a knowledge of the behaviour of soil in tension is still required for an effective control of cracking of earth dams. Laboratory tests were undertaken to study the tensile behaviour of Mica Till, a soil representing typical core materials generally used for dams in western Canada. The effects of the moisture content, the strain rate, the compactive effort, and the addition of bentonite to till on the flexibility characteristics of till were examined.

2.3 A Brief Review of Previous Studies on the Tensile Behaviour of Soils

A systematic study on the tensile strength of compacted soils, by testing relatively large specimens under direct tension, was reported by Tschebotarioff et al. (1953). The soil sample had the shape of a briquette, similar to the one normally used in testing cement mortar in tension. The specimen was 52" in total length and 3" in thickness. The width was reduced from 18" at the ends to 6" at the test section, which had a length of 16". The specimen, compacted by standard proctor tampers, was supported horizontally on ball bearings to avoid friction. The important findings of this study were as follows:

(1) The tensile strength and the strain at failure of a clay depended on the type of clay mineral in the soil. Montmorillonite exhibited the highest tensile strength and tensile strain at failure whereas the corresponding quantities for kaolinite were the lowest.

(2) The tensile strength was affected by the water content, the time elapsed between mixing and testing and the rate of strain.

(3) The addition of bentonite to sand increased the tensile

strength of bentonite by about 50% when the mixture had a composition of about 15% bentonite and 85% sand. Further addition of sand decreased both the tensile strength and the tensile strain at failure of the mixture.

From the preceding observation one can expect the possibility of considerably improving the tensile behaviour of a relatively non-plastic soil such as till by the addition of an optimum quantity of bentonite.

Narain (1962) studied the tensile behaviour of six soil types of which five were obtained from earth embankments with known construction conditions. The sixth soil was a limestone clay of relatively high plasticity that had a plasticity index of 45% and a liquid limit of 72%. The soils from embankments varied from non-plastic to a plasticity index of 16. For a given soil type, relationships were obtained between the tensile strain at the initiation of cracking and the compactive effort, moulding water content and the rate of loading. All the tensile tests were performed on soils moulded into beams 3" wide, 2.75" deep and 22.125" long. The soil was compacted in ten equal horizontal layers with an actuated vibrator having a 2.5" square base plate, weighing 16 lbs. Different compactive efforts could be simulated by adjusting the time of compaction. Loss of moisture from the specimen was prevented by coating the specimen with a layer of 50% petrowax plus 50% petrolatum oil. The beams were loaded at the centre by adding dead weights at rates that caused failure in 2 days to 6 months. From the deflections of beams obtained by cathetometer observations of tungsten pins inserted into the beams, the tensile stresses and strains were computed. The computation of stresses and strains was based on a solution obtained, using the elastic theory, for a rectangular beam with known displacement boundary conditions. The rupture of beam invariably occurred near the midspan after the formation of the first crack. Parallel compression tests were conducted on all the soils to compare their behaviour in compression with that in tension. The main conclusions drawn from these tests were as follows:

(1) The ratio of tensile strains at cracking to the compressive strain at failure varied widely from 0.01 to 0.1 with no consistent pattern, indicating that compression tests are of little value in assessing the tensile strains in soils at cracking.

(2) An increase of moulding water content from 2% to 3% dry of optimum to nearly optimum substantially increased the flexibility of soil. At comparable moisture contents with respect to the optimum, an increase of compactive effort substantially decreased the flexibility.

(3) Clays of high plasticity are, in general, more flexible than clays of low plasticity. However, the flexibility of soils with low plasticity could not be correlated with their plasticity characteristics.

(4) Rapid straining of soils caused failure at lower tensile strains and stresses compared to those obtained from slow rates of testing.

Inglis and Frydman (1963) examined the suitability of the different tensile test methods for soils. Direct tension tests, indirect tension tests and flexure tests were performed on soil specimens of different sizes and different compositions. In order to cover a wide range of strengths in the specimens tested, Portland cement was added to kaolin and sand in varying small amounts. It was concluded that an indirect test would be useful and sensitive for stabilized materials as extreme as kaolin and uniformly graded coarse sand. Simplicity in test operation, low variability, and sharp failure were observed. The length of the specimen did not affect the test results significantly indicating that relatively thin specimens could be tested with minimum compaction inhomogeneities.

Hasegawa and Ikeuty (1966) tested a soil with a plastic limit of 80%, a liquid limit of 98%, and an optimum water content of 82% in direct tension, using briquette shaped specimens, similar to those used by Tschebotarioff et al. (1953) but of much smaller dimensions. The overall length of the specimen was 19 cm. with a middle test section of 2 cm. x 2 cm. in cross section and 7 cm. in length. The tensile load was transmitted to the specimen through thin steel plates embedded into the specimen at the enlarged ends during compaction. The specimen was kept horizontal and the friction was avoided by floating the specimen on mercury. The tensile strain was measured by observing through a cathetometer, the movement of two ceramic marks, kept initially at a distance of 5 cm. apart. The failure took place perpendicular to the axis of loading but at different locations along the length of the specimen, sometimes occurring even at the ends. A maximum strain of 5.5% was measured for the soil tested. A decrease of tensile strength and increase of failure strain with the increase in moisture content were observed.

Narain and Rawat (1970) tested six soil types, covering a wide range of plasticity characteristics, under a diametral compression to determine their tensile strength at different moulding water contents. The specimen, 4" dia. x 4.6" in size, was supported on 5/8" wide and 1/4" thick rubber strips for even distribution of the load along its length. The good reproducibility of the results reported, indicates the suitability of the indirect tension test (Brazilian test) for compacted soils. Comparison of the ratio of unconfined compressive strength to the tensile strength at the optimum water content for different soils tested showed that the ratio was less for the more plastic soils.

Fang and Chen (1971) developed a new simple test, known as the double punch test, for testing soils in tension. The test consists of loading a cylindrical soil specimen by applying two steel punches at the centre on both top and bottom surfaces of the specimen. A simple formula, based on the theory of plasticity was developed for computing the tensile strength of soils. The test results for various materials including concrete, mortar, soil, and bituminous concrete were compared with those of the indirect test and good agreement among the results were reported. However the measurement of tensile strain during a double punch test on soil specimen appears to be difficult.

2.4 Different Types of Test for Tensile Testing of Soils

Based on the experiences reported in previous investigations on tensile testing of soil, stabilized soil, concrete, rock and bituminous concrete, a general evaluation of the common tensile test methods appears to be possible.

2.4.1 Direct or Uniaxial Tension Test

A direct tension test, although quite simple in interpretation, is rather difficult to apply to soils and other materials which have a low tensile strength. The main difficulty arises in the satisfactory application of load to the ends of the specimen. A number of methods such as freezing the ends of specimen (Haefeli, 1951), cementing the ends of specimen to loading blocks with a quick-setting polyester resin (Bofinger, 1970), enlarging the ends of the specimen to form a briquette (Tschebotarioff _et al_., 1953) and embedding loading plates in the enlarged ends of specimen (Hasegawa and Ikeuty, 1966) were adopted. Slight eccentricities in loading, stress concentrations at the ends, and compaction planes in the case of cylindrical specimens (Ingles and Frydman, 1963) affect the reproducibility of test results to a considerable extent. When soils are to be tested at high water contents or when the dimensions of the specimen are large, the horizontal application of load is preferred. This necessitates an elaborate arrangement for the application of load without friction and eccentricity (e.g., Tschebotarioff et al., 1953).

2.4.2 Flexure or Beam Test

This test is considerably easier to conduct than the direct tension test. The preparation of the specimen and the application of load do not require as much care. To some extent the loading conditions in this type of test are similar to the field loading conditions of an earth dam which, for purpose of analysis, can be considered as a beam (Narain, 1962). However, as the failure is induced at the surface, skin effects produced by the uneven distribution of compaction pressures, especially in soils of low plasticity tend to influence the results to a large extent (Ingles and Frydman, 1963). Since a part of cross section of the beam passes into the plastic range, the stress distribution in the specimen is not defined. Hence the tensile strength computed by the simple bending theory will be in error. However, Bofinger (1970), using a theory that accounts for a different moduli in tension and compression and plastic behaviour of soil, obtained extreme fibre flexural stresses which are not markedly different from the strengths of soil-cement specimens obtained by direct tension tests.

2.4.3 Indirect Tension Test or Brazilian Test

An indirect tension test that involved loading of a circular cylinder or disc with compressive loads along two diametrically opposite generators, was developed by Carneiro and Barcellos (1953) in Brazil and also by Akazawa (1953) in Japan. A relatively uniform tensile stress perpendicular to and along the diametral plane containing the applied load usually causes splitting failure along the loaded plane (Fig. 2.1). The test was originally developed for concrete and mortar specimens, however its use has been found satisfactory for materials such as rock (Mellor and Hawkes, 1971), stabilized soils (Thompson, 1965), bituminous mixtures (Breen and Stephens, 1966) and soils (Narain and Rawat, 1970). Based on the previous investigations it is generally recognized that an indirect tension test has the following advantages:

(1) Specimen preparation and its handling are considerably easier.

(2) Equipment needed for the test is similar to that of a compression test.

(3) Failure is relatively insensitive to the surface conditions and compaction planes of the specimen and is initiated in a region of relatively uniform tensile stress.

(4) Variation of the test results is low.

(5) For brittle materials and when performed properly, the test is capable of giving a good measure of uniaxial tensile strength (Mellor and Hawkes, 1971).

However, since the formula used to compute the tensile stress in the test is based on the assumption of homogeneous, isotropic elastic material there will be an error in the estimate of tensile strength of real materials. In addition the relationship between the tensile stress and tensile strain cannot be obtained directly because of the biaxial stress conditions of the test (Bofinger, 1970).

2.4.4 Choice of the Type of Test for Present Studies

The simplicity in preparation and handling of test specimens and the consistency of test results lead to the adoption of the indirect tension test in this investigation. The error caused in the estimate of tensile strength of materials whose moduli differ in tension and compression is examined in Section 2.5.2. A procedure to derive the tensile stress-strain relationship is indicated in Section 2.5.3.

2.5 Theoretical Consideration of the Indirect Tension Test

2.5.1 Theoretical Stress Solutions

Hertz (1883) obtained a stress solution for a disc or cylinder compressed normally by line loads along diametrically opposite generators. Later, a number of investigators (e.g., Timoshenko and Goodier, 1951; Wright, 1955; Frocht, 1957) considered the same problem. Hondros (1959) gave a complete stress solution for the case where the load is distributed over finite arcs, valid for conditions of both plane stress and plane strain. Colback (1966) observed that the presence of a diametrical fracture plane originating from centre is essential if the test is to be accepted as valid. Favourable conditions for the acceptability of the test are generally obtained by distributing the applied load over small areas. A distributed load, when applied over a length less than a tenth of the diameter of the specimen, prevents local compressive failure without significantly altering the stress conditions at the centre of specimen that are valid for a line load. Fig. 2.1 compares the theoretical distribution of vertical and horizontal principal stresses along the vertical or loading diameter for conditions of line loading and distributed loading over an arc of length equal to 1/12 of the diameter of the specimen. The two principal stresses along the vertical diameter for distributed loading are given by Hondros (1959) as:

$$\sigma_\theta = + \frac{P}{\pi R t \alpha} \{ \frac{[1-(r/R)^2]\sin 2\alpha}{1-2(r/R)^2\cos 2\alpha + (r/R)^4} - \tan^{-1}[\frac{1+(r/R)^2}{1-(r/R)^2} \tan \alpha]\} \tag{2.1a}$$

$$\sigma_r = - \frac{P}{\pi R t \alpha} \{ \frac{[1-(r/R)^2]\sin 2\alpha}{1-2(r/R)^2\cos 2\alpha + (r/R)^4} + \tan^{-1}[\frac{1+(r/R)^2}{1-(r/R)^2} \tan \alpha]\} \tag{2.1b}$$

where P is the applied load, R is the radius of the specimen, t is the thickness of the specimen, 2α is the angular distance over which P is assumed to be distributed radially (normally $\leq 15°$), and r is the distance from the centre of the specimen (Fig. 2.1). At the centre of specimen the stresses are given by:

$$\sigma_\theta = + \frac{P}{\pi R t} \left(\frac{\sin 2\alpha}{\alpha} - 1\right) \quad (2.2a)$$

$$\sigma_r = - \frac{P}{\pi R t} \left(\frac{\sin 2\alpha}{\alpha} + 1\right) \quad (2.2b)$$

For line loading the stresses along vertical diameter are given (Frocht, 1957) by:

$$\sigma_\theta = + \frac{P}{\pi R t} \quad (2.3a)$$

$$\sigma_r = - \frac{P}{\pi R t} \left\{\frac{4}{[1-(r/R)^2]} - 1\right\} \quad (2.3b)$$

It will be noted that, for $\alpha \leq \tan^{-1}(1/10)$, both Eqs. 2.2 and 2.3 give the same stresses at centre, viz.,

$$\sigma_\theta = \frac{P}{\pi R t} \quad (2.4a)$$

$$\sigma_r = - \frac{3P}{\pi R t} \quad (2.4b)$$

Fig. 2.1 shows that a distributed load gives a finite value of compressive stress at the point of load application whereas the compressive stress in the case of a line load is infinite. Because of the stress condition that exists at the centre ($3\sigma_\theta + \sigma_r = 0$) the initiation of tensile failure for a brittle material, according to Griffith's criterion, should occur at the centre of the specimen. The tensile stress corresponding to the initiation of failure at centre is then equal to the uniaxial tensile strength of the material. When the load P_f corresponding to the failure is known, the tensile strength of the material tested can be obtained from:

$$\sigma_t = \frac{P_f}{\pi R t} \tag{2.5}$$

It is interesting to note that an identical formula for the failure tensile stress could be derived assuming the material to be perfectly plastic (Chen, 1970).

2.5.2 Effect of Different Elastic Moduli in Tension and Compression

In the derivation of the stress solution discussed in the previous section it was assumed that the elastic moduli in tension and compression were equal. In general, for materials of very low tensile strength it is observed that the modulus in tension is considerably smaller in magnitude than that in compression. Bofinger (1970) observed that for an inactive clay (liquid limit 53% and plastic limit 20%) when stabilized with 6 to 10% ordinary Portland cement, the ratio of modulus in compression to that in tension varied from 7.5 to 11.1. Because of different elastic moduli in compression and tension, the tensile strength of the material estimated with the use of the Eq. 2.5 will be higher than the correct value. A numerical solution that considers different elastic moduli in tension and compression has been obtained here with the use of the finite element method. When moduli differ in tension and compression the material can be considered as bilinear and the solution technique by successive approximations suggested by Wilson (1963) can be used to obtain a numerical solution to the problem. The stress-strain relationship for a bilinear material is of orthotropic form and can be written in terms of principal coordinate system for plane stress condition as:

$$\begin{Bmatrix} \sigma_t \\ \sigma_c \\ 0 \end{Bmatrix} = \frac{1}{1-\nu_t\nu_c} \begin{bmatrix} E_t & \nu_c E_t & 0 \\ \nu_t E_c & E_c & 0 \\ 0 & 0 & G \end{bmatrix} \begin{Bmatrix} \varepsilon_t \\ \varepsilon_c \\ 0 \end{Bmatrix} \tag{2.6a}$$

where
- σ_t the tensile principal stress
- σ_c the compressive principal stress
- ε_t the tensile principal strain
- ε_c the compressive principal strain
- E_t the modulus in tension
- E_c the modulus in compression
- ν_t the Poisson's ratio associated with tension
- ν_c the Poisson's ratio associated with compression
- G the shear modulus prescribed independently.

From symmetry considerations of the constitutive matrix given above

$$\nu_c E_t = \nu_t E_c \tag{2.6b}$$

Writing $E_c/E_t = n$ and $G = gE_c$ the constitutive matrix can be expressed as:

$$[\bar{c}] = E_c \begin{bmatrix} \frac{1}{n-\nu_c^2} & \frac{\nu_c}{n-\nu_c^2} & 0 \\ \frac{\nu_c}{n-\nu_c^2} & \frac{n}{n-\nu_c^2} & 0 \\ 0 & 0 & g \end{bmatrix} \qquad (2.7)$$

The constitutive matrix $[\bar{c}]$ is defined if E_c, ν_c, n and g are prescribed. For an isotropic material the extreme values of g corresponding to Poisson's ratios of zero and 0.5 are 0.5 and 0.33 respectively. As g is an independently prescribed quantity it is reasonable to assume that about 0.4 represents approximately an average condition for soils that have different moduli in tension and compression. However, solutions for different values of g ranging from 0.2 to 0.5 are obtained. The variation of n is considered from 1 to 15. The finite element procedure is given in detail in Appendix D. Fig. 2.2 compares the finite element solution with the theoretical solution for the distribution of tensile and compressive stresses along the horizontal diameter of the specimen. A close agreement between the solutions can be noticed. Finite element solutions for $E_c/E_t = 10$ and $g = 0.4$ are also shown in Fig. 2.2 for two values of ν_c namely 0.10 and 0.35. An increase in compressive stress and decrease in tensile stress when compared to the isotropic case, at the centre of the specimen can be seen. The solution is little affected by the value of Poisson's ratio used in the analysis as can be seen from Fig. 2.2. Fig. 2.3 gives the tensile and compressive stress at the centre of specimen obtained by the finite element method for different values of E_c/E_t and g. The stresses are not significantly sensitive to the variation of g especially over the range between 0.3 and 0.5. Hence it is reasonable, in the absence of a correct estimate of g, to assume that the variation of the stresses at centre as dictated by the ratio E_c/E_t for an average value of g equal to 0.4 serves the purpose of evaluating an indirect tension test. Based on this, the variations of the tensile and compressive stresses at the centre with the ratio E_c/E_t for the value of $g = 0.4$ is plotted in Fig. 2.4. This plot was used in subsequent computations (Section 2.9). The distribution of the tensile and compressive stresses along the horizontal diameter of the specimen for various values of E_c/E_t is shown in Fig. 2.5.

2.5.3 Evaluation of the Tensile Stress-Strain Relationship

Since the indirect tension test involves a biaxial stress state at the centre of the specimen, the tensile strain obtained from the test includes that caused by the compressive stress in the vertical direction. To obtain the tensile stress-strain relationship it is necessary to deduct the tensile strain due to the compressive stress from the observed tensile strain. As the tensile stress at failure for soils is generally low, the compressive stress that exists at the centre of the specimen while it fails in tension is also low, this being equal to three times the tensile stress at failure. For the range of this low compressive stress an appropriate compression modulus (E_c) and a Poisson's ratio (ν_c) can be obtained by conducting an unconfined compression test on the same soil. The observed tensile strain at the centre of specimen in an indirect tension test can be expressed for plane stress condition as:

$$\varepsilon_{xc} = \frac{\sigma_{xc}}{E_t} + \nu_c \frac{\sigma_{yc}}{E_c} \tag{2.8}$$

where σ_{xc}, σ_{yc} represents respectively the tensile and compressive stress at the centre, ε_{xc} the observed tensile strain at centre and E_t the modulus in tension. The tensile strain due to tensile stress alone can be obtained from:

$$\frac{\sigma_{xc}}{E_t} = \varepsilon_{xc} - \nu_c \frac{\sigma_{yc}}{E_c} \tag{2.9}$$

Initially, as E_t is not known, σ_{xc} and σ_{yc} can be computed for $E_c/E_t = 1$. From tensile stress-strain relationship obtained after the first trial, E_t is derived and the ratio E_c/E_t computed. In the second trial the appropriate values of σ_{xc} and σ_{yc} are derived from Fig. 2.4 for the known E_c/E_t and used in Eq. 2.9 to obtain the new tensile stress-strain relationship. Now the E_t can be derived from the present tensile stress-strain relationship and the E_c/E_t can be recomputed and compared with previous value of E_c/E_t. The procedure can be repeated until close agreement is achieved between the successive values of E_c/E_t. An example illustrating the procedure appears in Section 2.9.

2.6 Experimental Set-Up for Laboratory Tensile Tests

2.6.1 Load Measuring Device

Since the tensile stress to be measured for soils is small, the load measuring device should be sufficiently sensitive to record small loads. The system should be rigid causing negligible deformation in the load measuring device. The recording equipment should be such that it is possible to record measurements of load and deformation at close intervals. This will lead to a precise evaluation of the stress-strain relationship especially at the failure of specimen.

All tensile tests were performed on a strain controlled loading machine having various constant speeds including a minimum of 0.000013"/minute. The load was measured by a sensitive, 300 lb. capacity tension-compression miniature transducer load cell, (Fig. 2.6) manufactured by Intertechnology Ltd., Don Mills, Ontario. The load cell is temperature compensated, has 50% over load capacity, and could be operated satisfactorily in a moist room at 95% relative humidity and at a temperature of 45°F to reduce the loss of moisture from the specimen. The load cell is supplied with 10 volts d.c. and the output is picked on one of the channels of the d.c. strain gauge control (Figs. 2.7 and 2.8). The channels were scanned and recorded by a Hewlett-Packard data acquisition system (Figs. 2.7 and 2.8). The readings could be taken at intervals of time ranging from 1 second to 1 hour. The minimum load that could be recorded with the system is 0.1685 lbs., equivalent to 0.01 millivolts.

2.6.2 Tensile Deformation Measuring Device

Tensile deformation measurement in soils is rather involved because of the difficulty in attaching the tensile deformation measuring device to the soil specimen and the need to measure extremely small tensile deformations. In the present studies a clip gauge shown in Figs. 2.9, 2.10(a) and 2.10(b) was used to measure the displacement between two brass guage blocks attached to the specimen on either side of its centre by means of Phenyl Salicylate. Similar clip gauges were successfully used in the past by the Alberta Research Council, Highways Division, Edmonton to obtain the tensile deformations of soil-cement specimens.

The clip gauge consists of two arms of 1¼" long, ¼" wide and 0.015" thick "feeler gauge" material firmly soldered to two brass blocks as shown in Fig. 2.9(a). The two arms were provided with brass knife edge points at their ends so that the clip gauge sits snugly between the grooved sides of the gauge blocks (Fig. 2.10(a)). The brass ends of the clip gauge were kept at a fixed distance apart on either end of a spacer by means of a screw and a pin (Fig. 2.9(a)). The thickness of the spacer selected was such that a distance of 0.915" between the ends of knife edge points was obtained in the unstrained state. When the gauge sits within the grooves of the gauge blocks the distance between the knife edge points is 0.84" so that a maximum tensile strain of 8.92% can be read over the entire range of the clip gauge. A distance greater than 0.915" was not found to be desirable as in this case the two arms of clip gauge in the initial strained position, exerted excessive pressure on the gauge blocks causing them to come off the specimen. The two cantilever arms, which tend to reach the unstrained position as the specimen undergoes tensile deformation, were fitted with two Budd's metal film strain gauges (type C6-111, gauge factor 2.4, 120 ohms) to measure the tensile deformation (Fig. 2.9(a)). To achieve a maximum signal output, one of the gauges was fixed on the compression side of one arm while the other was on the tension side of the other arm. Two resistors of 120 ohms each were put into the circuit to make it a full bridge circuit (Fig. 2.9(b)). The transducer amplifier indicator (Figs. 2.7 and 2.8) supplies 3 volts a.c. at 3kHz to the strain gauge circuit, receives back the a.c. signal from the circuit, amplifies and converts into a d.c. signal which is read by the data acquisition system. As the tensile deformations were to be read from both ends of the specimen, two clip gauge units with two transducer amplifier indicators have been used (Figs. 2.7 and 2.8). The minimum tensile strain that could be read with the set up used is 0.002%, equivalent to 0.01 millivolts. A L.V.D.T. (linear variable differential transformer) of 6 volts was fixed to the loading head (Fig. 2.10(b)) to check the rate of loading of the specimen.

2.7 Experimental Set-Up for Laboratory Compression Tests

The unconfined compression tests were conducted on the same loading machine with the same load cell used for the tensile tests. The tests were performed on 4" dia. x 8" long samples with lateral strain measurement (Fig. 2.11). The lateral strain measuring device used is a modification of the lateral strain indicator described by Bishop and Henkel (1962) for performing compression test on 4" dia. samples under zero lateral strain. The modification was the replacement of the diaphragm-mercury indicator by an L.V.D.T. of 24 volts with a thin wire tied to the lower end of the core while the upper end was supported by a spring (Fig. 2.12). The relative movement of two curved metal pads which bear lightly on the surface of the sample is magnified twice by the hinged ring which embraces the sample and is imparted to the thin wire, stretching across the two ends of the ring (Fig. 2.12). The wire causes the vertical movement of the core of L.V.D.T. equivalent to twice the amount of the lateral displacement of the specimen. Lateral strains are measured here to compute the Poisson's ratio during the unconfined compression of the specimen. The vertical displacement of the specimen is measured by a 6 volt L.V.D.T. attached to the loading plunger of the triaxial cell as shown in Fig. 2.11.

2.8 Description of Laboratory Tests

2.8.1 Description of Soil Used for Tensile and Compressive Tests

Mica Till was used in all tensile and compressive tests to represent the tensile and compressive stress-strain characteristics of a typical brittle core material of an earth dam.

Some tension tests were performed on Mica Till mixed with 6% bentonite to study the effect of adding a plastic material to the core material. Mica Till tested, has the following properties:

Liquid limit	18.2%
Plastic limit	14.7%
Plasticity index	3.5
Proctor maximum dry density (material passing #4 sieve)	132.0 pcf
Proctor optimum water content (material passing #4 sieve)	9.2%

The gradation curve for Mica Till for sizes less than 3/4" is shown in Fig. 2.13. Mica Till mixed with 6% commercial bentonite (liquid limit 591%, plastic limit 87%, and activity 5.6) has the following properties:

Liquid limit	42.0%
Plastic limit	21.2%
Plasticity index	20.8
Proctor maximum dry density (material passing #4 sieve)	126.0 pcf
Proctor optimum water content (material passing #4 sieve)	10.8%

2.8.2 Tests Performed

Fifty-two tension tests and four unconfined compression tests were performed altogether as detailed in Table 2.1.

2.8.3 Soil Preparation and Compaction of the Sample for Tension and Compression Tests

The till obtained from borrow area of Mica dam had a water content of about 12%. The soil was forced through a #4 sieve and the material passing the sieve was air dried for a week. The dried soil was stored in plastic bags. Twenty-six hundred grams of the air dried soil was mixed with the required quantity of distilled water by weight in a mechanical mixer for 3 minutes. The soil thus mixed was forced through a #4 sieve to remove all lumps. A uniform mixture was achieved without difficulty because of the non-plastic nature of soil. However, when 6% bentonite was mixed with Mica Till it was relatively difficult to force the soil through a #4 sieve when the water content was well above optimum. In such cases the lumps were broken by hand. The loss of water during mixing and compaction was compensated by adding about 0.5% more water than required. The soil mixed with water was kept in a moisture proof plastic bag and stored for 24 hours in a moist room.

The soil was compacted in a mould 4" in diameter and 1.53" high fitted with a collar. An automatic compactor with a hammer weighing 5.5 lbs. and a height of fall 12" was used for compacting the specimen. A specimen of 4" diameter and 1.53" was obtained after trimming. Three such specimens were obtained from each batch of 2600 grams of air dried soil. All the tensile test specimens were prepared using dynamic compaction. The effect of type of compaction such as kneading or vibratory compaction was not studied. The number of blows was maintained at 25 for M, B and T series of the tests (Table 2.1) and varied only for the C series in which the effect of compactive effort was studied. Greater compactive effort was simulated by increasing the number of blows while the height of fall and the weight of the hammer were kept constant at 12" and 5.5 lbs. respectively. The thickness of sample selected was 1/3 the height of the standard proctor sample. A sample 4" dia. x 1.53" was preferred over the full proctor sample (4" dia. x 4.59") for the following reasons:

(1) The quantity of soil to be handled for each specimen is smaller.

(2) Non-homogeneity caused due to compaction of standard proctor sample in three layers is avoided.

(3) For the evaluation of tensile strains a plane stress condition can be assumed with the size of sample selected while it is neither a plane strain nor a plane stress condition for the full proctor sample. Also a plane stress condition simplifies the evaluation of tensile strain when modulus in compression differs from that in tension (Sections 2.5.2, 2.9, and Appendix D). In the case of a plane strain analysis the Poisson's ratio associated with the third direction also enters the constitutive matrix.

(4) A thinner specimen would lead to a better correspondence between the tensile deformations measured on the two ends of the specimen.

For the compression tests the soil mixed with water as described above, was compacted in a 4" diameter by 8" high, 3 part split mould in 5 equal layers. Twenty-five blows of a standard 5.5 pound hammer with a 12" drop were given on each layer.

The compaction curves obtained on different size samples are compared in Fig. 2.14. A close agreement among the moisture-density relationships can be noted.

2.8.4 Specimen Preparation for Tension Test

The compacted soil specimen for a tension test was weighed for the determination of its density. Two gauge blocks are fixed to both ends of the specimen to receive the tensile clip gauges. To facilitate correct location of the gauge blocks at both ends of the specimen, a gauge-block locating jig, from here on in referred to as jig, was used. The jig as shown in Fig. 2.16 had four straight edges fixed to a brass disc of 4" diameter. The disc had two square holes to receive the two gauge blocks of 3/8" x 3/8" size separated by a fixed distance of 0.84". Two straight edges were fixed on the ends of the diameter joining the gauge blocks while the other two were fixed on the ends of the diameter perpendicular to the former. The soil specimen was kept on a wooden block with two holes to receive the gauge blocks, the jig was placed on the specimen and the four generators on the circumference of the specimen were marked along the four straight edges of the jig (Figs. 2.15 and 2.16). Marking the generators facilitated the setting of gauge blocks on the other end of the specimen exactly in opposite positions and at the same gauge length of 0.84". After marking the generators a few a standard 5.5 pound hammer with a 12" drop were given on each layer.

The compaction curves obtained on different size samples are compared in Fig. 2.14. A close agreement among the moisture-density relationships can be noted.

2.8.4 Specimen Preparation for Tension Test

The compacted soil specimen for a tension test was weighed for the determination of its density. Two gauge blocks are fixed to both ends of the specimen to receive the tensile clip gauges. To facilitate correct location of the gauge blocks at both ends of the specimen, a gauge-block locating jig, from here on in referred to as jig, was used. The jig as shown in Fig. 2.16 had four straight edges fixed to a brass disc of 4" diameter. The disc had two square holes to receive the two gauge blocks of 3/8" x 3/8" size separated by a fixed distance of 0.84". Two straight edges were fixed on the ends of the diameter joining the gauge blocks while the other two were fixed on the ends of the diameter perpendicular to the former. The soil specimen was kept on a wooden block with two holes to receive the gauge blocks, the jig was placed on the specimen and the four generators on the circumference of the specimen were marked along the four straight edges of the jig (Figs. 2.15 and 2.16). Marking the generators facilitated the setting of gauge blocks on the other end of the specimen exactly in opposite positions and at the same gauge length of 0.84". After marking the generators a few drops of phenyl salicylate at 200°F temperature were dropped into the square holes and the gauge blocks were set in position by lightly pressing them into the molten liquid. The jig was removed from the specimen without disturbing the blocks. In a few minutes the liquid set and held the gauge blocks firmly to the specimen. To the other end of the specimen also the gauge blocks were attached in a similar manner after turning the specimen upside down and orienting it properly so that the lines marked previously coincided with the straight edges of the jig. Any phenyl salicylate that entered the grooves of the gauge blocks was removed with a sharp knife. The specimen was then held on a stand (Fig. 2.17(a)) and dipped into a mixture of 50% petrowax and 50% petrolatum kept in a molten condition at about 55°C. A thin and pliable coat of the mixture thus formed not only prevents the loss of moisture from the specimen but also forms a protective coat to prevent the edges from spalling. The specimen thus prepared was cured in the moist room for about 2 weeks before testing.

Before performing the tensile test the wax covering the gauge blocks of the specimen was removed to insert the knife edge points of the clip gauge into the grooves of the gauge blocks. A strip of wax along the thickness of the specimen was removed at both ends of the vertical diameter so that the surface of soil was in direct contact with the loading strips. The loading strips used were butyl rubber 0.385" wide and 0.185" thick. From the preliminary tests it was found that the type of rubber used was neither too soft nor too rigid for the proper distribution of load to the samples tested. The width chosen for the loading strips was slightly less than a tenth of the diameter of the sample so that the theoretical stress distributions at the centre of the specimen for a concentrated load was valid. A greater width for the loading strip causes the specimen to mobilize greater resistance than that needed to cause the initial fracture. A typical brittle failure observed in all the tension tests performed is shown in Fig. 2.17(b).

2.8.5 Tension Test Operation

All the tension tests were performed in the moist room at 45°F and 95% relative humidity. The variations in temperature and the relative humidity were ±2°F and ±5% respectively. The purpose of conducting the test in a moist room was to avoid loss of moisture from the specimen especially during long term tests. The specimen was properly positioned in the loading machine before the application of the load as shown in Figs. 2.10(a) and 2.10(b). While the load was applied to the specimen the load cell, the two strain gauges and the L.V.D.T. readings were recorded on a paper by the data acquisition system at an interval of time, set on the digital clock.

2.8.6 Computation of Tensile Stress and Strain

The readings obtained in volts and millivolts on the recording paper were converted to the proper units by using the appropriate calibration factors determined prior to testing. It was assumed that a tensile crack was initiated at the peak load and the tensile stress at failure was computed using Eq. 2.5. From the tensile deformations recorded at peak load from both ends of the specimen the tensile strains were computed and were averaged. The resulting strain was taken as the average observed tensile strain at failure. The average tensile strain was observed over a gauge length of 0.84". To obtain the tensile strain at the centre of the specimen, the average observed tensile strain has to be multiplied by a coefficient which can be evaluated from the tensile strain distribution on the horizontal diameter of the specimen. This tensile strain distribution can in turn be computed from the stress distribution shown in Fig. 2.5. For the plane stress condition the horizontal tensile strain at a distance r from the centre can be expressed as:

$$\varepsilon_x = \frac{\sigma_x}{E_t} + \frac{\nu_c}{E_c}\sigma_y$$

or

$$\frac{\pi Rt}{P}\varepsilon_x E_t = \sigma_x \frac{\pi Rt}{P} + 3\nu_c \frac{E_t}{E_c}\sigma_y \frac{\pi Rt}{3P} \qquad (2.10)$$

The tensile strain at the centre can be expressed as:

$$\varepsilon_{xc} = \frac{\sigma_{xc}}{E_t} + \frac{\nu_c}{E_c}\sigma_{yc}$$

or

$$\frac{\pi R t}{P} \varepsilon_{xc} E_t = \sigma_{xc} \frac{\pi R t}{P} + 3\nu_c \frac{E_t}{E_c} \sigma_{yc} \frac{\pi R t}{3P} \tag{2.11}$$

From Eqs. 2.10 and 2.11

$$\frac{\varepsilon_x}{\varepsilon_{xc}} = \frac{\sigma_x \frac{\pi R t}{P} + 3\nu_c \frac{E_t}{E_c} \sigma_y \frac{\pi R t}{3P}}{\sigma_{xc} \frac{\pi R t}{P} + 3\nu_c \frac{E_t}{E_c} \sigma_{yc} \frac{\pi R t}{3P}} \tag{2.12}$$

Using Eq. 2.12 and Fig. 2.5 $\frac{\varepsilon_x}{\varepsilon_{xc}}$ along the horizontal diameter can be computed for a given value of ν_c and E_c/E_t. From the distribution of $\frac{\varepsilon_x}{\varepsilon_{xc}}$ along the horizontal diameter the central tensile strain, ε_{xc}, can be related to the strain $\varepsilon_{x\ell}$, observed over a length ℓ as:

$$\varepsilon_{x\ell} = \frac{\varepsilon_{xc} \int_{-\ell/2}^{\ell/2} \frac{\varepsilon_x}{\varepsilon_{xc}} \cdot dr}{\ell} \tag{2.13}$$

or

$$\varepsilon_{xc} = C_\ell \times \varepsilon_{x\ell} \tag{2.14}$$

where

$$C_\ell = \frac{\ell}{\int_{-\ell/2}^{\ell/2} \frac{\varepsilon_x}{\varepsilon_{xc}} \cdot dr} \qquad (2.15)$$

The variation of coefficient C_ℓ determined by graphical integration of Eq. 2.15 for $\nu_c = 0.365$, $\ell = 0.84"$, and for E_c/E_t ranging from 1 to 15 is shown in Fig. 2.18. The use of this coefficient in the evaluation of the tensile stress-strain relationship is shown in Section 2.9.

The terms pertaining to the tensile strain used in all the subsequent sections mean as follows: Observed tensile strain is the tensile strain computed from the tensile deformation measured over a gauge length of 0.84". Average observed tensile strain is the tensile strain obtained by averaging the observed tensile strains computed for both ends of the specimen. Observed central tensile strain is the tensile strain at the centre of the specimen obtained by multiplying the average observed tensile strain by a coefficient (Eq. 2.15). Tensile strain ("true" tensile strain) is the strain caused at the centre of the specimen by the tensile stress alone. This strain is obtained by deducting from the observed central tensile strain, the tensile strain caused by the compressive stress at the centre of specimen.

2.9 An Example to Illustrate the Procedure of Deriving the Tensile Stress-Strain Relationship

As mentioned in Section 2.5.3, in a biaxial indirect tension test, the observed central tensile strain consists of strains due to both tensile and compressive stress at the centre of the specimen. The following example illustrates the procedure for deriving the tensile stress-strain relationship (Section 2.5.3).

An unconfined compression test performed on a 4" dia. x 8" sample with lateral strain measurement yielded the results presented in Fig. 2.19. The water content at failure was 10.65%, about 1.5% greater than the optimum. The compressive stress-strain relationship and the Poisson's ratio, computed from measured lateral and axial strains throughout the test, are shown in Fig. 2.19. An increase in Poisson's ratio with axial strain can be noticed. A tension test was also performed on 4" dia. x 1.53" sample at the same rate of loading (0.005"/min.) as that used in the compression test. The results of the tension test are shown in Fig. 2.20 and Table 2.2. The water content at failure (10.68%) was almost the same as that obtained in the compression test. The tensile stress was computed using Eq. 2.4(a). This formula is valid when the modulus in compression is equal to that in tension. In Fig. 2.20 the tensile stress is plotted against the observed tensile strains, computed from the measured tensile deformation on both ends of the specimen over a gauge length of 0.84". In the same figure the relationship between the tensile stress and the average of the observed tensile strains is also shown.

The relationship between the tensile stress and tensile strain is obtained using the following steps (Table 2.3):

Step 1: A representative value for E_c and ν_c is chosen from the compression test results for the range of compressive stress realized in the tension test. For the example considered, the failure tensile stress from Fig. 2.20 is 0.525 psi and the corresponding compressive stress at the centre of specimen would be 1.575 psi, i.e., three times the tensile stress. From Fig. 2.19 representative values for E_c and ν_c can be selected for a range of compressive stress between zero and 1.575 psi. These are 260.9 psi and 0.365 respectively.

Step 2: The relationship between central tensile stress and central observed tensile strain, shown by a solid line in Fig. 2.21, is derived by multiplying the observed average tensile strain, shown by a solid line in Fig. 2.20, by a coefficient equal to 1.048. This coefficient, corresponding to $E_c/E_t = 1$, is obtained from Fig. 2.18 in which the value of coefficient is plotted against E_c/E_t for a ν_c equal to 0.365.

Step 3: From the relationship between central tensile stress and the observed central tensile strain the relationship between the tensile stress and the tensile strain, for $E_c/E_t = 1$ is obtained. This relationship is shown by a solid line passing through solid circles in Fig. 2.21. This relationship is obtained by deducting the tensile strain at the centre caused by the compressive stress from the observed central tensile strain (Eq. 2.9, Section 2.5.3).

Step 4: The secant modulus (E_t) at 2/3 of the failure tensile stress is obtained from the tensile stress-strain relationship derived in Step 3. The value is 31.99 psi (Table 2.3) and the corresponding ratio of E_c/E_t is 8.16.

The relationship in Step 3 is obtained for $E_c/E_t = 1$, whereas the actual E_c/E_t computed from the relationship is equal to 8.16. Steps 2, 3 and 4 are repeated for the $E_c/E_t = 8.16$, making use of Figs. 2.18 and 2.4, and the new value of E_c/E_t is computed. The procedure is repeated until the values of E_c/E_t obtained in two successive cycles of computation agree reasonably with each other (Table 2.3). In this example the final relationship between tensile stress and strain, derived for a value of $E_c/E_t = 11.64$, gives $E_c/E_t = 12.10$ which is reasonably close to 11.64. Further calculations are not necessary because the corresponding change in the final tensile stress-strain relationship is negligible. In Fig. 2.21 the final tensile stress-strain relationship is shown by a solid line through squares.

2.10 Discussion of Tension and Compression Test Results

Since the tensile deformations were measured on the same gauge length in all the tests performed, the influence of various factors has been studied in terms of the observed failure strains instead of "true" tensile failure strains.

Similarly the tensile strength of the soil as influenced by different factors was computed using the formula given by Eq. 2.5. Since the purpose of the present study was mainly to compare the influence of different factors on the tensile characteristics of soil, the somewhat simplified approach adopted here was considered to be appropriate enough to bring out the salient points.

2.10.1 Effect of Water Content

The tensile strength of the low-plastic till tested, decreases with an increase in water content at failure (Fig. 2.22). The observed average tensile strain at failure on the other hand increases with the increase in water content at failure (Fig. 2.23). The increase in strain becomes disproportionately high at water contents greater than the optimum. Assuming for the present studies, the ratio of the failure tensile stress to the observed average tensile strain as a measure of stiffness of the soil in tension it can be seen from Fig. 2.24 that the stiffness decreases with an increase in the water content at failure.

2.10.2 Effect of Compactive Effort

As stated in Section 2.8.3, the amount of compactive effort was varied by changing the number of blows. The weight of the hammer (5.5 lbs.) and the height of fall (12") were constant for all the tests. The water content-dry density relationships obtained for 25, 50 and 70 blows are shown in Fig. 2.25. The tensile stress at failure increases with the compactive effort for water contents below the optimum and decreases slightly with the compactive effort for water contents above the optimum (Fig. 2.26). The observed average tensile strain at failure and the stiffness of the soil in tension are plotted against water content at failure in Figs. 2.27 and 2.28 respectively. Increasing the compactive effort for water contents greater than about 7% causes a decrease in the stiffness of the soil in tension. This appears to be due to the effect of some softening induced by over compacting the non-plastic Mica Till at water contents above and close to the op^imum. However, increasing the compactive effort at water contents well below the optimum increases the stiffness as well as the tensile strength of soil.

2.10.3 Effect of Rate of Loading

The effect of rate of loading on the tensile strength and on the observed average tensile strain at failure is shown for water contents at 9% and 10.4% in Figs. 2.29 and 2.30. Both the tensile strength and the strain at failure attain the minimum values at a certain rate of loading depending on the water content at failure. Tschebotarioff *et al*. (1953) reported a decrease in tensile strength and tensile strain at failure with an increase of the duration of the test. The test duration for the tests conducted by Tschebotarioff *et al*. (1953) ranged approximately from 5 to 430 minutes. Narain (1962) reported an increase in the tensile strength and tensile strain at failure with the increase of the test duration. The duration of tests conducted by Narain (1962) ranged from 2 days to 6 months. The two opposite effects of test duration on the tensile characteristics of compacted soils reported by Tschebotarioff _et al_. (1953) and Narain (1962) appear to be mainly due to the different ranges of test durations used in the experiments. The test durations of the present tension tests cover the range of test durations reported by Tschebotarioff _et al_. (1953) and extend to the lowest of the range reported by Narain (1962). From Figs. 2.29 and 2.30 it can be seen that the duration of test has a significant effect on the tensile characteristics of a compacted soil. The critical rate of loading at which the minimum tensile strength is mobilized is almost the same as that needed to produce the minimum tensile strain at failure. However the critical rate of loading is influenced by the water content at failure (Figs. 2.29 and 2.30). From a practical point of view, it can be concluded that a fairly rapid loading, comparable to the test durations lasting between 1 to 2 days, causes conditions favourable to the formation of cracks. Considering only the effect of rate of loading, it is unlikely that extremely rapid or extremely slow rates of loading would cause tensile failures in compacted soils of low to medium plasticity. By conducting a number of representative laboratory tension tests at different rates of loading it appears possible to define the minimum tensile strength and the minimum tensile strain at failure for a given compacted soil of the type tested here.

2.10.4 Effect of Adding Bentonite

As a means of increasing the flexibility of the core of an earth dam a small percentage of bentonite may be added to the almost non-plastic till. For example, in the case of Duncan Dam (Chapter V) about 6% bentonite was added to the core material. To study the effect of adding the bentonite, tension tests were conducted on a mixture of Mica Till and 6% by weight of commercial bentonite. Fig. 2.31 shows the water content-dry density relationships for Mica Till with and without bentonite. Addition of 6% bentonite decreased the maximum dry density by 6 pcf and increased the optimum water content by 1.6%. The liquid limit and plasticity index are also increased by 23.8% and 17.3 respectively.

The effect of water content at failure on the tensile strength of Mica Till is shown in Fig. 2.32 with and without bentonite. A significant difference between the variation of the tensile strength for water contents below optimum is evident. For Mica Till without bentonite the tensile strength decreases steadily with the water content while for Mica Till with 6% bentonite the tensile strength increases up to the optimum water content and then decreases beyond the optimum.

The tensile strain at failure increases with water content at failure both for Mica Till and Mica Till with bentonite (Fig. 2.33). However the increase in failure strain is more rapid in the case of Mica Till for water contents greater than optimum. To achieve the required flexibility, the soil mixed with bentonite requires a higher percentage of water than that needed for a soil without bentonite. The stiffness of Mica Till with and without bentonite is shown against the tensile strength in Fig. 2.34. For Mica Till without bentonite a decrease in stiffness is followed by a decrease in tensile strength. On the other hand for Mica Till with bentonite a decrease in stiffness up to the optimum water content is followed by a slight increase in tensile strength. Beyond the optimum moisture content, the tensile strength decreases with the stiffness. Comparing the two soils at a given stiffness it will be noted that till with bentonite has a greater tensile strength than till without bentonite. The decrease in tensile strength for water contents beyond the optimum is more rapid in the case of Mica Till without bentonite than that with bentonite. The addition of bentonite to till makes it possible to increase the flexibility without appreciably decreasing the tensile strength. In Fig. 2.35, the percent decrease in tensile strength that occurs with an increase of water content of 2% above the optimum for different soils is shown. The results for soils from A to F were obtained from the work of Narain and Rawat (1970). The results for soils G and H are from the present work. As can be seen from Fig. 2.35, the percent decrease in tensile strength is more for soils of low plasticity than that of soils of high plasticity.

2.10.5 Comparison of Compression and Tensile Characteristics

The stress-strain relationship obtained from unconfined compression tests on Mica Till are shown in Fig. 2.36. The variation of the compressive strength and strain at failure with water content is shown in Fig. 2.37. A comparison of compression and tensile characteristics of Mica Till appears in Fig. 2.38. The ratio of compressive strength to tensile strength increases with the water content. This is due to the fact that the reduction of tensile strength with water content is more rapid than that of compressive strength. The ratio of compressive failure strain to the tensile failure strain decreases initially and stays relatively constant for water contents greater than 7%. The secant moduli, assumed here as the ratio of the failure stress to failure strain, are also compared in Fig. 2.38. The ratio of secant moduli increases with the water content. This increase is mainly due to the greater percent reduction of tensile strength with water content as compared to the percent reduction of compressive strength (Figs. 2.22 and 2.37).

2.11 Summary

Soils are extremely weak in tension. The tensile strength of an earth dam core, comprised of soils of low to medium plasticity, can be assumed to be zero for purposes of design and analysis. The tensile strength measured here for a till of low plasticity, compacted at a water content 1.5% greater than the optimum, is only about 0.5 psi. Considering different methods of tensile testing, the Brazilian or the indirect tension test offers the maximum facility for testing soils in tension. However, because of the biaxial stress state that exists, the interpretation of the test becomes somewhat involved. When the moduli in tension and compression are not equal, as is usually the case for soils of low to medium plasticity, the theoretical stress solutions obtained under isotropic conditions over-estimate the tensile strength of the material. Numerical solutions, using the finite element method, for cases involving different moduli in tension and compression, have been obtained in this report to estimate the tensile strength of soils. By conducting parallel unconfined compression tests, the relationship between tensile stress and tensile strain can be determined from the data of an indirect tension test.

At water contents greater than the optimum the flexibility of a soil increases accompanied by a considerable decrease in tensile strength. The percent decrease of the tensile strength is higher for a less plastic soil compared to that of a more plastic soil. Addition of bentonite with the appropriate water content aids in increasing the flexibility of the soil, at the same time without a considerable reduction in the tensile strength. For a compacted till of low plasticity, the rate of loading has a significant influence on the tensile strength mobilized at failure and the associated tensile strain. Rates of loading comparable to a laboratory test duration of one to two days appears to be critical for the type of soil tested in this investigation.

The ratio of unconfined compressive strength to the tensile strength increases with the water content. The ratio for the soil tested varied from 11 to 31.2 for water contents 3.56% below optimum to 1.45% above optimum respectively. As the water content increases, for a low plastic soil the tensile strength decreases very rapidly while the reduction in compressive strength is comparatively less. The ratio of modulus in compression to that in tension also increases with the water content. The ratio for the till tested varied from 2.68 to 15.40 for water contents 3.56% below the optimum to 1.45% above the optimum.

TABLE 2.1

DETAILS OF TENSION AND COMPRESSION TESTS PERFORMED

Name of the Series and Type of Test	Purpose	Name of Sample	Percent Water Added at the Time of Mixing	Rate of Test (inches/min.)	Number of Blows Per Layer Administered by a 5.5 lb. Hammer with 12" Fall	Number of Samples Tested
M Tension	To study the influence of water content	M5/1,M5/2,M5/3	5.5	0.005	25	3
		M6/1,M6/2	6.5	0.005	25	2
		M6/3	6.0	0.005	25	1
		M7/1,M7/2	7.5	0.005	25	2
		M9/1,M9/2,M9/3	9.5	0.005	25	3
		M11/1,M11/2, M11/3	11.0	0.005	25	3
C Tension	To study the influence of compactive effort	C6/50	6.0	0.005	50	1
		C6/70	6.0	0.005	70	1
		C7/50	7.5	0.005	50	1
		C7/70	7.5	0.005	70	1
		C9/50	9.5	0.005	50	1
		C9/70	9.5	0.005	70	1
		C11/50	11.0	0.005	50	1
		C11/70	11.0	0.005	70	1
T Tension	To study the influence of the rate of loading	S21,S22,S23	9.5	0.001300	25	3
		S31,S41,S51	9.5	0.000100	25	3
		S61,S62,S63	9.5	0.000013	25	3
		T21,T22,T23	11.0	0.001300	25	3
		T31,T41,T51	11.0	0.000100	25	3
		T61,T62,T63	11.0	0.000013	25	3
B Tension	To study the influence of adding 6% bentonite	B6/1,B6/2,B6/3	6.6	0.005	25	3
		B8/1,B8/2,B8/3	8.6	0.005	25	3
		B10/1,B10/2, B10/3	10.6	0.005	25	3
		B12/1,B12/2, B12/3	12.6	0.005	25	3
UC Unconfined Compression	To compare the behaviour of soil in tension and compression	UC6	6.0	0.005	25	1
		UC7	7.5	0.005	25	1
		UC9	9.5	0.005	25	1
		UC11	11.0	0.005	25	1

Total Number of Tests: Tension 52
Compression 4

TABLE 2.2

COMPUTATION OF TENSILE STRESS AND STRAIN FROM EXPERIMENTAL DATA

Load Cell Reading in Milli-volts (1)	Load in Millivolts (2)	Tensile stress in psi (2) x 1.75 (3)	Strain Gauge Reading from Bottom End of Specimen in Millivolts (4)	Observed Tensile Strain from Bottom End in Millivolts (5)	Observed Tensile Strain from Bottom End in Percent (5)x0.1417 (6)	Strain Gauge Reading from Top End of Specimen in Millivolts (7)	Observed Tensile Strain from Top End of Specimen in Millivolts (8)	Observed Tensile Strain from Top End in Percent (8)x0.259 (9)	Average Observed Tensile Strain [(6)+(9)]/2 (10)
1.58	0	0	1.55	0	0	50.40	0	0	0
1.63	0.05	0.088	2.76	1.21	0.171	49.47	0.93	0.241	0.206
1.66	0.08	0.140	3.46	1.91	0.271	49.02	1.38	0.357	0.314
1.68	0.10	0.175	4.12	2.57	0.364	48.62	1.78	0.461	0.413
1.70	0.12	0.210	4.52	2.97	0.421	48.42	1.98	0.513	0.467
1.72	0.14	0.245	5.51	3.96	0.561	47.90	2.50	0.648	0.605
1.74	0.16	0.280	6.73	5.18	0.734	47.30	3.10	0.803	0.769
1.76	0.18	0.315	8.04	6.49	0.920	46.68	3.72	0.963	0.942
1.78	0.20	0.350	9.94	8.39	1.189	45.85	4.55	1.178	1.184
1.80	0.22	0.385	11.40	9.85	1.396	45.26	5.14	1.331	1.364
1.82	0.24	0.420	14.47	12.92	1.831	44.09	6.31	1.634	1.733
1.84	0.26	0.455	17.18	15.63	2.215	43.07	7.33	1.898	2.057
1.86	0.28	0.490	21.27	19.72	2.794	41.46	8.94	2.315	2.555
1.88	0.30	0.525	24.58	23.03	3.263	40.28	10.12	2.621	2.942
1.86	0.28	0.490	35.99	34.44	4.880	35.32	15.08	3.906	4.393

Note: Bottom or top end refer to the position of the specimen while it was compacted.

TABLE 2.3

DETERMINATION OF TENSILE STRESS-STRAIN RELATIONSHIP

	E_c/E_t = 1.0				E_c/E_t = 8.16				E_c/E_t = 11.64			
Tensile Stress at Centre of Specimen	Observed Average Tensile Strain Over a Length of 0.84"	Observed Tensile Strain at Centre of Specimen (2)x1.048	Tensile Strain Due to Compressive Stress (1)x300 v_c/E_c	Tensile Strain Due to Tensile Stress Alone (3)-(4)	Tensile Stress at Centre of Specimen (1)x0.70	Observed Tensile Strain at Centre of Specimen (2)x1.074	Tensile Strain Due to Compressive Stress (1)x372 v_c/E_c	Tensile Strain Due to Tensile Stress Alone (7)-(8)	Tensile Stress at Centre of Specimen (1)x0.67	Observed Tensile Strain at Centre of Specimen (2)x1.0845	Tensile Strain Due to Compressive Stress (1)x397 v_c/E_c	Tensile Strain Due to Tensile Stress Alone (11)-(12)
(psi) (1)	(%) (2)	(%) (3)	(%) (4)	(%) (5)	(psi) (6)	(%) (7)	(%) (8)	(9)	(10)	(11)	(12)	(13)
0	0	0	0	0	0	0	0	0	0	0	0	0
0.088	0.206	0.216	0.037	0.179	0.061	0.221	0.046	0.175	0.059	0.223	0.049	0.174
0.140	0.314	0.329	0.059	0.270	0.098	0.337	0.073	0.264	0.094	0.341	0.078	0.263
0.175	0.413	0.433	0.073	0.360	0.123	0.444	0.091	0.353	0.117	0.448	0.097	0.351
0.210	0.467	0.489	0.088	0.401	0.147	0.502	0.109	0.393	0.141	0.506	0.117	0.389
0.245	0.605	0.634	0.103	0.531	0.172	0.650	0.128	0.522	0.164	0.656	0.136	0.520
0.280	0.769	0.806	0.118	0.688	0.196	0.826	0.146	0.680	0.188	0.834	0.156	0.678
0.315	0.942	0.987	0.132	0.855	0.221	1.012	0.164	0.848	0.211	1.022	0.175	0.847
0.350	1.184	1.241	0.147	1.094	0.245	1.272	0.182	1.090	0.235	1.284	0.194	1.090
0.385	1.364	1.429	0.162	1.267	0.270	1.465	0.200	1.265	0.258	1.479	0.214	1.265
0.420	1.733	1.816	0.176	1.640	0.294	1.861	0.219	1.642	0.281	1.879	0.233	1.646
0.455	2.057	2.156	0.191	1.965	0.319	2.209	0.237	1.972	0.305	2.231	0.253	1.978
0.490	2.555	2.678	0.206	2.472	0.343	2.744	0.255	2.489	0.328	2.771	0.272	2.499
0.525	2.942	3.083	0.220	2.863	0.368	3.160	0.273	2.887	0.352	3.191	0.292	2.899
0.490	4.393	4.604	0.206	4.398	0.343	4.718	0.255	4.463	0.328	4.764	0.272	4.492

E_c = 260.9 psi; v_c = 0.365

At 2/3 of the maximum tensile stress:

$$E_t = \frac{100 \times 0.35}{1.094} = 31.99 \text{ psi}$$

and E_c/E_t = 8.76.

E_c = 260.9 psi; v_c = 0.365

At 2/3 of the maximum tensile stress:

$$E_t = \frac{100 \times 0.245}{1.090} = 22.47 \text{ psi}$$

and E_c/E_t = 11.64.

E_c = 260.9 psi; v_c = 0.365

At 2/3 of the maximum tensile stress:

$$E_t = \frac{100 \times 0.235}{1.090} = 21.56 \text{ psi}$$

and E_c/E_t = 12.10.

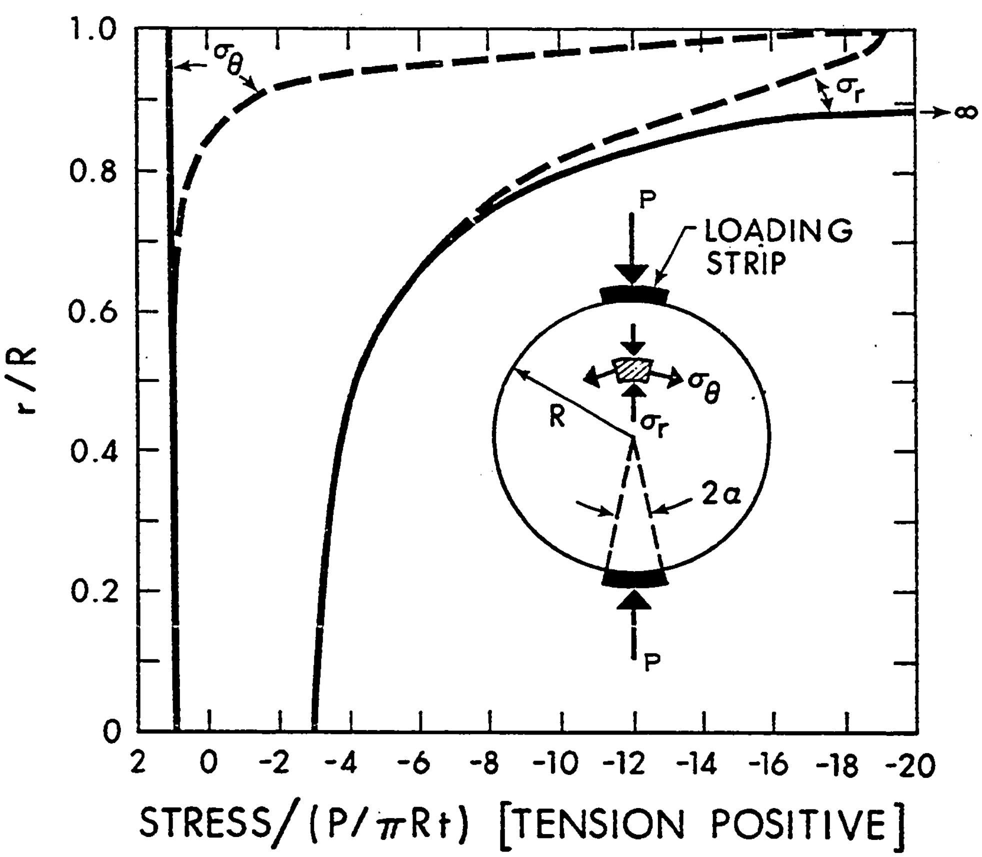

SOLUTION FOR LINE LOADING

SOLUTION FOR STRIP LOADING

WITH $\alpha=\tan^{-1}1/12$ [HONDROS, 1959]

FIG. 2.1 THEORETICAL SOLUTIONS FOR STRESSES ALONG THE VERTICAL DIAMETER OF A SPECIMEN SUBJECTED TO DIAMETRAL COMPRESSION

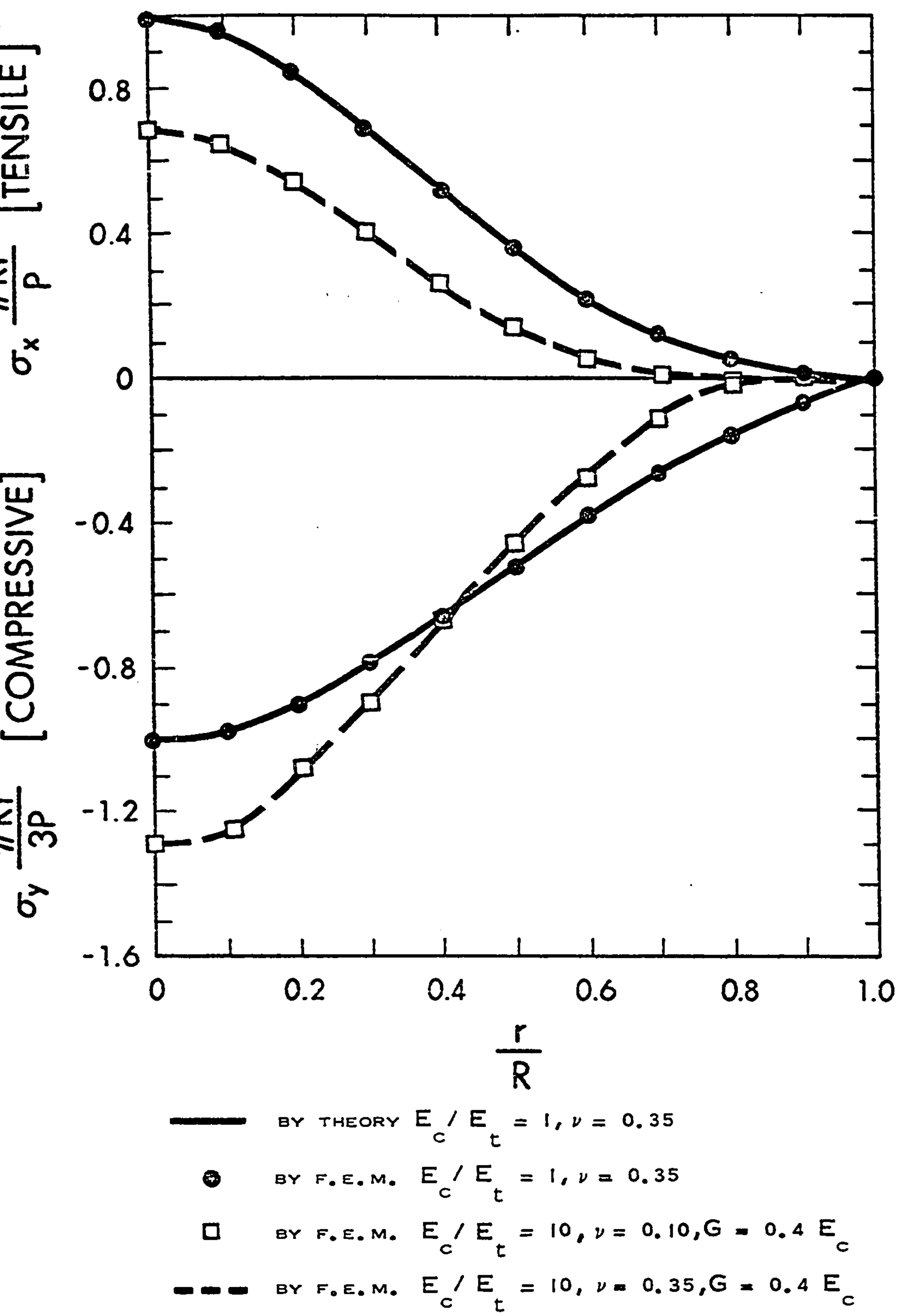

FIG. 2.2 VARIATION OF STRESSES ALONG THE HORIZONTAL DIAMETER OF A SPECIMEN UNDER DIAMETRAL COMPRESSION [COMPARISON OF THEORETICAL AND FINITE ELEMENT SOLUTIONS AND EFFECT OF POISSON'S RATIO ON STRESS DISTRIBUTION]

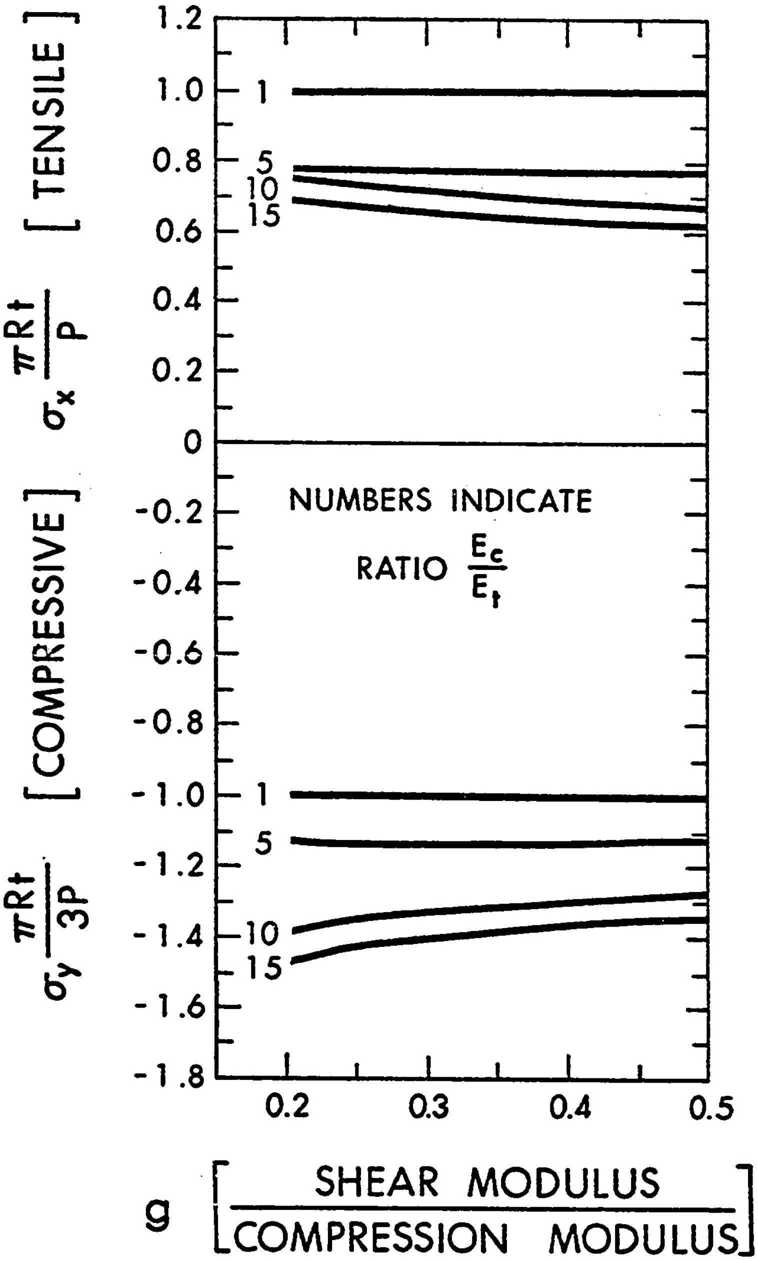

FIG. 2.3 VARIATION OF COMPRESSIVE AND TENSILE STRESS AT THE CENTRE OF SPECIMEN WITH SHEAR MODULUS FOR DIFFERENT RATIOS OF E_c/E_t

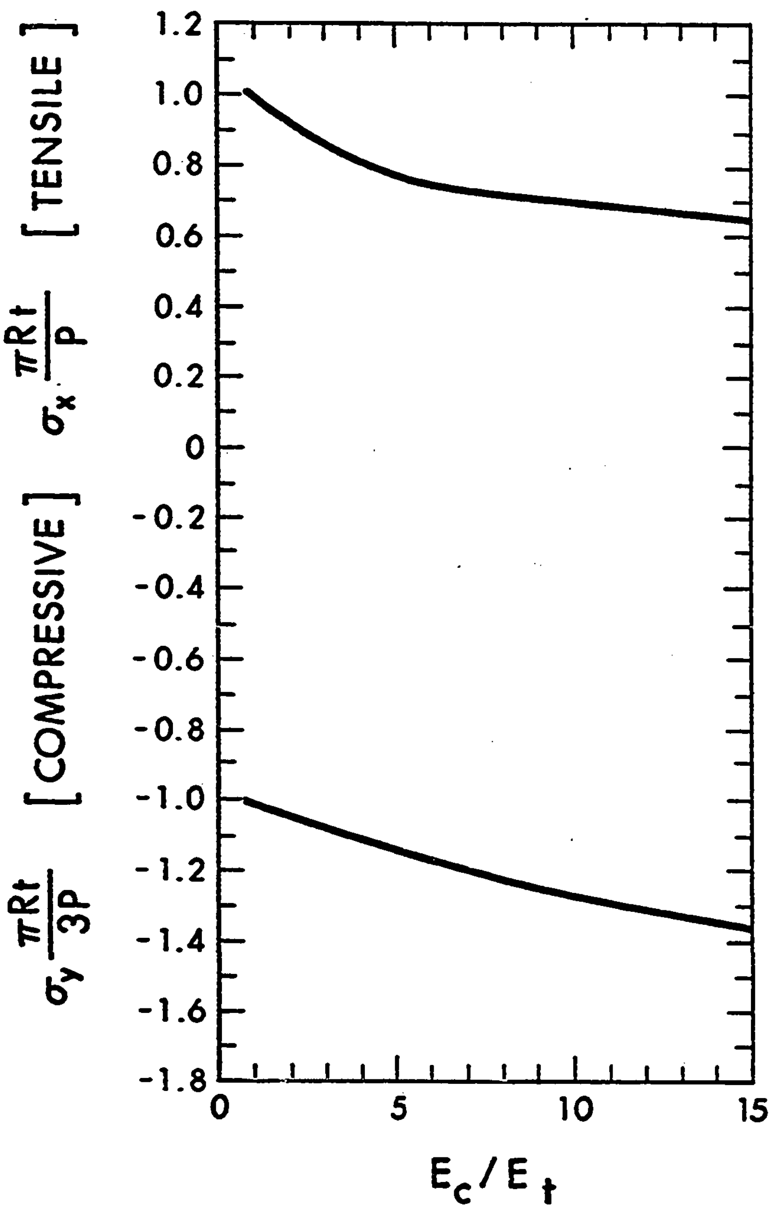

FIG. 2.4 VARIATION OF TENSILE AND COMPRESSIVE STRESS AT THE CENTRE OF SPECIMEN UNDER DIAMETRAL COMPRESSION WITH THE RATIO E_c/E_t [STRESSES CORRESPOND TO G/E_c EQUAL TO 0.4]

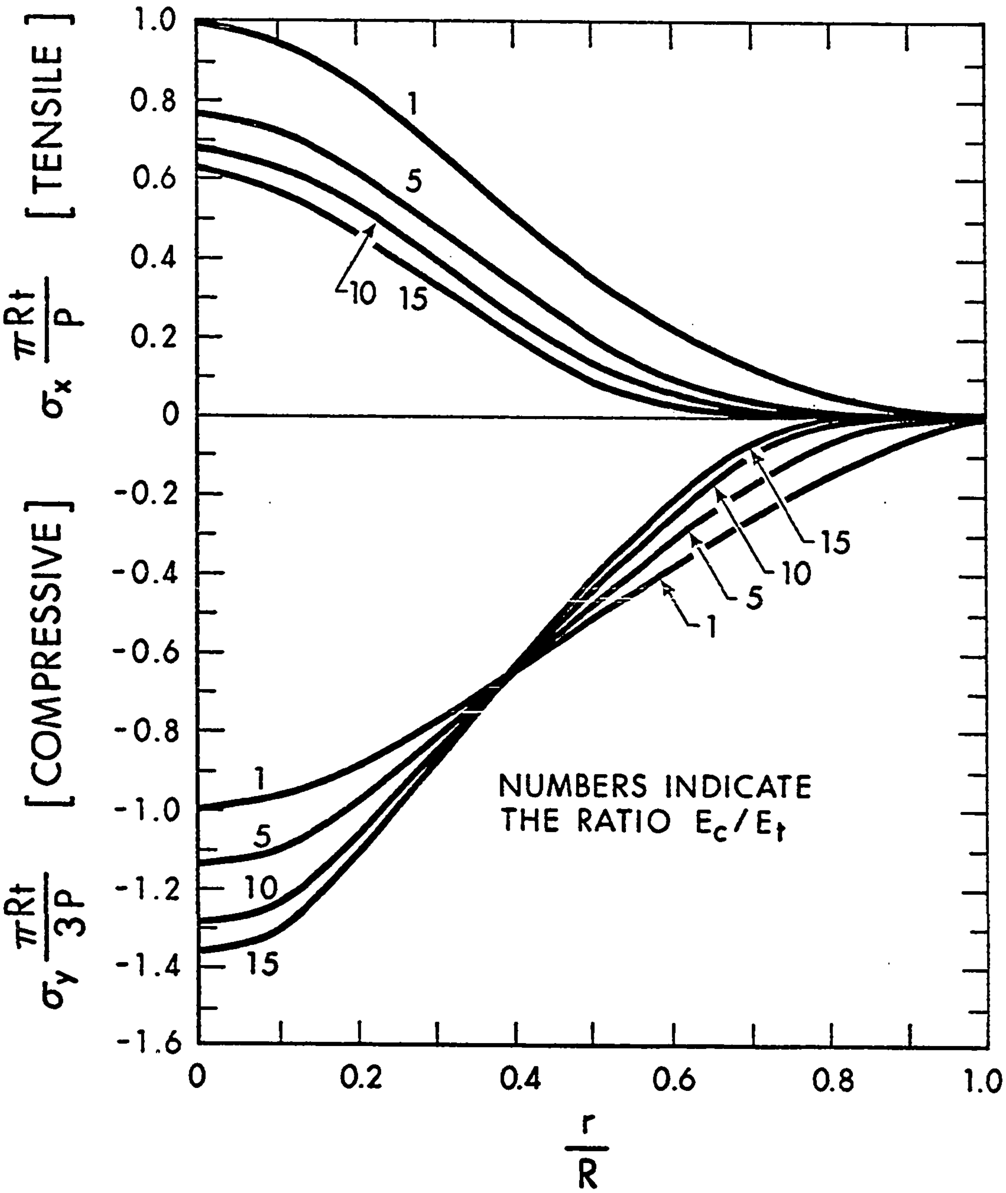

FIG. 2.5 VARIATION OF VERTICAL AND HORIZONTAL STRESS ALONG THE HORIZONTAL DIAMETER OF SPECIMEN UNDER DIAMETRAL COMPRESSION FOR DIFFERENT E_c/E_t RATIOS [STRESSES COMPUTED FOR G/E_c EQUAL TO 0.4]

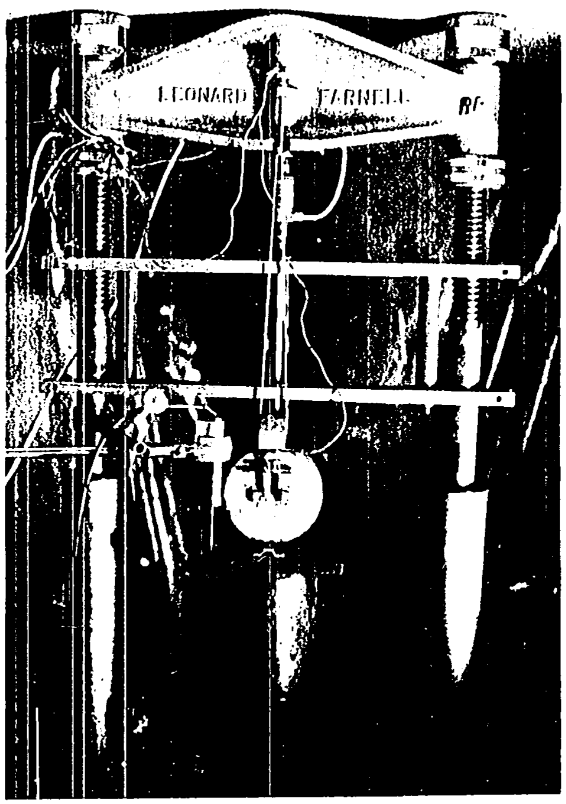

FIG. 2.6 TENSILE TEST SET-UP WITH SPECIMEN IN POSITION

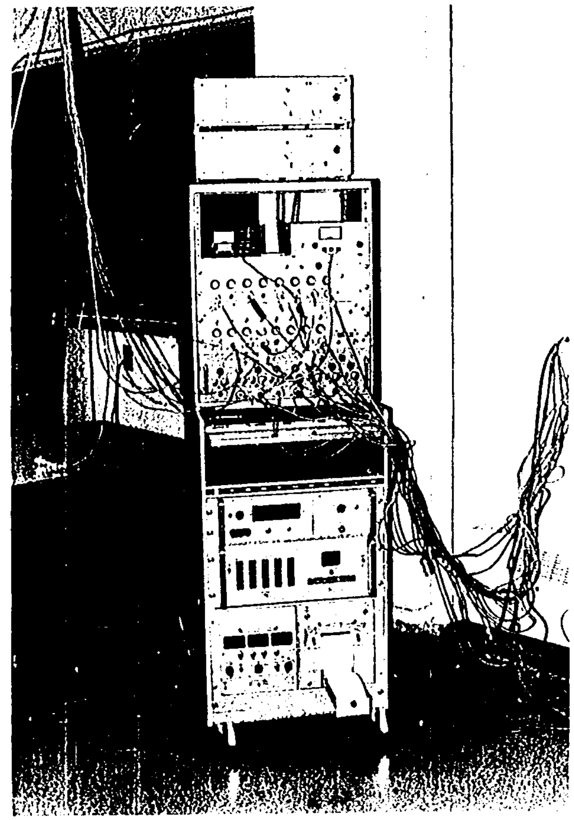

FIG. 2.7 VIEW SHOWING DATA ACQUISITION SYSTEM AND TRANSDUCER AMPLIFIERS

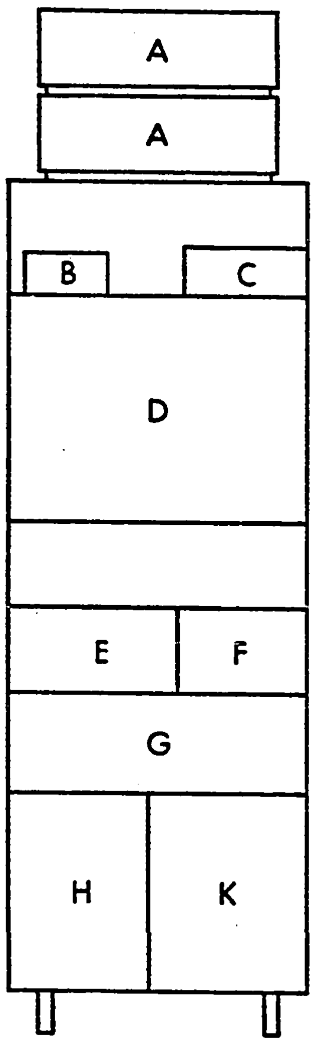

A TRANSDUCER AMPLIFIER-INDICATOR, DAYTRONIC MODEL 300D

B TRANSFORMER FOR 10V SUPPLY

C TRANSFORMER FOR 24V SUPPLY

D D.C. STRAIN GAUGE CONTROL, SANBORN MODEL 958-300

E DIGITAL VOLT METER, HEWLETT-PACKARD MODEL 3440A

F HIGH GAIN/ AUTO RANGE UNIT, HEWLETT-PACKARD MODEL 3443A

G INPUT SCANNER, HEWLETT-PACKARD MODEL 2901B

H DIGITAL CLOCK, HEWLETT-PACKARD MODEL H31571B

K DIGITAL RECORDER, HEWLETT-PACKARD MODEL H48562A

FIG. 2.8 SCHEMATIC DIAGRAM SHOWING THE DATA ACQUISITION SYSTEM AND TRANSDUCER AMPLIFIERS

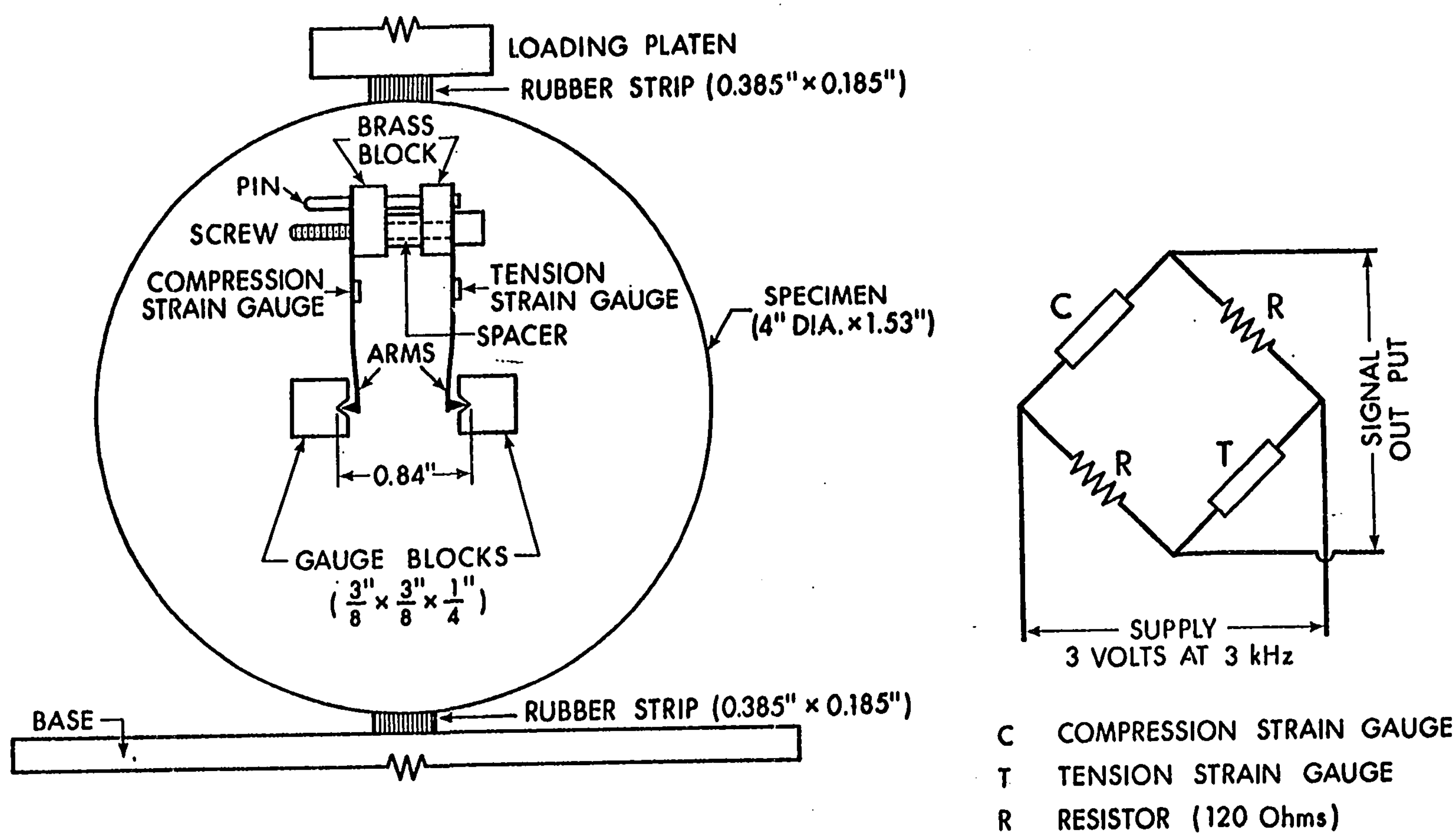

[A] CLIP GAUGE POSITIONED ON THE SPECIMEN BETWEEN GAUGE BLOCKS

[B] FULL BRIDGE CIRCUIT FOR THE CLIP GAUGE

FIG. 2.9 DETAILS OF THE CLIP GAUGE FOR TENSION TEST

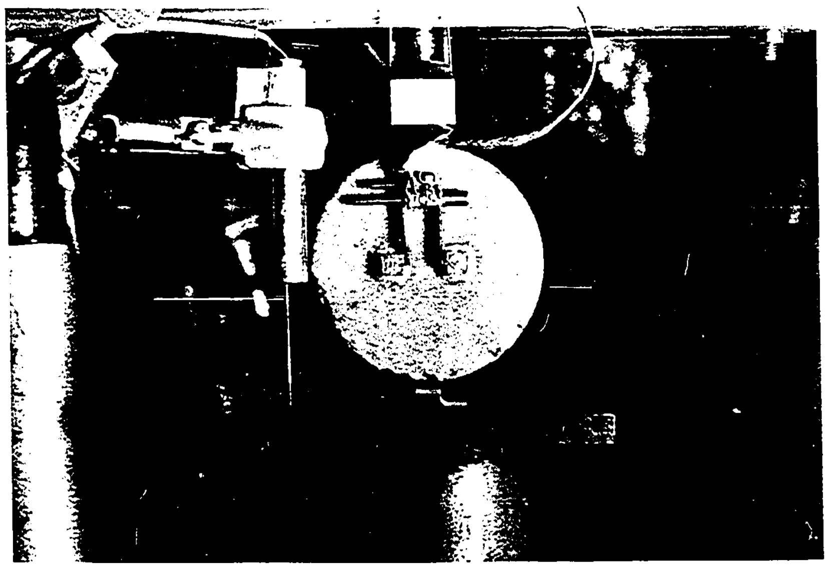

FIG. 2.10[A] A CLOSE-UP VIEW OF SPECIMEN WITH CLIP GAUGE IN POSITION

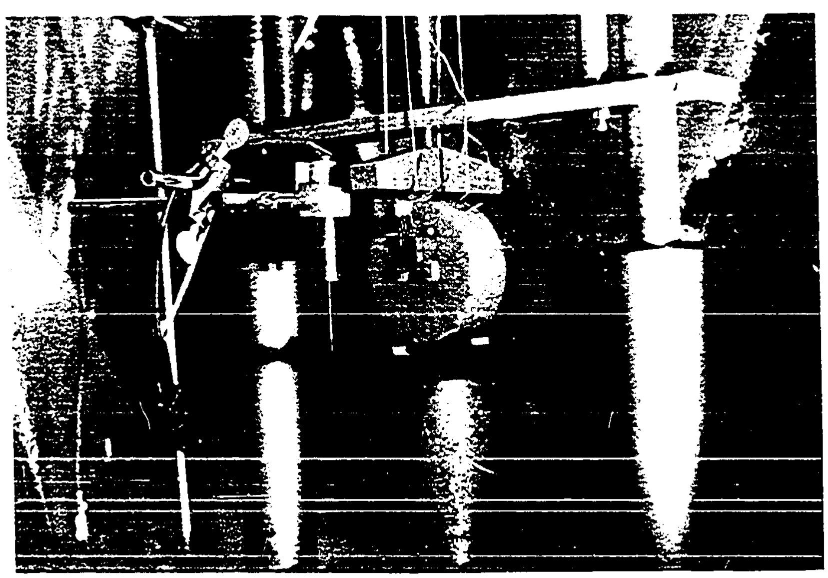

FIG. 2.10[B] A SIDE VIEW OF SPECIMEN WITH CLIP GAUGE IN POSITION

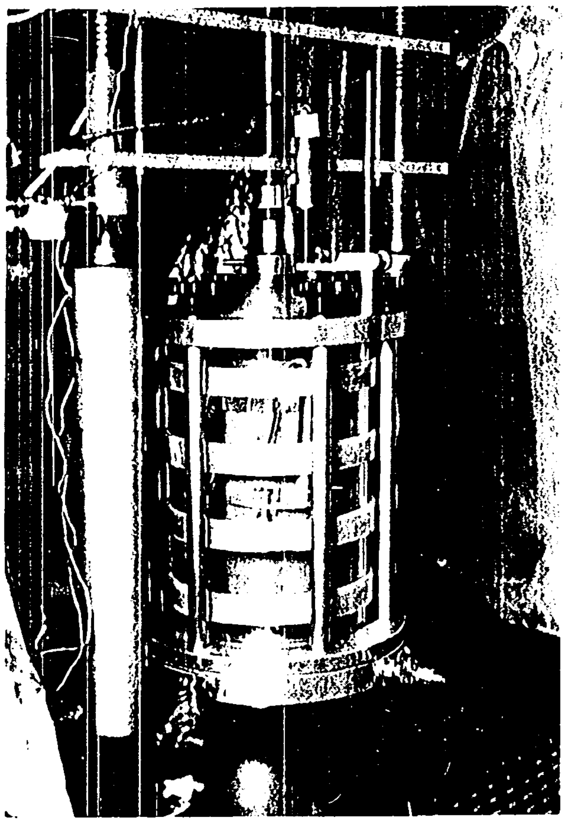

FIG. 2.11 SET-UP FOR UNCONFINED COMPRESSION TEST

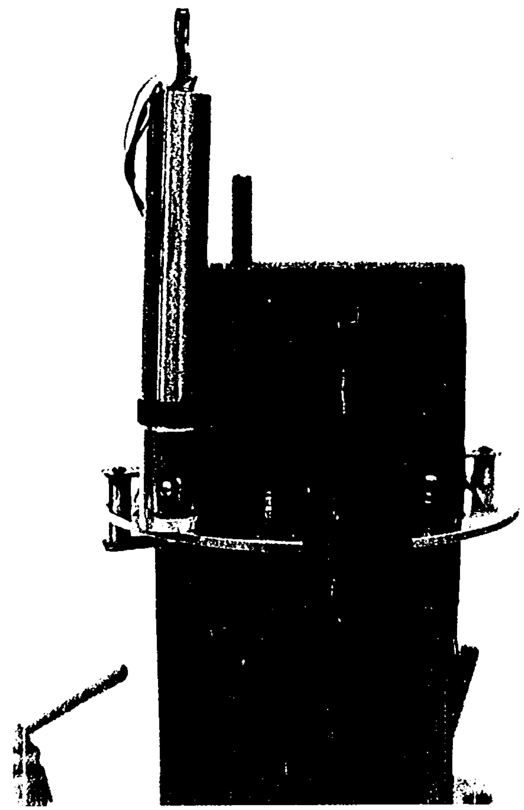

FIG. 2.12 A CLOSE-UP VIEW OF THE LATERAL STRAIN INDICATOR

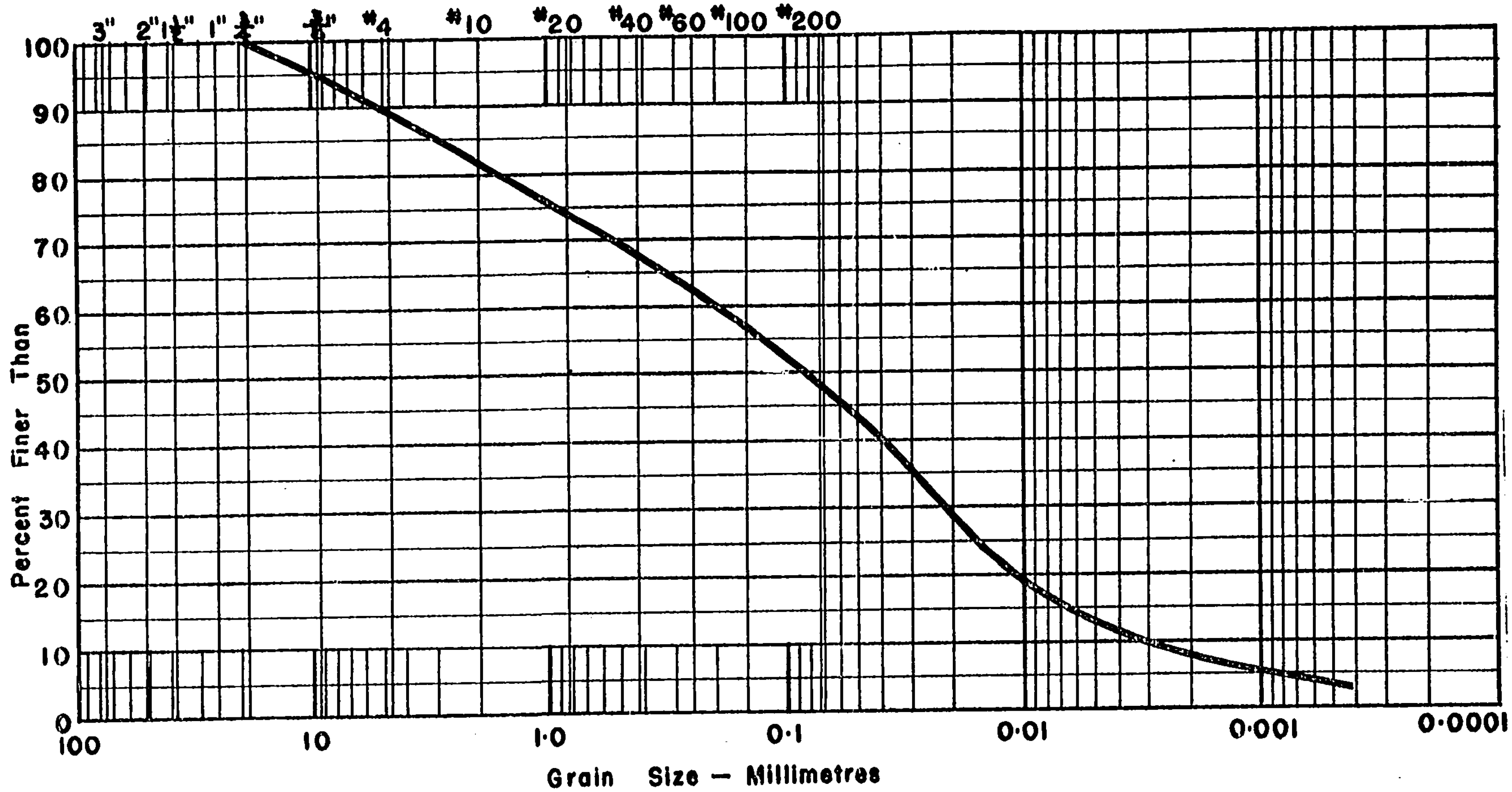

FIG. 2.13 GRAIN SIZE DISRTIBUTION FOR MICA TILL

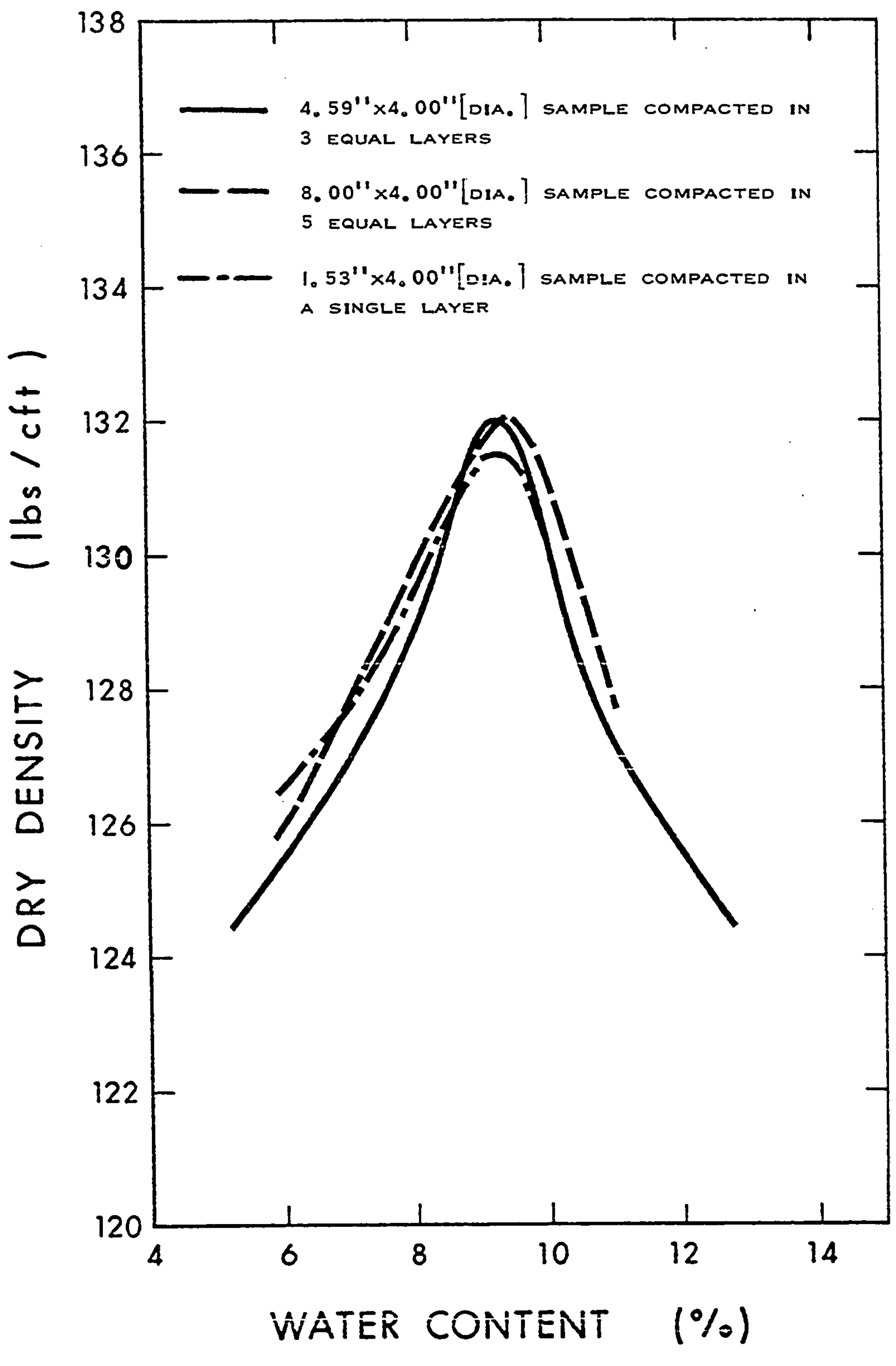

FIG. 2.14 WATER CONTENT-DENSITY RELATIONSHIPS FOR SAMPLES OF DIFFERENT SIZES PREPARED UNDER PROCTOR STANDARD COMPACTION

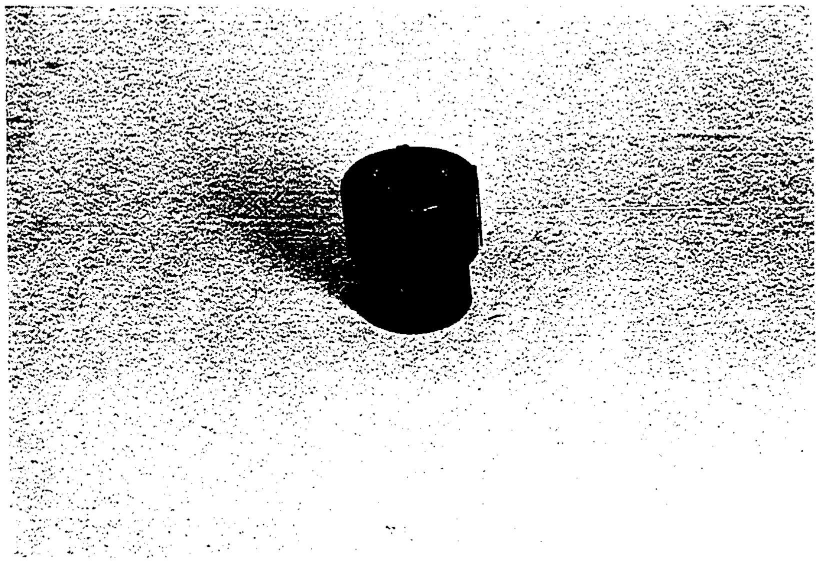

FIG. 2.15 SPECIMEN WITH GAUGE BLOCK JIG IN POSITION

FIG. 2.16 COMPONENTS FOR ATTACHING GAUGE BLOCKS TO SOIL SPECIMEN

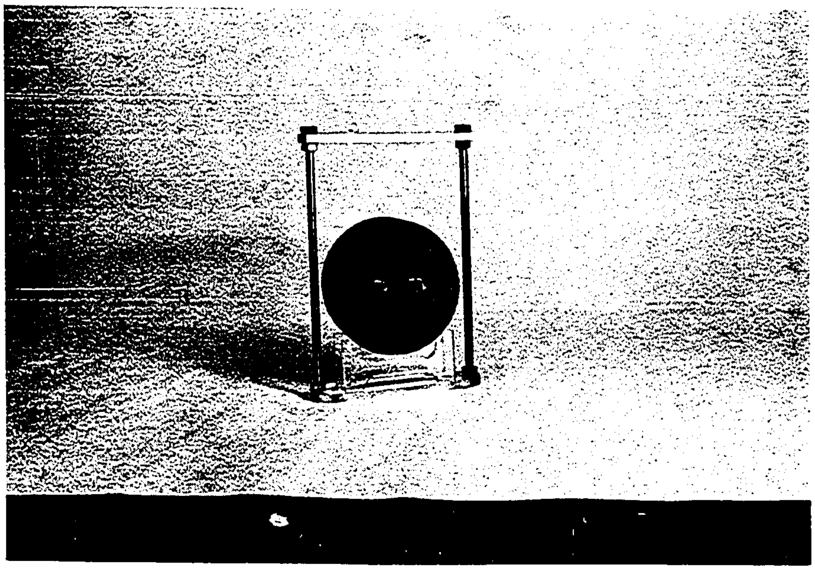

[A] SPECIMEN KEPT ON A STAND BEFORE WAXING

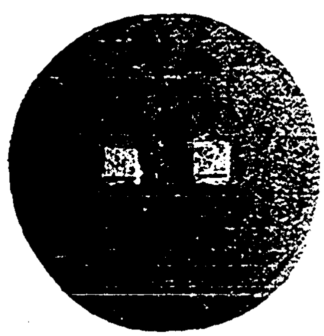

[B] TYPICAL BRITTLE FAILURE OF SPECIMEN

FIG. 2.17 TENSILE TEST SPECIMEN BEFORE AND AFTER FAILURE

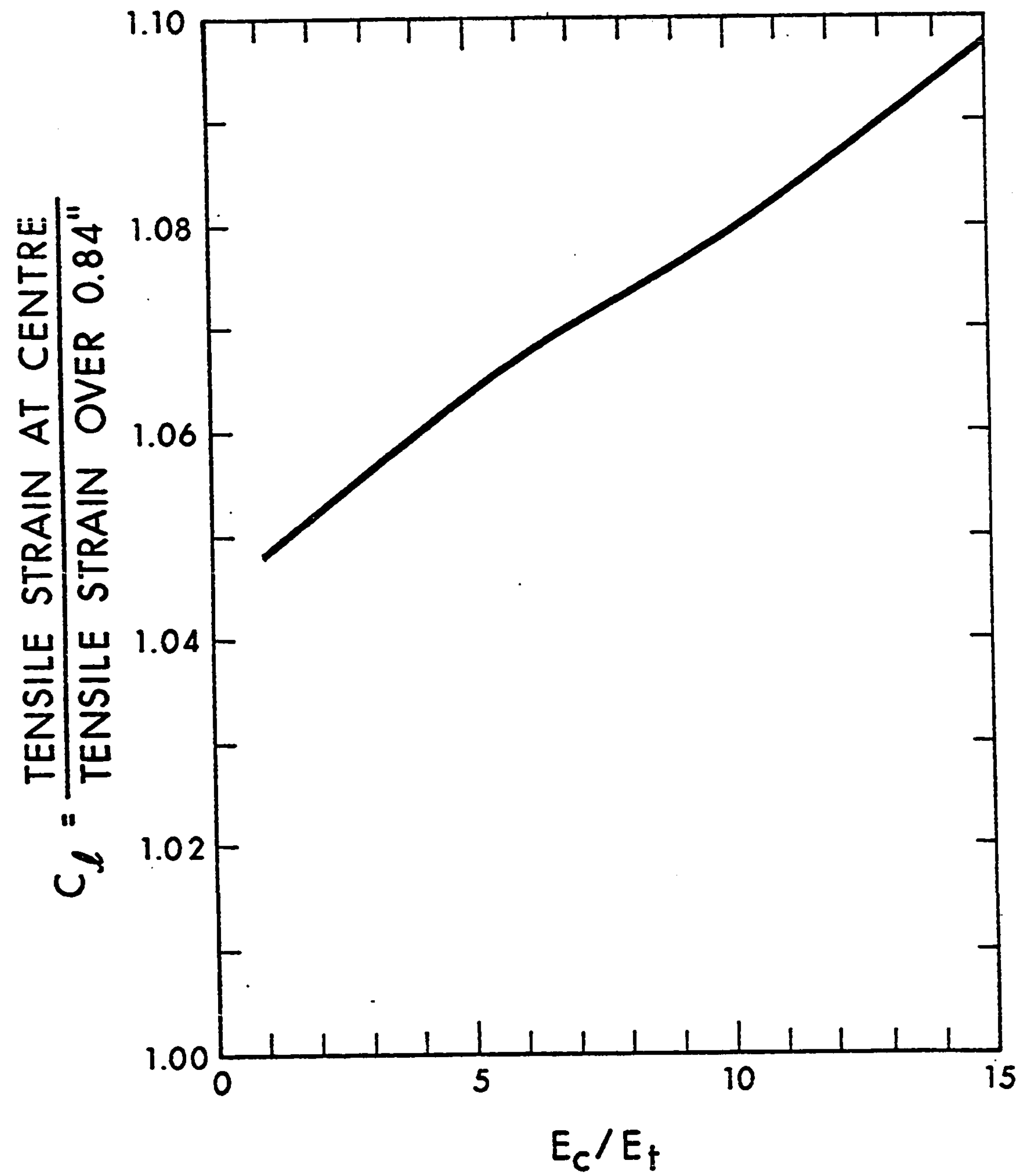

FIG. 2.18 VARIATION OF COEFFICIENT $[C_\ell]$ WITH E_c/E_t FOR POISSON'S RATIO EQUAL TO 0.365

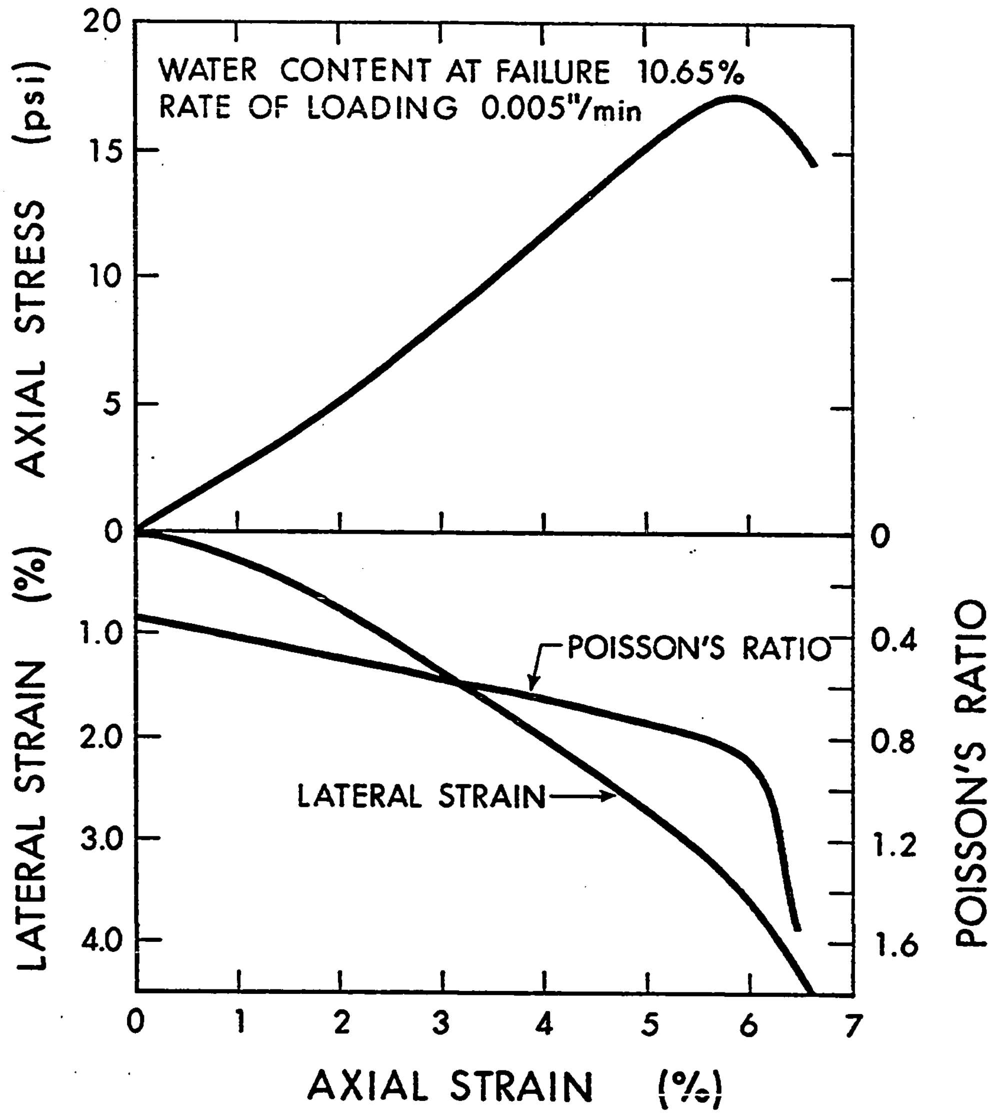

FIG. 2.19 STRESS-STRAIN RELATIONSHIP AND THE VARIATION OF LATERAL STRAIN AND POISSON'S RATIO WITH AXIAL STRAIN FOR MICA TILL TESTED UNDER UNCONFINED COMPRESSION

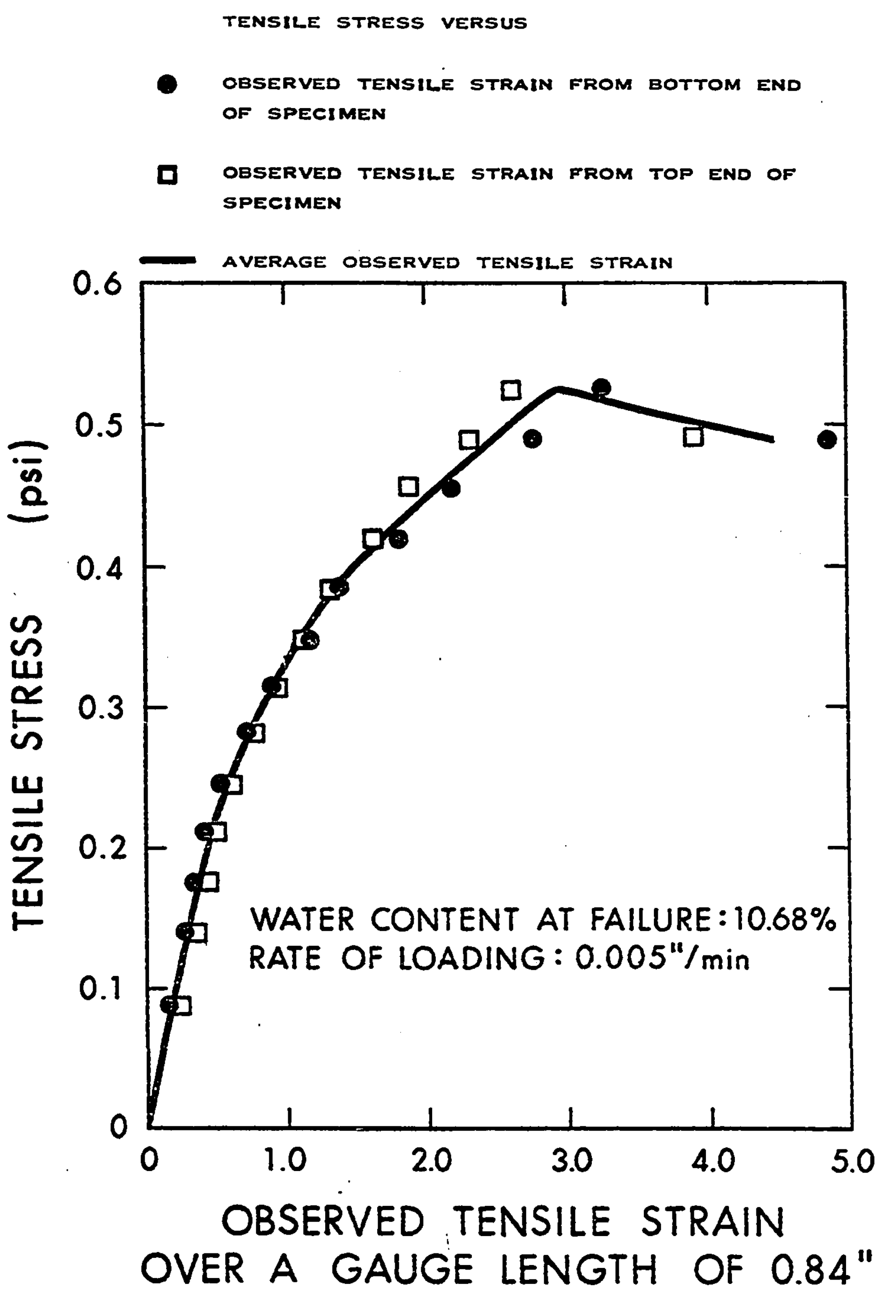

FIG. 2.20 RELATIONSHIP BETWEEN TENSILE STRESS AND THE OBSERVED TENSILE STRAIN FOR MICA TILL

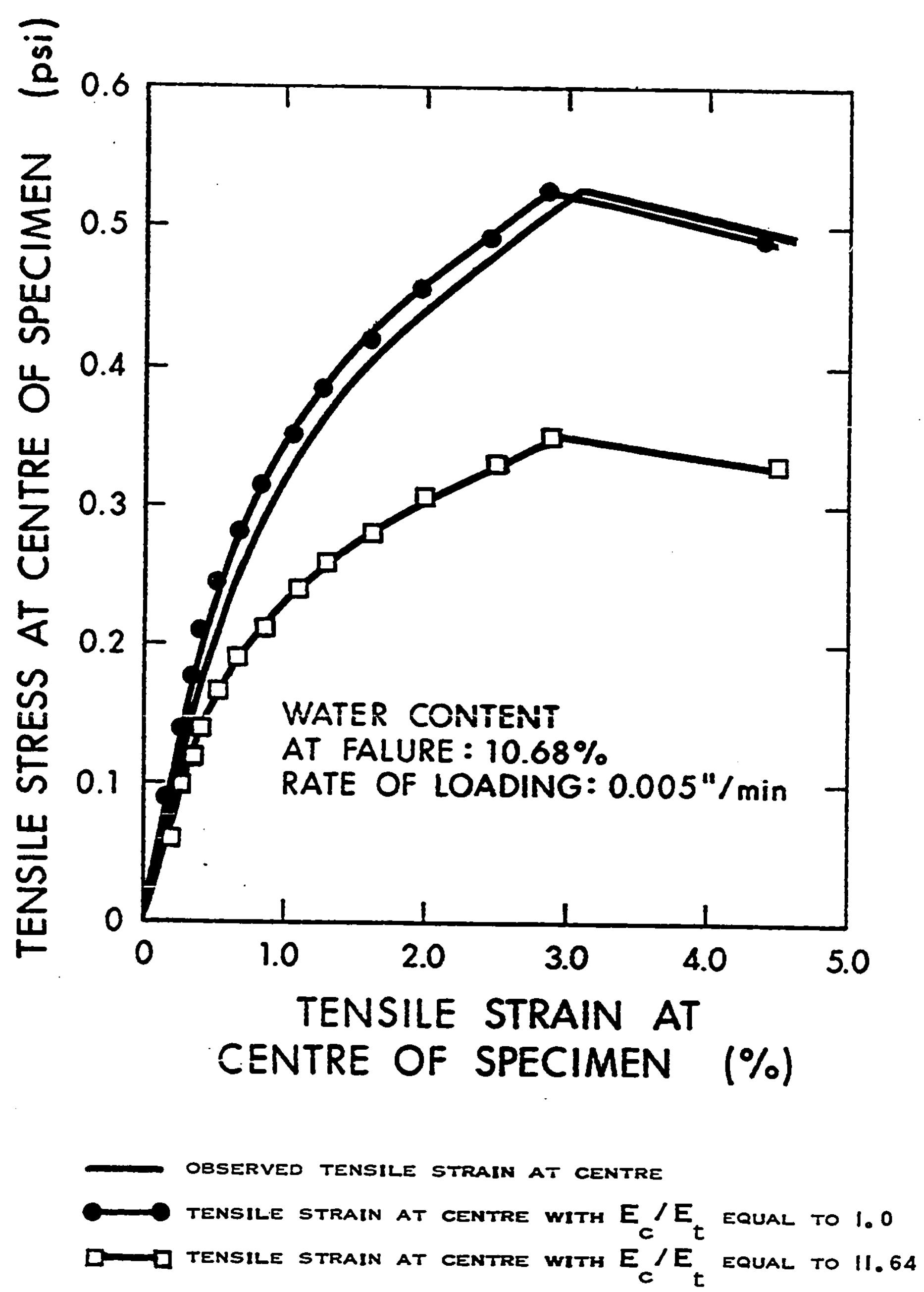

FIG. 2.21 COMPARISON OF TENSILE STRESS-STRAIN RELATIONSHIPS DERIVED FROM TENSILE TEST DATA OF MICA TILL

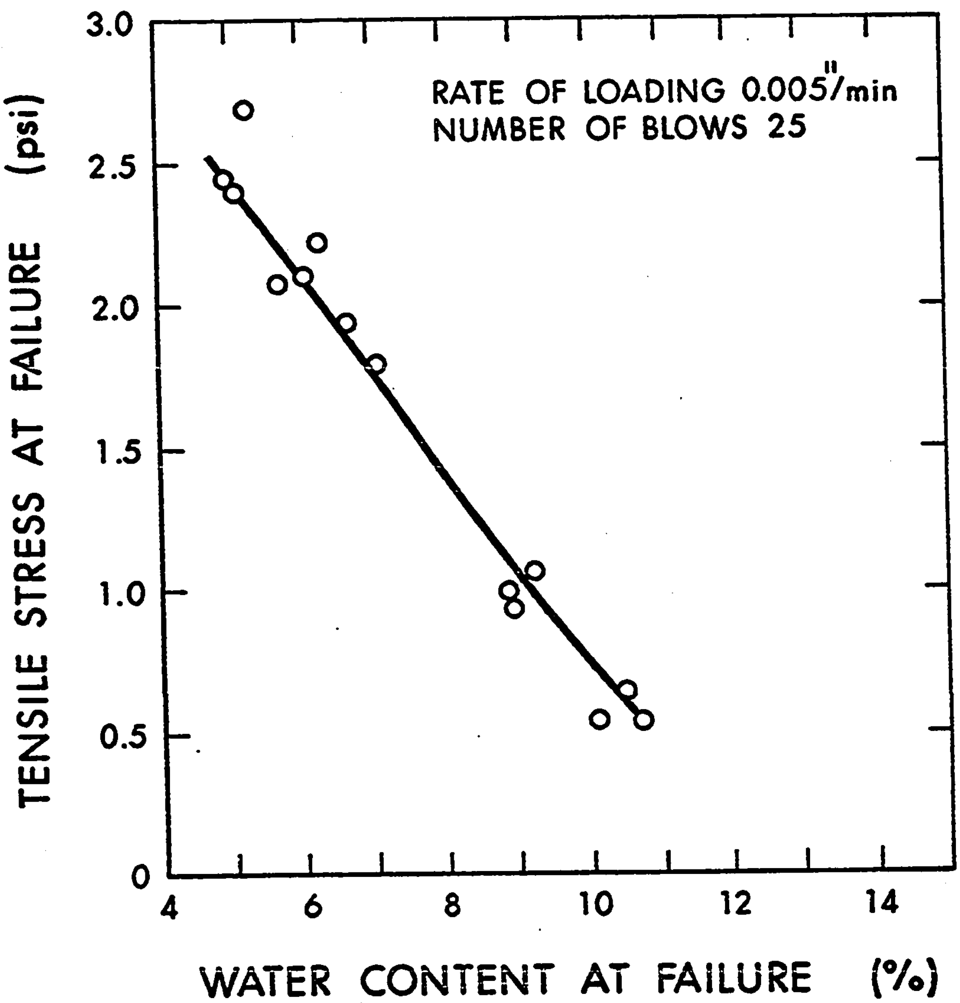

FIG. 2.22 EFFECT OF WATER CONTENT ON THE TENSILE STRESS AT FAILURE FOR MICA TILL

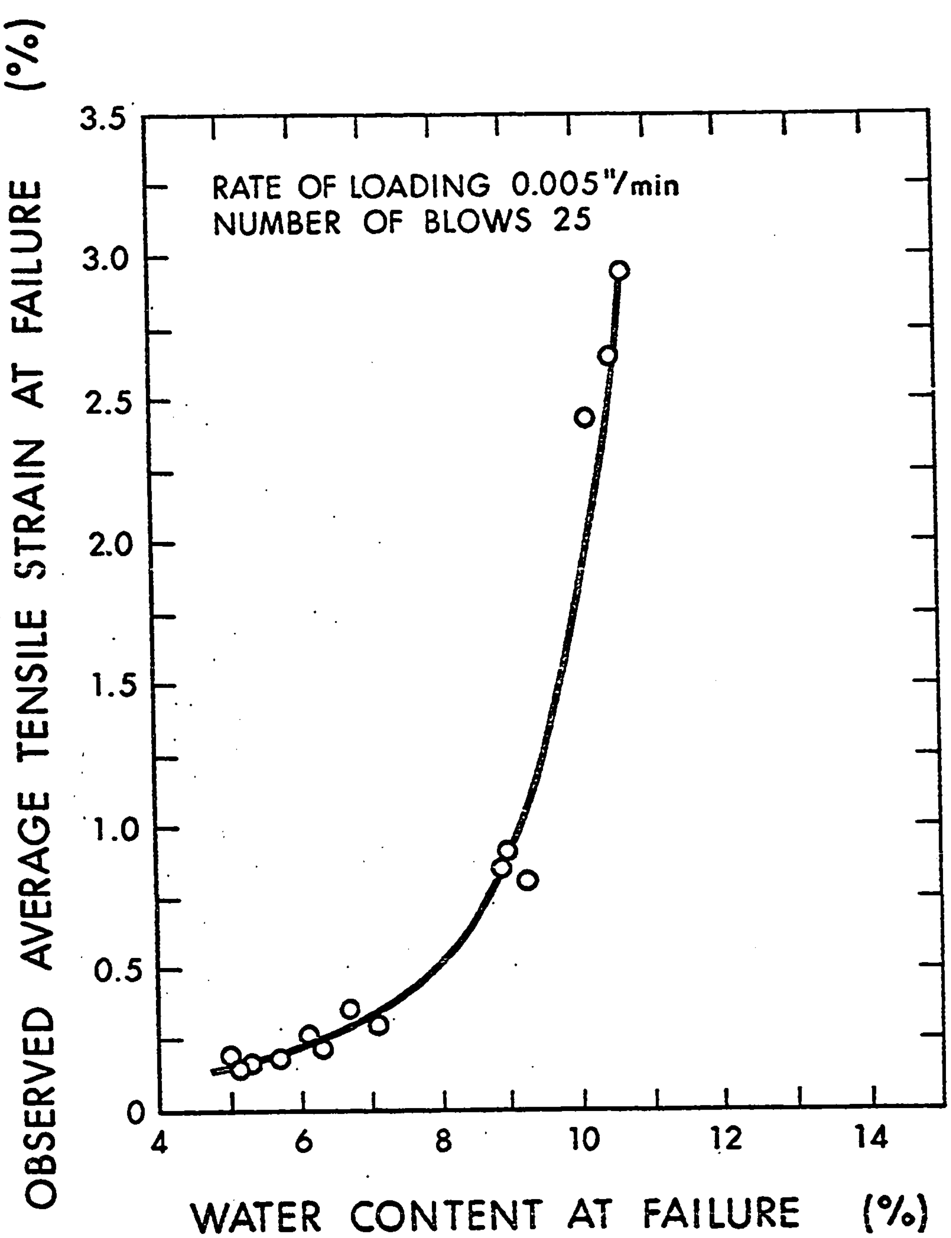

FIG. 2.23 EFFECT OF WATER CONTENT ON THE TENSILE STRAIN AT FAILURE FOR MICA TILL

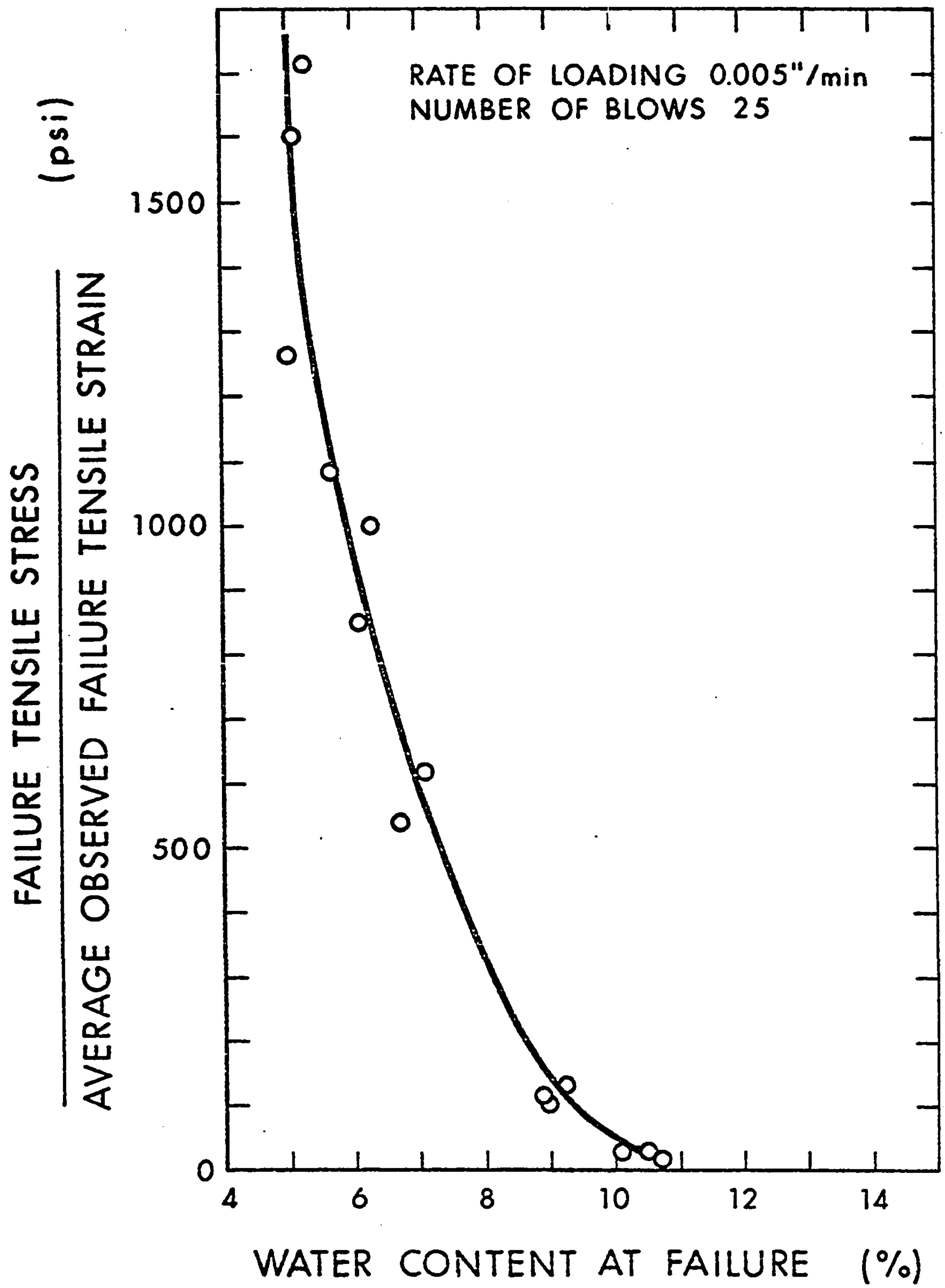

FIG. 2.24 VARIATION OF STIFFNESS IN TENSION WITH WATER CONTENT FOR MICA TILL

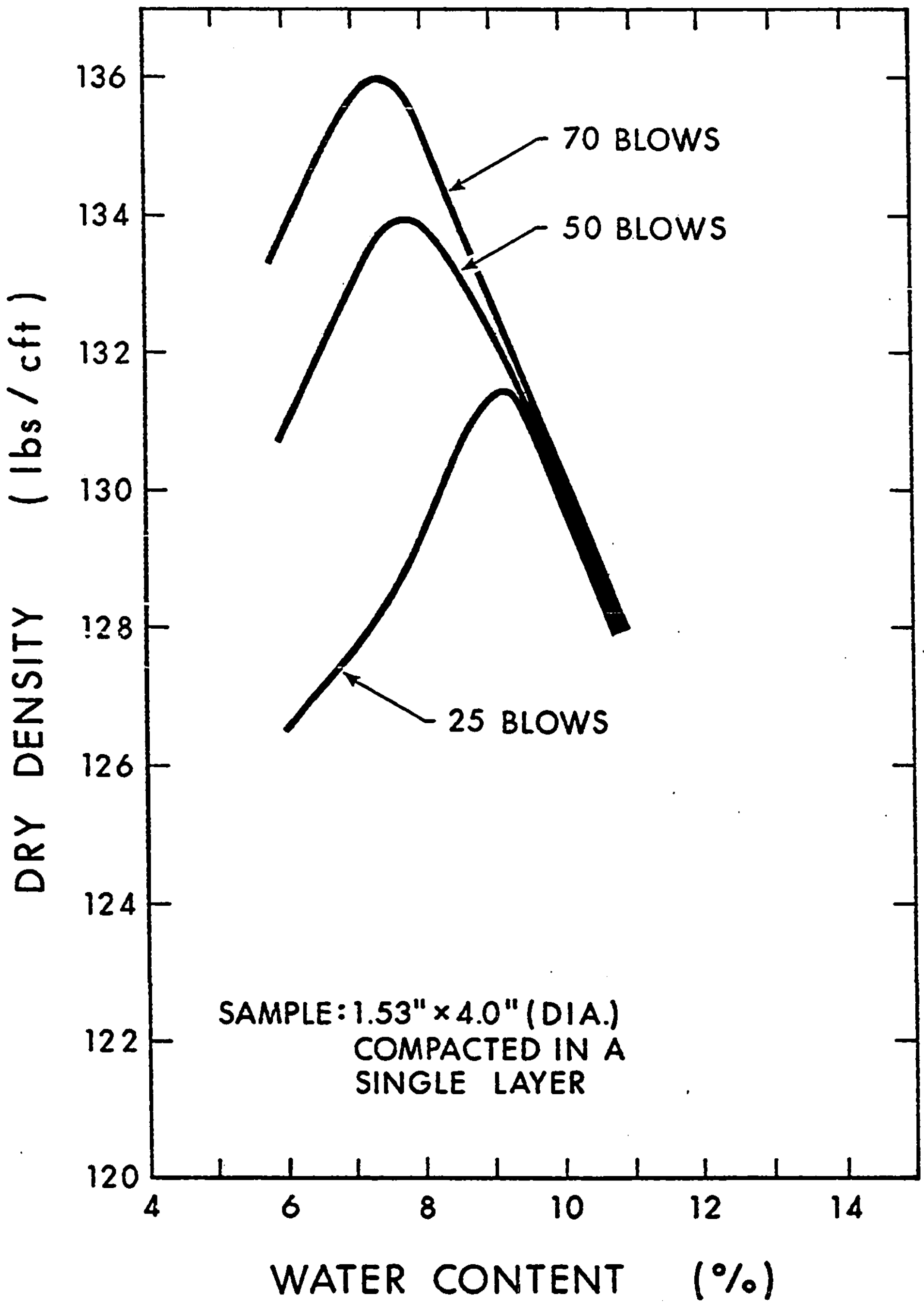

FIG. 2.25 WATER CONTENT-DENSITY RELATIONSHIPS FOR MICA TILL AT DIFFERENT COMPACTIVE EFFORTS

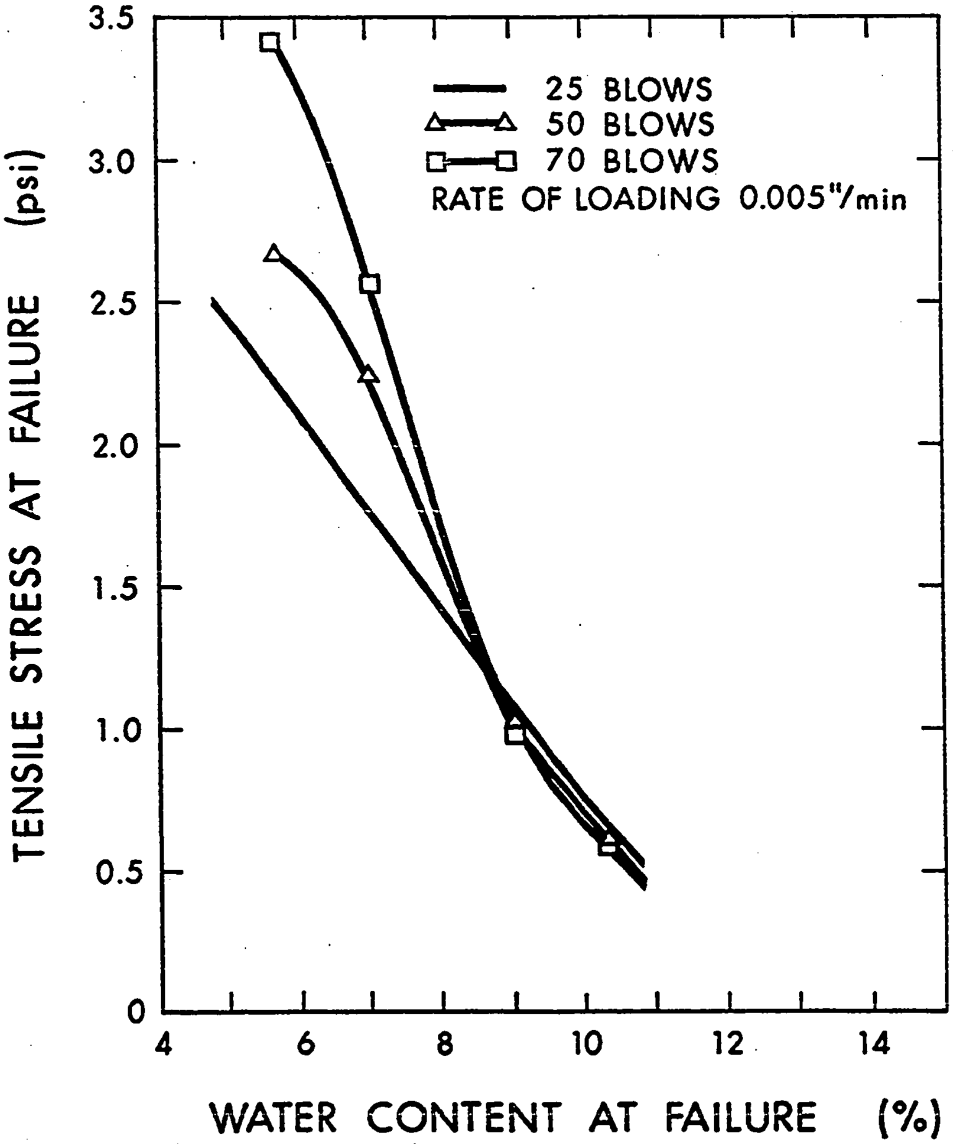

FIG. 2.26 VARIATION OF TENSILE STRENGTH WITH WATER CONTENT FOR MICA TILL AT DIFFERENT COMPACTIVE EFFORTS

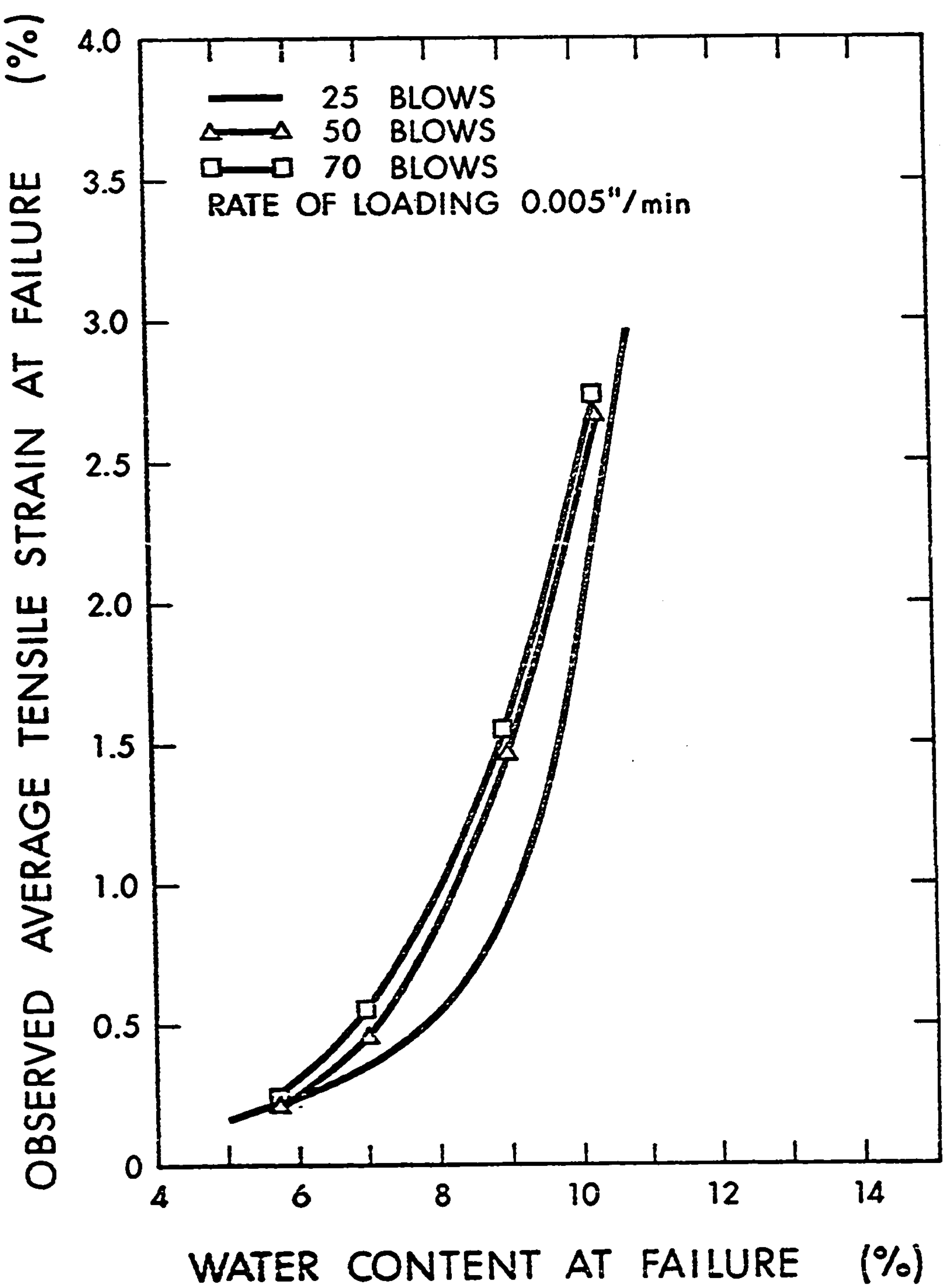

FIG. 2.27 VARIATION OF TENSILE STRAIN AT FAILURE WITH WATER CONTENT FOR MICA TILL AT DIFFERENT COMPACTIVE EFFORTS

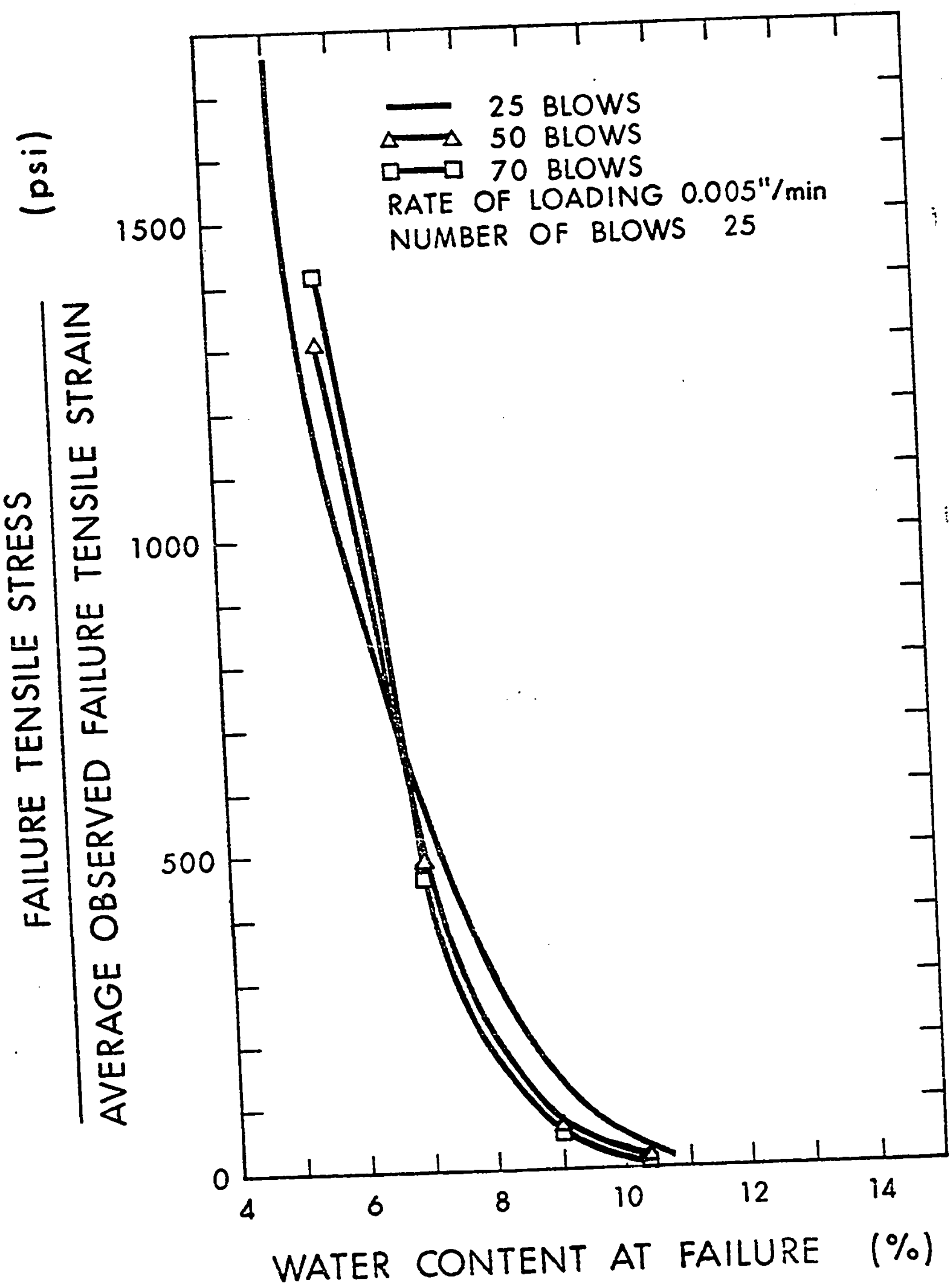

FIG. 2.28 VARIATION OF STIFFNESS IN TENSION WITH WATER CONTENT FOR MICA TILL AT DIFFERENT COMPACTIVE EFFORTS

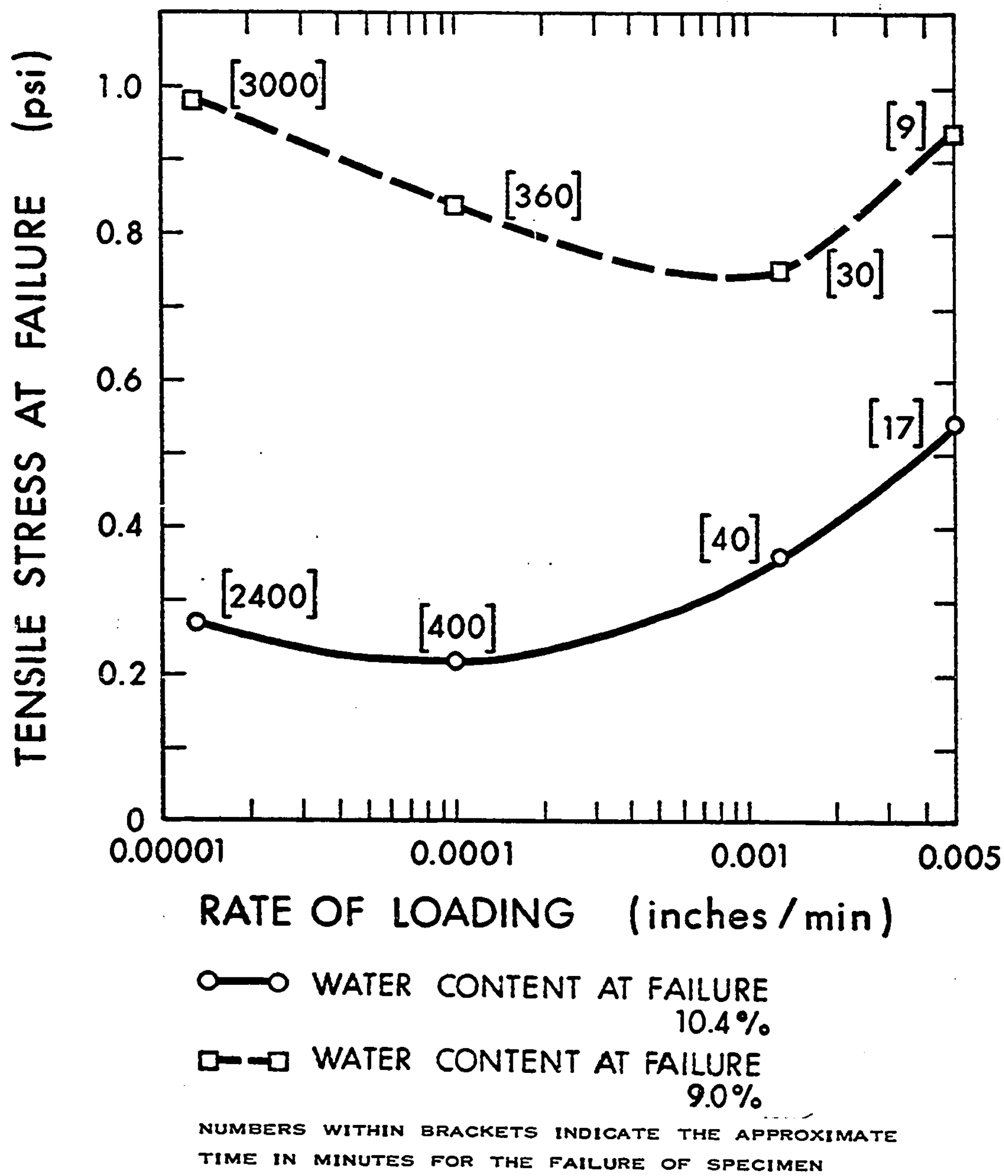

FIG. 2.29 EFFECT OF RATE OF LOADING ON THE TENSILE STRENGTH OF MICA TILL

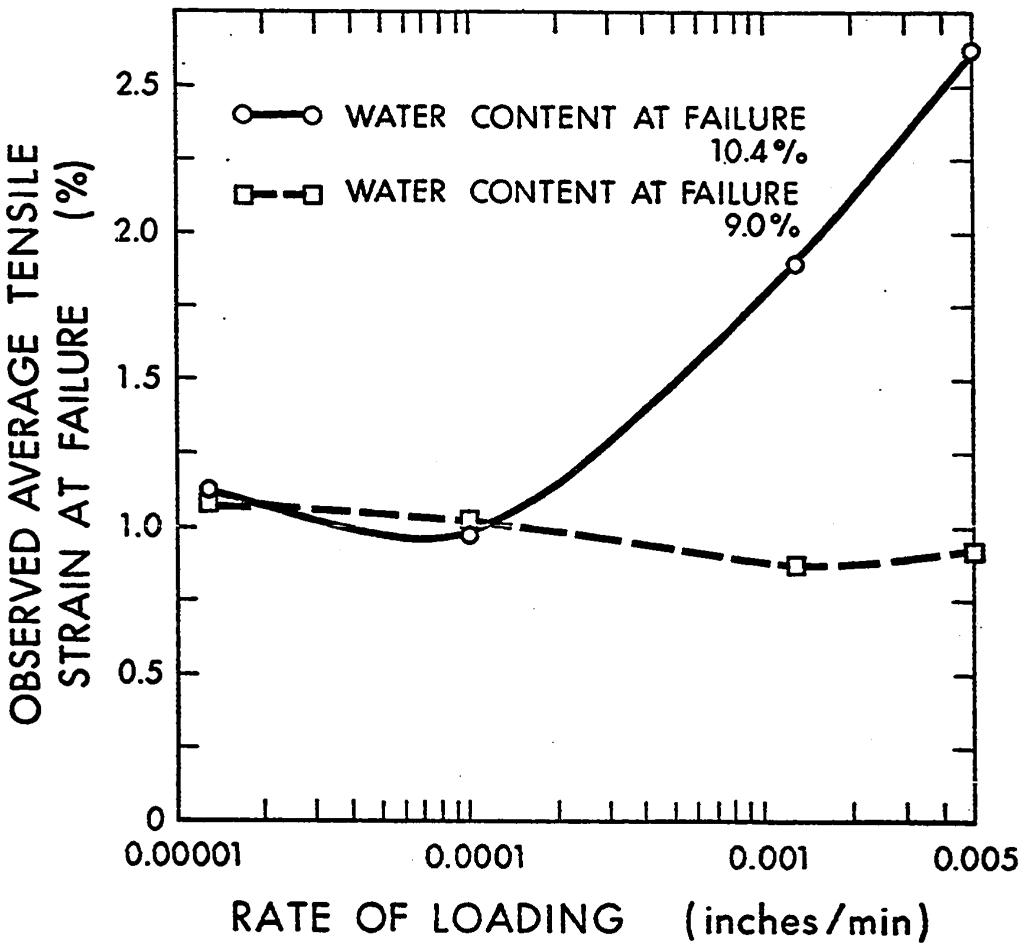

FIG. 2.30 EFFECT OF RATE OF LOADING ON THE TENSILE STRAIN AT FAILURE FOR MICA TILL

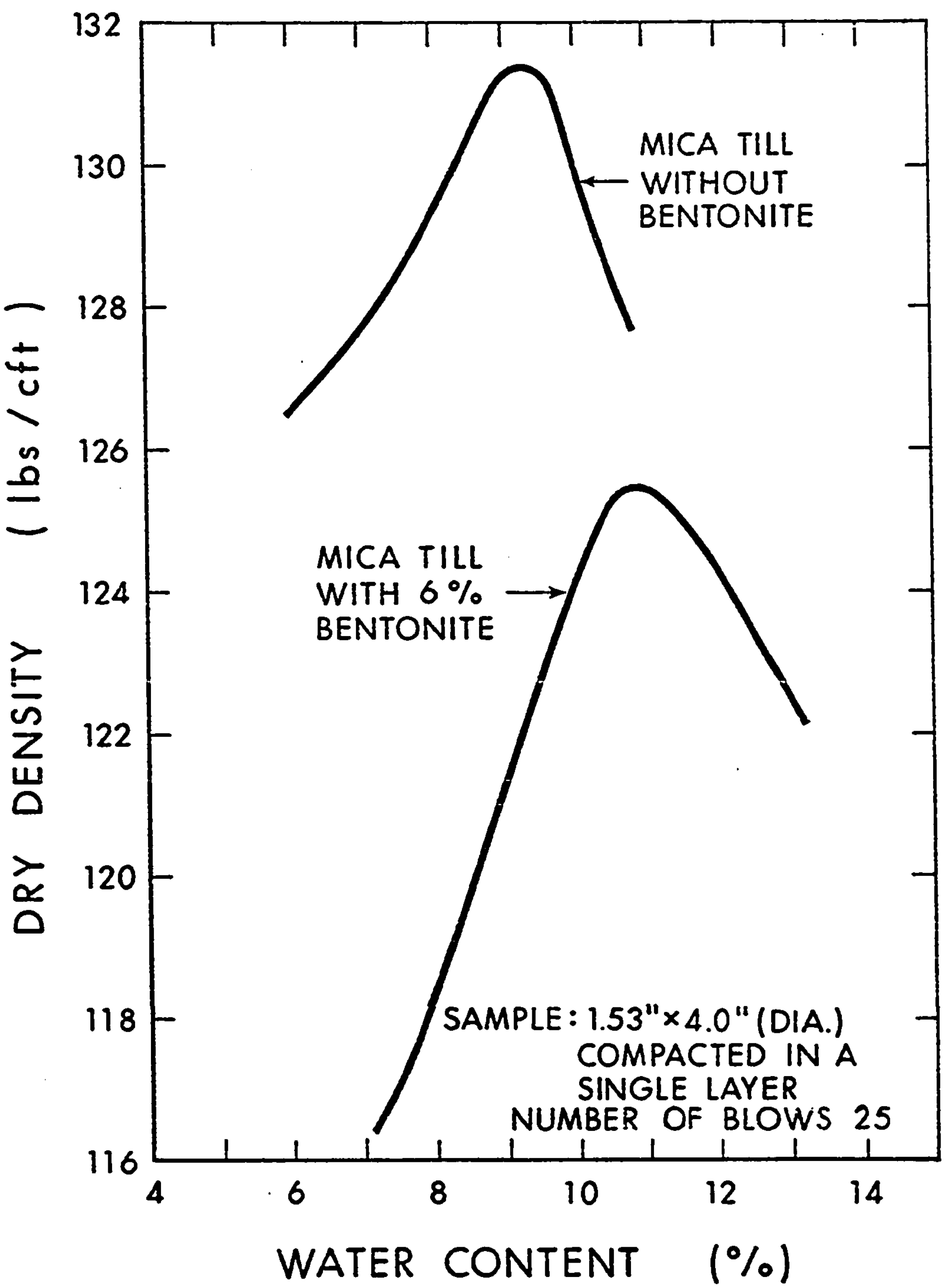

FIG. 2.31 WATER CONTENT-DENSITY RELATIONSHIPS OF MICA TILL WITH AND WITHOUT THE ADDITION OF BENTONITE

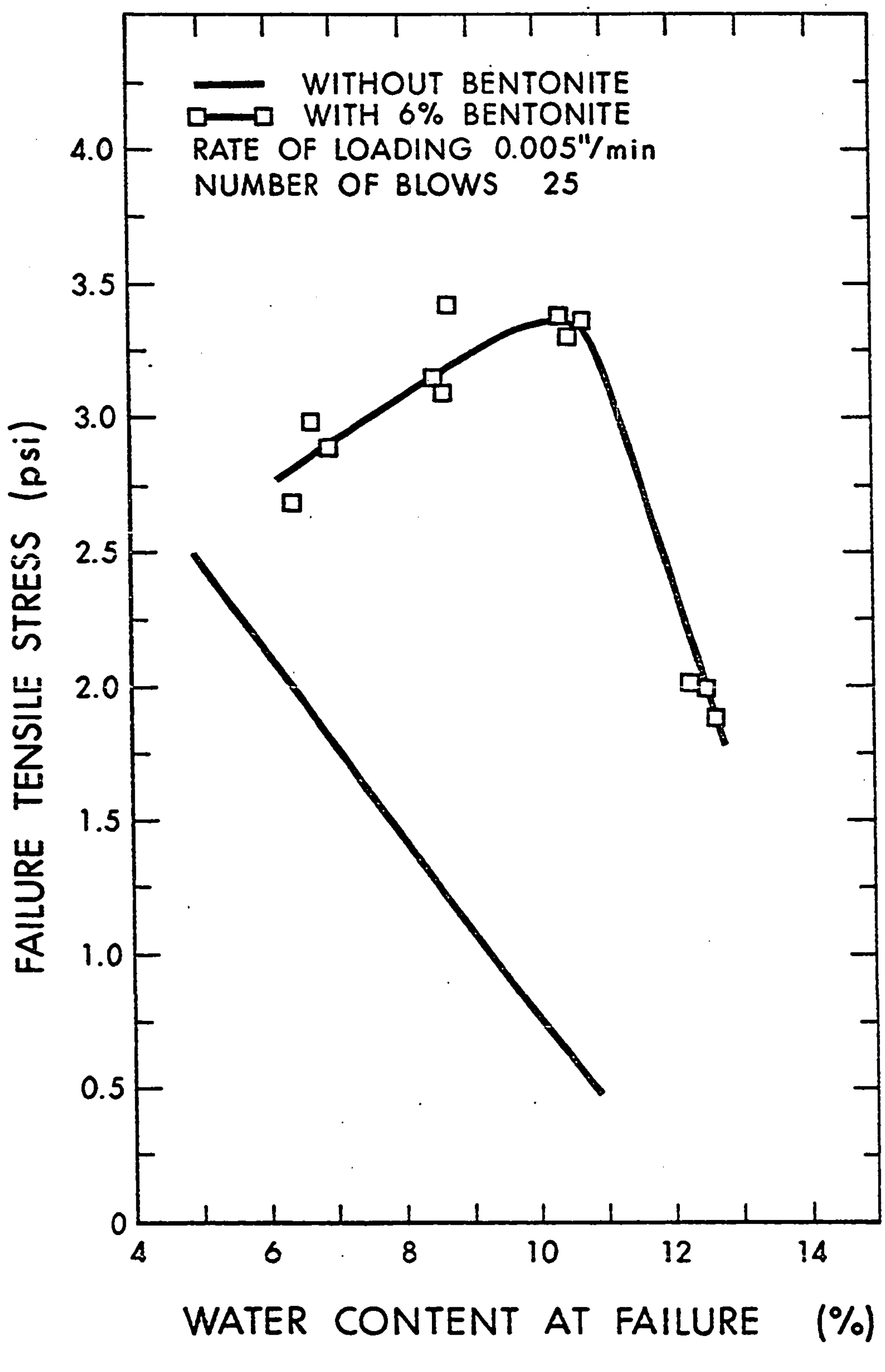

FIG. 2.32 COMPARISON OF TENSILE STRENGTH OF MICA TILL WITH AND WITHOUT THE ADDITION OF BENTONITE

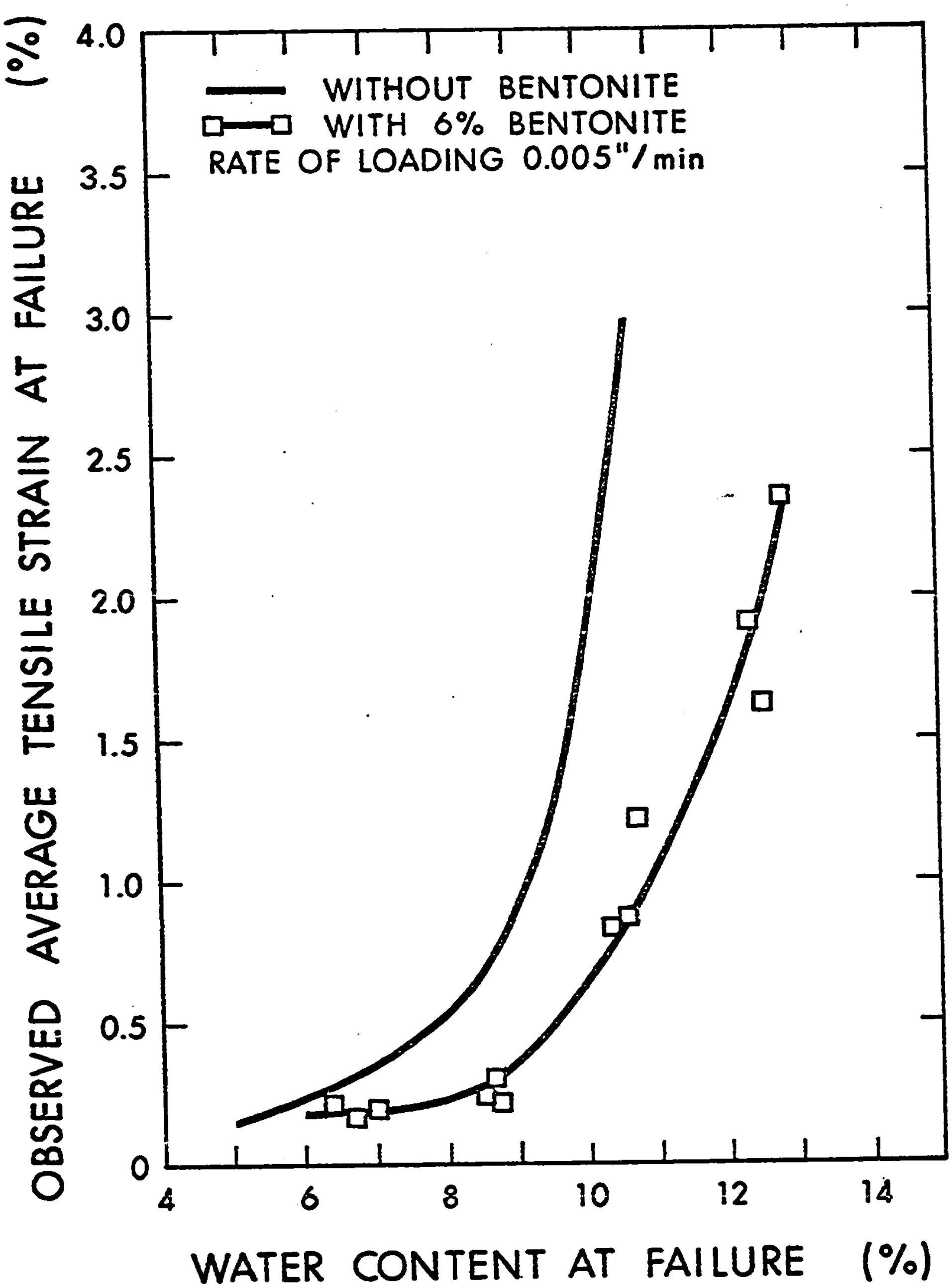

FIG. 2.33 COMPARISON OF TENSILE STRAIN AT FAILURE FOR MICA TILL WITH AND WITHOUT THE ADDITION OF BENTONITE

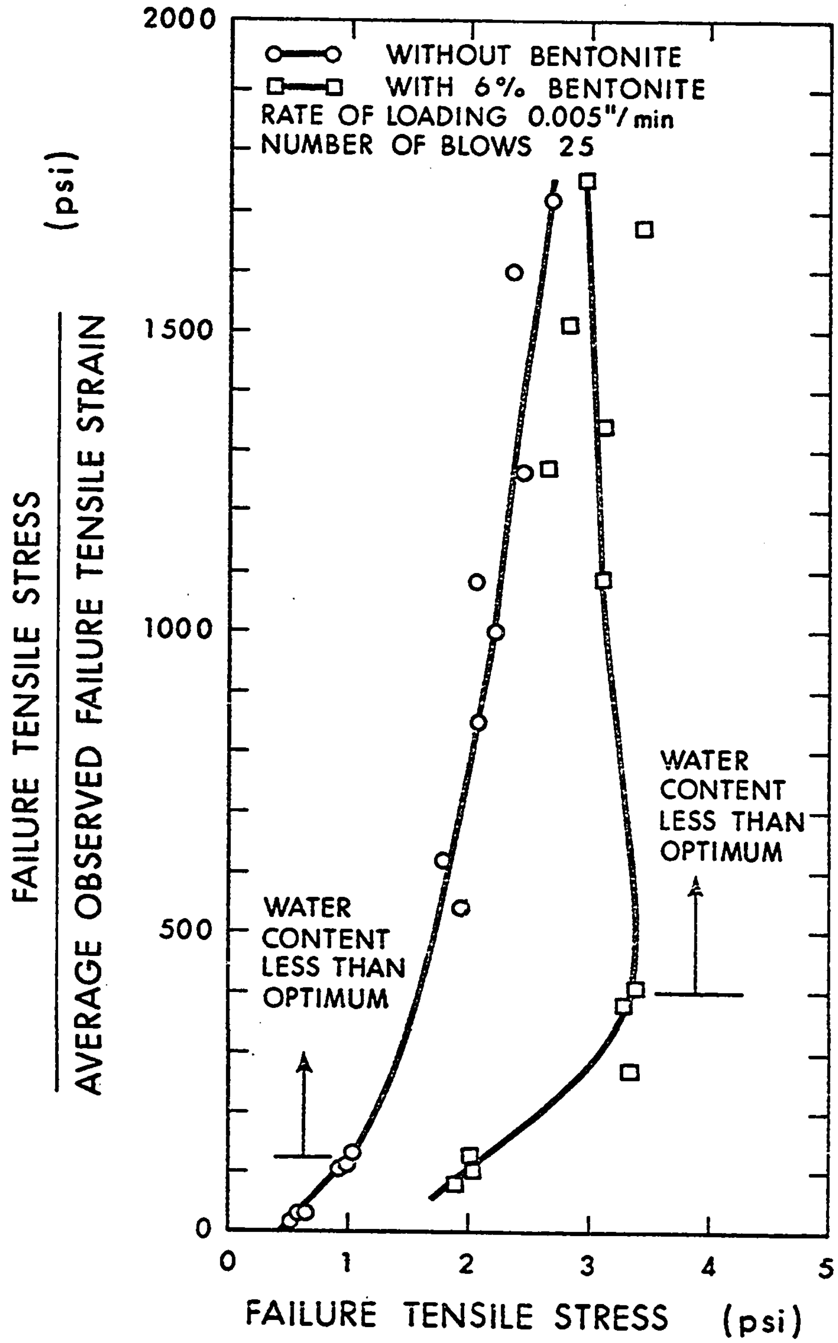

FIG. 2.34 COMPARISON OF STIFFNESS IN TENSION FOR MICA TILL WITH AND WITHOUT THE ADDITION OF BENTONITE

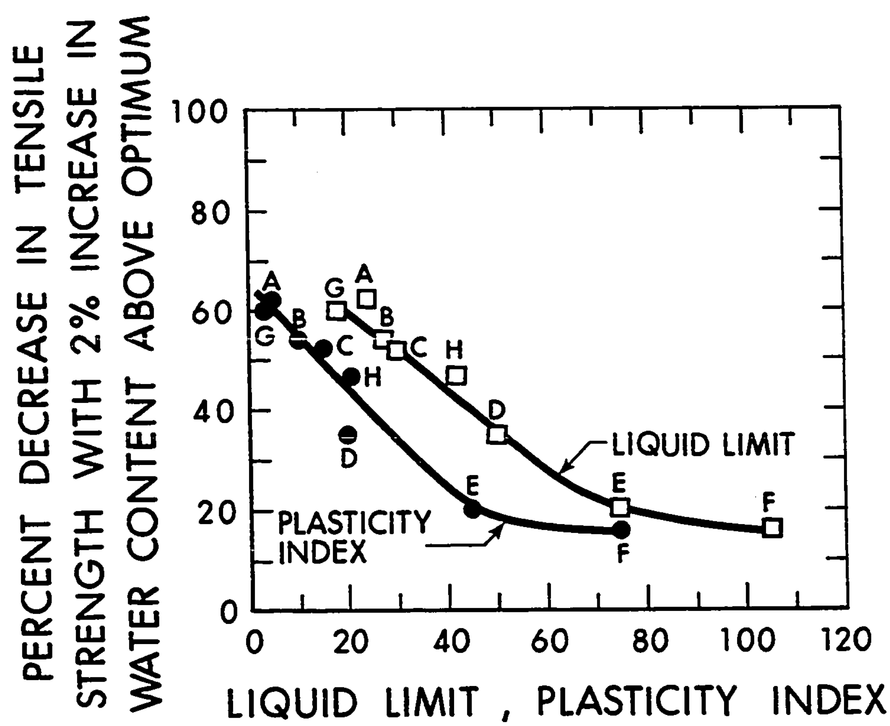

A TO F SOILS FOR WHICH THE DATA IS AFTER NARAIN AND RAWAT [1970]

G MICA TILL

H MICA TILL WITH 6% BENTONITE

FIG. 2.35 PERCENT DECREASE IN TENSILE STRENGTH CAUSED BY A 2% INCREASE IN WATER CONTENT ABOVE OPTIMUM FOR SOILS WITH DIFFERENT CONSISTENCY LIMITS

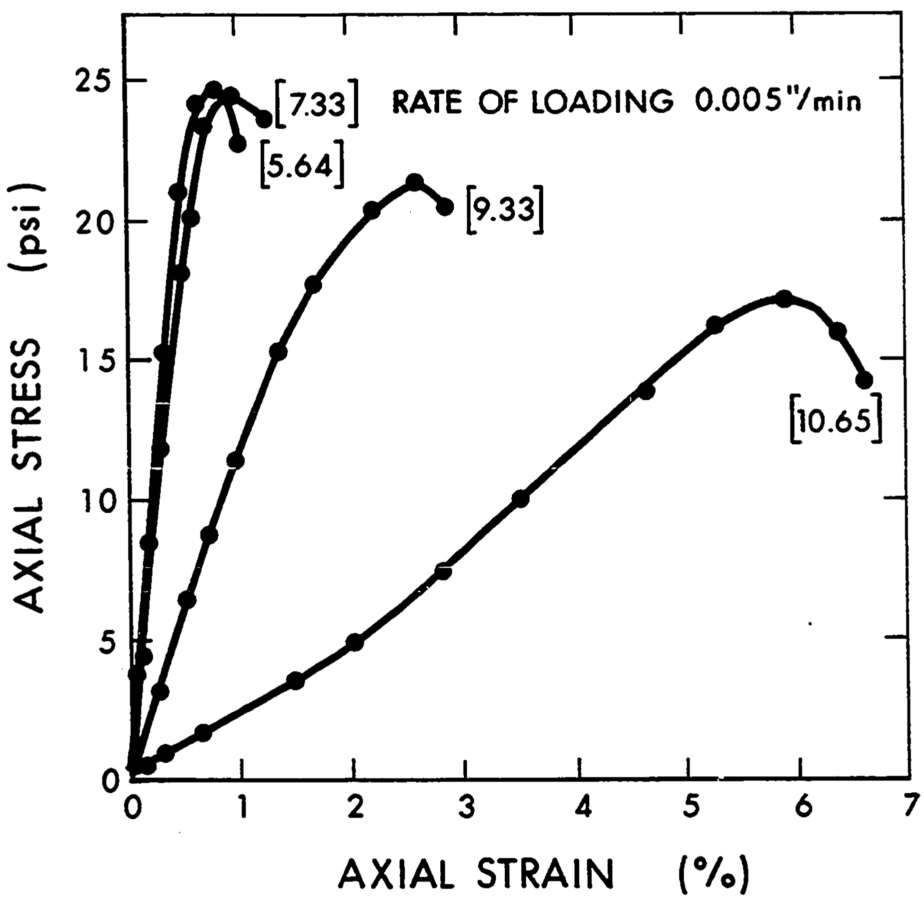

[ ] INDICATES THE WATER CONTENT AT FAILURE

FIG. 2.36 STRESS-STRAIN RELATIONSHIPS OF MICA TILL TESTED UNDER UNCONFINED COMPRESSION

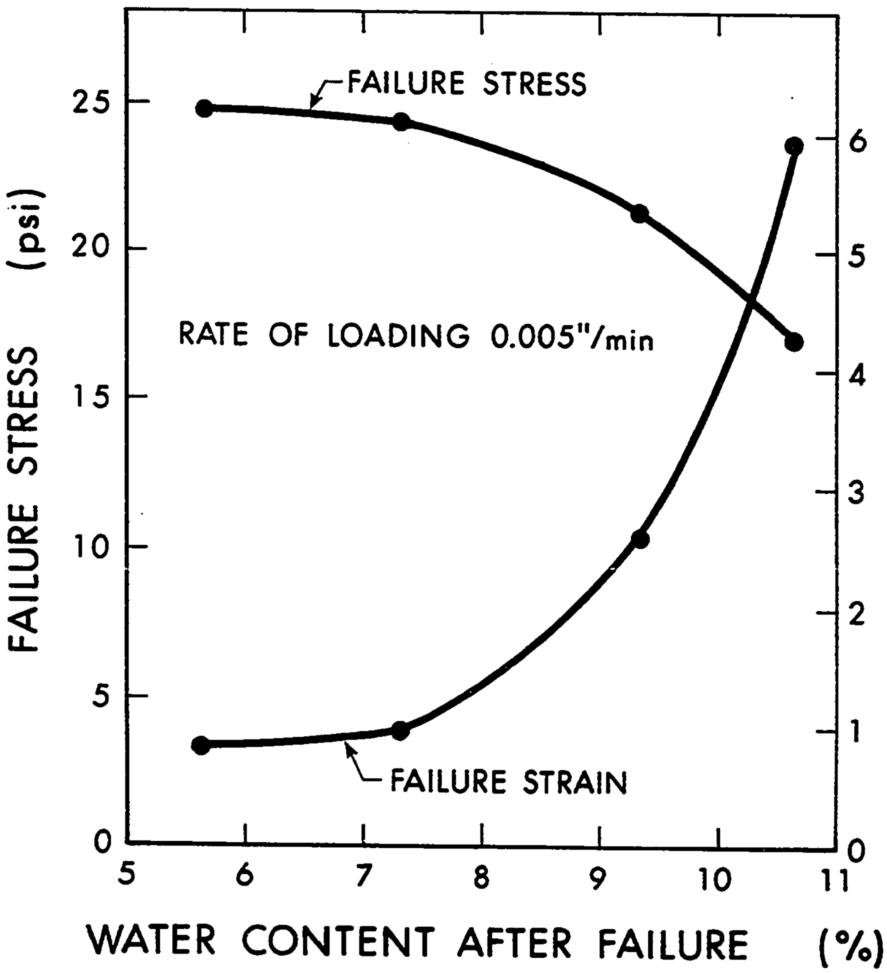

FIG. 2.37 VARIATION OF THE FAILURE STRESS AND STRAIN WITH WATER CONTENT FOR MICA TILL TESTED UNDER UNCONFINED COMPRESSION

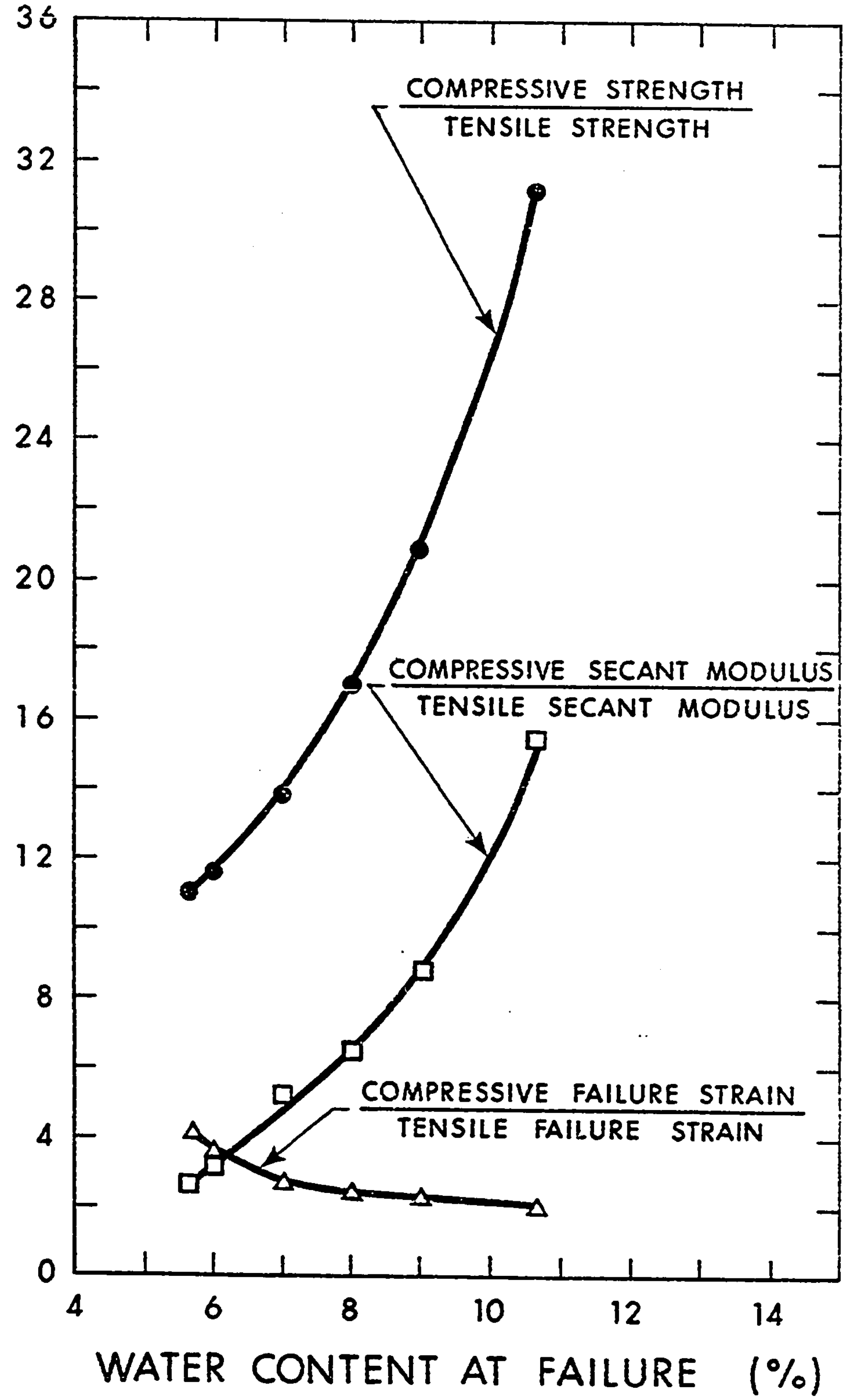

FIG. 2.38 COMPARISON OF COMPRESSIVE AND TENSILE CHARECTERISTICS OF MICA TILL AT DIFFER--ENT WATER CONTENTS

CHAPTER III

SIMULATION PROCEDURES FOR LINEAR AND NON-LINEAR FINITE ELEMENT ANALYSES

3.1 Scope

This chapter discusses the simulation procedures developed for the finite element analyses and the validity of their application to the problem of cracking of earth dams.

3.2 Introduction

Classical theory of elasticity, with the assumptions of isotropy, homogeneity, linear elastic stress-strain relationships, and simplified boundary conditions has been used in the past (e.g., Jurgensen, 1934; Terzaghi, 1943; Scott, 1963; Harr, 1966) to obtain closed form solutions for a certain limited number of boundary value problems, concerned with the determination of stress and strain fields in soil masses. Since the ideal conditions assumed in obtaining such solutions are rarely satisfied in practical problems, these analytical procedures can be used only to a very limited extent in the field of soil mechanics.

Finite difference numerical analyses (e.g., Bishop, 1952; Dolezalova, 1970) that assume linear elastic stress-strain relationships, were used for solving some boundary value problems concerned with earth dams.

The finite element method, which has more flexibility than other methods for dealing with complex boundary conditions, non-homogeneous materials, and non-linear stress-strain relationships, has been in active use for some ten years. It has been shown by a number of workers (e.g., Clough and Woodward, 1967; Girijavallabhan and Reese, 1968; Kulhawy et al., 1969; Chang and Duncan, 1970; Desai and Reese, 1970; Kulhawy and Duncan, 1970) that with a proper application of the finite element method one can obtain reasonably good solutions for problems concerned with the stresses and strains in soil masses. It is evident that success in obtaining a good solution depends to a considerable extent on close simulation of field behaviour of the structure. At present, research on the application of finite element method to soil problems is largely directed towards developing suitable simulation procedures to obtain close agreement between the results of analysis and field or experimental observations. In the present investigation, the finite element method has been used because of its capabilities.

3.3 Use of Isotropic Elastic Theory and Its Limitations

The stress-strain relationships for soils are non-linear, partially inelastic, and depend on stress path and stress level. Geometric anisotropy and stress-induced anisotropy are quite common in soils. Volume changes take place not only due to changes in all around pressure but also due to factors such as pure shear and rotation of principal stress axes.

A theory that completely describes the deformation properties of soils is not available yet, although the application of such a theory in the analysis is highly desirable (Scott and Ko, 1969). Some attempts have been made to introduce volume changes due to shear into the analysis (e.g., Chang et al., 1967; Smith and Kay, 1971). The limitations that exist in the experimental determination of soil parameters needed for the application of more complex non-linear theories, seriously limit, at present, the finite element analysis. Until sufficient progress in the development of suitable laboratory procedures for obtaining stress-strain relationships under conditions that simulate field behaviour of soil is achieved, the use of simple isotropic elastic theory appears to be reasonable. The parameters needed for such a theory are easily obtained from conventional laboratory tests. Perhaps the most significant disadvantage, from a practical engineering point of view, in using the small-strain isotropic elastic theory to represent soil behaviour is that it cannot account for the dilatancy effect of soils (Scott and Ko, 1969).

Despite these limitations successful solutions using isotropic elastic theory have been reported in literature (e.g., Clough and Woodward, 1967; Girijavallabhan and Reese, 1968; Kulhawy et al., 1969; Chang and Duncan, 1970; Desai and Reese, 1970; Kulhawy and Duncan, 1970). These solutions are based on the assumption of a piecewise linearity between the stress and strain. The appropriate stress-strain relationships used in the analyses were derived from conventional triaxial tests. A conventional triaxial test refers here to a test in which the deviatoric stress is increased under a constant cell pressure.

Based on the comments of the previous paragraphs, isotropic elastic theory for small strains has been applied to the finite element analyses performed in this work. Piecewise linearity between stress and strain has been assumed during each increment of the load. The appropriate stress-strain relationships, dependent on stress level, have been derived from the conventional triaxial tests. The volume change data of the triaxial tests has been used to derive the second parameter needed.

3.4 Types of Analyses Performed

Different types of finite element analyses, pertaining to the studies on cracking of earth dams, were performed in this work. Explanatory definitions of the analyses are given with each type:

(1) Linear analysis is an analysis in which the two elastic parameters defined either by K and G or by E and ν are maintained constant in the analysis.

(2) Non-linear analysis is an analysis in which the loads are applied in a number of small increments. A piecewise linear relationship between stress and strain has been assumed during each increment of the load. The

elastic parameters during a certain increment of load are defined either by K and G or by E and ν. The displacements, stresses and strains determined in each increment of loads are accumulated to obtain the total values corresponding to all increments of loads.

(3) Single step linear analysis is an analysis in which the loads are applied instantaneously and the analysis is performed with constant values of elastic parameters defined either by K and G or by E and ν.

(4) Incremental linear analysis is an analysis in which loads are applied in a number of small increments with the elastic parameters used in all the increments remaining constant.

(5) "No tension" analysis is an analysis in which soil is considered incapable of sustaining tension and the tensile principal stresses are removed by replacing them by equivalent nodal forces. The "no tension" analysis procedure has been elaborated in detail by Zienkiewiecz et al. (1968).

In all types of analyses listed above Poisson's ratio is not allowed to exceed 0.49. Generally the results of an analysis obtained for Poisson's ratio exceeding 0.49 and very close to 0.5 are not accurate (Herrmann, 1964). For Poisson's ratio equal to 0.5 the analysis cannot be performed as some elements of the constitutive matrix become infinite. These limitations are inherent in the formulation based on the minimum potential energy principle. Using a variational principle which is equivalent to the elastic field equations expressed in terms of the displacements and a function of mean pressure, Herrmann (1964) showed that sufficiently accurate results can be obtained for all values of Poisson's ratio ranging from 0 to 0.5. The formulation proposed by Herrmann (1964) is particularly suited to incompressible materials such as rubber. Such a formulation is not used in this work for two reasons:

(1) For soils which dilate during shear, Poisson's ratio exceeds the permissible value of 0.5 hence volume change behaviour of such a soil cannot be represented by a value of Poisson's ratio equal to 0.5.

(2) By limiting Poisson's ratio to 0.49, reasonably good correlations between the results of analysis and field or experimental observations have been achieved in a number of cases (e.g., Girijavallabhan and Reese, 1968; Kulhawy et al., 1969; Chang and Duncan, 1970; Kulhawy and Duncan, 1970) involving nearly incompressible soils ($\nu \approx 0.5$).

3.5 Two Dimensional Finite Element Analyses

The two dimensional finite element analyses in this work were performed by using the computer program given in Appendix A. In this program constant strain triangular elements each having six degrees of freedom are used. More refined elements such as quadrilateral elements, each having four constant strain triangular elements (Covarrubias, 1969) or two linear strain triangular elements are possible (Felippa, 1966). However the results obtained using constant strain triangular elements for the cases considered in this work are in good agreement with those of Covarrubias (1969) who used more refined quadrilateral elements along with constant strain triangular elements. The comparison of results appears in Section 4.4 of Chapter IV. The equations are solved by Gauss-Seidel iterative procedure. The original computer program which could perform a linear single step analysis was developed by Wilson (1963). The program was modified to incorporate the following additional facilities:

(1) the automatic generation of element and nodal data,

(2) the performance of an incremental analysis with an option to analyze each step once or twice,

(3) the calculation of elastic parameters from the laboratory test data needed for each increment of loads,

(4) the performance of a "no tension" analysis.

The iterative method of solution of equations, used in the program is particularly suitable for the "no tension" analysis, because it involves an iterative procedure. Since the element stiffness formulation for a constant strain triangle is well known it will not be discussed here. Details regarding the computer program for two dimensional finite element analysis are in Appendix A.

3.6 Three Dimensional Finite Element Analyses

The three dimensional analyses were performed using a computer program (Appendix B) developed by the author. In this program, isoparametric hexahedral elements, each having twenty-four degrees of freedom, are used. Each element is specialized to represent triangular prisms and tetrahedra (Appendix B). The equations are solved in blocks using the direct Gaussian elimination method and the necessary integrations for the evaluation of element stiffness and stresses are performed numerically by using Gaussian quadrature formulae. The program includes facilities that:

(1) automatically generate nodal and element data,

(2) perform a single step linear analysis,

(3) perform an incremental analysis with an option to analyze each step once or twice,

(4) calculate elastic parameters for each increment of loads from the laboratory test data.

Provision for "no tension" analyses has not been made due to the excessive amount of computation effort needed for the iterative procedure in a three dimensional analysis.

The selection of isoparametric hexahedral elements for the three dimensional analysis is based on the comparative studies on three dimensional finite elements conducted by Clough (1969). His conclusions regarding the performance of the various types of three dimensional elements are as follows:

(1) the isoparametric hexahedral elements are distinctly

superior to any tetrahedron assemblages, both with respect to the individual element properties and in application to idealized structural systems. Also the isoparametric elements have the advantage of isotropy whereas the stiffness of the tetrahedron assemblages are slightly different along their three axes.

(2) based on the comparative efficiency studies of 8 node and 20 node isoparametric hexahedral elements, it is recommended that an 8 node element be used in standard three dimensional programs for analysis of general elastic solids and the 20 node element be applied primarily in systems or local regions when the plate bending mechanism is likely to dominate the behaviour.

From the preceding conclusions it can be seen that an 8 node isoparametric hexahedral element would be well suited for the analysis of earth dams in which shear effects dominate the behaviour of the structure.

The details regarding the main features of the program, its limitations and the computation time needed are discussed in Appendix B. The element stiffness formulation for the isoparametric hexahedral element used in this work is discussed in Appendix C.

3.7 Determination of the Elastic Parameters for Non-Linear Analysis

Since an incremental loading procedure is used to simulate the construction sequence of an earth dam, the elastic parameters to be used during each increment of the load are to be calculated from laboratory or field test data. The elastic parameters are either K and G or E and ν. Generally two approaches are possible to feed the test data into the computer for the evaluation of the parameters. In one approach the test data is supplied in digital form and in the other it is supplied in functional form.

In the digital form, a number of closely spaced points on a stress-strain curve are given as input. Hence the modulus calculated by considering two adjacent points (by chord slope) approximates the tangent modulus. Because of their dependency on the stress level, the relationships between stress and strain must be supplied at a number of closely spaced values of stress levels. From the set of data supplied in digital form the moduli are calculated at the required stress level.

In the second approach, the stress-strain relationships are supplied in functional form assuming either hyperbolic stress-strain relationships (Kulhawy et al., 1969; Duncan and Chang, 1970) or using mathematical spline functions (Desai, 1971). The hyperbolic representation involving the use of a small number of parameters with identifiable physical significance has the advantage that it is easier to compare the properties of different soils, and to develop experience and judgment in terms of the parameters (Duncan and Chang, 1972). However, in general, it involves greater approximations to the measured stress-strain behaviour than those obtained by the spline function representation (Desai, 1971; Duncan and Chang, 1972). In the present work the digital form was used because, although it may involve more computation time for interpolation than other methods, no approximation of the stress-strain relationships is necessary.

3.8 Validity of Triaxial Test Data for Interpolating the Elastic Parameters

The conventional triaxial tests are performed by increasing the deviatoric stress with constant cell pressure. Several other stress paths consistent with the type of problem considered can be simulated in the triaxial tests. However, because of the axisymmetric conditions maintained in triaxial tests the behaviour of the soil under plane strain or general three dimensional conditions cannot be simulated. To simulate such conditions a plane strain test apparatus or a "true" triaxial test apparatus in which stresses and strains can be controlled in all three directions is needed. Since the data from such tests are not readily available, the conventional triaxial tests may continue to find their application in the analyses, at least for some years to come. Triaxial data obtained from tests performed on representative soil samples with the proper simulation of stress paths and drainage conditions could be of a considerable value in reasonably predicting the deformations and stresses. However research is needed to develop suitable laboratory tests, the data from which can be used in the analyses for reasonably accurate predictions. On the other hand if the conventional triaxial test data obtained under a particular stress path are used for problems involving different types of stress paths, the results predicted by the analysis are bound to be inaccurate for some cases. Duncan and Chang (1972), based on the investigations conducted under different stress paths, indicated that the simple incremental procedures using the conventional triaxial test data result in a reasonably good prediction of strains for unloading-reloading stress-paths and for a range of stress-paths in the primary loading range. However the predictions are poor for primary loading under constant or nearly constant stress-ratios (σ_3/σ_1) and for certain other types of stress paths.

In the present work only the conventional triaxial test data have been used for the following reasons:

(1) Data from either plane strain tests or "true" triaxial tests are not available.

(2) As the present work is primarily concerned with the evaluation of tension zones caused by tensile stresses, it is to be expected that the stresses computed would be less sensitive to the changes in the derived elastic parameters than the computed displacements or strains.

3.8.1 Simulation of the Drainage Conditions

Duncan (1972) and Lowe (1972) discussed the importance of a proper simulation of the drainage conditions in the finite element analysis. The data from the unconsolidated undrained tests are used to simulate the undrained conditions while the consolidated drained test data are used for the fully drained conditions. However, the simulation of partial drainage conditions in the analysis is rather difficult. Because of the uncertainty involved in the evaluation of the amount of drainage that occurs in the field, the laboratory test results simulating a partial drainage condition will be of limited value. Chang and Duncan (1970) performed two types of analyses for an excavation problem involving a partial drainage in the clayey soil. In one of the analyses no drainage was assumed to occur within the clayey soils while in the other full drainage was assumed to occur in all types of soils. The extreme drainage conditions assumed in the two analyses resulted in two sets of displacements that bounded the observed displacements.

In earth dams with relatively thin cores of low plastic till a certain amount of drainage is normally expected to occur within the impervious and semi-pervious zones during the period of construction. The stress-strain relationships used in the analysis are to be derived from the laboratory tests that simulate the proper stress paths and the partial drainage, consistent with the field conditions. For the purpose of the present investigation such tests were not performed. Instead the results from the consolidated undrained tests were used to simulate the behaviour of the impervious and the semi-pervious materials (Chapter V). It was believed that such an approach would simulate a condition that lies between the two extreme possibilities of the fully drained and the undrained conditions.

3.9 Method of Deriving the Moduli of Elasticity

The derivation of the moduli proposed in this work consists of converting the conventional triaxial test data to a form involving the three stress invariants, the axial strain, and the octahedral shear strain. The elastic parameters based on the three stress invariants are computed in the finite element analysis for each element. The proposed method has the following advantages:

(1) Approximations involved in representing the test data are eliminated by using a digital form for the actual stress-strain relationships.

(2) The method proposed to derive the moduli in terms of stress invariants, removes the necessity of making an assumption regarding the intermediate principal stress.

(3) Even though the derivation procedure given here was developed for the conventional triaxial tests, the generality of the use of stress invariants can easily be applied with suitable modifications to other types of tests (e.g., triaxial tests with different stress paths, plane strain tests, etc.).

One obvious disadvantage of the method is that it involves greater computational effort than other methods that consider functional form of representing the test data. However, the time involved in the calculations is a minor part of that needed for the solution of equations in the finite element analysis. In the subsequent sections the procedure of derivation of moduli and its accuracy are discussed.

3.9.1 Derivation Procedure

From the deviatoric stress versus axial strain (ε_1) and volumetric strain (ε_v) versus axial strain relationships of the triaxial test results, two plots can be generated. The first plot is the octahedral shear stress (τ_{oct}) versus axial strain for a set of chosen values of $J_3/(\sigma_{oct})^2$ where J_3 is the third stress invariant and σ_{oct} is the octahedral normal stress. The dimensions of $J_3/(\sigma_{oct})^2$ is that of stress. To determine the octahedral shear (τ_{oct}) and $J_3/(\sigma_{oct})^2$ one has to consider the three stress invariants in order that the three principal stresses are uniquely represented. The second plot is the octahedral shear strain (γ_{oct}) plotted against the axial strain. Fig. 3.1 shows a typical conventional plot of the triaxial test data obtained by performing consolidated undrained triaxial tests on a silty sand representing the semi-pervious material of Duncan Dam (Chapter V). The net volumetric expansion is neglected as shown by the dotted lines. Fig. 3.2 shows the relationships between τ_{oct} and ε_1 and γ_{oct} and ε_1 for a set of chosen values of $J_3/(\sigma_{oct})^2$. For clarity the relation between γ_{oct} and ε_1 is shown only for two values of $J_3/(\sigma_{oct})^2$ (0 psi and 80 psi). The triaxial data are given as data input to the computer program and the conversion to the stress invariant form is a part of the program.

The following expressions were used to calculate the stress invariants and γ_{oct} from the conventional triaxial test data:

$$\sigma_{oct} = (\sigma_1 + 2\sigma_3)/3 \qquad (3.1)$$

$$\tau_{oct} = (\sqrt{2}/3)(\sigma_1 - \sigma_3) \qquad (3.2)$$

$$J_3 = \sigma_1(\sigma_3)^2 \qquad (3.3)$$

$$\gamma_{oct} = (\sqrt{2}/3)(3\varepsilon_1 - \varepsilon_v) \qquad (3.4)$$

The following procedure was used for the determination of the elastic parameters:

(1) The three stress invariants were computed from the three known principal stresses in an element. For a two dimensional plane strain analysis, the intermediate principal stress was computed from

$$\sigma_2 = \nu(\sigma_1 + \sigma_3)$$

where ν was a trial value of Poisson's ratio (say 0.35). Since ν in turn depends on the stress condition, an iterative method was used.

(2) For the values of τ_{oct} and $J_3/(\sigma_{oct})^2$ computed, the incremental ratio, $(\Delta\tau_{oct}/\Delta\varepsilon_1)$ was interpolated from the τ_{oct} versus ε_1 plot. Similarly from the γ_{oct} versus ε_1 plot,

the incremental ratio, $(\Delta\gamma_{oct}/\Delta\varepsilon_1)$ is interpolated for the same value of $J_3/(\sigma_{oct})^2$ and the corresponding axial strains used for interpolating $(\Delta\tau_{oct}/\Delta\varepsilon_1)$. The shear modulus was obtained from:

$$G = (\Delta\tau_{oct}/\Delta\varepsilon_1)/(\Delta\gamma_{oct}/\Delta\varepsilon_1) \qquad (3.5)$$

Since the value $(\Delta\gamma_{oct}/\Delta\varepsilon_1)$ obtained above corresponds to a particular constant value of σ_3 in the triaxial test, Poisson's ratio was computed from:

$$\nu = (3/2\sqrt{2})(\Delta\gamma_{oct}/\Delta\varepsilon_1) - 1 \qquad (3.6)$$

and was limited to a maximum of 0.49. The bulk modulus was computed from:

$$K = G(2/3)(1 + \nu)/(1 - 2\nu) \qquad (3.7)$$

When one of the principal stresses becomes negative (tensile) it was artificially set to zero hence $J_3/(\sigma_{oct})^2$ should be zero. Under isotropic compression $J_3/(\sigma_{oct})^2$ would be equal to σ_3.

In case of a two dimensional analysis steps 1 and 2 were repeated until the intermediate principal stress values computed in two consecutive trials agree closely with each other.

The elastic parameters used in a particular increment of load can be derived from the stress state corresponding to the conditions that existed before the increment of load. The solution obtained by such a procedure was called a "past stress" solution by Kulhawy et al. (1969). Since this procedure usually gives a poor result, it was recommended that the use of the "average stress" be made for the derivation of moduli. The "average stress" was defined as the average of stresses that exist immediately before and after the load increment. A similar procedure has been used in this work to improve the solutions of the non-linear analysis. The incremental load was added to the existing load and the stresses were computed using the elastic parameters calculated on the basis of "past stresses" and these stresses are termed the "present stresses" (Kulhawy et al., 1969). The elastic parameters based on the "present stresses" were calculated. The average elastic parameters were computed from those calculated on the basis of "past stresses" and "present stresses" and were used in the reanalysis of the same increment. This procedure termed the "average moduli" procedure here, has been used in this work because of computational advantages in terms of storage. It is obvious that the "average moduli" or "average stress" procedure takes twice as much time as the "past stress" solution.

3.9.2 Studies to Check the Accuracy of the Procedure of Derivation of Elastic Parameters

To check the accuracy of the present method of derivation of elastic parameters, a weightless soil block 4" x 4" x 1" was considered to be loaded vertically, in five increments, of 20 lbs. each which cause a vertical incremental stress of 5 psi. The problem was analyzed both in two and three dimensions. The finite element idealizations for two and three dimensional analyses for a half of the soil block (because of symmetry) are shown in Fig. 3.3. The nodal loads imposed in each increment are also shown. The initial moduli for the first increment of load for all these studies were derived from the experimental data (Fig. 3.2) for the condition: $\tau_{oct} = 0$ and $J_3(\sigma_{oct})^2 = 0$. The following cases were studied:

(1) Plane stress analysis using the elastic parameters derived from "past stresses".

(2) Plane stress analysis using "average moduli".

(3) Three dimensional analysis using "average moduli" for the unconfined compression of the soil block.

Fig. 3.4 shows the comparison between the "past stress" solution and "average moduli" solution, the latter agreeing very well with the experimental curve obtained under unconfined compression (Fig. 3.1). The three dimensional analysis gives the same result as the two dimensional one for the particular case. The better accuracy of the "average moduli" approach led to its adoption in all the subsequent studies in this work unless otherwise stated.

3.9.3 Effect of Intermediate Principal Stress on Stress-Strain Results

The effects of the assumption regarding the intermediate principal stress on the stress-strain results are of interest. The following studies have been conducted for this purpose:

(1) Two dimensional plane strain analysis assuming that $\sigma_2 = \sigma_3$.

(2) Two dimensional plane strain analysis assuming that $\sigma_2 = \nu(\sigma_1 + \sigma_3)$.

(3) Two dimensional plane strain analysis with lateral restraint in the x-direction (Fig. 3.3). This has been done merely to compare the solution with plane stress and plane strain solutions.

Fig. 3.5 indicates that the assumption $\sigma_2 = \sigma_3$ gives greater strains compared to the correct strains obtained from $\sigma_2 = \nu(\sigma_1 + \sigma_3)$. This is due to the lower moduli calculated for the former assumption. However the difference between the results is not significant for the lower range of axial strains (up to 2% for present case). Fig. 3.6 compares the results for conditions of plane stress, plane strain and plane strain with lateral restraint. The progressively increasing slope of the stress-strain curve or the "locking" effect can be seen in the case of the plane strain analysis with lateral restraint.

3.10 Isotropic Compression

Compression under an all around stress is dealt with by considering the initial-tangent Young's moduli and Poisson's ratios at the appropriate confining stresses. In terms of stress invariants they correspond to the initial-tangent shear and bulk moduli at the appropriate confining stresses. An example of isotropic compression is shown in Fig. 3.7. The axial stress (σ_1) is plotted against axial strain (ε_1) both for isotropic and deviatoric compression for a silty sand tested at a water content 3% greater than the optimum in a triaxial apparatus for consolidated undrained conditions. The deviatoric compression results are shown only for σ_3 equal to 15 psi and 40 psi for clarity. The predicted isotropic compression curve obtained by using the incremental procedure described previously agrees reasonably well with the experimental curve even though the drainage condition is not the same for the isotropic and deviatoric compressions.

3.11 Summary

Satisfactory simulation procedures for two and three dimensional finite element analyses with a method of deriving moduli based on stress invariants and "average moduli" have been developed. The main limitation of the procedure is the restriction of Poisson's ratio to a maximum value of 0.49. However this is not serious because the dilatancy effects of soil become more important at comparatively large strains such as those caused due to shear failures. Since the present studies are concerned essentially with the tensile cracking of earth dams, and not with the shear failure of earth dam, it is believed that the above limitation has no significant effect on the prediction of tensile zones in earth dams.

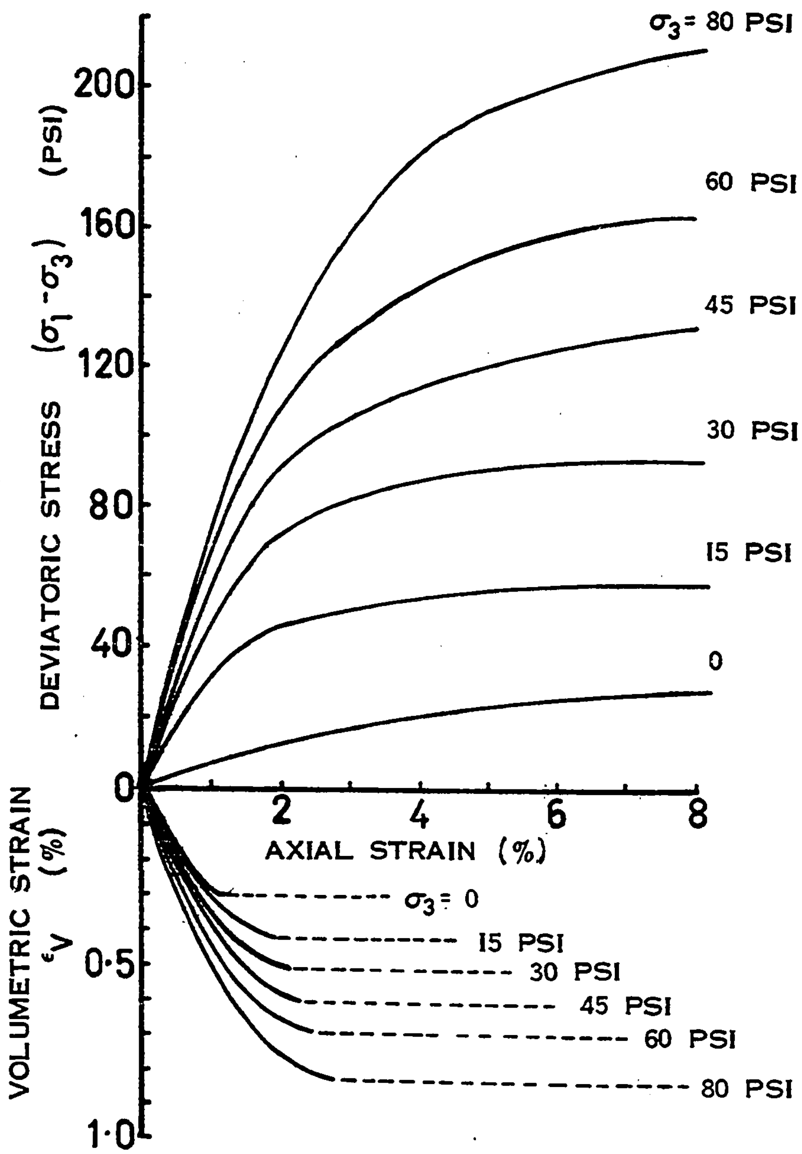

FIG. 3.1 TRIAXIAL TEST DATA FOR A SILTY SAND PLOTTED IN THE CONVENTIONAL MANNER

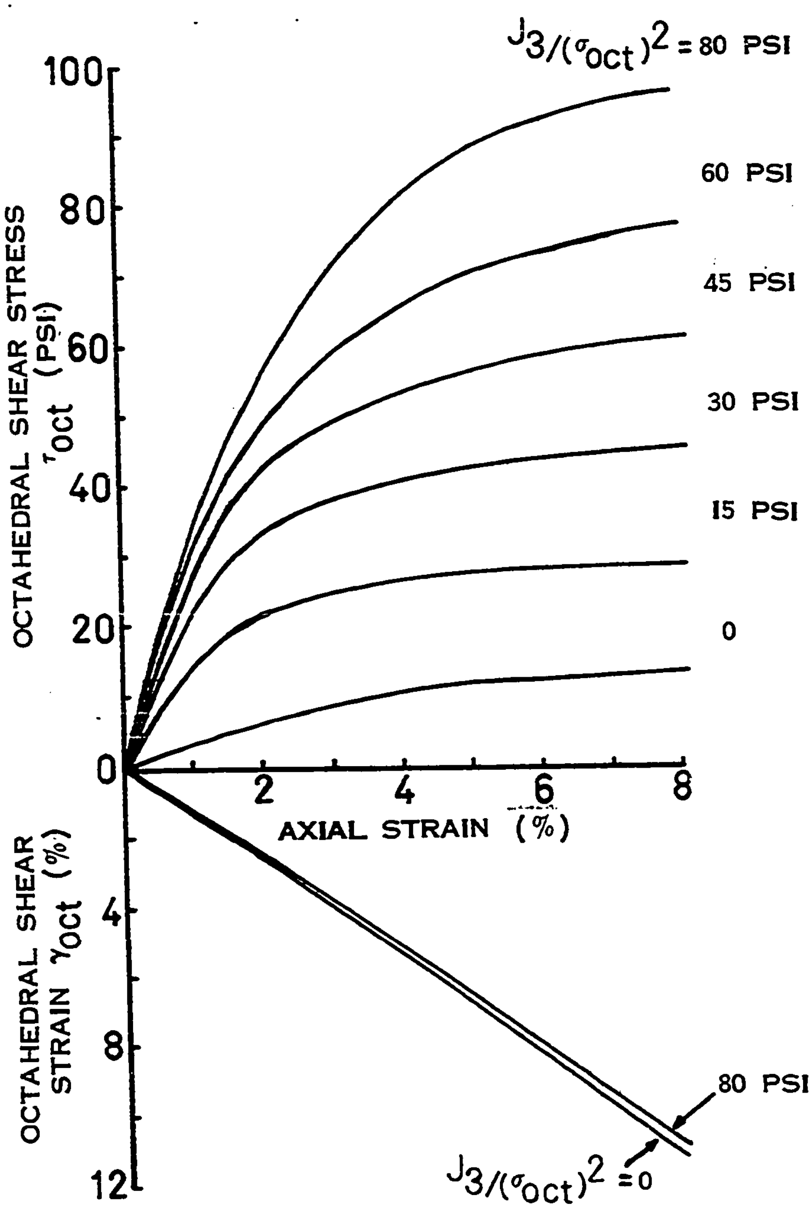

FIG. 3.2 TRIAXIAL TEST DATA FOR A SILTY SAND PLOTTED IN TERMS OF STRESS AND STRAIN INVARIANTS AND AXIAL STRAIN

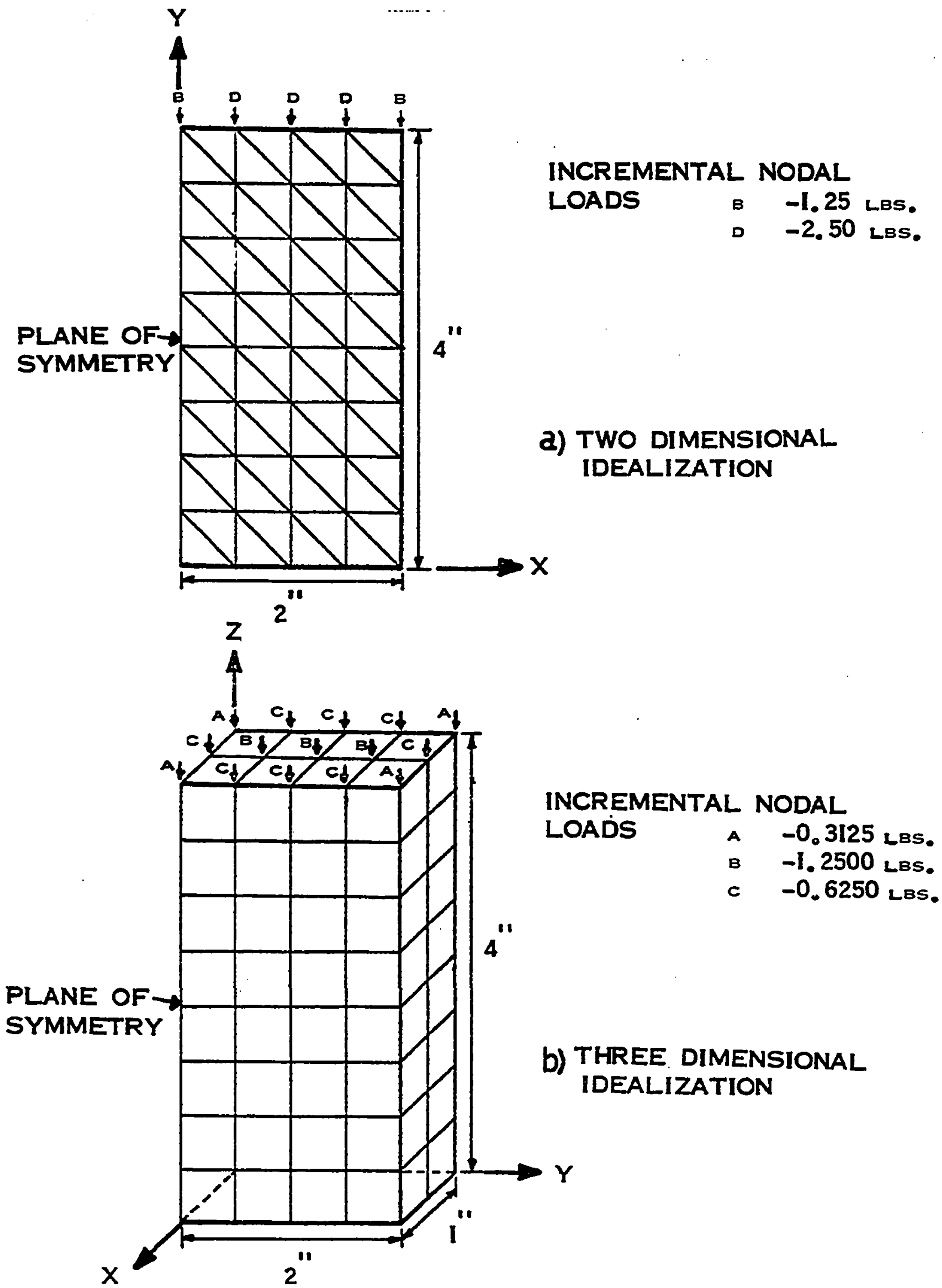

FIG. 3.3 FINITE ELEMENT IDEALIZATION OF A SOIL BLOCK

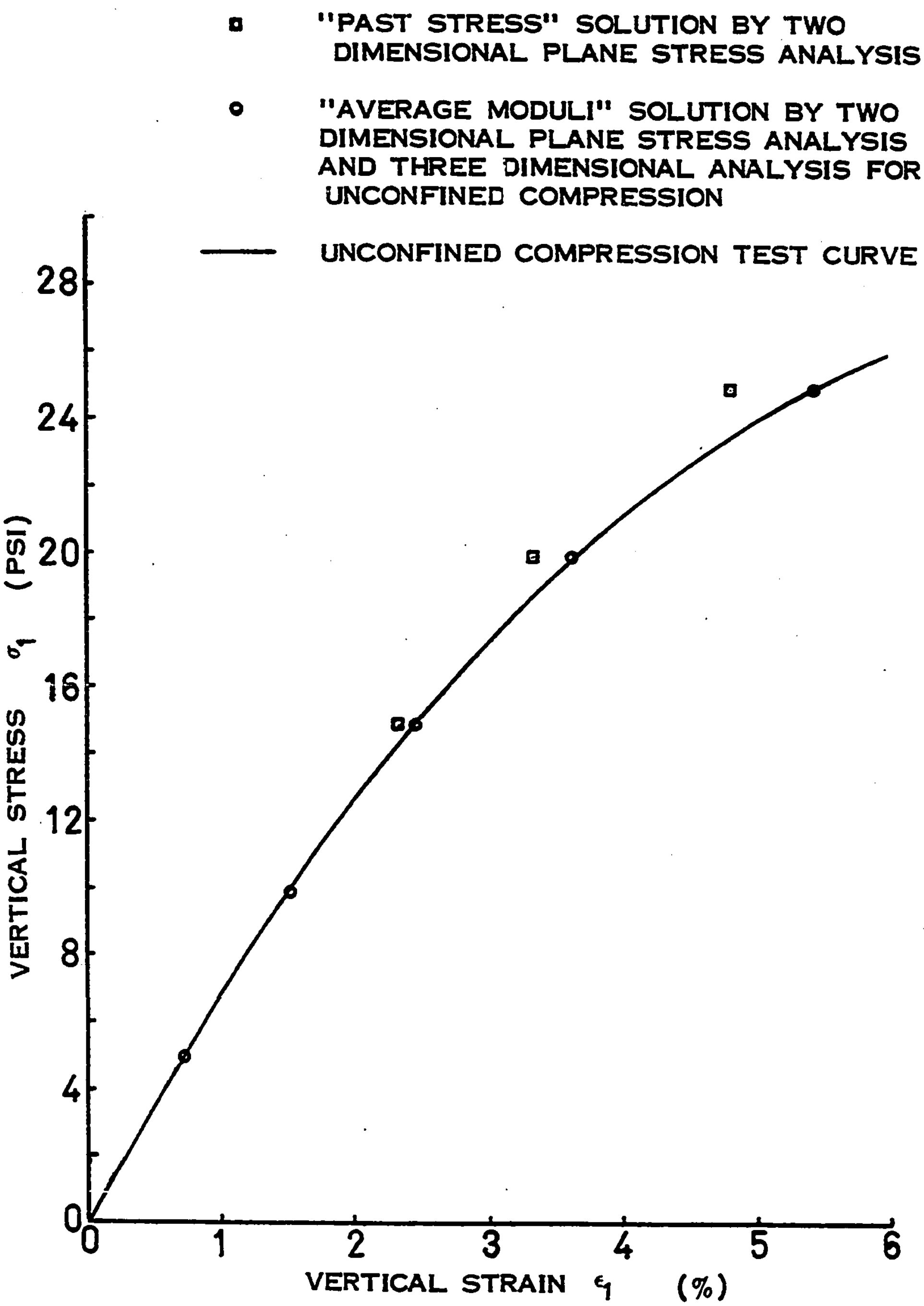

FIG. 3.4 COMPARISON OF "PAST STRESS" AND "AVERAGE MODULI" SOLUTIONS IN AN INCREMENTAL ANALYSIS PERFORMED IN FIVE INCREMENTS

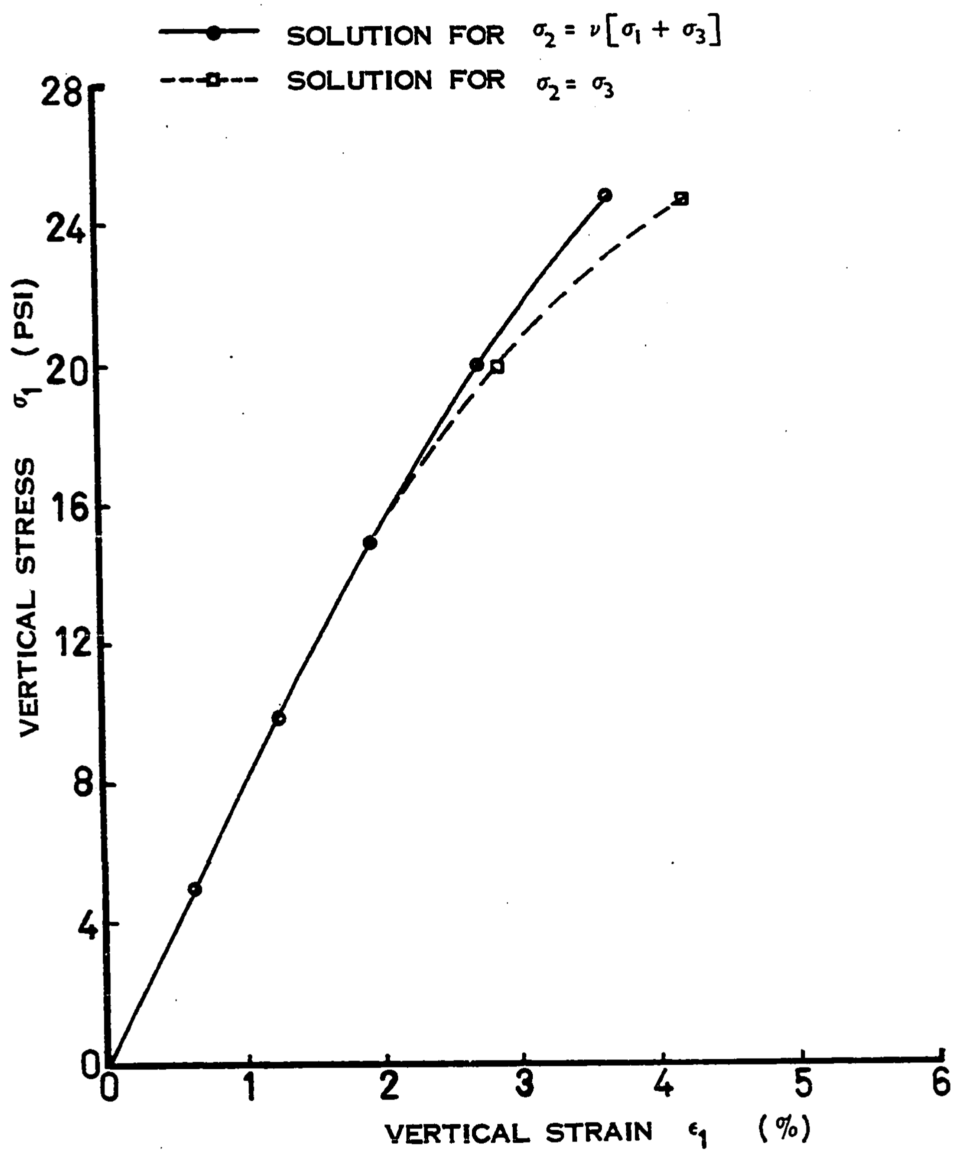

FIG. 3.5 COMPARISON OF INCREMENTAL NONLINEAR PLANE STRAIN SOLUTIONS WITH DIFFERENT ASSUMPTIONS REGARDING THE INTERMEDIATE PRINCIPAL STRESS [ANALYSES IN FIVE INCREMENTS]

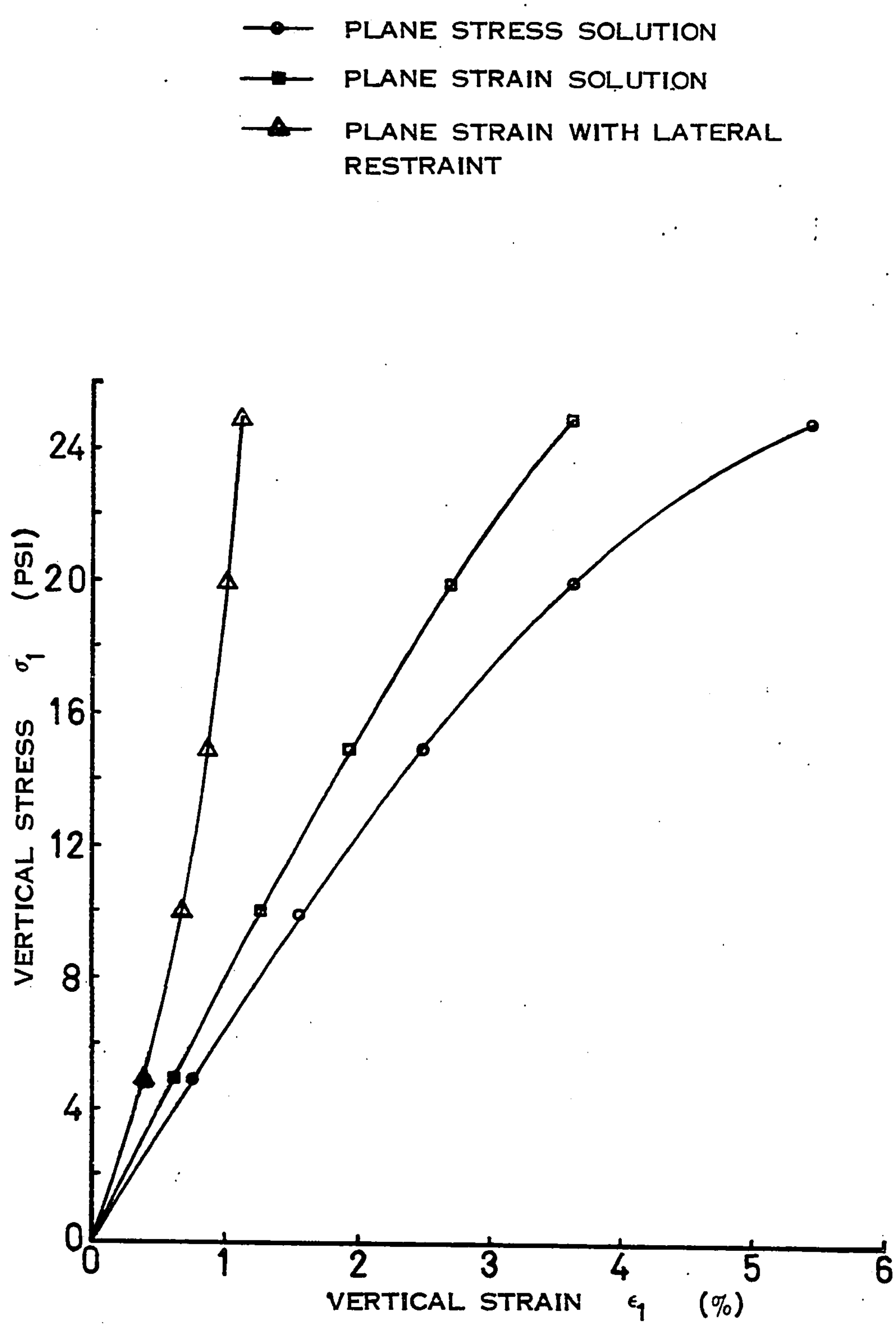

FIG. 3.6 COMPARISON OF INCREMENTAL NONLINEAR SOLUTIONS OBTAINED FOR DIFFERENT BOUNDARY CONDITIONS [ANALYSES IN FIVE INCREMENTS]

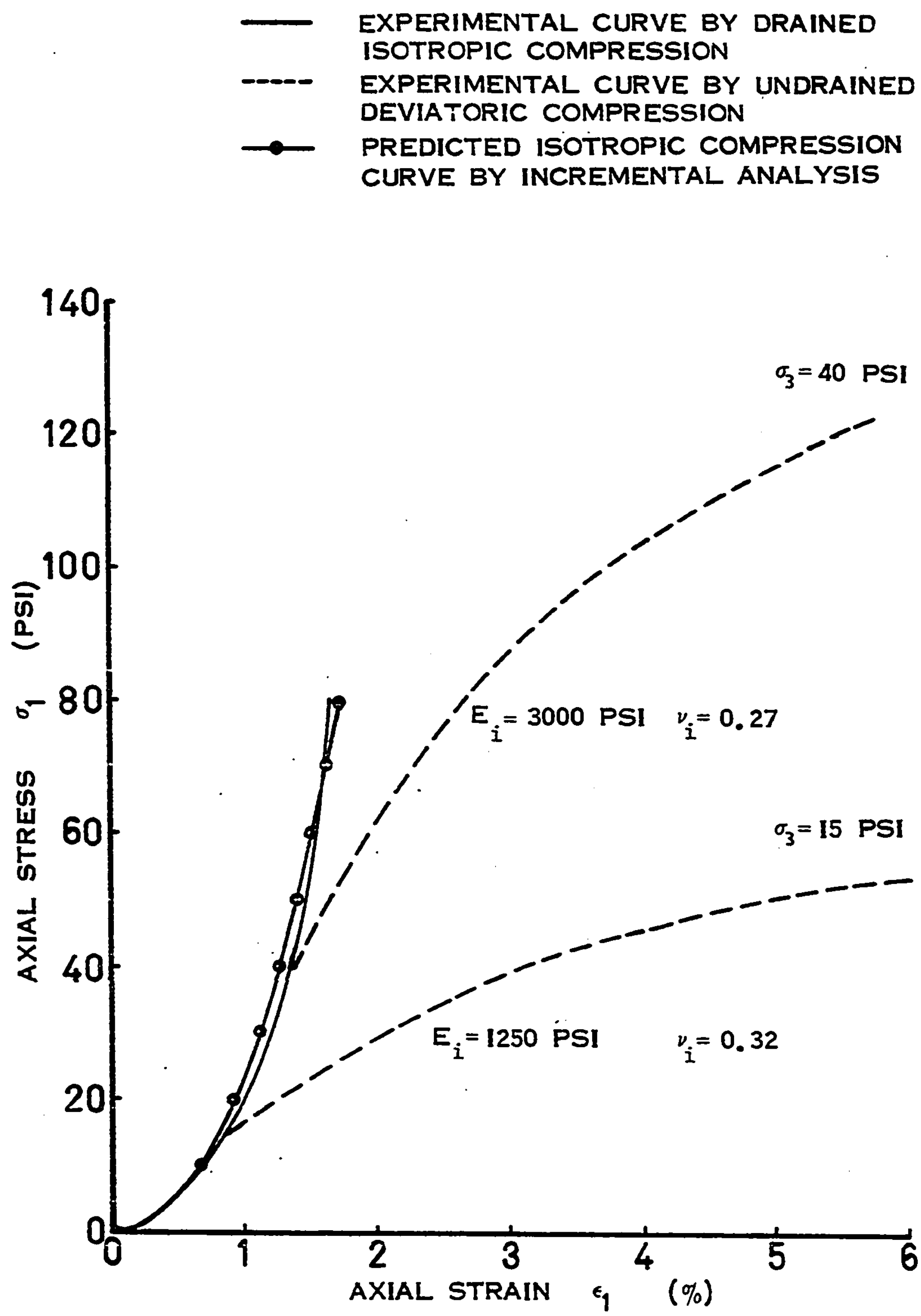

FIG. 3.7 COMPARISON OF PREDICTED AND EXPERIMENTAL STRESS-STRAIN RELATIONSHIP FOR ISOTROPIC COMPRESSION

CHAPTER IV

IMPORTANCE OF CERTAIN FACTORS IN THE ANALYSIS OF CRACKING OF DAMS

4.1 Scope

In this chapter the importance of considering the construction step sequence, non-linear stress-strain relationships, no tensile strength for soils, and three dimensional effects in the analysis of cracking of dams are discussed.

4.2 Introduction

Several factors contributing to the development of tensile cracks in earth dams were outlined in Section 1.3.1 of Chapter I. The influence of the shape (Covarrubias, 1969) and the steepness (Dolezalova, 1970) of the valley walls on the development of tension zones during the construction of a dam has been studied elsewhere. The effects of considering a number of steps that simulate the construction sequence, and the non-linear stress-strain characteristics of soil in the analysis have been discussed by Strohm and Johnson (1971). The studies conducted by Strohm and Johnson were restricted to the period during and at the end of construction of the dam.

As mentioned in Section 1.6 of Chapter I, an analysis should be able to simulate field conditions as closely as possible so that the predictions regarding cracking of dams would be of some practical value. In order to develop a procedure for reasonable prediction of cracking it is necessary to study the influence of certain assumptions made in the analysis on the predicted results. As outlined in Section 1.8 of Chapter I the parametric studies carried out in this work are restricted to the period, during and at the end of construction of a dam. The studies are directed towards evaluating the influence of construction sequence, non-linear stress-strain relationships of soil, zero tensile strength for soil, and three dimensional effects on the predicted results. The first two factors, even though considered by Strohm and Johnson (1971) before have been studied and included in the present studies for the sake of completeness.

4.3 Selection of Sections for Parametric Studies

The section shown in Fig. 4.1 represents a half of the maximum longitudinal section passing through the centre line of an earth dam founded in a narrow, steep, symmetrical valley. The same section, though not with the same number of elements, was used in all two dimensional analyses. The abutment was assumed to be rough and rigid. The same section was also considered previously by Covarrubias (1969) and Strohm and Johnson (1971). Therefore comparison of results to test the accuracy of the present analyses was facilitated. In order to evaluate the three dimensional effects on a comparative basis, the same symmetrical triangular valley was used for the three dimensional model. In this case, the dam was symmetrical in the transverse direction also, with a centrally located core having sides inclined at 1:10 and outer slopes of 2:1. A view of one quadrant of the three dimensional model with the type and size of the spatial elements used is shown in Fig. 4.2.

4.4 Accuracy of Two Dimensional Analyses

Since the accuracy of the finite element analysis depends to a large extent on the type of element and the number of elements chosen for the analysis, it is of interest to compare the results of the present work with other available solutions. For this purpose the section shown in Fig. 4.1 was analyzed under plane strain conditions in a single lift assuming linear stress-strain relationships. One hundred constant strain triangular elements as shown in Fig. 4.1 were chosen. The elastic parameters used are shown in Fig. 4.3. The results obtained by Covarrubias (1969) for the same problem using slightly more refined quadrilateral elements are compared with the present results in Fig. 4.3. The horizontal and vertical displacements compared at the crest of the dam are almost identical. In Fig. 4.4 the extent of tension zones computed by Covarrubias (1969), Strohm and Johnson (1971), and the present analysis are compared for the same problem. The good agreement of results shown in Fig. 4.3 and 4.4 indicates that the number and type of element selected are satisfactory for subsequent analyses on the same section to elicit parametric effects.

4.5 Influence of the Construction Step Sequence

Since an earth dam is constructed in a number of layers of small thicknesses, an analysis that simulates the construction step sequence is necessary to predict the stresses and strains in a realistic manner (Clough and Woodward, 1967; Kulhawy et al., 1969). It is not economically possible to deal with a large number of steps in an analysis. Hence it is necessary to determine the number of steps that result in reasonable prediction of stresses and strains. To assess this feature, two dimensional linear elastic analyses were performed for a different number of steps. The maximum vertical displacement at centre line of valley, the maximum horizontal tensile stress and strain at the crest are compared for different number of steps in Fig. 4.5. The vertical displacement compared includes the settlement due to self weight of each layer as it is placed. It can be seen from Fig. 4.5 that all the three quantities compared are reduced with the number of steps and the reduction becomes insignificant after ten steps. Based on these results it is considered that ten steps would be sufficient for the purpose of present parametric studies.

4.6 Two Dimensional Linear, Non-Linear, and "No Tension" Analyses

Since the deformational behaviour of soil is essentially non-linear, the computation of realistic stresses and strains requires that a non-linear stress-strain relationship be used in the analysis, even though such relationships are employed within the framework of the theory of isotropic elasticity. In order to compare the results of linear and non-linear analyses, a typical set of conventional triaxial test results, obtained by performing consolidated undrained tests on a silty sand was selected (Fig. 4.6). The soil tested represents the semi-pervious material of Duncan Dam (Chapter V). For the purpose of linear analyses an average linear stress-strain relation that represents the stress conditions at the mid height of the dam and close to the centre line of valley is also shown in Fig. 4.6. The initial tangent Poisson's ratio corresponding to the preceding linear relation is 0.26. The curves relating volume changes to axial strain are discontinued after they become horizontal. Poisson's ratio was taken as 0.49 for subsequent stress levels. A density of 2.16 G/CM^3 was used in all analyses and the construction was simulated by ten lifts in every case. As described in Section 3.9.1 the elastic moduli were derived in terms of stress invariants and each step was analyzed twice to use the "average moduli".

The results illustrating the development of tension zones in the incremental linear analysis are shown in Fig. 4.7. Since it was assumed that soil can withstand a substantial amount of tension, it can be seen from the final stage of the analysis shown in Fig. 4.7, that a fairly large zone remains in tension. However since soils in general and the soils used in the analyses here in particular have very low tensile strengths, it is more appropriate to ignore the tensile strength in the analysis. In other words it may be assumed that as soon as an element goes into tension cracking would take place in that element. To simulate such a condition Zienkiewicz et al. (1968) suggested a "no tension" analysis in which the tensile principal stress in an element is artifically replaced by a system of equivalent nodal forces for that element thereby the redistribution of stresses due to removal of tensile stress in an element after cracking is achieved in a number of iterations. This method of analysis is found to be more efficient than one in which the tensile element is treated as anisotropic by assigning a very low elastic modulus in the direction of the tensile principal stress and the analysis is performed iteratively. Kulhawy et al. (1969) treated a tensile failure, similar to a shear failure, by assigning a zero value of shear modulus to the element in which tensile failure occurs. Strohm and Johnson (1971) assigned an overall low Young's modulus to the element in which tension failure took place. Since a "no tension" analysis is more realistic and efficient than other methods it has been used here. After removing the tensile stress the element is assigned moduli calculated from unconfined compression test data since the confining stress is zero.

The effect of a "no tension" analysis on the development of the tensile zone, major and minor principal stresses, and the displacements is of interest. The results of incremental linear analyses performed with and without the removal of tensile stresses are compared in Fig. 4.8. The extent of the tensile zone, as indicated by the contour of the zero minor principal stress, is smaller when tension is removed. The distribution of the minor principal stress is affected to a fair degree by the "no tension" analysis whereas the major principal stress and the vertical displacement along the centre line are relatively insensitive to the removal of tension. The variation in the distribution of the minor principal stress that occurs due to the "no tension" analysis depends to a large extent on the magnitude of the tensile stresses removed. If the tensile stresses removed are very small the "no tension" analysis does not significantly alter the results regarding the development of tension zones. In such cases analyses performed without the removal of tensile stresses may be preferred as it considerably saves the computation effort needed especially in a three dimensional analysis.

The growth of tension zones in an incremental non-linear analysis is illustrated in Fig. 4.9. It can be seen that the extent of the tension zone and the magnitude of tensile stresses developed are quite small compared to the results obtained in a linear analysis. A similar result was also obtained by Strohm and Johnson (1971). In this analysis it was assumed that the intermediate principal stress is equal to the minor principal stress (i.e., $\sigma_2 = \sigma_3$) while calculating the elastic moduli. For the elements in which tension occurs the modulus is calculated from the stress-strain curve corresponding to unconfined conditions. A "no tension" analysis is not performed as the tensile stresses developed are very small in magnitude.

4.7 Effect of the Intermediate Principal Stress

It is of interest to assess the effect of the intermediate principal stress on the analytical results. To determine any effects the intermediate principal stress was computed from:

$$\sigma_2 = \nu(\sigma_1 + \sigma_3)$$

and its value was utilized in calculating the stress invariants for deriving the moduli. An iterative procedure was used because of the dependence of Poisson's ratio on stress. Results obtained from such an analysis are compared in Fig. 4.10 with those obtained by assuming σ_2 is equal to σ_3. It is apparent that the intermediate principal stress has practically no effect on the horizontal stress and strain at the crest of dam. However, vertical displacements at the centre line of the valley are about 2.5% greater for the analysis in which it is assumed that σ_2 is equal to σ_3.

The small difference between the results obtained for the plane strain cases analyzed can be attributed to the condition, close to a confined compression with relatively small vertical strains, that exists over a major portion of the valley. Under small vertical strains the effect of intermediate principal stress is not significant (Fig. 3.5, Chapter

III). Because of the closeness to confined compression $\sigma_2 \approx \sigma_3$.

4.8 Three Dimensional Effects

4.8.1 General

Finite element analyses for embankments are performed mostly for plane strain conditions even though some solutions were obtained recently by three dimensional analysis (e.g., Frazier, 1969; Lefebvre and Duncan, 1971; Palmerton, 1972). The major drawback of a three dimensional analysis is its high computational cost compared to a two dimensional analysis. However, for certain situations a three dimensional finite element analysis for an embankment structure becomes very useful and sometimes irreplaceable. A three dimensional analysis may be preferred when the complex boundary geometry and boundary conditions cannot be represented by the plane strain conditions assumed in a two dimensional analysis. Considering the complexity of the problem of cracking of earth dams founded on irregular, non-homogeneous, compressible foundations, it appears that a three dimensional analysis is more relevant than a two dimensional analysis. Under such conditions a three dimensional analysis may be justified as its cost forms only a minor part of the total cost of the project.

4.8.2 Three Dimensional Studies

Palmerton (1972) compared the results of plane strain and three dimensional analyses performed on an earth dam located in a narrow triangular valley, similar to that in Figs. 4.1 and 4.2. The plane strain analysis was performed only on the maximum transverse section. The analyses used non-linear stress-strain relationships in the hyperbolic functional form and an incremental construction was simulated. Considerable differences in stress conditions were observed between plane strain and three dimensional analyses but the displacements predicted by both analyses were more or less similar. The differences between the stresses were mainly due to the arching action aided by the valley walls.

From these results it appears that a two dimensional analysis performed on the maximum transverse section of an earth dam founded in a symmetrical or nearly symmetrical narrow rigid valley may provide useful information regarding the displacements which can be verified easily by field observations at the maximum section.

In the present studies, the results of three dimensional analyses performed on the dam shown in Fig. 4.2 are compared with those of two dimensional analyses. For the purpose of comparison linear three dimensional analyses in single and multiple increments were performed. Linear analyses were performed to facilitate comparison of two and three dimensional analyses at the same moduli values.

Fig. 4.11 and Fig. 4.12 show the comparison of vertical displacement and horizontal stress and strain at the crest of the dam respectively. As seen from the comparison the results obtained by plane strain and three dimensional analyses are not significantly different. The difference between the maximum vertical displacement of the crest obtained by the two types of analysis is 4.7%. Incremental linear analyses with five construction steps were performed for two and three dimensional sections shown in Figs. 4.1 and 4.2. The results of horizontal and vertical stresses in the core, and the vertical displacements at the centre line of the valley obtained by plane strain and three dimensional incremental linear analyses are compared in Fig. 4.13. The horizontal and vertical stresses near the crest obtained by both analyses are very much the same. However, significant differences in stresses are evident in the lower portion of the dam, the stresses being smaller in magnitude in the three dimensional case. The difference between the maximum vertical settlements at the centre line of the valley is about 13.6%.

From these studies it emerges that the results of plane strain analyses are useful to predict, with some reliance, the tensile stresses close to the crest of a homogeneous earth dam founded in a narrow symmetrical steep valley.

However, when the rigidity of the core differs from that of the shell the predictions by plane strain analyses lead to large errors in tensile stresses near the crest. This is revealed by the comparisons shown in Fig. 4.14. The plane strain analysis predicts much higher magnitudes of tensile stresses compared to the three dimensional analysis when the core is ten times softer than the shell. The reverse is true when the shell is softer than core. The results are similar both in a single step and 5-step incremental analyses even though the absolute magnitude of stresses developed in the incremental analysis is considerably less.

The reason for these large differences in stresses can be understood from the displacement patterns shown in Fig. 4.15. The displacement results were obtained from three dimensional linear 5-step incremental analyses for two ratios of elastic moduli of core to shell. The ratios chosen for rigid and soft core are 10 and 0.1 respectively. The displacement of the surface points in the x-y plane are shown by dotted lines for the rigid core case and by full lines for the soft core case. The displacement vectors both in magnitude and direction and the locations of the zones in which tensile stresses develop are also shown for both cases. The following features can be observed from this figure:

(1) For the rigid core case, the displacements in the core are away both from the crest and the abutment.

(2) For the soft core case, the displacements in the x-direction are towards the crest, and in the y-direction they are away from the abutment.

(3) Plane strain conditions along the maximum longitudinal section, assumed in a two dimensional analysis, will not be satisfied in both cases.

(4) Longitudinal tensile strains produced in a core of a given flexibility close to the crest are influenced by the flexibility of shell. A shell more flexible than

core produces greater longitudinal tensile strains in core than those produced by a shell stiffer than core. For example in Fig. 4.15 the displacements shown by dotted line would increase by ten times if an analysis is performed with the modulus of core equal to 200 KG/CM^2 (same as that used for the soft core case) and with the modulus of shell equal to 20 KG/CM^2. Larger longitudinal strains produced in a rigid core due to greater flexibility of shell result in larger tensile stresses in comparison to the case of a soft core with a rigid shell.

(5) In a rigid core both longitudinal and transverse cracks are possible whereas in the case of a soft core the cracks that are likely to occur in the core are mainly in the transverse direction. The locations where tensile stresses developed in the transverse and longitudinal directions, for the two cases studied, are shown in Fig. 4.15.

The distribution of vertical and horizontal stresses in core and shell for two cases discussed above is shown in Fig. 4.16. Large reductions in both horizontal and vertical stresses in the soft core can be seen. Such reductions are usually the cause of hydraulic fracturing, a factor that could cause internal cracks leading to piping failures (Bjerrum, 1967; Kjaernsli and Torblaa, 1968; Sherard _et al_., 1972). Fig. 4.17 shows the effect of the difference in flexibilities between core and shell on the maximum tensile principal stress developed in the core. The results were obtained by performing three dimensional linear analyses in a single step for different ratios of moduli of core to shell ranging from 0.01 to 100.0. The variation of the maximum tensile stress is predominant between ratios 0.1 to 10.0. For ratios less than 0.07, representing conditions seldom realized in practice, the computed stress may not be reliable and it is thought that the dashed line is more representative. While the result shown in Fig. 4.17 is applicable to the geometry and the conditions assumed in the analysis, it nevertheless indicates that by controlling the compaction and moisture content of shell and core, placement conditions of the fill can be specified which will contribute significantly to the design of dams against cracking.

4.9 Considerations of the Flexibility of the Core to Control Cracking

One of the common methods used to control the cracking of earth dams is to place the fill at water contents 1 to 2% greater than the optimum. It is assumed that the increase in flexibility of the core thus achieved, prevents the core from cracking due to tensile stresses. However, when the flexibility of the core is to be increased, it is necessary to distinguish between two common situations:

(1) A dam built on a highly compressible foundation, will undergo differential settlement which causes tensile cracks in the core (e.g., Duncan Dam, Chapter V). The stresses in the core are governed mainly by the settle-

ment of the foundation and the flexibility of the core. When the flexibility of the core is increased the tensile stresses in the critical zones are generally reduced.

(2) The tensile zones developed in the core of a dam built in a valley with more or less rigid abutments and incompressible foundations are governed mainly by the settlement that occurs within the core. Two dimensional finite element analyses under plane strain conditions were performed on the section shown in Fig. 4.1 for the following three cases to illustrate the effect of increasing the flexibility of the core and the non-homogeneity of the core on the development of tensile zones:

(i) A homogeneous dam (Fig. 4.18(a)) consisting of material with $E = 200$ KG/CM^2 and $\nu = 0.35$.

(ii) A homogeneous dam (Fig. 4.18(a)) consisting of material with $E = 100$ KG/CM^2 and $\nu = 0.35$.

(iii) A homogeneous dam (Fig. 4.18(b)) consisting of two materials with

(a) $E = 100$ KG/CM^2 and $\nu = 0.35$ in the tensile zone as determined in case (i) or case (ii) and

(b) $E = 200$ KG/CM^2 and $\nu = 0.35$ elsewhere in the dam.

Fig. 4.18(a) compares the tensile zone and the tensile strain along the crest for cases (i) and (ii). An increase in the flexibility of the core does not change the tensile stresses or the extent of the tensile zone because, for the type of boundary considered, the stresses are independent of the values of the moduli used in the analysis. The tensile strains along the crest, on the other hand, increase with the flexibility of the core.

Fig. 4.18(b) shows the results of a finite element analysis performed on a non-homogeneous section. This section consists of two types of material. A material with a high flexibility is incorporated in the tensile zones determined previously for homogeneous section (case (i) or case (ii)), whereas material with a low flexibility is retained elsewhere in the dam. The non-homogeneity of the material in the dam causes a favourable stress redistribution, the magnitude of tensile stresses is lowered as well as reducing the extent of the tensile zone. The tensile strains along the crest are slightly more than those obtained in case (i). Introducing another type of material of higher flexibility than that corresponding to 100 KG/CM^2 into the tensile zone indicated by tensile stresses in Fig 4.18(b), further reduces the tensile stresses and the extent of tensile zone.

For the type of boundary considered above, the reduction of tensile zones or even their elimination would become possible if materials with appropriate flexibility characteristics are properly distributed within the suspected tensile zones. An overall increase in flexibility of material throughout the core, for the type of boundary considered, is of little use in controlling of tensile cracks. A finite element analysis with non-homogeneous modelling can be employed conveniently, as shown, to assess the relative influence of changing the placement conditions of the fill in the critical zones of a dam.

4.10 Summary

An analysis which considers realistic boundary conditions, representative non-linear stress-strain characteristics of soils and the construction step sequence is a considerable contribution to the proper evaluation of tensile zones in earth dams both during and at the end of construction. A single step linear analysis, even though simple and straightforward, exaggerates the tensile zones and results in unrealistic displacements and stress distributions. Consideration of incremental loading is of utmost importance even for an approximate evaluation of displacements. The influence of the intermediate principal stress on the results of a plane strain analysis is small when geometry analyzed almost represents conditions of confined compression with relatively small strains. This generally occurs for a valley having a narrow profile. The removal of tensile stresses in cracked zones ("no tension" analysis) influences the results of the non-linear incremental analysis of cracking only to a minor extent. As a non-linear incremental analysis in general results in tensile stresses of low magnitude compared to those obtained by a linear incremental analysis, the redistribution of stresses caused by the removal of tensile stresses does not significantly alter the extent of tensile stresses subsequently computed in the upper layers. As the "no tension" analysis involves an iterative procedure its use in a three dimensional analysis increases the cost of computation considerably. Because of its rather minor effect on the results, and also due to the high cost of computation involved, a "no tension" analysis was not introduced into the three dimensional finite element program for the purpose of the present work. The extension of the "no tension" analysis to three dimensional problems is however possible. While a two dimensional analysis provides reasonably accurate solutions in the analysis of cracking of homogeneous earth dams founded in narrow steep valleys, significant errors could be caused when core and shell differ in their deformational properties. The tensile stresses are under-estimated when the shell is more flexible than core whereas they are over-estimated when the shell is less flexible than core. For certain boundary conditions a finite element analysis with a non-homogeneous modelling of dam may be used to assess the relative influence of changing the flexibility of the fill. Such an assessment is useful in designing dams against tensile cracking.

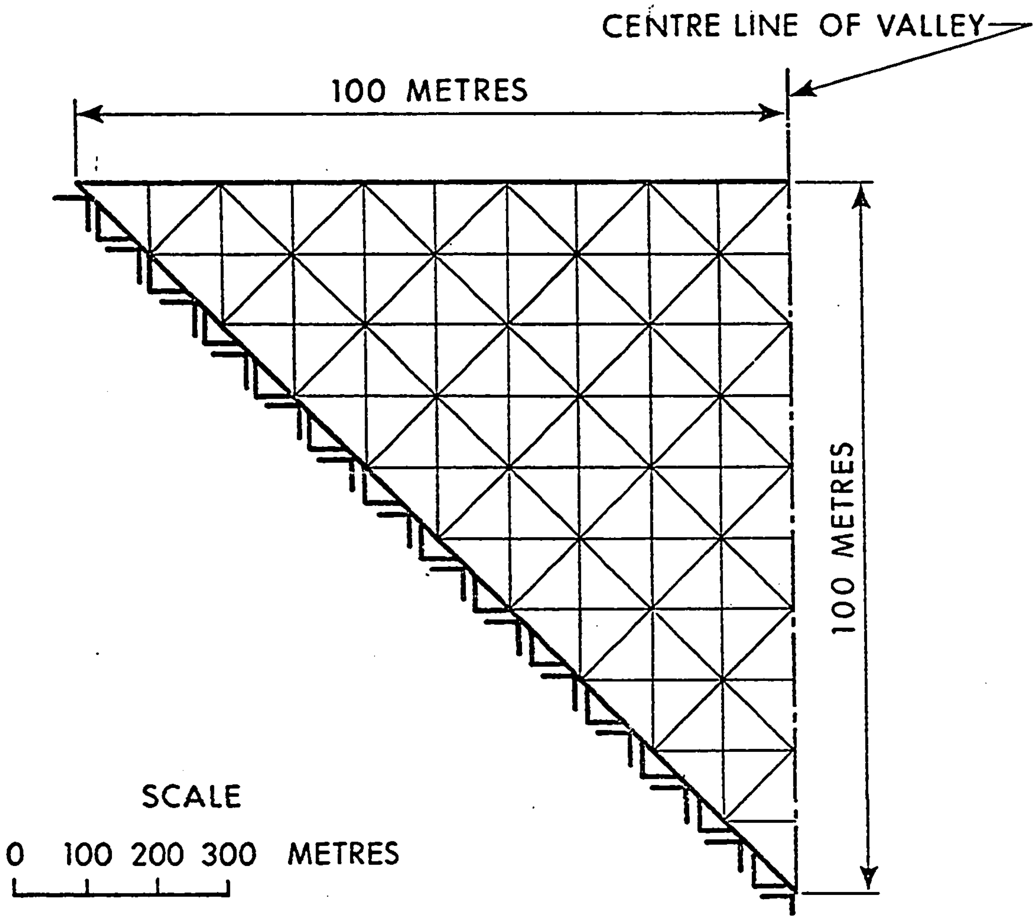

FIG. 4.1 SECTION ASSUMED IN TWO DIMENSIONAL ANALYSES

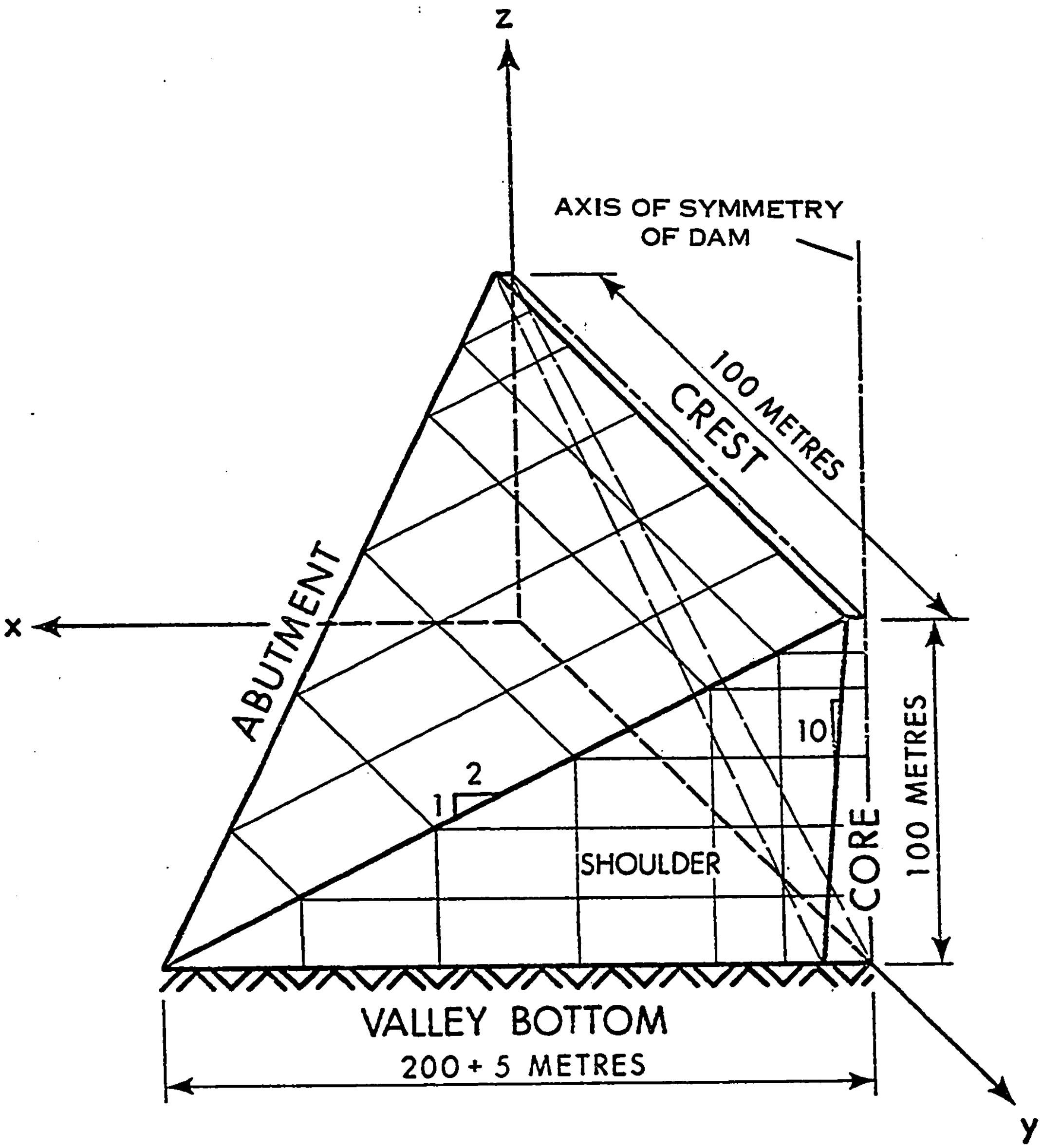

FIG. 4.2 QUADRANT OF DAM ASSUMED IN THREE DIMENSIONAL ANALYSES

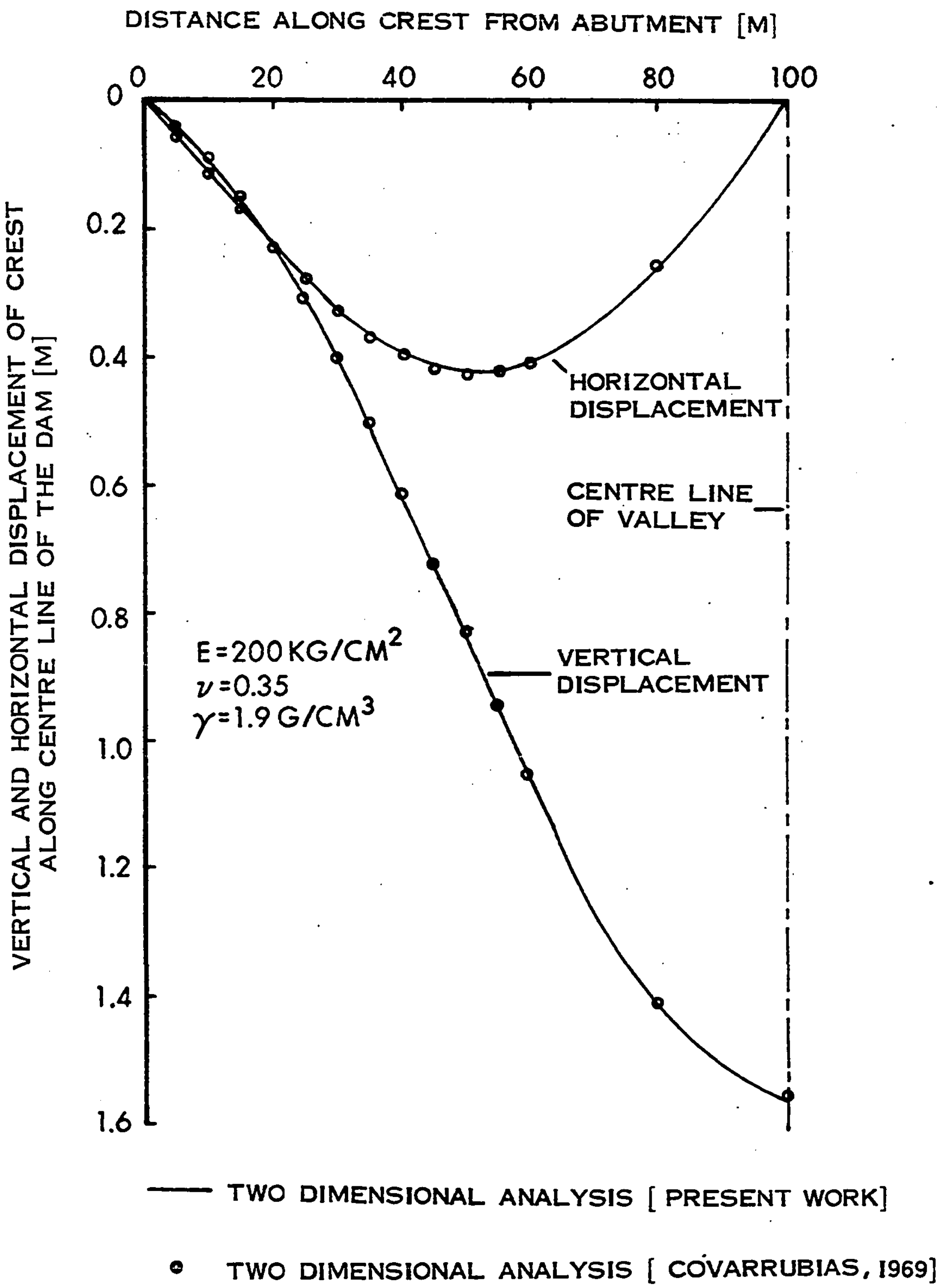

FIG. 4.3 COMPARISON OF VERTICAL AND HORIZONTAL DISPLACEMENTS FOR TWO DIMENSIONAL SINGLE STEP ANALYSES

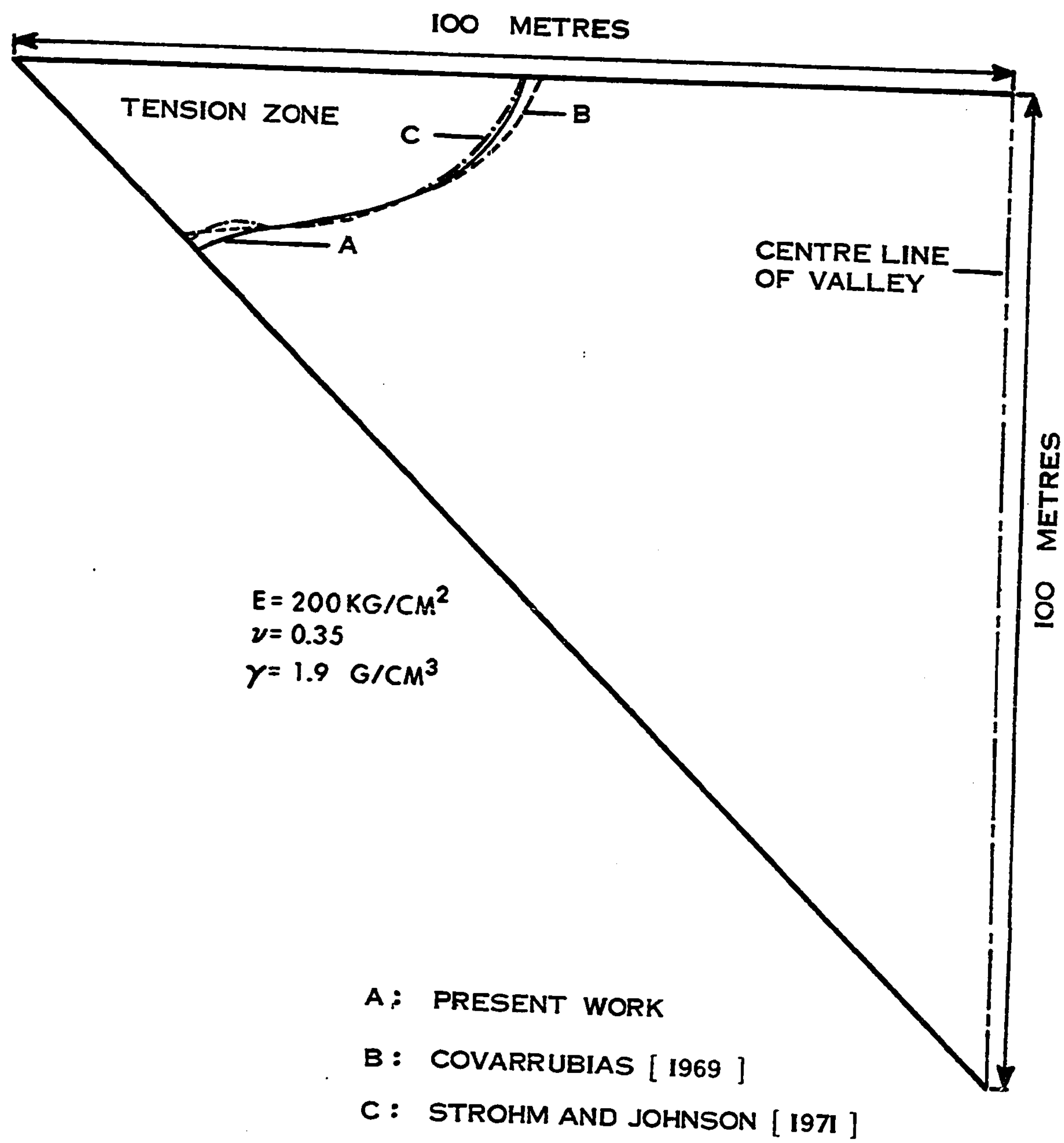

FIG. 4.4 COMPARISON OF TENSION ZONES COMPUTED BY SINGLE STEP TWO DIMENSIONAL LINEAR ELASTIC ANALYSES

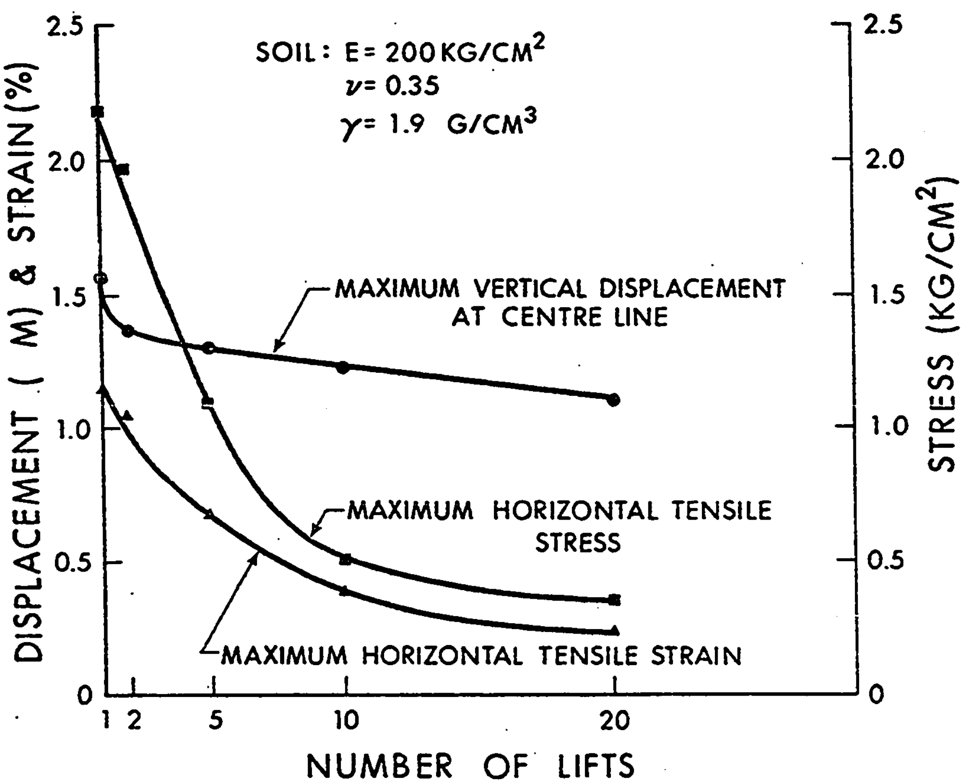

FIG. 4.5 EFFECT OF NUMBER OF LIFTS ON MAXIMUM HORIZONTAL STRESS, STRAIN AND VERTICAL DISPLACEMENT OF TWO DIMENSIONAL SECTION

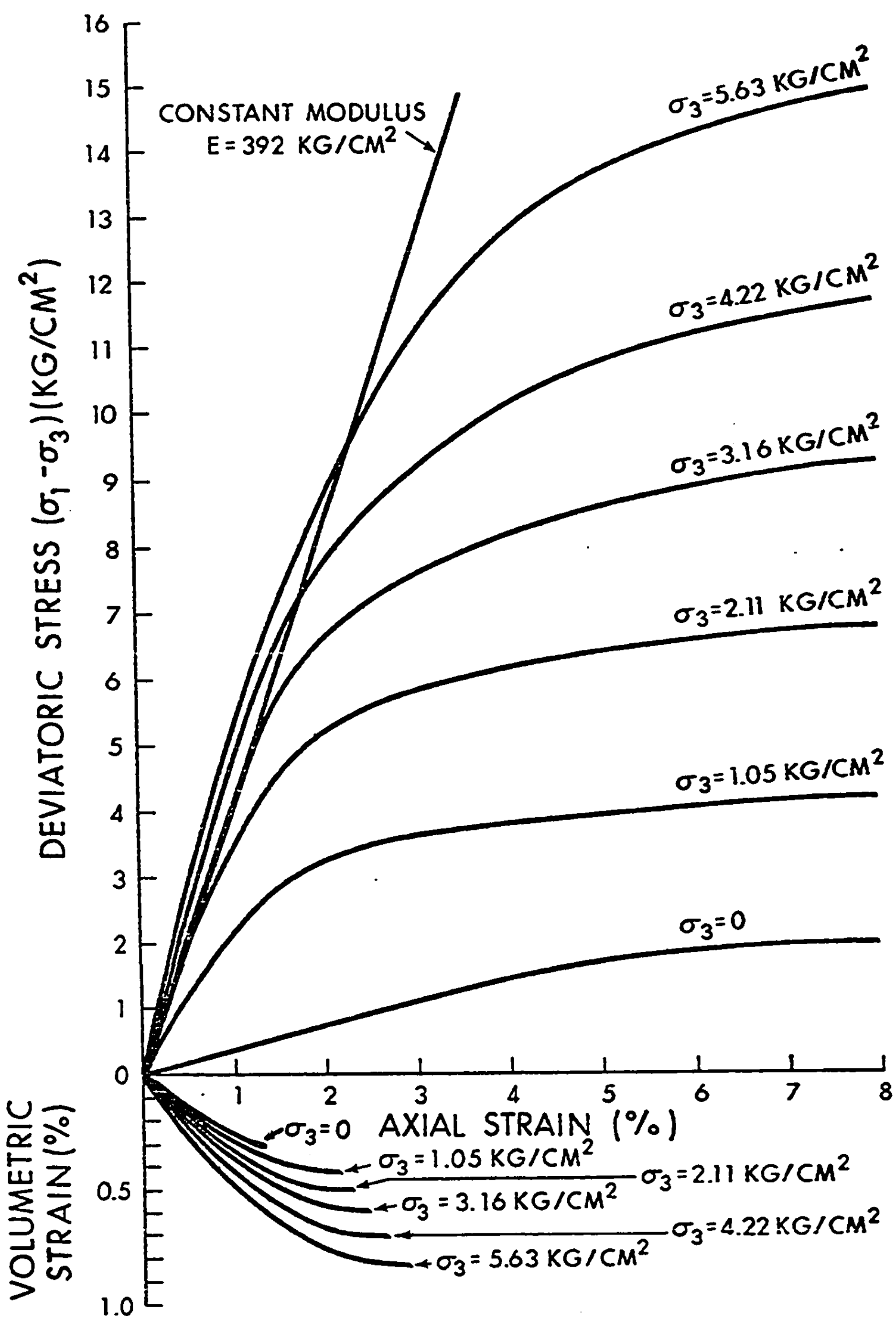

FIG. 4.6 STRESS STRAIN RELATIONSHIPS FOR SILTY SAND

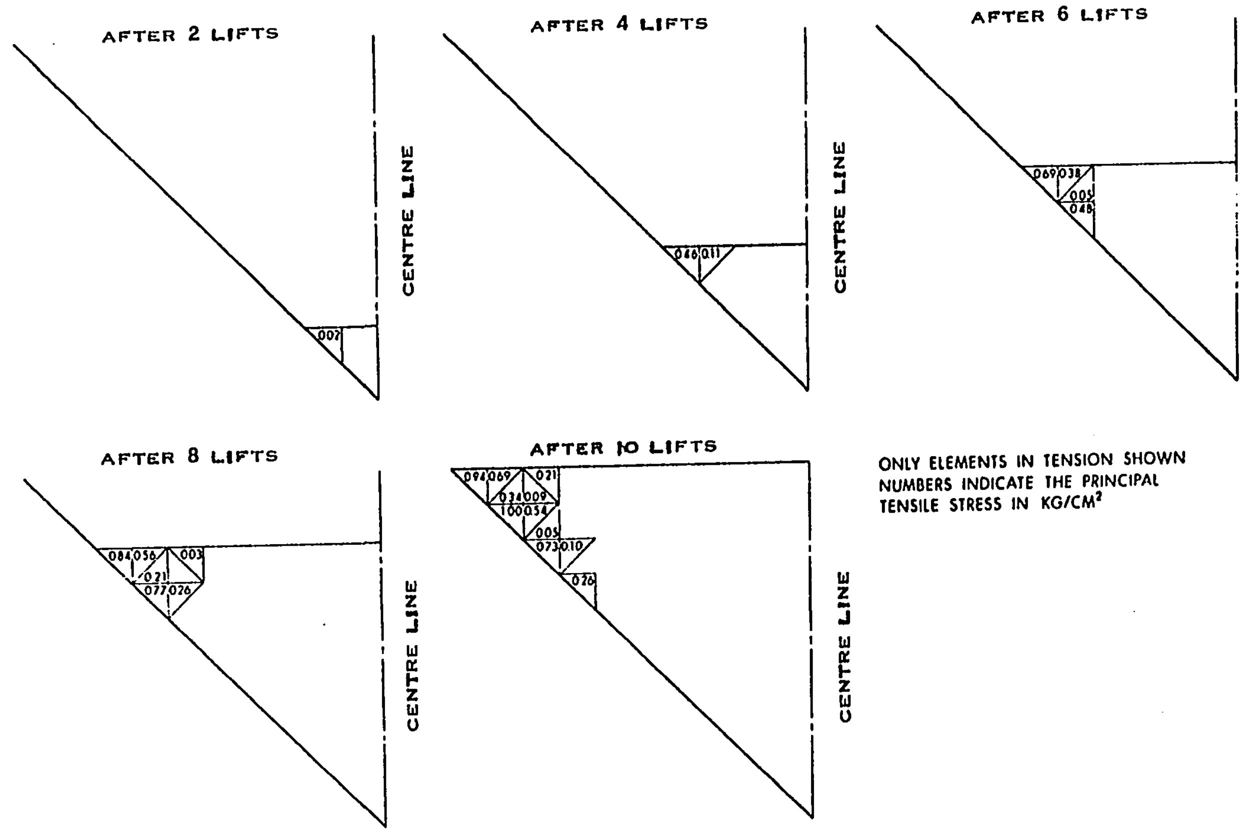

ANALYZED FOR : $E = 392\ KG/CM^2$, $\nu = 0.26$, $\gamma = 2.16\ G/CM^3$

FIG. 4.7 TENSILE ZONES DEVELOPED FOR LINEAR ANALYSIS AFTER CERTAIN NUMBER OF LIFTS

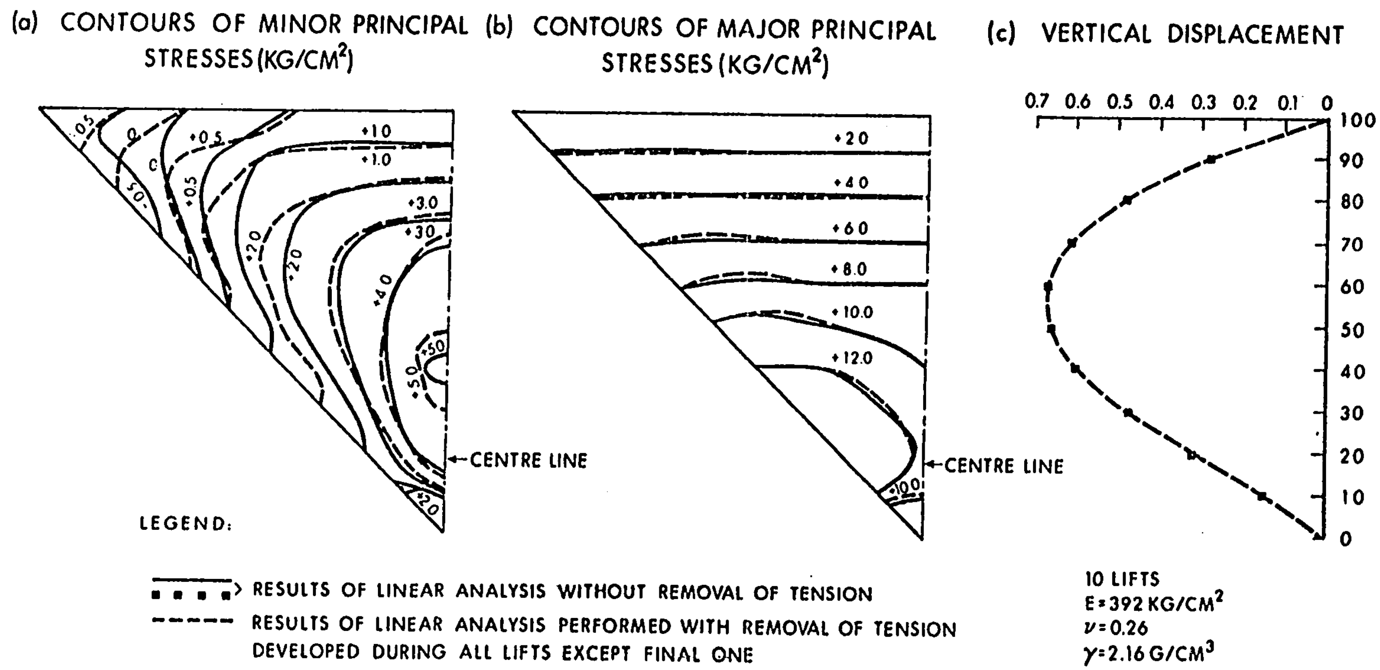

FIG. 4.8 COMPARISON OF LINEAR ANALYSIS WITH AND WITHOUT REMOVAL OF TENSION

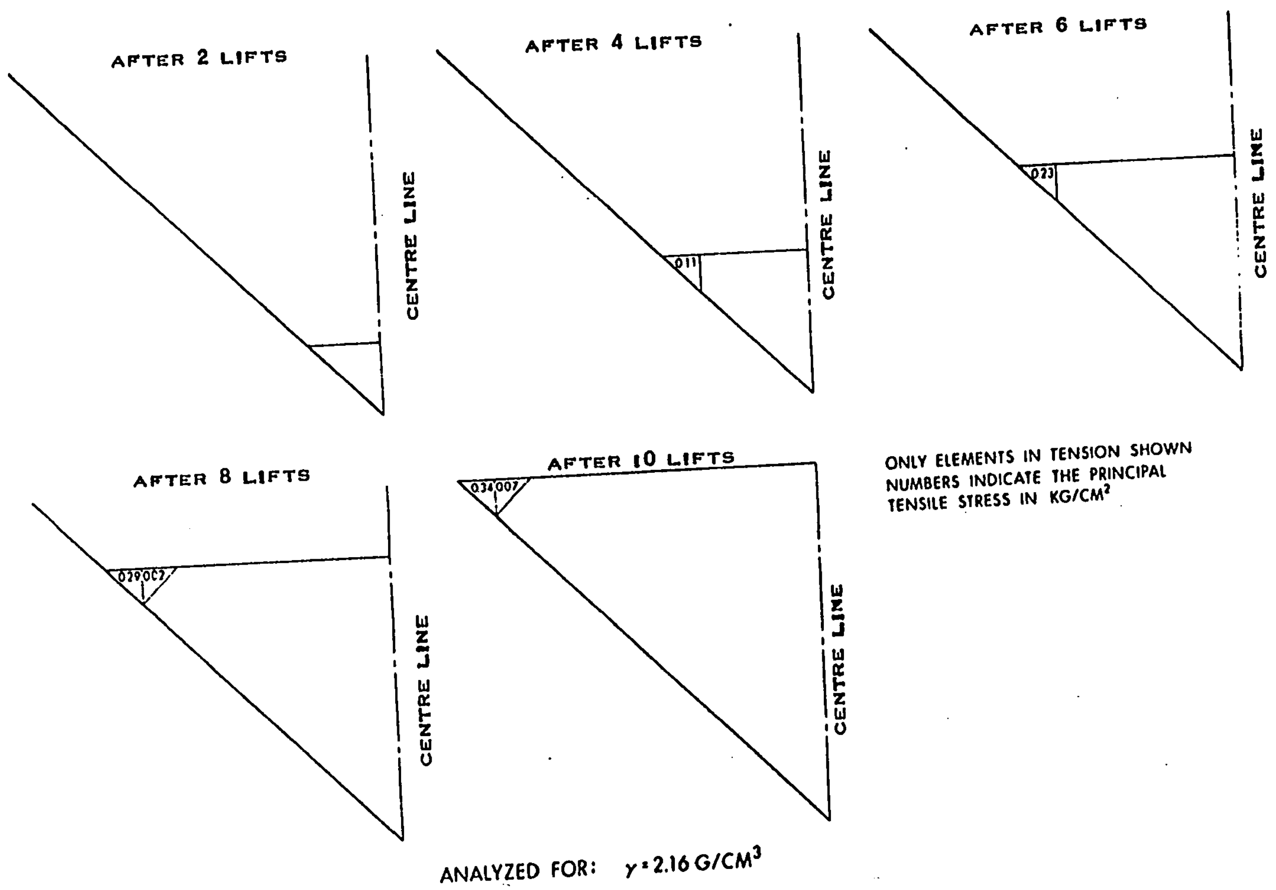

FIG. 4.9 TENSILE ZONES DEVELOPED FOR NONLINEAR ANALYSIS AFTER CERTAIN NUMBER OF LIFTS

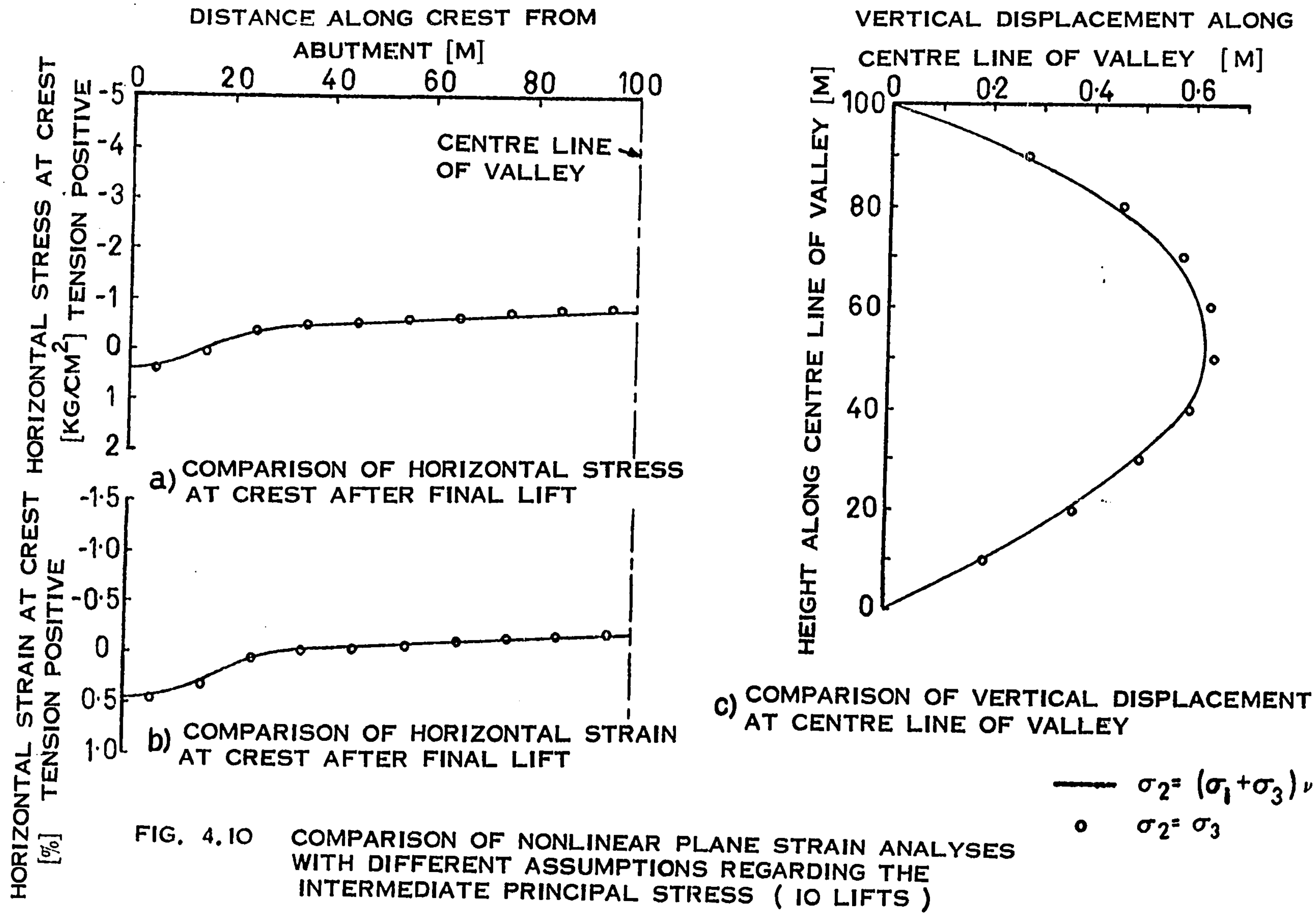

a) COMPARISON OF HORIZONTAL STRESS AT CREST AFTER FINAL LIFT

b) COMPARISON OF HORIZONTAL STRAIN AT CREST AFTER FINAL LIFT

c) COMPARISON OF VERTICAL DISPLACEMENT AT CENTRE LINE OF VALLEY

FIG. 4.10 COMPARISON OF NONLINEAR PLANE STRAIN ANALYSES WITH DIFFERENT ASSUMPTIONS REGARDING THE INTERMEDIATE PRINCIPAL STRESS (10 LIFTS)

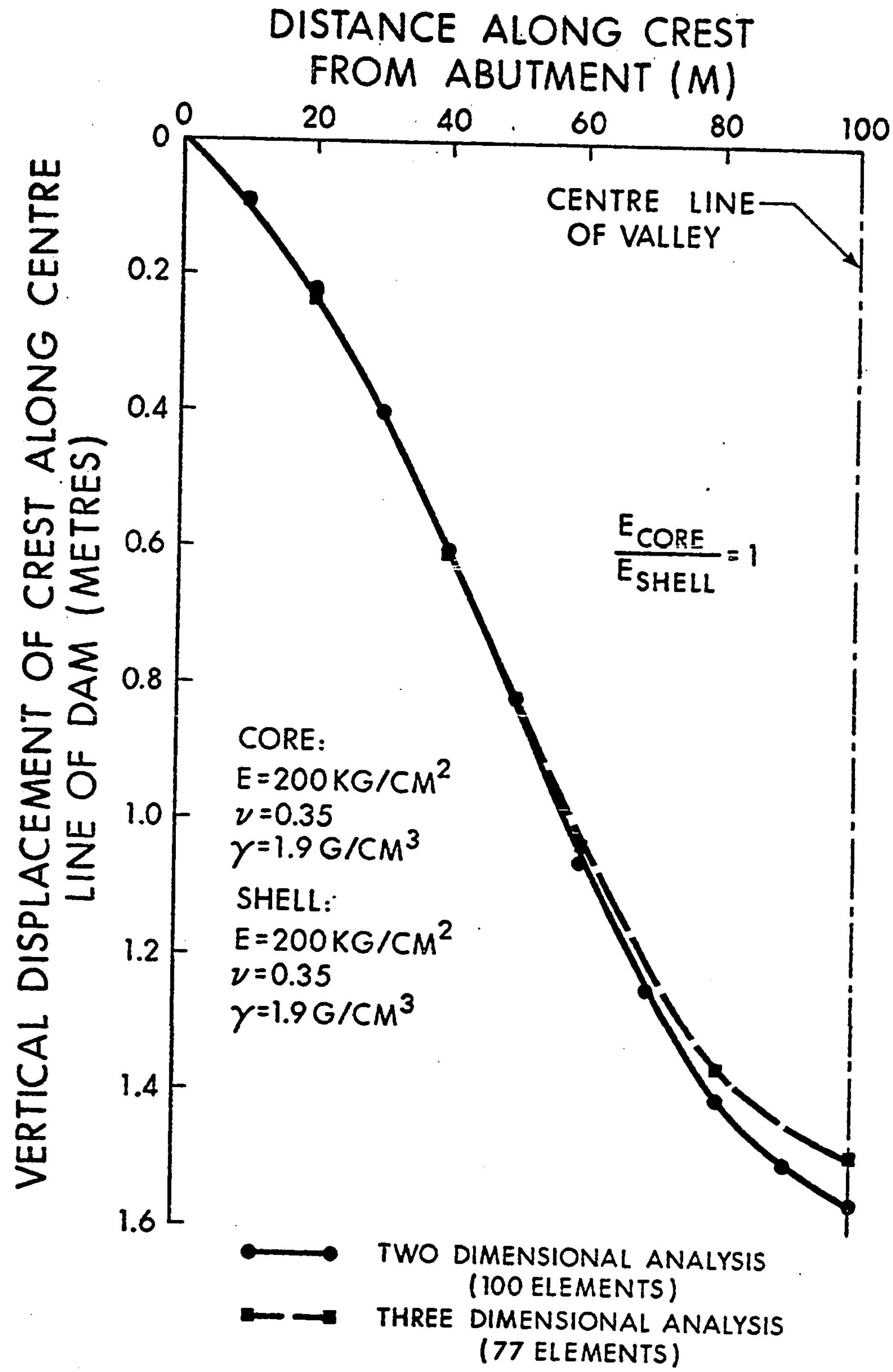

FIG. 4.11 VERTICAL DISPLACEMENT ALONG CREST FOR TWO AND THREE DIMENSIONAL ANALYSIS, SINGLE LIFT

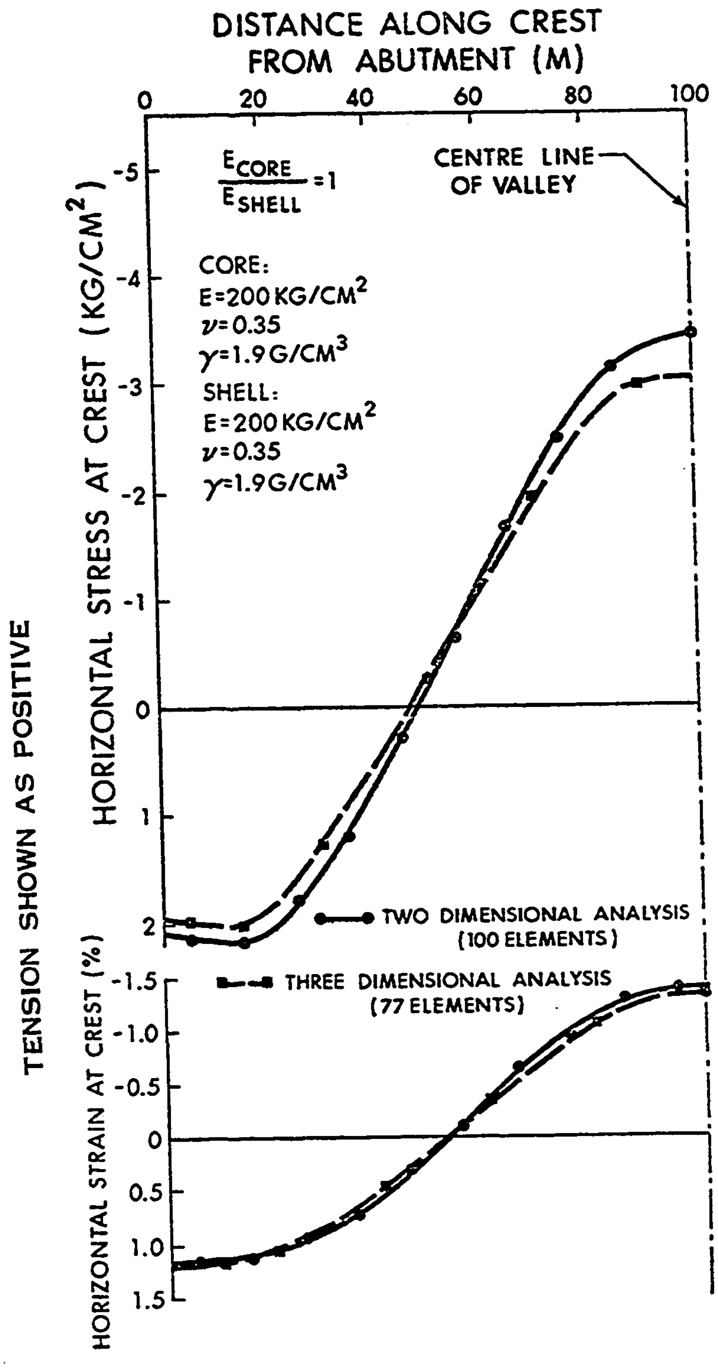

FIG. 4.12 HORIZONTAL STRESS AND STRAIN ALONG CREST FOR TWO AND THREE DIMENSIONAL ANALYSES IN SINGLE LIFT

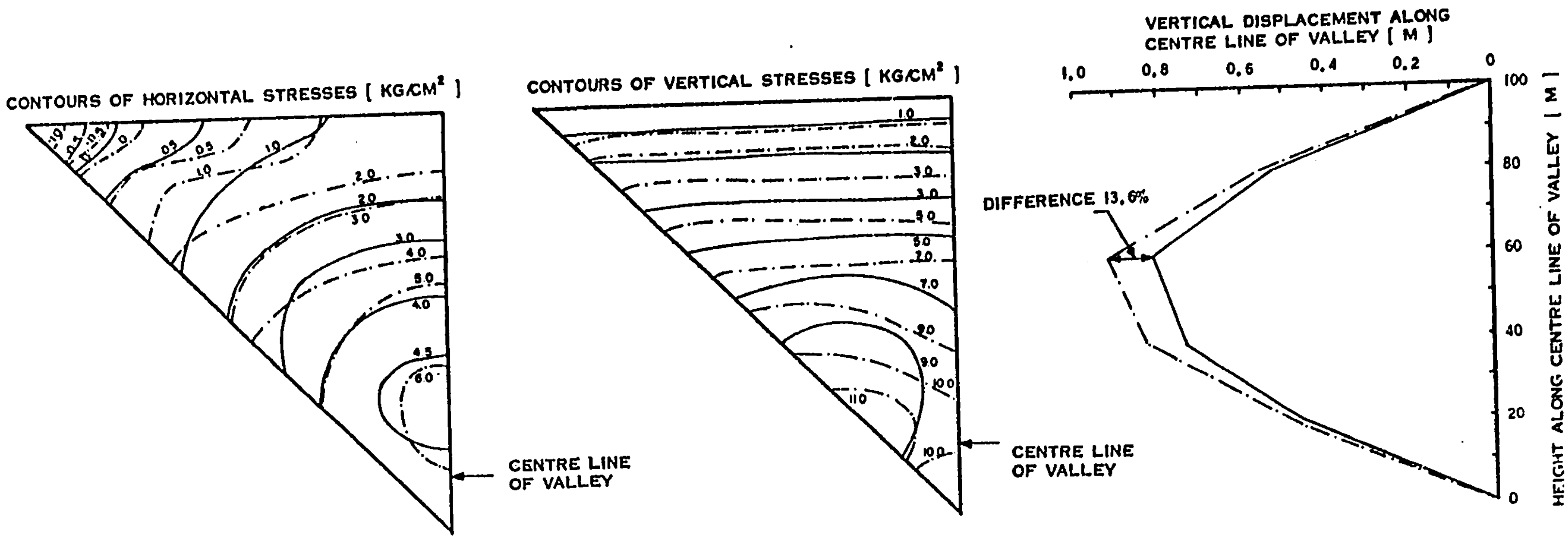

LEGEND: _._._ RESULTS OF TWO DIMENSIONAL LINEAR ANALYSIS IN 5 INCREMENTS
____ RESULTS OF THREE DIMENSIONAL LINEAR ANALYSIS IN 5 INCREMENTS
[NEGETIVE STRESSES INDICATE TENSION]

$E = 200\ KG/CM^2$
$\nu = 0{,}35$
$\gamma = 1{,}90\ G/CM^3$

FIG. 4.13 COMPARISON OF RESULTS OF TWO AND THREE DIMENSIONAL INCREMENTAL LINEAR ANALYSES PERFORMED ON A HOMOGENEOUS DAM [5 INCREMENTS]

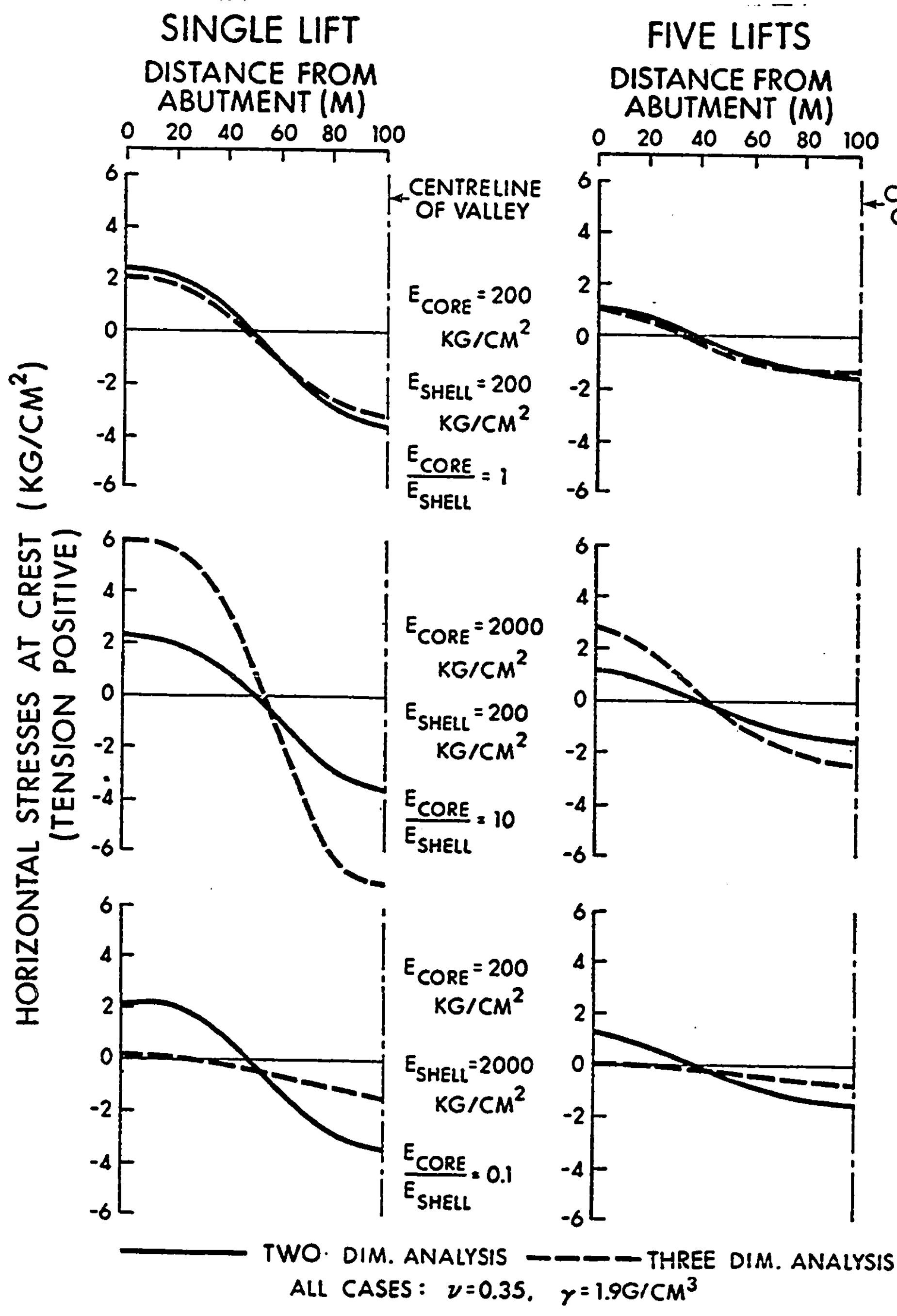

FIG. 4.14 COMPARISON OF HORIZONTAL STRESSES ALONG CREST FOR TWO AND THREE DIMENSIONAL ANALYSES AT DIFFERENT RATIO OF MODULI OF CORE TO SHELL

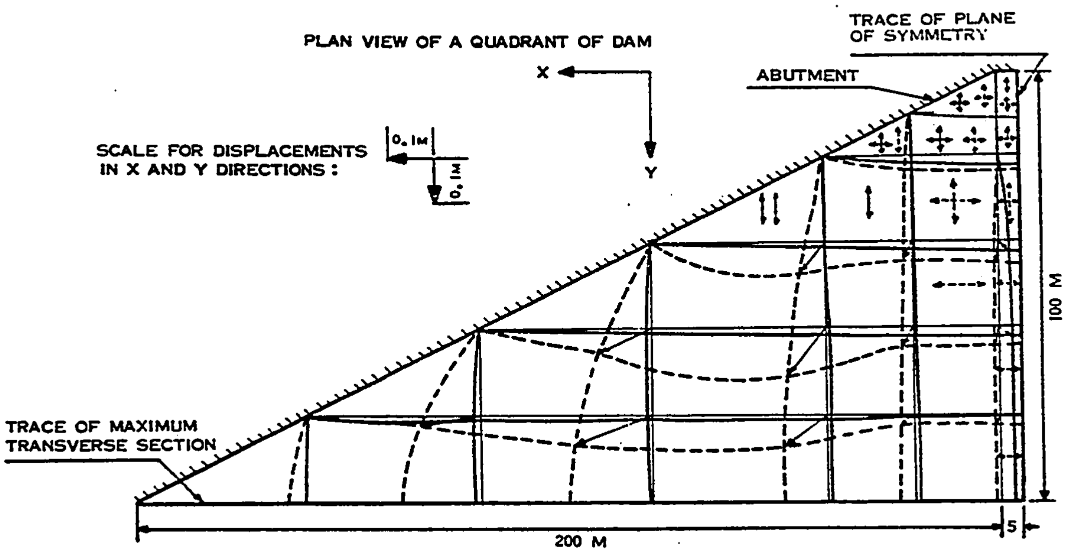

LEGEND :

---- MOVEMENT OF POINTS ON TOP SURFACE OF DAM OBTAINED WITH : E_{CORE} = 2000 KG/CM^2, E_{SHELL} = 200 KG/CM^2, ν = 0.35, γ = 1.9 G/CM^3

—— MOVEMENT OF POINTS ON TOP SURFACE OF DAM OBTAINED WITH : E_{CORE} = 200 KG/CM^2, E_{SHELL} = 2000 KG/CM^2, ν = 0.35, γ = 1.9 G/CM^3

◄--► INDICATES EXISTENCE OF TENSILE STRESS IN TRANSVERSE DIRECTION WHEN E_{CORE}/E_{SHELL} = 10.0

INDICATES EXISTENCE OF TENSILE STRESS IN LONGITUDINAL DIRECTION WHEN E_{CORE}/E_{SHELL} = 10.0

◄—► INDICATES EXISTENCE OF TENSILE STRESS IN TRANSVERSE DIRECTION WHEN E_{CORE}/E_{SHELL} = 0.1

INDICATES EXISTENCE OF TENSILE STRESS IN LONGITUDINAL DIRECTION WHEN E_{CORE}/E_{SHELL} = 0.1

DISPLACEMENT VECTOR IN THE HORIZONTAL PLANE

FIG. 4.15 COMPARISON OF DISPLACEMENT PATTERN AND DEVELOPMENT OF TENSILE CRACKS ON THE SURFACE OF DAM FOR MODULAR RATIOS OF CORE TO SHELL EQUAL TO 10 AND 0.1. RESULTS BY THREE DIMENSIONAL LINEAR ANALYSES IN 5 INCREMENTS

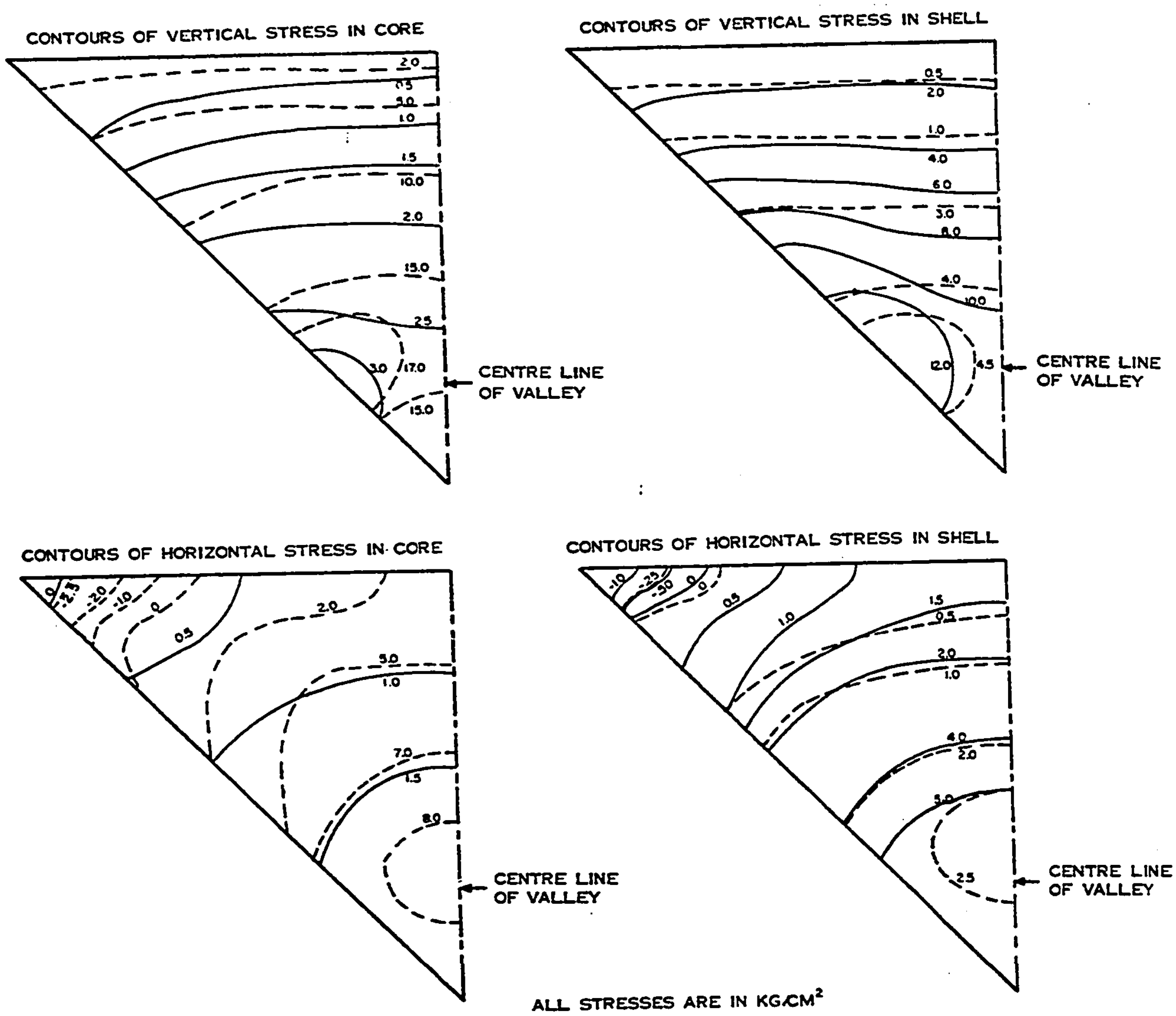

ALL STRESSES ARE IN KG/CM^2
NEGETIVE STRESSES
INDICATE TENSION

LEGEND:

– – – RESULTS WHEN: E_{CORE} =2000 KG/CM^2, E_{SHELL} = 200 KG/CM^2, $\nu = 0.35, \gamma = 1.9$ G/CM^3

——— RESULTS WHEN: E_{CORE} = 200 KG/CM^2, E_{SHELL} = 2000 KG/CM^2, $\nu = 0.35, \gamma = 1.9$ G/CM^3

FIG. 4.16 COMPARISON OF STRESSES IN CORE AND SHELL CLOSE TO THE MAXIMUM LONGITUDINAL SECTION OF DAM FOR MODULAR RATIOS OF CORE TO SHELL EQUAL TO 10 AND 0.1. RESULTS BY THREE DIMENSIONAL LINEAR ANALYSES IN 5 INCREMENTS

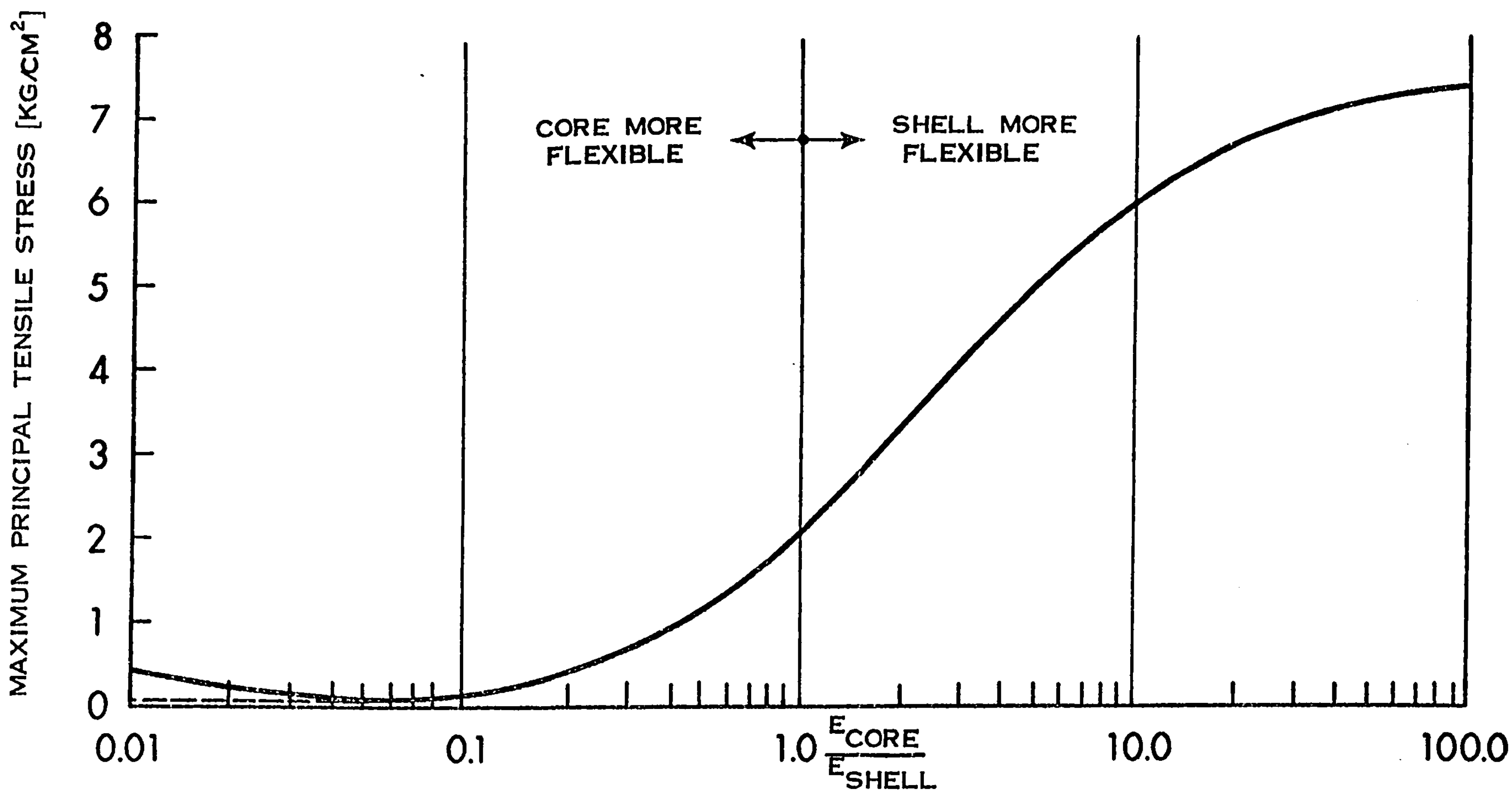

FIG. 4.17 COMPARISON OF MAXIMUM TENSILE STRESSES IN CORE FOR DIFFERENT RATIOS OF MODULI OF CORE TO SHELL

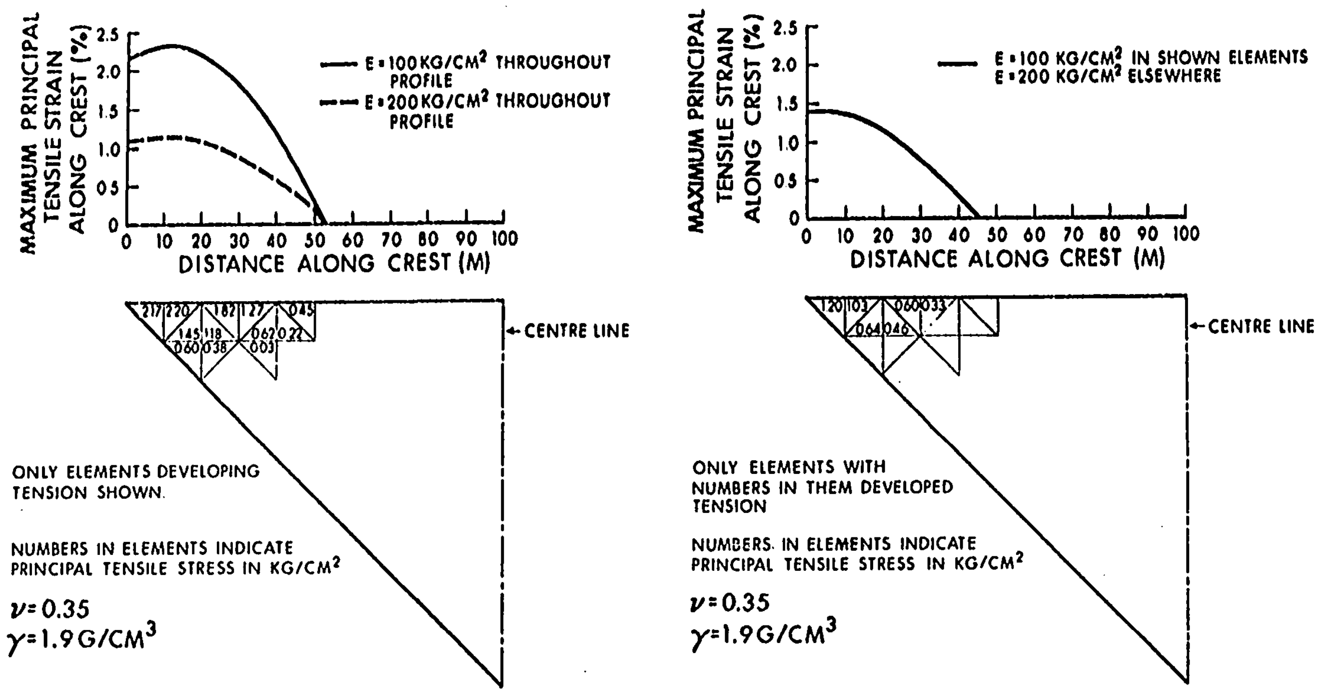

(a) SAME MODULUS THROUGHOUT PROFILE

(b) $E = 100\ KG/CM^2$ IN ELEMENTS SHOWN
$E = 200\ KG\ CM^2$ ELSEWHERE

FIG. 4.18 EFFECT OF THE NONHOMOGENEITY OF CORE ON THE REDUCTION OF TENSILE ZONES

CHAPTER V

ANALYSIS OF CRACKING AT DUNCAN DAM

5.1 Scope

In this chapter the analytical procedures developed in the previous chapters are applied to the analysis of the cracking of the Duncan Dam to assess their practical application.

5.2 Introduction

As pointed out in Chapter III, any analytical procedure that attempts to model a real structure mathematically in order to predict its behaviour can only yield approximate answers. This is a result of the various simplifications introduced into the analysis in representing factors such as the complex stress-strain behaviour of soils, geometry of the structure, the boundary conditions, and the history of construction. In addition, the laboratory stress-strain data used in the analysis can sometimes introduce an appreciable error in the prediction of in-situ behaviour (Alberro, 1972; Low, 1972). These factors introduce an unknown error into the model. The magnitude of this error can be assessed by comparison with an actual case history. Hence studies of the behaviour of well documented earth structures are of utmost importance for the evaluation of analytical procedures based on the finite element method (Chang and Duncan, 1970).

The recorded behaviour of the Duncan Dam in Southern British Columbia, Canada has proved to be particularly valuable for verifying the usefulness of the proposed procedures in the analysis of cracking of earth dams.

5.3 History of Cracking at Duncan Dam

5.3.1 Salient Features

A detailed account of cracking at Duncan Dam and the remedial measures taken for its successful completion are given by Gordon and Duguid (1970). Only the features relevant to the present analysis are described here.

Duncan Dam is an earthfill dam built during 1964-1967 on the Duncan River in British Columbia, Canada. The dam makes it possible to increase the power generation at downstream plants and also provides a measure for flood control.

The dam is about 120 feet high and 2500 feet long with an upstream sloping core. It was built across a valley, underlain by sediments about 1240 feet deep infilling a canyon. The stratigraphy of the foundation, shown in Fig. 5.1, is rather irregular with deposits ranging from the relatively incompressible gravel to silty clay layers, possessing considerable compressibility. The poor foundation conditions and previous experiments with dams on deep alluvial deposits dictated the use of conservatively flat side slopes. A typical cross-section of the dam is shown in Fig. 5.2. The designers of the dam anticipated large settlements and made provisions in the design and construction procedures to avoid excessive cracking (Gordon and Dugid, 1970). The main steps taken were the delayed placement of core-abutment ties, placement of overwet till core (1% to 2% greater than the optimum water content) and the self healing zoned section of the dam. Also the dam has been profusely instrumented with settlement gauges and piezometers both in longitudinal and transverse directions. The locations of the settlement gauges in plan view are indicated in Fig. 5.3. The positions of centrally located gauges (numbers 9 to 18) are shown in Fig. 5.1.

5.3.2 Observed Differential Settlement Cracks

The settlement records for the period from May, 1965 to October, 1966, taken from the construction reports, are plotted in Fig. 5.4. Each settlement line in Fig. 5.4 corresponds to the particular date indicated, and the corresponding level of fill is shown on the longitudinal section in Fig. 5.1. The settlement records clearly indicate a significant shift of the maximum settlement towards the left or east abutment. Although the maximum settlement agreed with the anticipated settlement in magnitude, its shift towards the left side was rather unexpected. These large differential movements resulted in transverse cracks in an area located on the upstream side of the dam and between the left abutment and settlement gauge No. 18. The extent of the area of visible cracking shown in Figs. 5.1 and 5.3 is between Sections 2 and 3 with the centre of the area located approximately 440 feet along the crest from the left abutment.

5.3.3 Sequence of Appearance of Cracks

The cracks did not all appear simultaneously and at the same level of construction of dam. The sequence of cracking is illustrated in Fig. 5.5. Cracking was first observed on August 14, 1966 on the upstream slope of the dam, about 210 feet from the centre line. Within a week the number of cracks increased with new ones appearing closer to the centre line of the dam, as indicated between Sections A and C in Fig. 5.5. It is of interest to note that during this particular week (August 15-22) the increment of settlement recorded by gauges Nos. 16 and 17 was about half a foot. As the settlement of the foundation continued and with the addition of some fill subsequent to August 14, 1966, further cracks appeared in the same zone in October, 1966. This time the cracking was located between Sections B and C as shown in Fig. 5.5. The approximate zones of cracks, as revealed by exploratory trenches and test shafts, and their sequence of development is shown in Fig. 5.6 along with the settlement of the base of dam in the transverse direction on August 14, 1966 and on October 28, 1966. The cracks revealed by the test shafts varied from one to three inches in width and extended downwards approximately to El. 1810.00, intercepting many large voids of about 10 inches in width.

Gordon and Dugid (1970) have described the measures subsequently adopted to control the cracking. These measures essentially consisted of preloading the area to the west of the cracked zone with a surcharge of 260,000 cubic yards of material to induce as much settlement as possible ahead of placing core and core-abutment tie, sluicing the gravel shell material with water to close all the previous cracks, increasing the capacity of gravel blanket and drains on the downstream side of the dam to handle more leakage, and changing the section of the dam in this area. The impervious core was brought closer to the upstream face where it could be placed as late as possible. An additional benefit of the surface core was its better accessibility for reworking any cracked area that might result from the settlement continuing at a substantial but decreasing rate for a number of years. The core material was made more plastic by mixing it with about 6% bentonite. This increased the plasticity index of core material from 4 to approximately 20. The downstream slope of the upper fill was flattened from 2:1 to 3:1 to increase the slope stability as a precaution against the saturation due to leakage through possible future cracks. The adoption of these measures and careful inspection since construction has resulted in satisfactory operation without any leakage.

5.4 Analysis of Cracking

The analysis presented here is concerned only with the period up to the end of October, 1966. The core material of Duncan Dam is a glacial till with the following characteristics (Gordon and Dugid, 1970):

Liquid limit	17.6%
Plasticity index	4.3
Proctor optimum moisture content	9.8%
Proctor maximum dry density	128 lbs./cft.

The grain size distribution is shown in Fig. 5.11. There is a considerable similarity between Duncan Till and Mica Till (Section 2.8.1). From the tensile studies conducted on Mica Till it can be concluded that a low plastic till such as Duncan Till will have a negligible tensile strength especially at water contents wet of optimum. The low tensile strength of the core material of Duncan Dam suggests the reasonable assumption that the cracks have appeared when one of the principal stresses became tensile. The problem of assessing the suitability of the finite element method for the prediction of cracking is one of calculating the zones of tension and comparing them with the zones of cracking observed in the actual structure.

A three dimensional finite element analysis has been used as it is more relevant in this present case than a two dimensional analysis. Nevertheless for the sake of comparison a two dimensional analysis has also been performed. During construction, the deformations and stresses in a fill dam result from the compression of the foundation and the gravity loading of the embankment itself. The effect of foundation settlement, which was the dominating factor in the case of Duncan Dam has been introduced into the analysis by specifying the incremental settlements derived from Fig.

5.4 at the base of the dam for various levels of construction as shown in Fig. 5.1. This represents a boundary condition of known displacements. The gravity loading was introduced by specifying the self-weight of only the newly added material of the fill. The analysis was performed in 5 lifts as shown in Fig. 5.1 with each lift analyzed twice. The three dimensional finite element idealization used is shown in Fig. 5.1 in the longitudinal direction and in Fig. 5.7 in the transverse direction. A total of 310 elements and 426 nodes were used. The material idealization consisting of core, pervious, semi-pervious, and common pervious types is also shown in Fig. 5.7.

The non-linear stress-strain relationships were introduced into the analysis in digital form as described in Chapter III. The triaxial test data used in the analysis for the materials are shown in Figs. 5.8, 5.9 and 5.10. Consolidated undrained test results were used for the impervious and the semi-pervious materials because it was thought that such data would be the most representative of the field conditions. These are somewhat in between the two extreme limits of unconsolidated-undrained and consolidated-drained conditions. This is partly because of the rapid loading during the embankment construction and partly due to the low pore pressures generally developed in the core and the semi-pervious zone. However it is recognized that the approach can only be approximate as the partial consolidation that occurs in the field cannot be represented accurately by the conventional consolidated undrained tests.

The stress-strain data used for core and semi-pervious zone in the analysis were derived from the available triaxial test results of Duncan Dam materials obtained prior to the construction of the dam. These tests were performed on samples comprising materials below 3/4" size. The test specimens were prepared in a 4" diameter by 8" high, 3 part split mould. Soil was compacted in five equal layers of approximately 1.7" thicknesses. Twenty-five blows of a standard 5.5 lb. hammer with a 12" drop were applied to each layer. Tests were performed on samples prepared at optimum water content and 3% greater than optimum. Since the placement water content was approximately at 1% to 2% greater than the optimum the stress-strain data used in the analysis was derived from the available test data by averaging the stress-strain relationships. Stress-strain data were not available for the pervious and the common-pervious material used in Duncan Dam, therefore drained triaxial test results of a gravelly material having similar gradations as at Duncan was used in the present analysis. The stress-strain relationships (Figs. 5.9 and 5.10) used in the analysis for the pervious and the common-pervious materials were derived from the available extensive triaxial test data obtained in connection with the design of Mica Dam for different gradations of sand and gravel. The test results were partly reported by Skermer and Hillis (1970). The tests were performed on 6" x 12" samples, at different cell pressures ranging up to 450 psi.

The corresponding gradations of pervious and common pervious material, for which the stress-strain relationships were derived, are shown in Fig. 5.11. The average gradation curves of pervious, semi-pervious and core material of the Duncan Dam are also shown in Fig. 5.11.

As discussed in Chapter III Poisson's ratio was limited to a maximum value of 0.49. "No tension" analysis was not performed for the reasons given in Section 4.10. The calculation of the elastic parameters in terms of K and G was done using the procedure described in Section 3.9.

The two dimensional analysis was performed assuming plane strain conditions along the central longitudinal section, the idealization of which is shown in Fig. 5.14. The analysis used 235 nodes and 388 constant strain triangular elements. The number of lifts and the construction levels were kept the same as for the three dimensional analysis (Fig. 5.1).

5.5 Results of Analyses

5.5.1 Three Dimensional Analysis

The aim of the analysis was to compare the locations of the tensile stresses computed for the idealized analytical model of the dam with the location of the cracks observed in the real structure. The zone of cracking, as noted earlier, was confined between transverse sections 2 and 3 (Figs. 5.3 and 5.5). It is convenient to deal with the development of the cracks between these sections by considering an intermediate section located at a distance of 440 feet from the left abutment (Fig. 5.5). This section is located approximately in the centre of the cracked area. To facilitate the comparison of progressive development of cracks along the transverse direction and height of the dam, vertical lines I, II, III and IV in Figs. 5.5 and 5.6 are considered. These are the vertical lines at which the sections A, B, C and D intersect the intermediate section, referred to above.

The distributions of minimum principal element stresses and strains along the vertical lines I, II, III and IV have been computed by three dimensional analysis for two different time instances, August 14 and October 28, which correspond to two different levels of filling and settlement of foundation. The results of the present three dimensional analysis along with those of a previous three dimensional analysis (Eisenstein et al., 1972) are shown in Fig. 5.12. The previous analysis differs from the present one only in the following respects:

(1) Because of the limitation on the number of material types that could be handled by the previous computer program only three types of material namely the pervious, core, and semi-pervious materials were considered in the previous analysis. The common-pervious material considered in the present analysis was assumed to be the same as the semi-pervious material. The zone represented by the common-pervious material of the present analysis

is in general stiffer than the corresponding zone of the previous analysis.

(2) The elastic moduli were calculated directly from the conventional plots of triaxial test data, instead of the stress invariant approach, used in the present analysis. The reference confining stress was assumed to be average of the minor and intermediate principal stresses that occur in an element. Whenever a principal stress assumed a negative value it was considered to be zero in calculating the confining stress needed for the derivation of moduli. When both the minor and intermediate principal stresses were negative, the confining stress was assumed to be zero.

The results by the previous and the present analysis are discussed below.

On August 14, 1966 the first cracks appeared in the area upstream of vertical line I and in its vicinity. The analytical results obtained for this stage show that the only tensile stress found is along the vertical line I and above an elevation of about 1830 feet. All other parts of the dam remain in compression at this time with regard to stresses, although principal tensile strains are common. Within a week, more cracks developed extending towards the centre line. However no analysis has been performed for conditions at this date (August 22, 1966).

In October, 1966 a new distinct crack was observed within the same transverse section but now extending between sections B and C (Fig. 5.5). The stresses calculated along vertical lines II and III clearly indicate tension between sections B and C for the conditions existing at the end of October. Tension is not indicated along vertical line IV and no cracks were detected in its vicinity. Therefore, the calculations indicate reasonably well the sequence of cracking along the transverse section. It is interesting to note that the previous and present analysis, although introducing slightly different elastic parameters into the computations, lead to the same conclusions as regards the sequence of cracking. This indicates that the most dominant factor in the analysis of cracking at Duncan Dam is the effect of the settlement of the foundation.

In order to verify the location of the cracks in the longitudinal direction, the distribution of minimum principal stresses and strains along centre line and section B are shown in Fig. 5.13. The stresses and strains are plotted for surface elements for two dates namely, August 14, 1966 and October 28, 1966. Since these stresses and strains obtained by the previous and the present analyses are almost the same (Fig. 5.12), the results of only the present analysis are shown in Fig. 5.13. From this figure, it can be seen that the analysis indicates the location of the cracks along the longitudinal section of the dam with reasonable accuracy. Some tensile stresses are also indicated adjacent to the right abutment and, indeed, limited cracking was observed in this area as well.

5.5.2 Two Dimensional Analysis

The distributions of minimum principal stress and strain along the central longitudinal section (Fig. 5.14) for two dimensional analysis are shown in Fig. 5.15. It can be seen that the location of the transverse section along which cracks appeared is predicted properly by the two dimensional analysis. However, the sequence of cracking and the distribution of cracks along the transverse section cannot be predicted as a plane strain condition is not satisfied on sections A, B and D (Fig. 5.5).

5.6 Summary

Duncan Dam, constructed on an extremely compressible foundation, was subjected to severe cracking due to large differential foundation settlement. Accurate and detailed observations of settlements and cracks at Duncan Dam constitute an important case history. Advantage of this was taken to test the usefulness of finite element analysis for assessing the cracking potential of earth structures.

The stresses and strains in Duncan Dam were computed using a three dimensional finite element program including the realistic boundary conditions, the non-linear stress-strain relationships and the actual construction step sequence. Two dimensional finite element analysis has also been performed assuming a plane strain condition along the central longitudinal section. The results of the three dimensional analysis predict reasonably well both the location and sequence of development of the cracks. The two dimensional analysis predicts reasonably well the location of cracks along the longitudinal section, although the sequence of development of cracks along the transverse section cannot be predicted. The agreement found between analysis and observation is noteworthy since it is unlikely that the stress-strain relationships used in the analysis are wholly representative of the in-situ behaviour. One might anticipate that sometimes the agreement between the observed and predicted displacements will be less impressive compared to the agreement between stresses. This is due to the fact that displacements are, in general, more sensitive to the variation of elastic parameters used in the analysis than are stresses. From the results of the finite element analyses performed on Duncan Dam, it may be concluded that the finite element method has a considerable potential in the analysis of cracking of earth dams. Reasonable predictions regarding the cracking of earth dams appear to be possible even with the use of simple, isotropic elastic theory in the analysis.

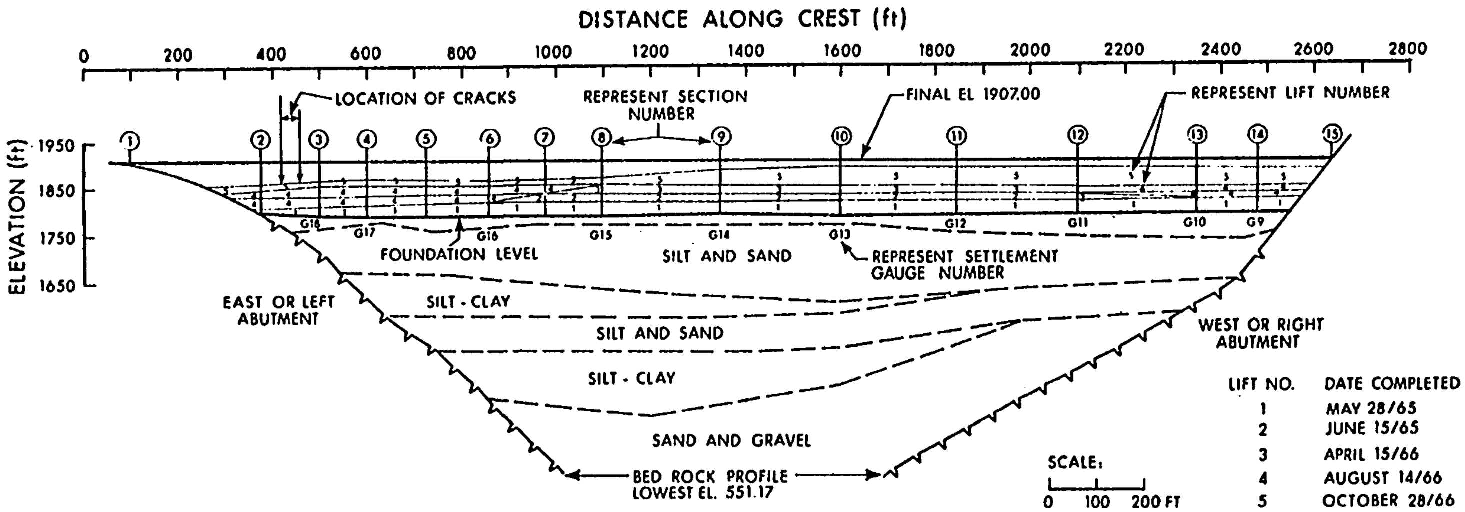

FIG. 5.1 LONGITUDINAL SECTION OF DUNCAN DAM SHOWING CONSTRUCTION SEQUENCE AND LOCATION OF CRACKS

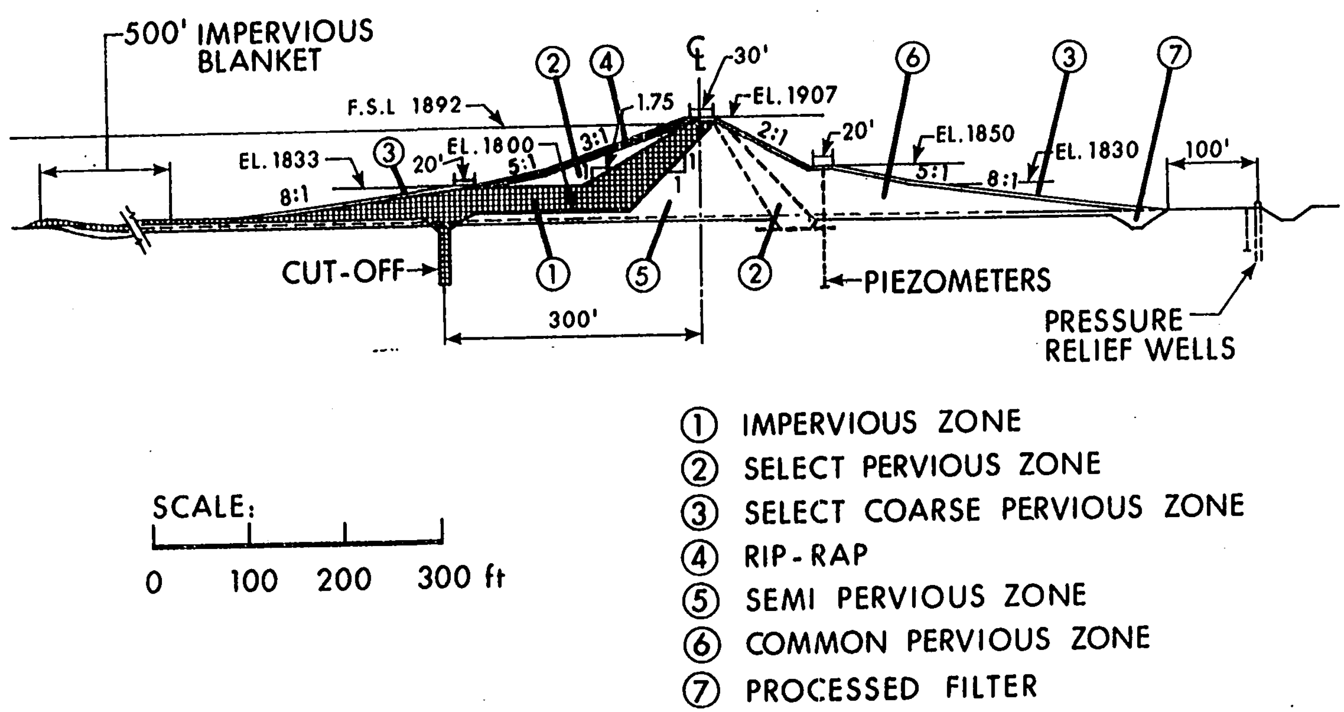

FIG. 5.2 A TYPICAL CROSS SECTION OF DUNCAN DAM [AFTER GORDON AND DUGUID, 1970]

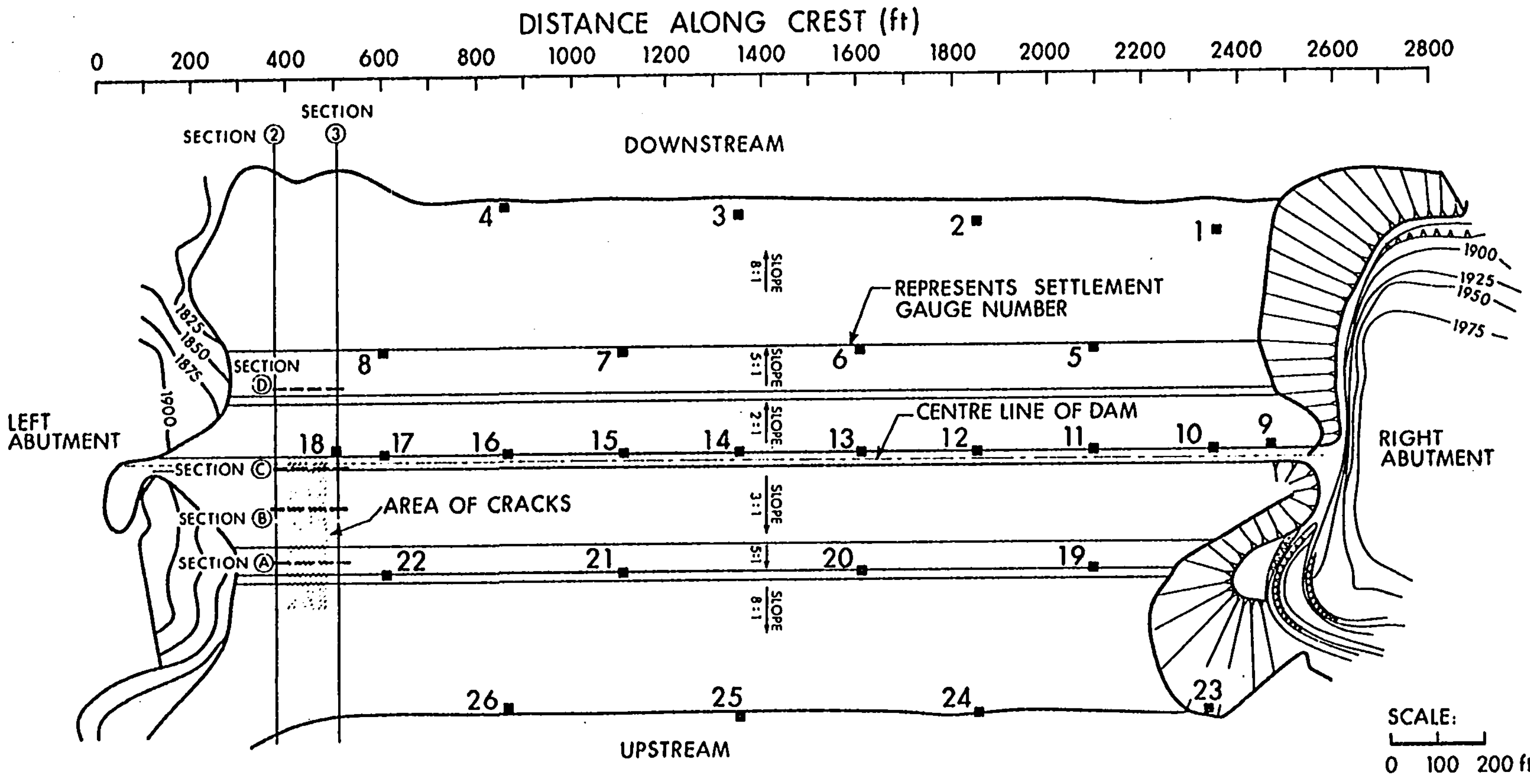

FIG. 5.3 PLAN VIEW OF DUNCAN DAM SHOWING LOCATION OF SETTLEMENT GAUGES AND AREA OF CRACKS

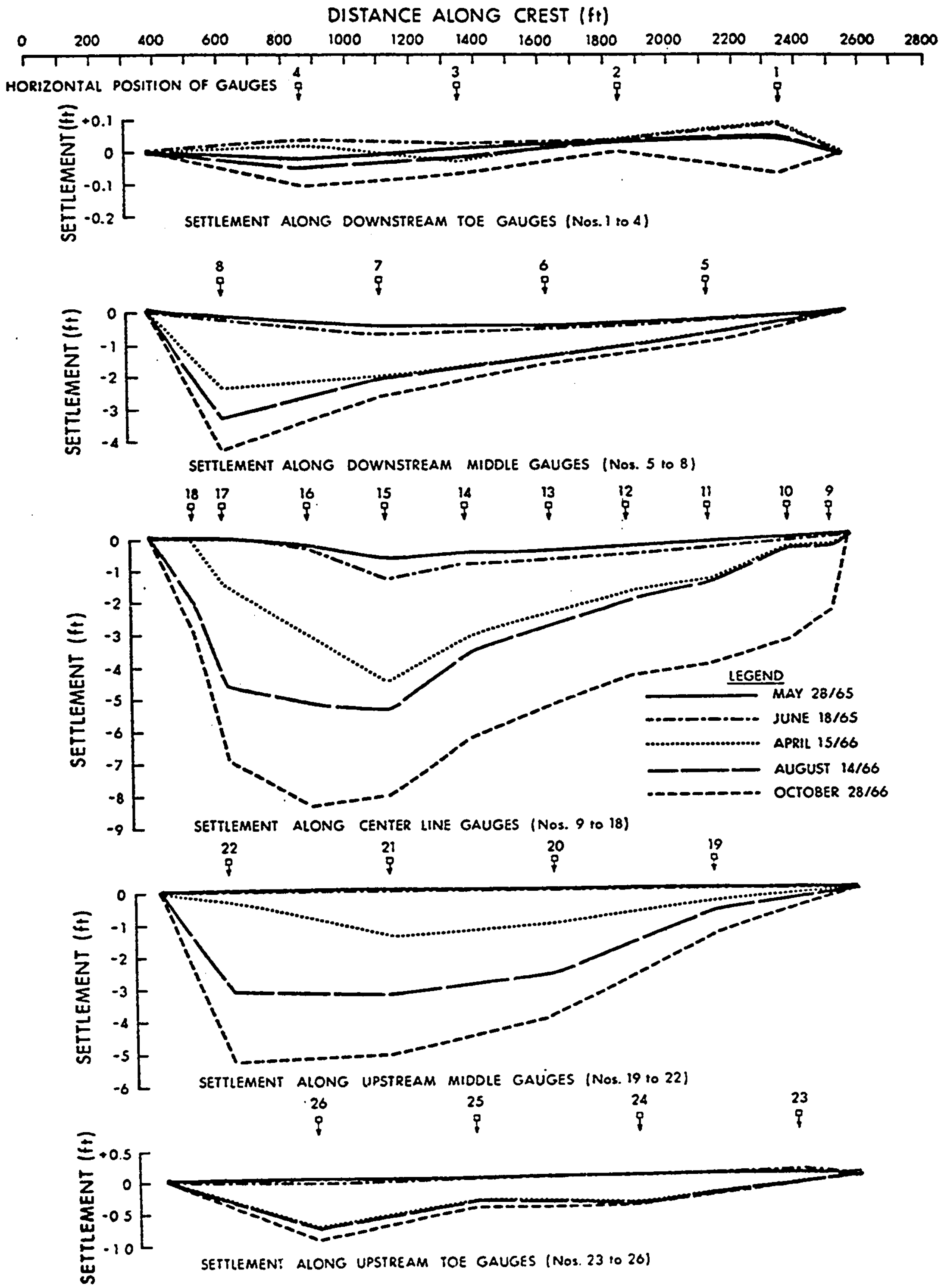

FIG. 5.4 SETTLEMENT ALONG LONGITUDINAL SECTIONS

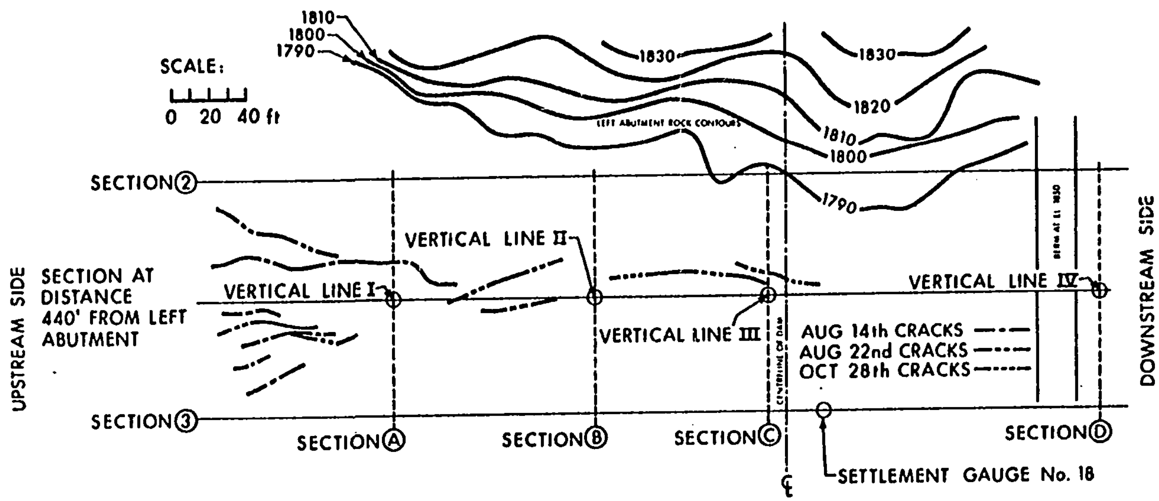

FIG. 5.5 SEQUENCE OF DEVELOPMENT OF CRACKS

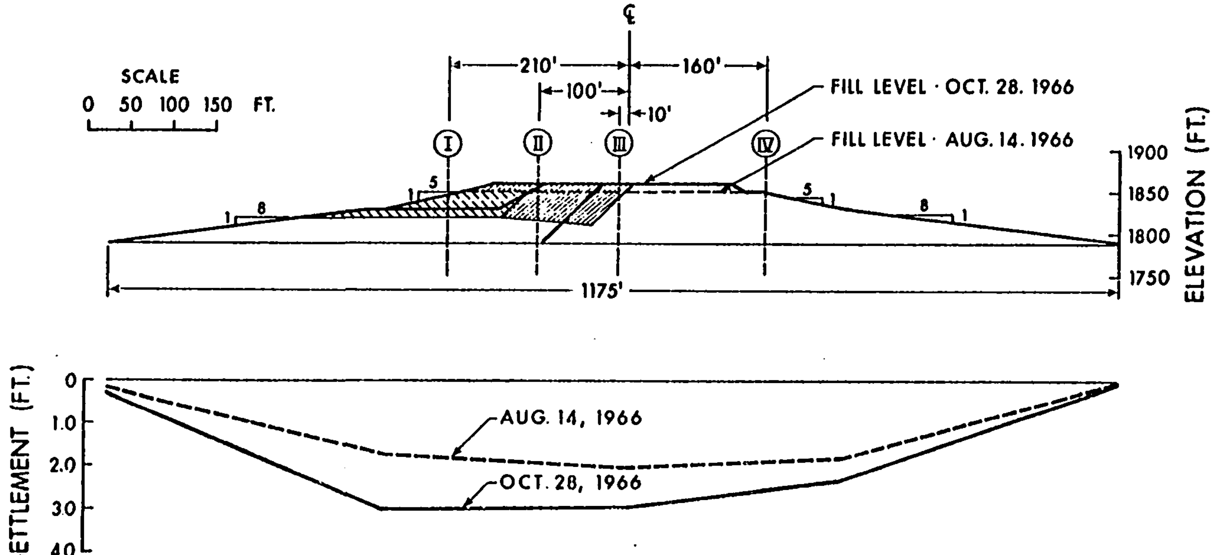

SETTLEMENT OF FOUNDATION ALONG THE SECTION

LEGEND

I, II, III, IV - VERTICAL LINES ALONG WHICH STRESSES AND STRAINS ARE STUDIED

℄ - CENTRE LINE OF DAM

ZONE OF ORIGINAL CRACKS OBSERVED DURING AUG. 1966

ZONE OF FURTHER CRACKS OBSERVED UP TO OCT. 1966

FIG. 5.6 SECTION OF DAM AT A DISTANCE OF 440 FEET FROM LEFT ABUTMENT SHOWING APPROXIMATE ZONES IN WHICH CRACKS DEVELOPED PROGRESSIVELY

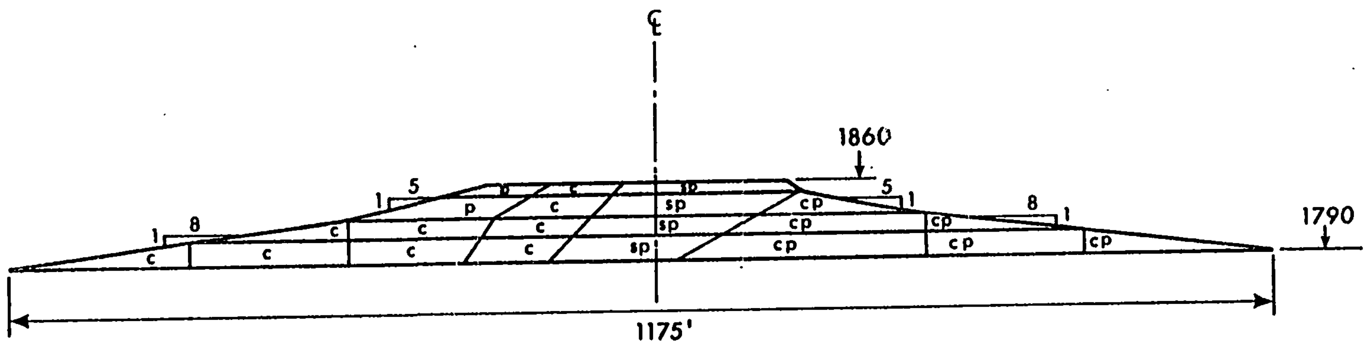

MATERIALS IN ELEMENTS: c - CORE
p - PERVIOUS
sp - SEMI PERVIOUS
cp - COMMON PERVIOUS

SCALE:
0 50 100 ft

FIG. 5.7 FINITE ELEMENT IDEALIZATION AT SECTION 3 FOR THREE DIMENSIONAL ANALYSIS

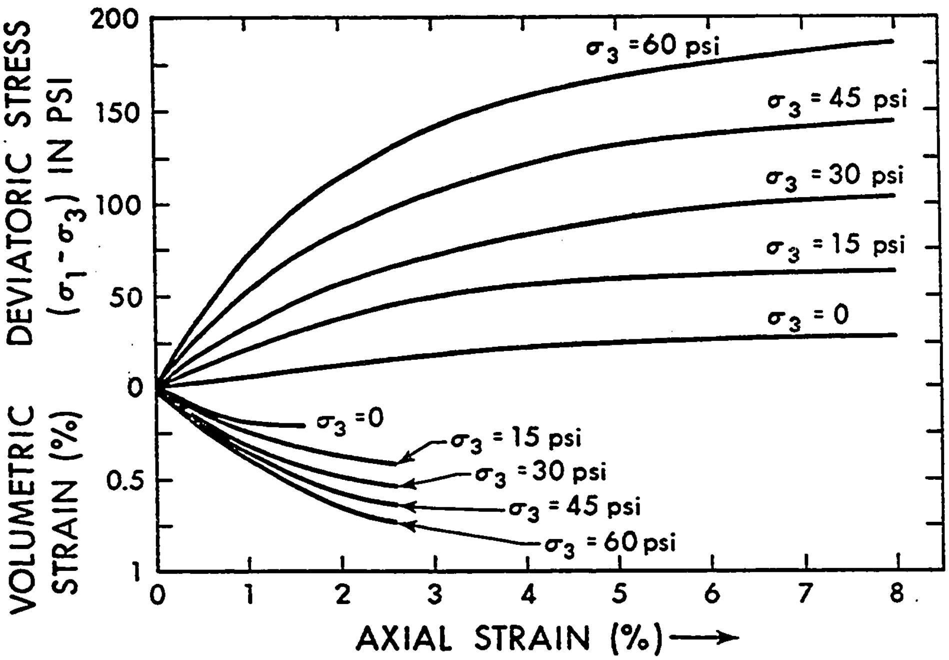

CORE MATERIAL

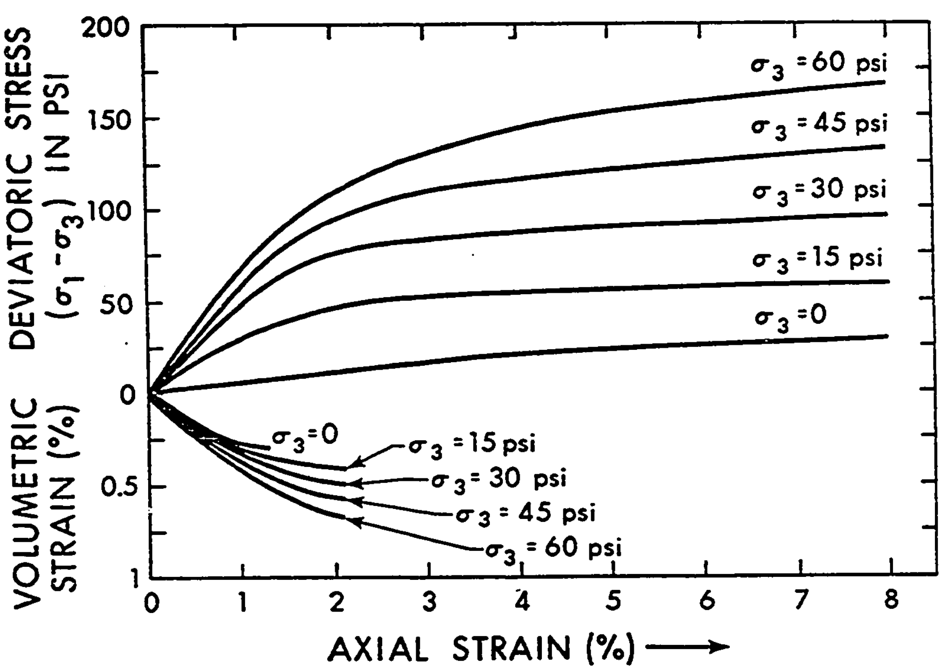

SEMIPERVIOUS MATERIAL

FIG. 5.8 CONSOLIDATED UNDRAINED TRIAXIAL STRESS-STRAIN RELATIONSHIPS FOR THE CORE AND SEMIPERVIOUS MATERIAL OF DUNCAN DAM

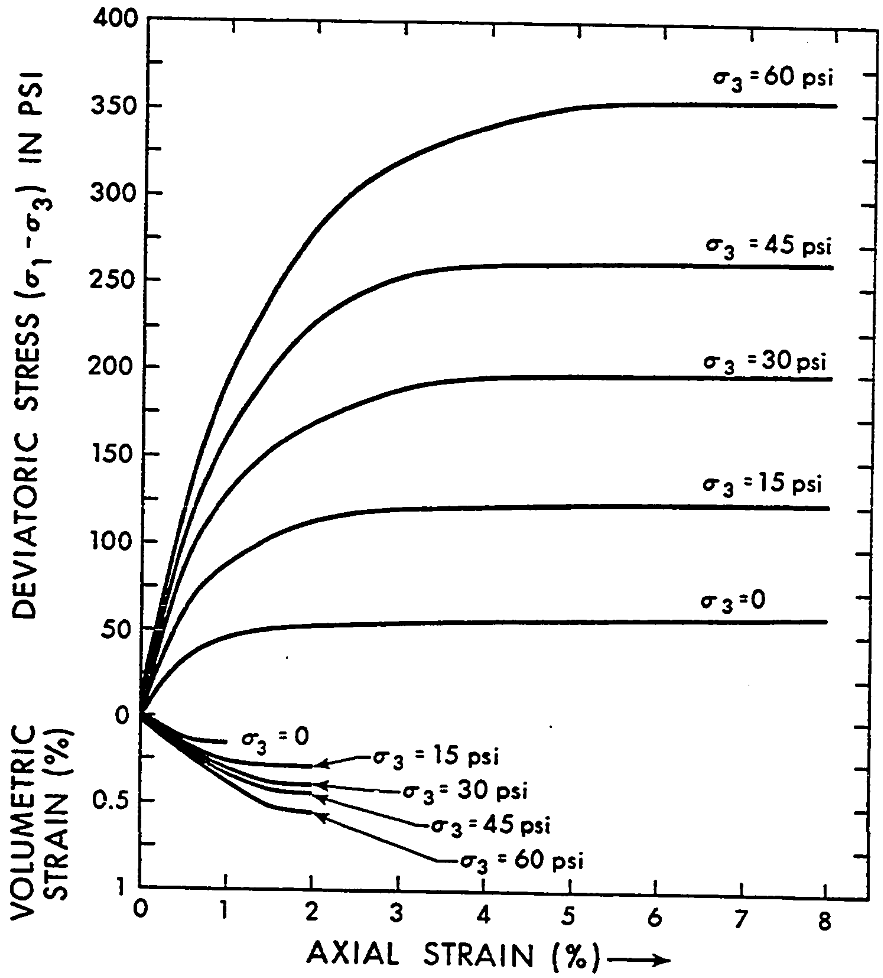

FIG. 5.9 CONSOLIDATED DRAINED TRIAXIAL STRESS-STRAIN RELATIONSHIPS FOR PERVIOUS MATERIAL

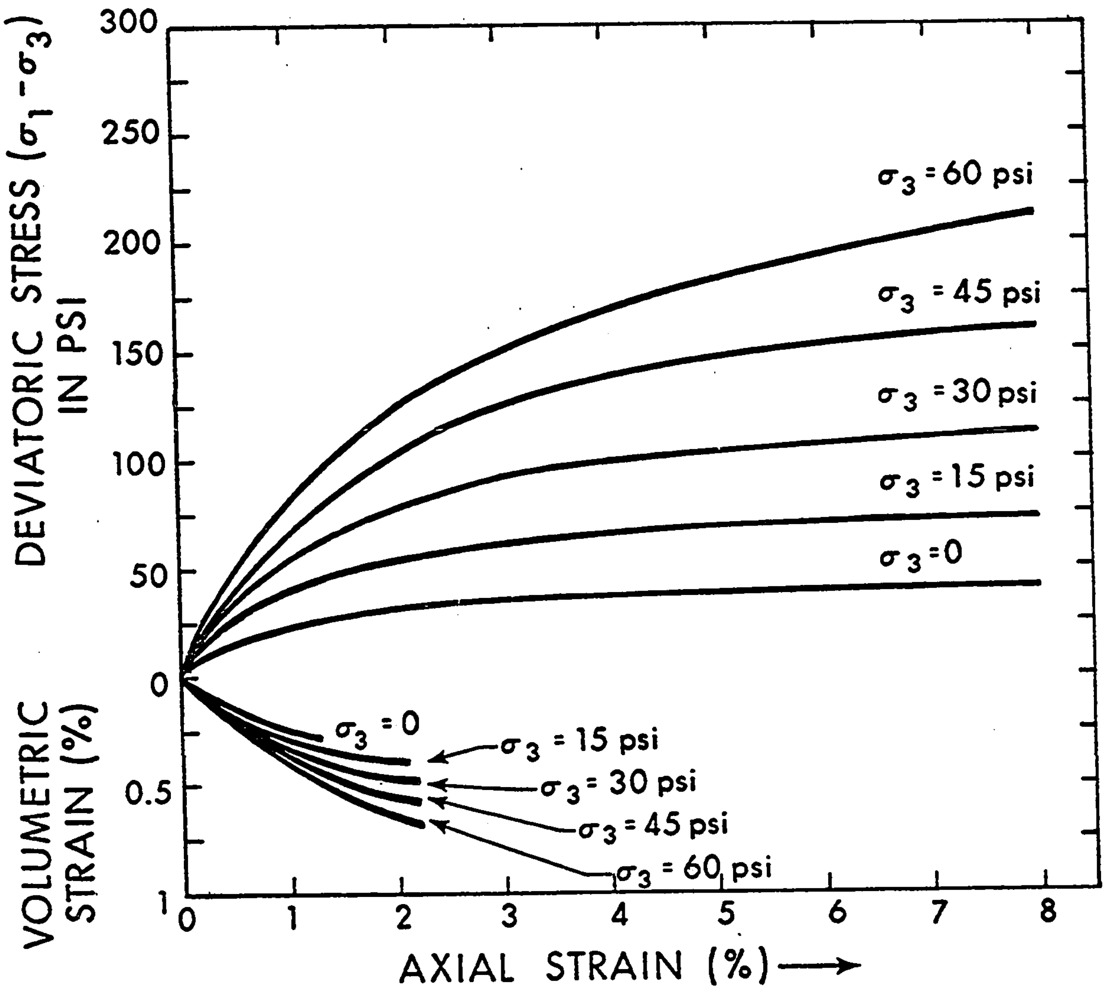

FIG. 5.10 CONSOLIDATED DRAINED TRIAXIAL STRESS-STRAIN RELATIONSHIPS FOR COMMON PERVIOUS MATERIAL

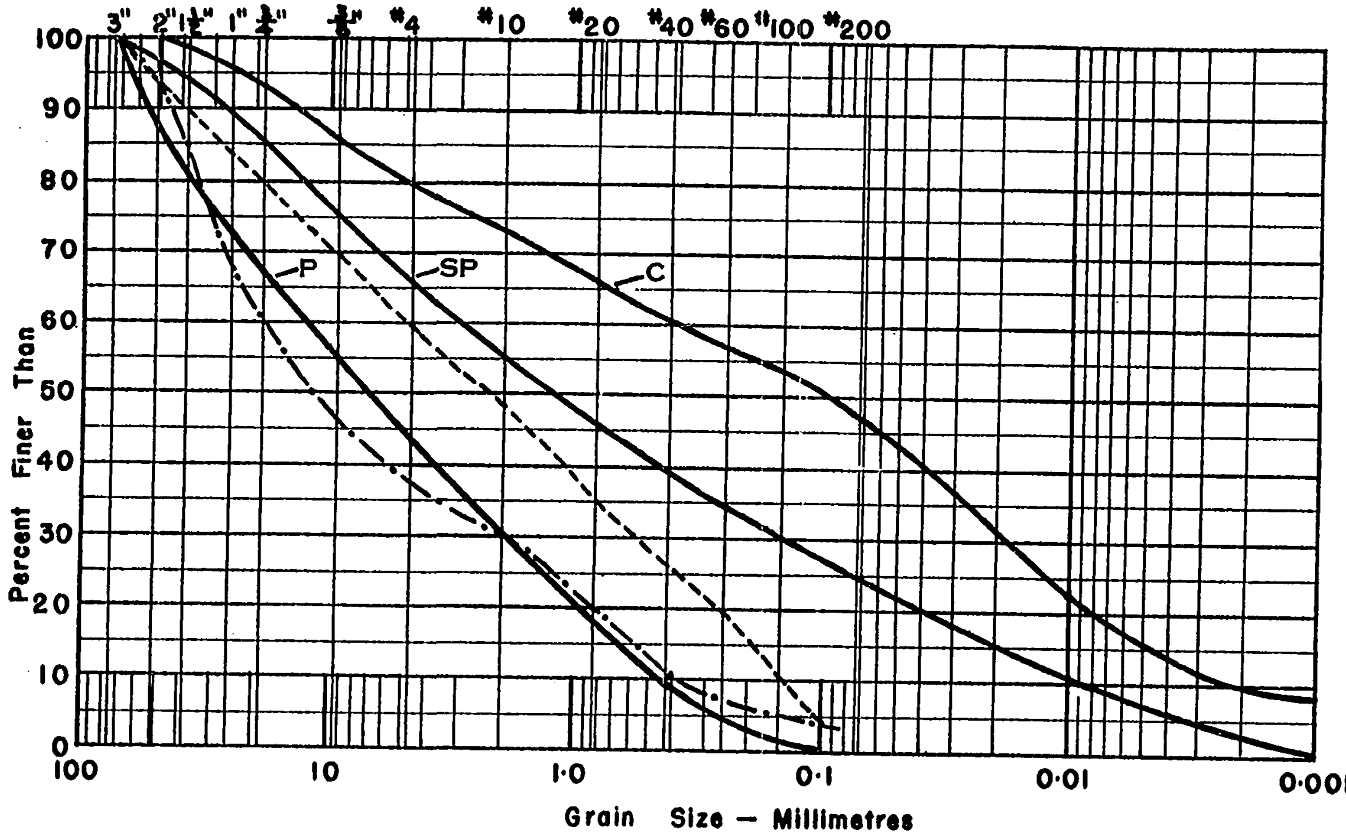

—··— GRADATION OF PERVIOUS MATERIAL USED IN ANALYSIS

—·— GRADATION OF COMMON PERVIOUS MATERIAL USED IN ANALYSIS

P PERVIOUS MATERIAL OF DUNCAN DAM

SP SEMIPERVIOUS MATERIAL OF DUNCAN DAM

C CORE MATERIAL OF DUNCAN DAM

FIG. 5.11 GRAIN SIZE DISTRIBUTION CURVES FOR MATERIALS OF DUNCAN DAM

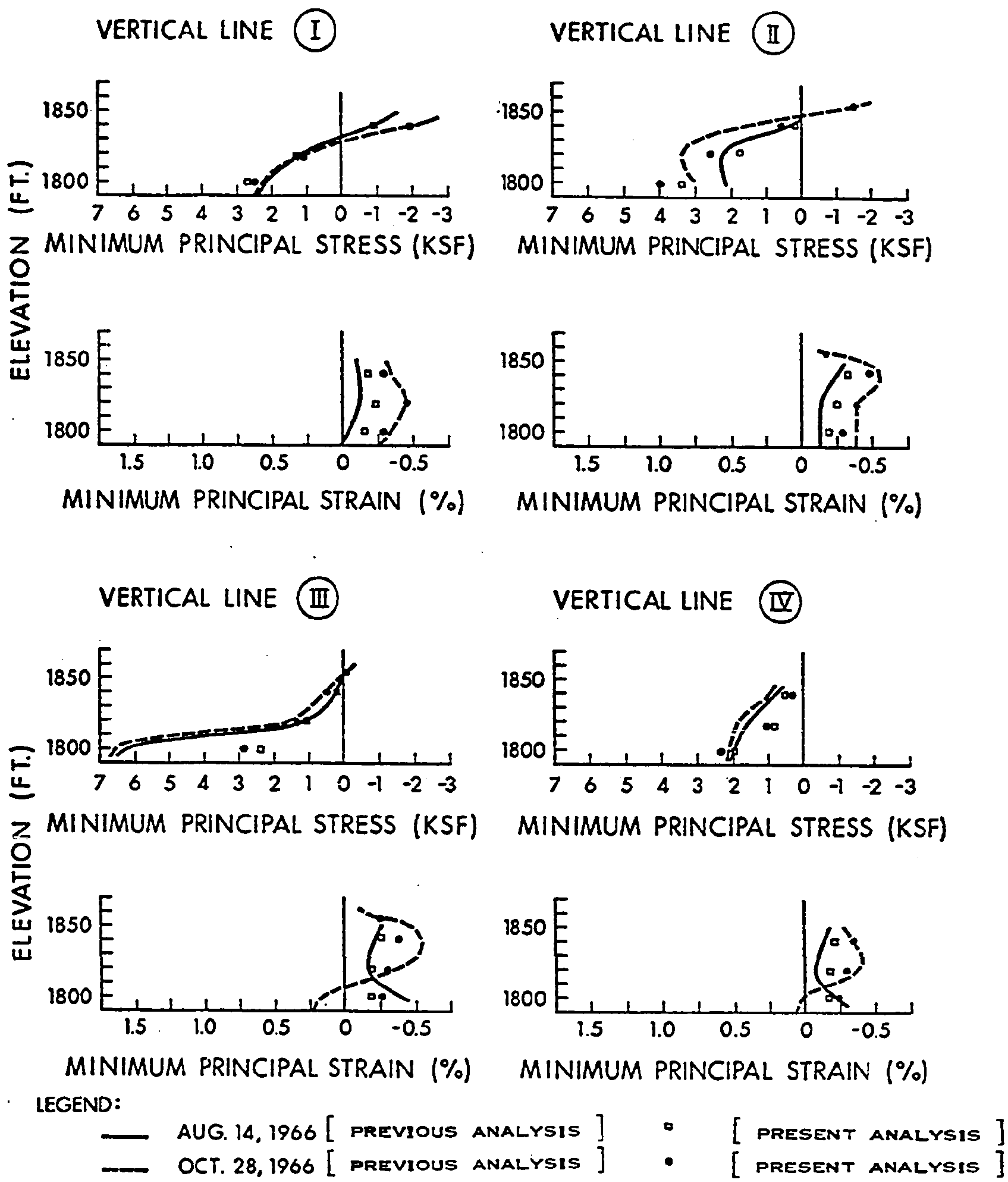

FIG. 5.12 DISTRIBUTION OF MINIMUM PRINCIPAL STRESSES AND STRAINS ALONG VERTICAL LINES I, II, III, AND IV

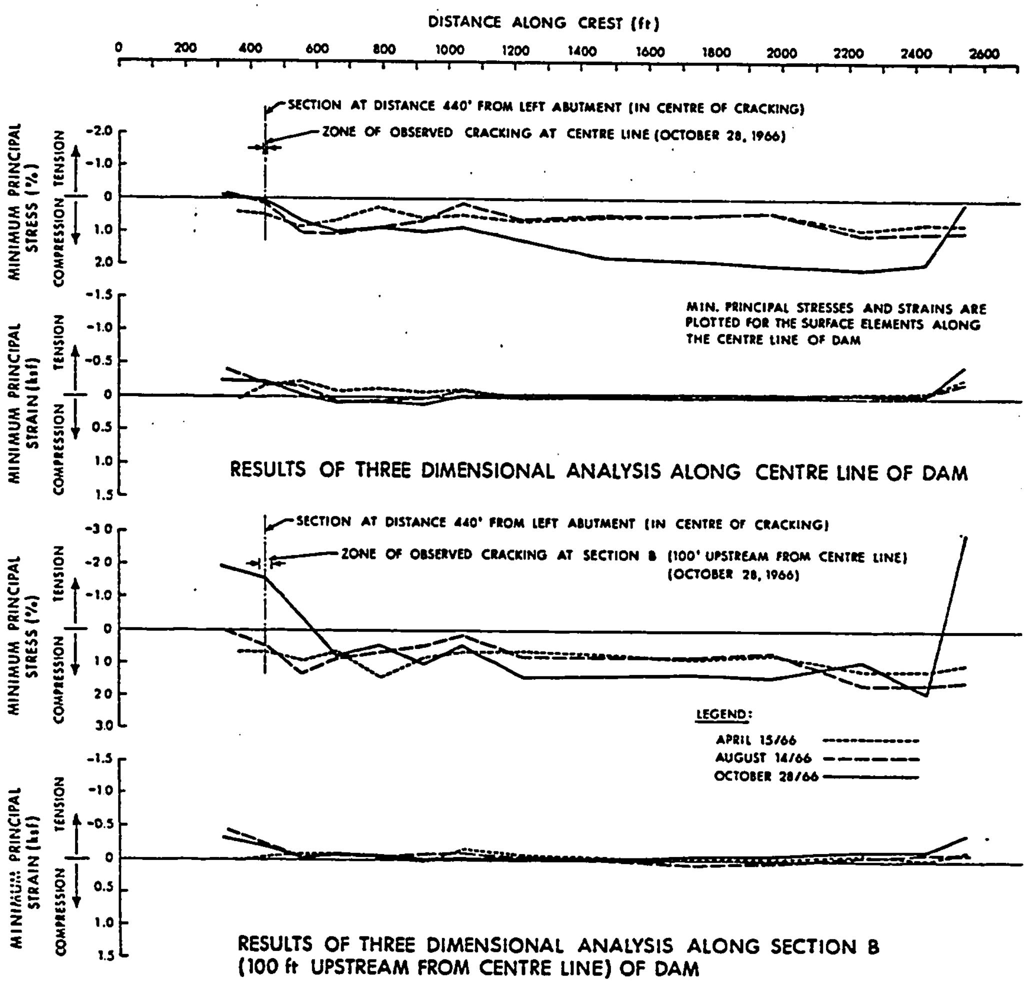

FIG. 5.13 MINIMUM PRINCIPAL STRESSES AND STRAINS ALONG TWO LONGITUDINAL SECTIONS FOR THREE DIMENSIONAL ANALYSIS

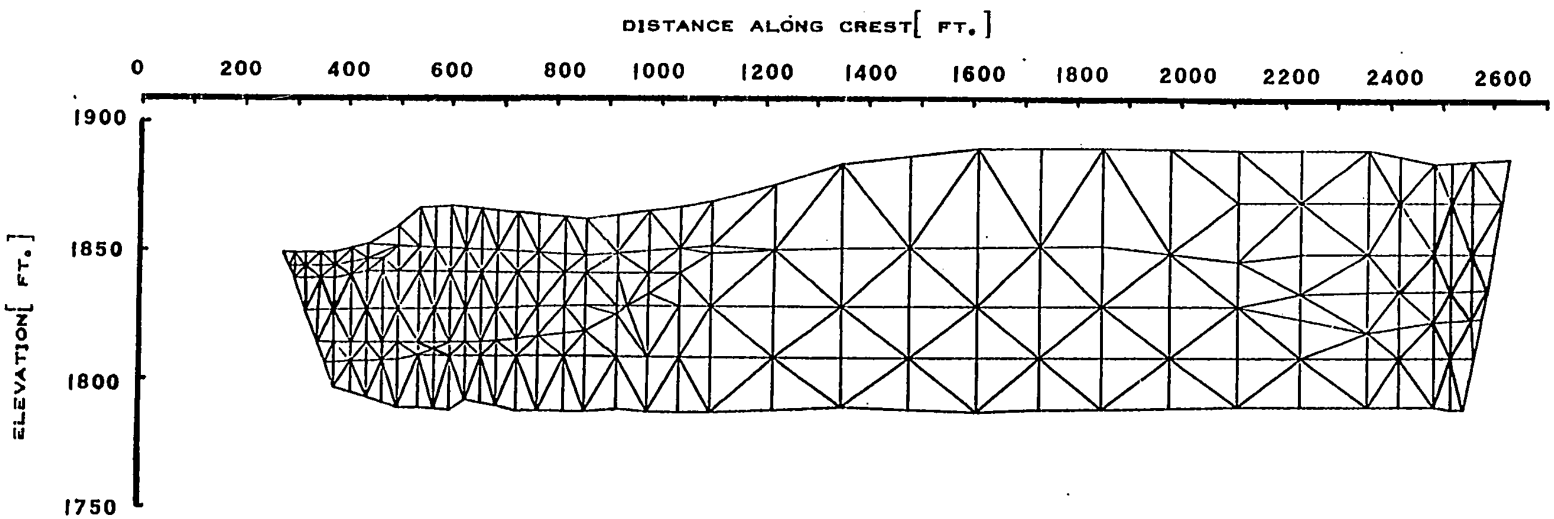

FIG. 5.14 FINITE ELEMENT IDEALIZATION ALONG CENTRAL LONGITUDINAL SECTION FOR TWO DIMENSIONAL ANALYSIS

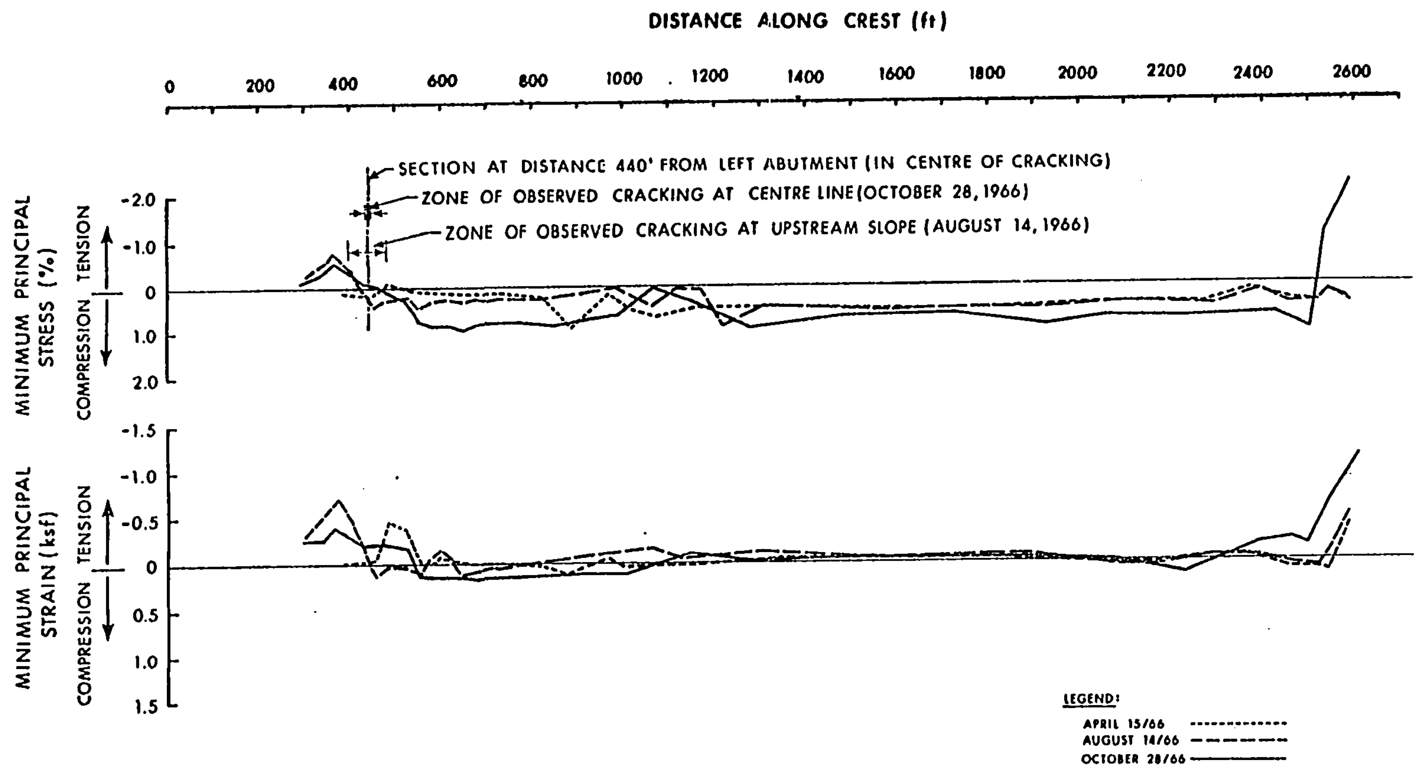

FIG. 5.15 MINIMUM PRINCIPAL STRESSES AND STRAINS ALONG THE CENTRAL LONGITUDINAL SECTION FOR TWO DIMENSIONAL ANALYSIS

CHAPTER VI

CONCLUSIONS AND SUGGESTIONS FOR FURTHER RESEARCH

6.1 General

The finite element method is a very useful and versatile tool for the analysis of cracking of earth dams. To obtain results that are useful in the prediction of cracking of earth dams during and at the end of the period of their construction, the geometry of the dam, the displacement boundary conditions, the construction step sequence, and the stress-strain relationships of soil are to be simulated properly in the analysis.

For a proper simulation of certain complex geometries and boundary conditions of the dam a three dimensional analysis becomes a necessity. In general a three dimensional analysis requires a considerable amount of computer memory and computer time. However, with the availability of large capacity computers three dimensional finite element analyses for large structures such as earth dams, are now feasible.

Any procedure, that attempts to simulate the real stress-strain behaviour of a soil, can only be approximate for the following main reasons:

(1) A satisfactory theory which can completely account for the deformational behaviour of soils is not presently available.

(2) The limitations that usually exist in the field and

laboratory test procedures make it difficult to obtain the necessary parameters to describe the deformation of soils under different conditions of loading.

Assuming piecewise linearity, isotropic elastic theory has been used in the present analysis of cracking of earth dams. Though the theory cannot account for the dilatancy effect of soils, it is simple and the parameters needed for its application to the analysis are easily obtained from the conventional laboratory tests. The acceptable agreement obtained in this work between the results of analysis and the field observations at Duncan Dam suggests that the theory used in the analysis is satisfactory for the prediction of cracking of earth dams.

6.2 Criterion for Failure of Soil in Tension

Soils are extremely weak in tension. From the results of the tensile studies conducted on a low plastic glacial till (Chapter II) it can be concluded that when the placement water content is above optimum the tensile strength of soil is practically equal to zero. Hence, a criterion for tensile failure, based on zero tensile strength for the core of the dam, appears to be appropriate. When the analysis is aimed at evolving a suitable design for an earth dam against tensile cracking it is prudent to neglect the tensile strength of the material of core. A criterion based on tensile strain at failure has been suggested (e.g., Narain, 1962). This has the following disadvantages when compared to the criterion based on zero tensile strength:

(1) The tensile strain at failure for a soil is a sensitive parameter depending on factors such as type of soil, water content, rate of strain, type and the amount of compaction, state of stress in the directions normal to the direction of tensile stress, and the type of tension test used. In comparison to the compression tests, tension tests are more difficult to perform as routine soil tests. The tensile strains are usually observed over large distances along the crest of dam whereas the laboratory tensile strains are observed on comparatively small specimens tested under certain particular stress states. As such the correlation achieved between the field and laboratory tensile failure strains can only be approximate.

(2) In general when compared to the strains the stresses computed in an analysis are less sensitive to the changes in elastic moduli. Because of the present limitations that exist in simulating the stress-strain behaviour of soil using laboratory test data it is unlikely that the stress-strain relationships used in the analysis would be wholly representative of the field behaviour of soil. Under these circumstances it appears reasonable to place more reliance on the computed stresses rather than on the computed strains.

(3) There is a possibility for a principal strain to be tensile while the three principal stresses remain com-

pressive. This situation does not lead to a tensile crack. The analysis of cracking at Duncan Dam (Chapter V) indicated the observed tensile cracks only occurred at locations where one of the principal stresses and the corresponding strain were tensile. This indicates that the criterion based on tensile strain alone is inadequate for the analysis of cracking. When the tensile strength of the soil is assumed to be zero no reliance on tensile tests need be made in the analysis.

Laboratory tensile tests are, however, useful for making comparative studies on tensile characteristics of soils. Such studies are useful in specifying the type of core material and its placement conditions for an effective control of cracking. In spite of the limitations outlined previously the laboratory tensile failure strains still provide useful information to aid in the interpretation of the field tensile strain measurement data.

6.3 Tensile Characteristics of Soil

The indirect tension test procedure, used in the present work for evaluating the tensile characteristics of a typical till, was found to be satisfactory. The test procedure can be used for soils with low to medium plasticity to ensure a brittle failure. A procedure to obtain the tensile stress-strain relationship for soils with different moduli in tension and compression is indicated.

Based on the laboratory tests performed on Mica Till with and without the addition of small amounts of bentonite the following conclusions are drawn:

(1) When the water content is above optimum the flexibility of a soil increases rapidly with the water content whereas the tensile strength decreases with the water content. The percentage decrease in tensile strength, with a given percentage increase in water content above optimum, is more in a low plastic soil compared to that of a soil with high plasticity. Hence the addition of highly plastic bentonite to a low plastic till aids in achieving the required flexibility without much reduction in the tensile strength.

(2) Rate of loading has considerable effect on the tensile stress and strain at failure. From the results obtained on Mica Till and from those reported by Tschebotarioff et al. (1953) and Narain (1962) there appears to exist, for compacted soils, a critical rate of loading that mobilizes the minimum tensile stress and strain at failure. A knowledge of the critical rate of loading is useful in obtaining the minimum tensile strain at failure for a given soil at a given water content.

(3) An increase in compactive effort decreased the flexibility and increased the tensile strength of till when the water content is well below the Proctor optimum. For water contents near and above the Proctor optimum the tensile strength decreased with the compactive effort. For the type of soil tested, over compaction at water

contents greater than the Proctor optimum hardly improves the tensile strength of soil.

6.4 Factors Affecting the Development of Tensile Zones in Earth Dams During Construction

The results of a finite element analysis, concerning the development of tensile zones in an earth dam during its construction depends on the simulation of a number of factors in the analysis. To evaluate the influence of different factors parametric studies were conducted. From the results of these parametric studies the following conclusions are offered.

6.4.1 Single Step and Incremental Loading

One of the important factors to be considered in the simulation of the construction of an earth dam in the analysis is the construction step sequence. While a single step analysis is simpler and less time consuming than an incremental analysis, it results in unrealistic displacements and exaggerated tensile zones. For a proper simulation of the construction step sequence an incremental analysis becomes a necessity. The optimum number of increments needed for an analysis is governed by the cost of computation and the accuracy of the results required. After a given number of load increments, the results become practically insensitive to further increments. In the case of a three dimensional analysis, because of its high cost of computation, the limitations on the number of increments becomes more severe than a two dimensional analysis.

6.4.2 Linear and Non-Linear Analyses

A non-linear analysis, which simulates the non-linear stress-strain behaviour of soils, is more realistic than a linear analysis. Comparison of linear and non-linear analyses showed that the tensile stresses obtained by a linear analysis are higher than those computed by a non-linear analysis. The non-linear behaviour of a soil can be simulated conveniently in an incremental analysis. A procedure to determine the elastic parameters from the laboratory test data, converted to a stress invariant form, is suggested. The use of this procedure offers the following advantages:

(1) An assumption regarding the third principal stress is not necessary.

(2) Approximations in representing the laboratory stress-strain relationships are eliminated because the experimental data is supplied in digital form.

A close agreement between the experimental stress-strain relationship and those obtained in the analysis is possible if each step is analyzed twice. The "average moduli" approach used in the analyses here is found to be satisfactory.

6.4.3 "No Tension" Analysis

In an incremental non-linear analysis the tensile stresses computed in the zones of tension are of small magnitude. Hence the local stress redistribution, that occurs due to the removal of tensile stresses from the tensile zones, does not alter the development of tensile zones computed subsequently in the upper layers. As a "no tension" analysis involves an iterative procedure considerable savings in the cost of computation can be effected in a three dimensional analysis by not removing the tensile stresses.

6.4.4 Three Dimensional Effects

The plane strain condition, generally assumed in the analysis of cracking of earth dams, is satisfied only for homogeneous dams with a symmetrical cross section. The non-homogeneity of the materials and complexity of the geometry of the dam are often the main reasons necessitating a three dimensional analysis. Where the material of core differs from that of the shell significant errors arise from a two dimensional analysis. The tensile stresses are under-estimated when shell is more flexible than core and they are over-estimated when shell is less flexible than core.

6.5 Control of Cracking by Non-Homogeneous Modelling

As indicated in Chapter IV (Section 4.9) a considerable reduction in tensile stresses is possible by changing the placement specifications of the fill in critical tensile zones. To derive suitable placement specifications, the finite element method can be used to a considerable advantage in analyzing the effect of changing the flexibility of core in the zones of computed tensile stresses.

6.6 Applicability of the Analysis of Cracking to a Real Structure

A three dimensional finite element analysis when applied to a case study of cracking at Duncan Dam, showed a reasonably good agreement between the computed and the observed tensile zones. This indicates, with proper simulation of the various factors (Section 6.3) in the analysis, the finite element method can be used with reliance for the analysis of cracking of earth dams during and at the end of their construction. Finite element analytical procedure may also be used as a design tool to control cracking in earth dams (Section 6.5).

6.7 Suggestions for Further Research

Based on the work presented here, the following further research and field studies on deformation and cracking of earth dams are suggested:

(1) The stress-strain relationships used in the analysis should be such that they enable a proper simulation to be made of the deformational behaviour of soil under different conditions of loading. To obtain such stress-strain relationships suitable laboratory test procedures should be evolved. A theory, which also considers the dilatancy effect of soils, is desirable, especially for problems involving large strains and failures due to shear.

(2) The analysis of cracking of earth dams presented here is limited to the period of construction of dam. It is desirable to consider other critical conditions such as the first filling of reservoir and earthquake loading.

(3) The tensile tests presented give, in broad terms, the behaviour of a typical low plastic core material under tension. Information obtained by more extensive tensile testing on different types of soil is useful in readily recognizing the soils susceptible to tensile cracking. In addition to obtaining information on the tensile behaviour of soils, it is highly desirable that research aimed at determining the factors contributing to the tensile strength of a soil be conducted. This will provide a better insight into the problem of tensile cracking.

(4) Effectiveness of different preventative measures, taken against cracking and subsequent erosion failure in earth dams, should be evaluated. Laboratory tests, aimed at determining the erodability of soil through cracks, the self-healing properties of soil, and the dependability of filters in prevention of erosion failures are of value.

(5) Information concerning stresses, deformations, development of tensile cracks, and erosion failures, obtained by reliable field observations is of a great value in testing the usefulness of the analytical and laboratory procedures developed for the analysis of cracking of

earth dams. In addition to recording the movements of the surface monuments, stress and strain observations should be obtained from the instruments located within the suspected, critical zones of tension. Such observations greatly contribute to the evaluation of the conditions responsible for tensile cracking.

REFERENCES

Akazawa, T. (1953), "Tension Test Method for Concrete", Bulletin No. 16, International Association of Testing and Research Laboratories, Paris, November, 1953, pp. 11-23.

Alberro, J. (1972), "Stress-Strain Analysis of El Infiernillo Dam", ASCE Speciality Conference on Performance of Earth and Earth-Supported Structures, June, 1972, Purdue University, Lafayette, Indiana, Vol. 1, Part 1, pp. 837-852.

ASCE Committee on Earth and Rockfill Dams (1967), "Progress Report: Problems in Design and Construction of Earth and Rockfill Dams", Journal of the Soil Mechanics and Foundations Division, ASCE, Vol. 93, No. SM3, May, 1967, pp. 129-136.

Bendel, H. (1962), "Die Berechnung von Spannungen und Verschiebungen in Erddammen", Mitt. Versuchanstalt f. Wasserbau und Erdbau, No. 55, ETH, Zurich.

Bishop, A.W. (1952), "The Stability of Earth Dams", Ph.D. Thesis, University of London, London.

Bishop, A.W. and Henkel, D.J. (1962), The Measurement of Soil Properties in the Triaxial Test, Second Edition, Edward Arnold, London, p. 72.

Bjerrum, L. (1967), Discussion, Ninth International Congress on Large Dams, Istanbul, Vol. VI, p. 456.

Bofinger, H.E. (1970), "The Measurement of the Tensile Properties of Soil-Cement", Ministry of Transport, Road Research Laboratory Report LR365, Crownthorne, Berkshire.

Breen, J.J. and Stephens, J.E. (1966), "Split Cylinder Test Applied to Bituminous Mixtures at Low Temperatures", Journal of Materials, Vol. 1, No. 1, American Society for Testing and Materials, March, 1966.

Brown, C.B. and King, I.P. (1966), "Automatic Embankment Analysis: Equilibrium and Instability Conditions", Geotechnique, Vol. 16, No. 3, September, 1966, pp. 209-219.

Carniero, F.L.L.B. and Barcellos, A. (1953), "Concrete Tensile Strength", Bulletin No. 13, International Association of Testing and Research Laboratories for Materials and Structures, Paris, March, 1953, pp. 97-127.

Casagrande, A. (1950), "Notes on the Design of Earth Dams", Journal of the Boston Society of Civil Engineers, Vol. 37, No. 4, October, 1950. (Reprinted in Contributions to Soil Mechanics 1941-1953, Boston Society of Civil Engineers, Boston, Mass., 1953, pp. 231-255).

Chang, C.Y. and Duncan, J.M. (1970), "Analysis of Soil Movements Around Deep Excavation", Journal of the Soil Mechanics and Foundations Division, ASCE, Vol. 96, No. SM5, September, 1970, pp. 1655-1681.

Chang, T.Y., Ko, H.Y., Scott, R.F. and Westman, R.A. (1967), "An Integrated Approach to the Stress Analysis of Granular Materials", Report of the Soil Mechanics Laboratory, California Institute of Technology, Pasadena, California.

Chen, W.F. (1970), "Extensibility of Concrete and Theorems of Limit Analysis", Journal of Engineering Mechanics Division, ASCE, Vol. 96, No. EM3, June, 1970, pp. 341-352.

Clough, G.W. and Duncan, J.M. (1970), "Finite Element Analyses of Port Allen and Old River Locks", Report No. TE69-3, Office of Research Services, University of California, Berkeley.

Clough, R.W. and Woodward, R.J., III (1967), "Analysis of Embankment Stresses and Deformations", Journal of the Soil Mechanics and Foundations Division, ASCE, Vol. 93, No. SM4, July, 1967, pp. 529-549.

Clough, R.W. (1969), "Comparison of Three Dimensional Finite Elements", Proc. of Symp. on Application of Finite Element Methods in Civil Engineering, ASCE, Nashville, November, 1969, pp. 1-26.

Colback, P.S.B. (1966), "An Analysis of Brittle Fracture Initiation and Propagation in the Brazilian Test", Proc. Congr. Intern. Soc. Rock Mech., 1 st., Lisbon, pp. 385-391.

Covarrubias, S.W. (1969), "Cracking of Earth and Rockfill Dams", Harvard Soil Mechanics Series, No. 82, April, 1969.

Desai, C.S. and Reese, L.C. (1970), "Analysis of Footings on Layered Soils", Journal of the Soil Mechanics and Foundations Division, ASCE, Vol. 96, No. SM4, July, 1970, pp. 1289-1310.

Desai, C.S. (1971), "Non-Linear Analyses Using Spline Functions", Journal of the Soil Mechanics and Foundations Division, ASCE, Vol. 97, No. SM10, October, 1971, pp. 1461-1480.

Dolezalova, M. (1970), "Effect of Steepness of Rocky Canyons Slopes on Cracking of Clay Cores of Rock-and-Earthfill Dams", Trans. Tenth Congress on Large Dams, Vol. 1, June, 1970, pp. 215-224.

Duncan, J.M. and Dunlop, P. (1969), "Slopes in Stiff-Fissured Clays and Shales", Journal of the Soil Mechanics and Foundations Division, ASCE, Vol. 95, No. SM2, March, 1969, pp. 467-492.

Duncan, J.M. and Chang, C.Y. (1970), "Non-Linear Analysis of Stress and Strain in Soils", Journal of the Soil Mechanics and Foundations Division, ASCE, Vol. 96, No. SM5, September, 1970, pp. 1629-1654.

Duncan, J.M. and Chang, C.Y. (1972), Discussion Closure of "Non-Linear Analysis of Stress and Strain in Soils", by Duncan, J.M. and Chang. C.Y., Journal of the Soil Mechanics and Foundations Division, ASCE, Vol. 98, No. SM5, May, 1972, pp. 495-498.

Duncan, J.M. (1972), "Finite Element Analyses of Stresses and Movements in Dams, Excavations and Slopes", State of the Art Report, WES Symp. on Appl. of Finite Element Method in Geotechnical Engg., Vicksburg, Miss., May, 1972.

Eisenstein, Z., Krishnayya, A.V.G. and Morgenstern, N.R. (1972), "An Analysis of Cracking at Duncan Dam", ASCE Speciality Conference on Performance of Earth and Earth-Supported Structures, June, 1972, Purdue University, Lafayette, Indiana, Vol. 1, Part 1, pp. 765-777.

Fang, H.Y. and Chen, W.F. (1971), "New Method for Determination of Tensile Strength of Soils", Preprint of Paper Presented at the 50th Annual Meeting of the Highway Research Board, Washington, D.C., January, 1971.

Felippa, C.A. (1966), "Refined Finite Element Analysis of Linear and Non-Linear Two Dimensional Structures", Ph.D. Thesis, University of California, Berkeley, California.

Finn, W.D.L. (1967), "Static and Seismic Behaviour of an Earth Dam", Canadian Geotechnical Journal, Vol. 4, No. 1, February, 1967, pp. 28-37.

Frazier, G.A. (1969), "Vibrational Characteristics of Three-Dimensional Solids, with Applications to Earth Dams", Ph.D. Thesis, Montana State University, Bozman, Montana.

Frocht, M.M. (1957), Photoelasticity, Vol. 2, John Wiley and Sons, Inc., New York.

Gates, R.H. (1968), "Inelastic Analysis of Slopes by the Finite Element Method", Ph.D. Thesis, University of Illinois.

Girijavallabhan, C.V. and Reese, L.C. (1968), "Finite Element Method for Problems in Soil Mechanics", Journal of the Soil Mechanics and Foundations Division, ASCE, Vol. 94, No. SM2, March, 1968, pp. 473-496.

Gordon, J.L. and Duguid, D.R. (1970), "Experiences with Cracking at Duncan Dam", Trans. Tenth Congress on Large Dams, Vol. 1, June, 1970, pp. 469-486.

Haefeli, R. (1951), "Investigation and Measurements of the Shear Strength of Saturated Choesive Soils", Geotechnique, Vol. 2, No. 3, pp. 186-208.

Harr, M.E. (1966), Foundations of Theoretical Soil Mechanics, McGraw-Hill Book Co., New York.

Hasegawa, H. and Ikeuty, M. (1966), "On the Tensile Strength of Disturbed Soils", Symposium on Rheology and Soil Mechanics, Edited by J. Kravtchenco and P.M. Sirieys, Springer, Berlin, pp. 405-412.

Herrmann, L.R. (1964), "Elasticity Equations for Incompressible and Nearly Incompressible Materials by a Variational Theorem", A.I.A.A. Journal, Vol. 3, No. 10, pp. 1896-1900.

Hertz, H. (1883), "Uber die Verteilung der Druckkrafte in einem elastischen Kreiscylinder", Zeitschrift fur Mathematik and Physik, Vol. 28.

Hondros, G. (1959), "The Evaluation of Poisson's Ratio and the Modulus of Materials of a Low Tensile Resistance by the Brazilian (Indirect Tensile) Test with Particular Reference to Concrete", Austrialian Journal of Applied Science, Vol. 10, No. 3, pp. 243-268.

Ingles, O.G. and Frydman, S. (1963), "An Examination of Some Methods for Strength Measurement in Soils", Proc. Fourth Australia-New Zealand Conference on Soil Mechanics and Foundation Engineering, August, 1963, Adelaide, pp. 213-219.

Jurgensen, L. (1934), "The Application of the Theories of Elasticity and Plasticity to Foundation Problems", Reprinted in Contributions to Soil Mechanics, 1925-1940, Boston Society of Civil Engineers, 1940, pp. 148-183.

Kjaernsli, B. and Torblaa, I. (1968), "Leakage Through Horizontal Cracks in the Core of Hyttejuvet Dam", Papers on Earth and Rockfill Dams in Norway, Publication No. 80, Norwegian Geotechnical Institute, Oslo, pp. 39-47.

Kulhawy , F.H., Duncan, J.M. and Seed, H.B. (1969), "Finite Element Analyses of Stresses and Movements in Embankments during Construction", Report No. TE69-4, Office of Research Services, University of California, Berkeley.

Kulhawy , F.H. and Duncan, J.M. (1970), "Non-Linear Finite Element Analysis of Stresses and Movements in Oroville Dam", Report No. TE70-2, Office of Research Services, University of California, Berkeley.

Lee, K.L. and Shen, C.K. (1968), "Horizontal Movements Related to Subsidence", Journal of the Soil Mechanics and Foundations Division, ASCE, Vol. 94, No. SM6, pp. 139-146.

Lefebvre, G. and Duncan, J.M. (1971), "Three Dimensional Finite Element Analyses of Dams", Contract Report S-71-6, U.S. Army Engineer Waterways Experiment Station, Vicksburg, Miss., May, 1971.

Leonards, G.A. and Narain, J. (1963), "Flexibility of Clay and Cracking of Earth Dams", Journal of the Soil Mechanics and Foundations Division, ASCE, Vol. 89, No. SM2, Part 1, March, 1963, pp. 47-98.

Lowe III, J. (1970), "Recent Development in Design and Construction of Earth and Rockfill Dams", Transactions 10th Congress on Large Dams, Montreal, Vol. 5, Q. 36, pp. 1-60.

Lowe III, J. (1972), Report, Session II: Earth and Earth-Rock Dams, ASCE Speciality Conference on Performance of Earth and Earth-Supported Structures, June, 1972, Purdue University, Lafayette, Indiana, Vol. 2, pp. 55-70.

Marsal, R.J. and Ramirez de Arellano, L. (1967), "Performance of El Infiernillo Dam, 1963-1966", Journal of the Soil Mechanics and Foundations Division, ASCE, Vol. 93, No. SM4, July, 1967, pp. 265-298.

Mellor, M. and Hawkes, I. (1971), "Measurement of Tensile Strength by Diametral Compression of Discs and Annuli", Engineering Geology, Vol. 5, No. 3, October, 1971, pp. 173-225.

Narain, J. (1962), "Flexibility of Compacted Clay", Ph.D. Thesis, Purdue University, Lafayette, Indiana.

Narain, J. and Rawat, P.C. (1970), "Tensile Strength of Compacted Soils", Journal of the Soil Mechanics and Foundations Division, ASCE, Vol. 96, No. SM6, November, 1970, pp. 2185-2190.

Nobari, E.S. and Duncan, J.M. (1972), "Movements in Dams Due to Reservoir Filling", ASCE Speciality Conference on Performance of Earth and Earth-Supported Structures, June, 1972, Purdue University, Lafayette, Indiana, Vol. 1, Part 1, pp. 797-815.

Nonveiller, E. and Anagnosti, P. (1961), "Stresses and Deformation in Cores of Rockfill Dams", Proc. Fifth International Conference on Soil Mechanics and Foundation Engineering, Vol. II, Duroid, Paris, pp. 673-680.

Palmerton, J.B. (1972), "Application of Three Dimensional Finite Element Analysis", WES Symp. on Appl. of Finite Element Method in Geotechnical Engg., Vicksburg, Miss., May, 1972.

Patrick, J.G. (1967), "Post-Construction Behaviour of Round Butte Dam", Journal of the Soil Mechanics and Foundations Division, ASCE, Vol. 93, No. SM4, July, 1967, pp. 251-263.

Pope, R.J. (1967), "Evaluation of Cougar Dam Embankment Performance", Journal of the Soil Mechanics and Foundations Division, ASCE, Vol. 93, SM4, July, 1967, pp. 231-250.

Schober, W. (1967), "Behaviour of Gepatsch Rockfill Dam", Proc. Ninth International Conference on Large Dams, Vol. III, Question 34, Istanbul, pp. 667-699.

Scott, R.F. (1963), Principles of Soil Mechanics, Addison Wesley, Reading, Mass.

Scott, R.F. and Ko, H.Y. (1969), State of the Art Report on "Deformation and Strength Characteristics", State of Art Volume, Seventh International Conference on Soil Mechanics and Foundation Engineering, Mexico, pp. 1-47.

Sherard, J.L. (1952), "Influence of Soil Properties and Construction Methods on the Performance of Homogeneous Earth Dams", Ph.D. Thesis, Harvard University, Cambridge, Mass.

Sherard, J.L., Decker, R.S. and Ryker, N.L. (1972), "Hydraulic Fracturing in Low Dams of Dispersive Clay", Paper Presented to the ASCE Speciality Conference on Performance of Earth and Earth-Supported Structures, June, 1972, Purdue University, Lafayette, Indiana, Vol. 1, Part 1, pp. 653-689.

Skermer, N.A. and Hillis, S.F. (1970), "Gradation and Shear Characteristics of Four Cohesionless Soils", Canadian Geotechnical Journal, Vol. 7, pp. 62-68.

Smith, I.M. and Kay, S. (1971), "Stress Analysis of Contractive or Dilative Soil", Journal of the Soil Mechanics and Foundations Division, ASCE, Vol. 97, No. SM7, July, 1971, pp. 981-997.

Strohm, W.E., Jr. and Johnson, S.J. (1971), "The Influence of Construction Step Sequence and Non-Linear Material Behaviour on Cracking of Earth and Rockfill Dams", Miscellaneous Paper S-71-10, U.S. Army Engineer Waterways Experiment Station, Vicksburg, Mississippi.

Tamez, E. and Springall, G. (1960), "The Use of Soils as Construction Materials for Earth Dams", Proc. First Pan-American Conference of Soil Mechanics and Foundation Engineering, Vol. III, Mexico, pp. 1269-1286.

Terzaghi, K. (1943), Theoretical Soil Mechanics, John Wiley and Sons, Inc., New York.

Thompson, M.R. (1965), "The Split-Tensile Strength of Lime-Stabilized Soils", Lime Stabilization, Highway Research Record, No. 92, Highway Research Board, pp. 69-79.

Timoshenko, S. and Goodier, J.N. (1951), "Concentrated Force at a Point of a Straight Boundary", Theory of Elasticity, Second Edition, McGraw-Hill, New York, p. 85.

Tschebotarioff, G.P., Ward, E.R. and DePhillippe, A.A. (1953), "The Tensile Strength of Disturbed and Recompacted Soils", Proc. Third International Conference on Soil Mechanics and Foundation Engineering, Vol. I, Zurich, pp. 207-210.

Vaughan, P.R., Kluth, D.J., Leonard, M.W. and Pradoura, H.H.M. (1970), "Cracking and Erosion of the Rolled Clay Core of Balderhead Dam and the Remedial Works Adopted for Its Repair", Trans. Tenth Congress on Large Dams, Vol. 1, pp. 73-93.

Wilson, E.L. (1963), "Finite Element Analysis of Two-Dimensional Structures", Structural Engineering Laboratory Report No. 63-2, University of California, Berkeley, California, (June, 1963).

Wilson, E.L. (1966), "Analysis of Plane Stress Structures", Computing Programming Series, University of California, Berkeley, California.

Wright, P.J.F. (1955), "Comments on an Indirect Tensile Test on Concrete Cylinders", Magazine of Concrete Research, Vol. 7, No. 20, London, July, 1955, pp. 87-96.

Zienkiewicz, O.C., Valliappan, S. and King, I.P. (1968), "Stress Analysis of Rock as a 'No-Tension' Material", Geotechnique, Vol. 18, pp. 56-66.

Zienkiewicz, O.C., Irons, B.M., Ergatoudis, J., Ahmad, S. and Scott, F.C. (1969), "Isoparametric and Associated Element Families for Two and Three Dimensional Analysis", Proc. Course on Finite Element Methods in Stress Analysis, Edited by Holand, I. and Bell, K., Trondheim Tech. University.

APPENDIX A

COMPUTER PROGRAM FOR TWO DIMENSIONAL FINITE ELEMENT ANALYSIS

A.1 Scope

This appendix contains a description of the computer program used for two dimensional finite element analyses and a listing of the program.

A.2 Language, Code and Limitations

Language. The computer program presented here was written in FORTRAN IV language and run on an IBM 360/67 computer with an MTS operating system at the University of Alberta, Edmonton.

Code. The title of the code is Finite Element Non-Linear Analysis in Two Dimensional Problems (FENA2D).

Limitations. The program in the present form can handle a problem less than or equal to the following size:

Number of elements	=	400
Number of nodes	=	250
Number of read elements	=	150
Number of read nodes	=	250
Number of boundary nodes	=	50
Number of materials	=	5
Number of cell pressures at which triaxial data is supplied	=	10

Number of axial strain
points at which triaxial
data is supplied = 20

If the size of a problem exceeds the above limits the dimensions have to be increased accordingly. The minimum required dimension for each array is given in A.4.1.

A.3 Development and the Main Features of Program

The program in its original form was developed by E.L. Wilson (University of California, 1962) to perform a two dimensional finite element analysis either for plane strain or plane stress condition using constant strain triangular elements. The analysis had to be linear and the loads were to be applied in a single step. The equations of equilibrium were solved by Gauss-Seidel iterative procedure.

Z. Eisenstein (University of Alberta, 1969) added to the above program the automatic generation of nodes and elements. The author (1970) modified the program to its present form, given in the listing, to perform, in addition to the linear single step analysis, a non-linear two dimensional analysis in a number of steps with an option to analyze each step once or twice. An option for a "no tension" analysis is possible. A facility to generate a uniform element pattern (detailed in A.5) in addition to the existing generation of non-uniform pattern is available.

The program consists of a Main and a Subroutine called TESTD. Only the main features of the program are given below since a detailed description appears in A.5.

(1) The input data regarding elements, nodes, boundary conditions, type of generation, number of materials and type of analysis are read.

(2) The nodes and elements are generated in the prescribed manner and the appropriate elastic parameters are assigned to each element. In the case of a non-linear analysis the triaxial test data are converted to the stress-invariant form by the subroutine TESTD. The elastic parameters for each element are determined from the converted form of the test data. The stresses considered for calculation of the initial moduli are those corresponding to the "at-rest" condition.

(3) The information regarding the number of steps, whether each step to be analyzed once or twice, whether "no tension" analysis to be performed or not is read. The number of elements, nodes and the boundary conditions for the particular step are also read.

(4) The element stiffness is formed for all the elements in the particular step, the equilibrium equations are set up and solved by Gauss-Seidel iterative procdure.

(5) The displacements, stresses and strains are computed and the elastic moduli are calculated from the test data in case of a non-linear analysis. If the step has to be repeated once more the "average moduli" are used. "No tension" analysis is performed if it is opted for.

(6) In the multiple step analysis the stresses, strains and displacements are accumulated. When a particular step

is to be repeated the added stresses, strains and displacements of that step are deducted from the total values before the analysis is repeated with the "average moduli".

A.4 Nomenclature

In Section A.4.1 that follows the variables that need a change in their dimension declaration according to the size of the problem are designated by parentheses after the variable name. The description and the minimum required size of the variable are also indicated. The variables defining the minimum sizes are given as input to the program.

A.4.1 Description and Size of Variables

Name	Description	Minimum Size When Applicable
ACOEF( )	Shear strength parameter associated with cohesion given by 2c cos ϕ/(1-sin ϕ)	(NUMAT)
AJ( )	X-distance between nodes i and j of an element	(NUMEL)
AK( )	X-distance between nodes i and k of an element	(NUMEL)
BCOEF( )	Shear strength parameter associated with σ_3 given by 2 sin ϕ/(1-sin ϕ)	(NUMAT)
BJ( )	Y-distance between nodes i and j of an element	(NUMEL)
BK( )	Y-distance between nodes i and k of an element	(NUMEL)

Name	Description	Minimum Size When Applicable
COED( )	Coefficient of thermal expansion assigned for each read or generated element	(NUMEL)
COEDR( )	Coefficient of thermal expansion assigned for each read element	(NUREL)
CONFAC	Conversion factor used to convert the triaxial test results to the units in which analysis is performed	
DSX( )	Displacement in X-direction given as input for already generated nodes	(NUMNP)
DSXQ( )	Total displacement in X-direction	(NUMNP)
DSXR( )	Displacement in X-direction given as input only for read nodes	(NURNP)
DSY( )	Displacement in Y-direction given as input for already generated nodes	(NUMNP)
DSYQ( )	Total displacement in Y-direction	(NUMNP)
DSYR( )	Displacements in Y-direction given as input only for read nodes	(NURNP)
DT( )	Temperature change in a read or generated element	(NUMEL)
DTR( )	Temperature change in a read element	(NUREL)
EBREAD( )	Bulk modulus read for each material type	(NUMAT)
EBULK( )	Bulk modulus assigned for each element	(NUMEL)
EMAX( )	Percent maximum principal strain in each element	(NUMEL)
EMIN( )	Percent minimum principal strain in each element	(NUMEL)
EPXV( )	Percent total X-strain in each element	(NUMEL)
EPYV( )	Percent total Y-strain in each element	(NUMEL)

Name	Description	Minimum Size When Applicable
ESHEAR( )	Shear modulus assigned for each element	(NUMEL)
ESREAD( )	Shear modulus read for each material type	(NUMAT)
ET( )	Young's modulus assigned for a read or generated element	(NUMEL)
ETR( )	Young's modulus assigned for a read element	(NUREL)
GAMV( )	Total percent shear strain in each element	(NUMEL)
GOCT( )	Percent octahedral shear strain	(NSTRN, NCELP,NUMAT)
HEAD( )	Heading for the identification of the problem	18
IANLYS	Code to identify whether the analysis is for plane stress or for plane strain condition	
IGEN	Code to identify whether the element generation is of uniform or non-uniform pattern	
ITOPT	Code to identify whether a step is to be analyzed once or twice.	
KOPT	Code to identify whether "no tension" analysis is to be performed or not	
M	Element or nodal number	
MAT( )	Material number assigned to each element	(NUMEL)
MATN	Number of elements to which material number other than 1 is to be assigned	
N	Element or nodal number	
NANLYS	Code to identify whether the analysis is linear or non-linear	

Name	Description	Minimum Size When Applicable
NAP( )	A vector to store the adjacent nodal points from a given node	(NUMNP)
NBOUN	Number of nodes at which the boundary displacements are specified in a particular step	
NCELP	Number of confining pressures at which triaxial test data is supplied as input	
NCPIN	Cycle interval for the print of the force unbalance	
NCYCM	Maximum number of iterations permitted in one step	
NFIX( )	Code to indicate the type of boundary displacement conditions prescribed	(NUMBC)
NLOAD	Number of nodes at which the loads are specified in a particular step	
NOBSET	Number of sets of elements for which the overburden factor is prescribed	
NOPIN	Cycle interval for the print of displacements and stresses	
NP( )	A vector used in the process of inversion of nodal point stiffness and modification of boundary flexibility	(NUMNP,10)
NPB( )	Nodal number at which the type of boundary displacement is specified	(NUMBC)
NPI( )	Nodal number for node i of a read or generated element	(NUMEL)
NPIR( )	Nodal number for node i of a read element	(NUMER)
NPJ( )	Nodal number for node j of a read or generated element	(NUMEL)
NPJR( )	Nodal number for node j of a read element	(NUMER)

Name	Description	Minimum Size When Applicable
NPK( )	Nodal number for node k of a read or generated element	(NUMEL)
NPKR( )	Nodal number for node k of a read element	(NUMER)
NPNUM( )	Nodal number of the read or generated nodes	(NUMNP)
NPNUR( )	Nodal number of the read nodes only	(NURNP)
NSET	Number of elements excluding the one read for which the same over-burden factor has to be assigned	
NSTEP	Number of steps for the analysis	
NSTRN	Number of axial strain points at which the triaxial data is supplied	
NTENS	Code to identify whether shear failure is to be considered or not	
NUMAT	Number of material types present in the given problem	
NUMBC	Number of boundary points at which displacements are prescribed in the problem	
NUMBCS	Number of boundary points at which displacements are specified in the step considered	
NUME( )	Element number for read or generated elements	(NUMEL)
NUMEL	Number of elements in the problem	
NUMELS	Number of elements in the step considered	
NUMER( )	Element number for read elements only	(NUREL)
NUMNP	Number of nodal points in the problem	
NUMNPS	Number of nodal points in the step considered	
NUREL	Number of read elements	

Name	Description	Minimum Size When Applicable
NURNP	Number of read nodal points	
OBFAC( )	Overburden factor	(NUMEL)
PA( )	Angle of inclination in degrees of the major principal stress with x-axis in an element	
RO( )	Density of the material in read or generated elements	(NUMEL)
ROR( )	Density of the material in read elements only	(NUREL)
ROREAD( )	Density of the material read for each material type	(NUMAT)
SD( )	Deviatoric stresses read from test data	(NSTRN, NCELP,NUMAT)
SIGINT( )	A vector used in the coversion of data from triaxial form to stress invariant form	(NCELP, NUMAT)
SIGINV( )	A vector used in the coversion of data from triaxial form to stress invariant form	(NSTRN, NCELP,NUMAT)
SL( )	Number of triaxial cell pressure values at which data is supplied	(NCELP, NUMAT)
SLOPE( )	Slope of the boundary along which a boundary point moves	NUMBC
ST( )	Number of percent axial strain values at which triaxial data is supplied	(NSTRN, NUMAT)
SXX( )	Vector used in the inversion of stiffness	(NUMNP,9)
SXY( )	Vector used in the inversion of stiffness	(NUMNP,9)
SYX( )	Vector used in the inversion of stiffness	(NUMNP,9)
SYY( )	Vector used in the inversion of stiffness	(NUMNP,9)

Name	Description	Minimum Size When Applicable
TAD( )	A vector used to identify the nodes at which displacements are specified	(NUMNP)
TAL( )	A vector used to identify the nodes at which loads are specified	(NUMNP)
THERM( )	Thermal stress in an element	(NUMEL)
TOCTD( )	Octahedral shear stress	(NSTRN, NCELP,NUMAT)
VS( )	Volumetric strain obtained from triaxial test	(NSTRN, NCELP,NUMAT)
VSTN( )	A vector used in the conversion of the triaxial test data to stress invariant form	(NSTRN, NCELP,NUMAT)
XMAX( )	Maximum principal stress in an element	(NUMEL)
XMIN( )	Minimum principal stress in an element	(NUMEL)
XLDR( )	X-load at read nodes only	(NURNP)
XLOAD( )	X-load at read or generates nodes	(NUMNP)
XORD( )	X-coordinate for read or generated nodes	(NUMNP)
XORDR( )	X-coordinate for read nodes only	(NURNP)
XU( )	Poisson's ratio assigned to read or generate elements	(NUMEL)
XUR( )	Poisson's ratio assigned to read elements	(NUREL)
XYV( )	Total shear stress in an element	(NUMEL)
XV( )	Total x-stress in an element	(NUMEL)
YLDR( )	Y-load at read nodes only	(NURNP)
YLOAD( )	Y-load at read or generated nodes	(NUMNP)
YORD( )	Y-coordinate for read or generated nodes	(NUMNP)

Name	Description	Minimum Size When Applicable
YORDR( )	Y-coordinate for read nodes only	(NURNP)
YV( )	Total y-stress in an element	(NUMEL)

A.5 Input Data Procedure

A.4.1 has to be referred for the explanations of the name of variables used in this section.

(1) Control cards (Number of Cards = 2)

(a) Card 1 (13A4)

1-72	HEAD	Title card for identification of the problem

(b) Card 2 (9I5)

1-5	NUMEL	
6-10	NUREL	
11-15	NUMNP	
16-20	NURNP	
21-25	NUMBC	
25-30	NUMAT	
31-35	NANLYS	Equal to zero for linear analysis; equal to 1 for non-linear analysis
36-40	IANLYS	Equal to zero for plane strain analysis; equal to 1 for plane stress analysis
41-45	IGEN	Equal to zero for non-uniform pattern of generation of element; equal to 1 for uniform pattern of generation of elements. The patterns are given below.

Uniform Pattern:

Non-Uniform Pattern:

(2) Element data cards (Number of cards = NUREL) (4I5)

1-5 NUMER( )

5-10 NPIR( )

11-15 NPJR( )

16-20 NPKR( )

Example for uniform element pattern generation:

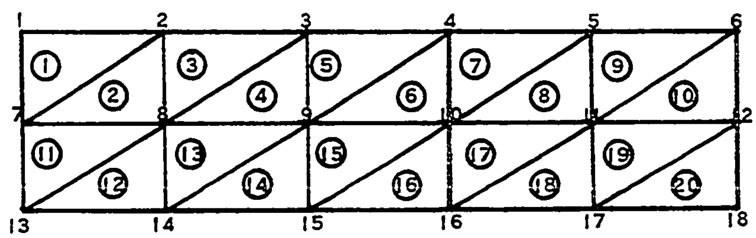

The element numbers have been circled. To generate the above mesh pattern it is necessary to supply the information regarding the first and the last element in each row. Here for example elements 1, 10, 11 and 20 are to be read in. The nodes i, j and k for these elements are to be given in the anticlock wise direction as shown below:

Name of Element	Node i	Node j	Node k
1	2	1	7
10	6	11	12
11	8	7	13
20	12	17	18

NUREL for this example is 4 and NUMEL is 20.

Example for non-uniform element pattern generation:

First Row

Second Row

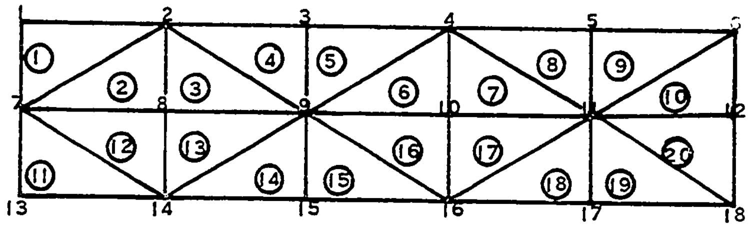

The element numbers have been circled. To generate the above mesh pattern it is necessary to supply information regarding the first and last elements in the first row and the first three lements and the last element in the second row. This is due to the difference between the orientation of the element 11 and the element 1. The following gives the nodal data to be supplied in the anticlock wise direction.

Name of Element	Node i	Node j	Node k
1	2	1	7
10	6	11	12
11	7	13	14
12	7	14	8
13	9	8	14
20	11	18	12

NUREL for this example is 6 while NUMEL is 20.

The intermediate elements will be assigned the same values of modulus, density, etc. as those read for the end elements.

(3) Nodal data cards (Number of cards = NURNP) (I5,4F10.0, 2F12.8)

1-5 NPNUR( )

6-15 XORDR( )

16-25 YORDR( )

26-35 XLDR( )

36-45 YLDR( )

46-57 DSXR( )

58-69 DSYR( )

When the intermediate nodes between the two extreme nodes are equally spaced in one coordinate direction with the distance in other coordinate direction being the same, the intermediate nodes are generated with equal distances between them, each distance being equal to the total distance between the extreme nodes read divided by the difference between the nodal numbers. The intermediate nodes are assigned the proper nodal numbers. The other quantities like displacements, loads, etc. for the intermediate nodes will be the same as those read for the extreme nodes.

(4) Boundary point displacement cards (Number of cards = NUMBC) (2I5,F8.3)

1-5 NPB( )

6-10 NFIX( )

11-18 SLOPE( )

The following codes have been used to define the mode of displacement at a given boundary point.

x-direction	y-direction	Sloping Boundary	NFIX( )	SLOPE( )
Zero displacement	Zero displacement		0	0
Zero displacement			1	0
	Zero displacement		2	0
		Free to move along a sloping boundary	2	tan θ

Sloping boundary is as shown:

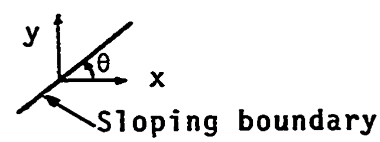

(5) Material type generation card (1 card) (I5)

1-5 MATN If there is only one material a blank card is required and the material number cards given in (6) below are omitted. All elements are automatically assigned a material number equal to 1.

(6) Material number cards (Number of cards = MATN) (2I5)

1-5 M Element number

6-10 MAT(M) Assigned material number

(7) Material properties cards (Number of cards = NUMAT) (5F10.0)

1-10 ROREAD( )

11-20 EBREAD( ) Normally assigned in a linear analysis

21-30 ESREAD( ) Normally assigned in a linear analysis

31-40 ACOEF( ) Needed if shear failure has to be considered

41-50 BCOEF( ) Needed if shear failure has to be considered

(8) Overburden factor control card (1 card) (I5)

1-5 NOBSET If the analysis is linear NOBSET = 0 and (9) is omitted

(9) Overburden factor cards (Number of cards = NOBSET)

(2I5,F10.0)

1-5	M	Element number
6-10	NSET	
11-20	OBFAC( )	To be given only if value is not equal to one.

The following example provides an explanation for (8) and (9).

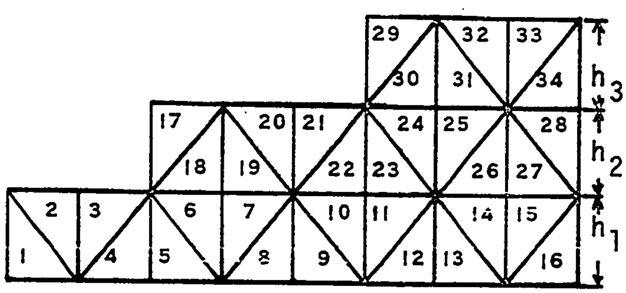

γ_3 density of material for elements 29 to 34

γ_2 density of material for elements 17 to 28

γ_1 density of material for elements 1 to 16

When a non-linear analysis has to be performed for gravity loaded structures the initial moduli are computed for each element considering the overburden pressure at the mid height of the element. In the sketch shown above there are 34 elements to be considered in a particular step. The overburden pressure at the mid height of a certain element say 16 is $(\gamma_1 h_1/2 + \gamma_2 h_2 + \gamma_3 h_3)$ where γ_1, γ_2 and γ_3 are the densities of the materials and h_1, h_2 and h_3 are the heights as shown. Now the overburden factor can be defined for the element 16 as follows:

$\mathrm{OBFAC}(16) = (\gamma_1 h_1/2 + \gamma_2 h_2 + \gamma_3 h_3)/(\gamma_1 h_1/2)$.

If for example $h_1 = h_2 = h_3 = h$ and $\gamma_1 = \gamma_2 = \gamma_3 = \gamma$ then the overburden factor control card and the overburden factor cards will be as given below.

NOBSET = 3

M	NSET	OBFAC(M)
5	5	3.0
11	5	5.0
23	5	3.0

OBFAC(M) = 1.0 is automatically set in the program and hence need not be supplied in the data. In the present example elements 1 to 4, 17 to 22 and 29 to 34 will have an overburden factor equal to unity.

(10) Triaxial test data control card (1 card) (2I5,F10.0)

1-5 NCELP

6-10 NSTRN

11-20 CONFAC

If the analysis is linear a blank card for (10) has to be substituted and (11), (12), (13) are to be omitted.

(11) Cell pressure card (1 card) (10F5.0)

If the test results are to be supplied say at 0, 5, 10, 30 and 40 psi cell pressure values, the input is as follows:

1-5	0.0
6-10	5.0
11-15	10.0
16-20	30.0
21-25	40.0

(12) Axial strain and deviatoric stress cards (Number of cards = NSTRN) (11F5.0)

Each card will have the axial strain punched in the first five columns and the deviatoric stresses corresponding to the various cell pressures (given in (11)) at that particular axial strain are punched in the subsequent columns.

(13) Axial strain and volumetric strain cards (Number of cards = NSTRN) (11F5.0)

Each card will have the axial strain punched in the first five columns and the volumetric strain corresponding to the various cell pressures (given in (11)) at that particular axial strain are punched in the subsequent columns. Volume expansion has to be neglected while giving the volumetric strain input.

(14) Option for "no tension" analysis (1 card) (I5)

1-5 KOPT Equal to zero when "no tension" analysis is not needed and equal to one when it is needed

(15) Option for analyzing each step once or twice (1 card) (I5)

1-5 ITOPT Equal to zero for analysis once and equal to one for analysis twice. If the analysis is linear ITOPT = 0.

(16) Number of steps and option for consideration of shear failure (1 card) (2I5)

1-5 NSTEP For a single step analysis NSTEP = 1

6-10 NTENS If shear failure is to be considered NTENS = 1, otherwise NTENS = 0

(17) Nodal loads control card (1 card) (I5)

1-5 NLOAD If NLOAD is equal to zero (18) is omitted

(18) Nodal loads specified in the step considered (Number of cards = NLOAD) (I5,2F10.0)

1-5 N Nodal number

6-15 YLOAD(N)

16-25 XLOAD(N)

(19) Nodal displacements control card (1 card) (I5)

1-5 NBOUN If NBOUN is equal to zero (20) is omitted

(20) Nodal displacements specified in the step considered (as many as the number NBOUN) (I5,2F10.0)

1-5 M Nodal Number

6-15 DSY(M)

16-25 DSX(M)

A.6 Output of Results

The following results are obtained as output:

(1) The complete nodal and element data with the initial values of the elastic parameters assigned to each element.

(2) Cumulative nodal displacements, element stresses, and strains for each step of the analysis.

(3) Element principal stresses and strains for each step of the analysis.

(4) Elastic parameters assigned to each element in each step of the analysis.

A.7 Listing of Program

A listing of the two dimensional program follows.

```
C
C
C TWO DIMENSIONAL FINITE ELEMENT PROGRAM WITH CONSTANT STRAIN TRIANGULAR
C
C ELEMENTS OF 6 DEGREES OF FREEDOM FOR EACH ELEMENT.PLANE STRAIN/ STRESS.
C
C LINEAR/ NONLINEAR. SINGLE/ MULTIPLE STEP ANALYSIS (WITH OPTION FOR
C
C REMOVAL  OF TENSILE STRESSES) CAN BE PERFORMED.
C
C
C
C ORIGINAL PROGRAM DEVELOPED BY E.L.WILSON (UNIVERSITY OF CALIFORNIA.1962)
C
C PROGRAM MODIFIED BY Z.EISENSTEIN (UNIVERSITY OF ALBERTA.1969) AND
C
C A.V.G. KRISHNAYYA (UNIVERSITY OF ALBERTA. 1970)
C
C
C
C       MAIN PROGRAM
C
C
C
C       DIMENSION AND COMMON STATEMENTS
C
C
C
      DIMENSION EBULK(400),ESHEAR(400),OBFAC(400),HEAD(18),
     1DSX(250),DSY(250),XLOAD(250),YLOAD(250),NP(250,10),SXX(250,9),
     2SXY(250,9),SYX(250,9),SYY(250,9),NAP(250),PA(400),
     3NPNUR(250),XORDR(250),YORDR(250),XLDR(250),YLDR(250),DSXR(250),
     4DSYR(250),TAD(250),MAT(400),TAL(250),          ET(400),
     5XU(400),RO(400),COED(400),DT(400),THERM(400),AJ(400),
     6BJ(400),AK(400),BK(400),GAMV(400),
     7SLOPE(50),NUMER(150),NPIR(150),NPJR(150),NPKR(150),ETR(150),
     8  ROR(150),XUR(150),COEDR(150),DTR(150),NPB(50),NFIX(50),LM(3),
     9A(6,6),B(6,6),S(6,6),THETA(50)
      COMMON/AREA1/SXX,SXY,SYX,SYY
      COMMON/AREA2/
     1       XORD(250),YORD(250),NPI(400),NPJ(400),NPK(400),NPNUM(250),
     1NUME(400),NUMNP,NUMEL                                  XV(400),
      DIMENSION DSXQ(250),DSYQ(250),
     1YV(400),XYV(400),EPXV(400),EPYV(400),XMAX(400),XMIN(400),EMAX(400)
     2,EMIN(400)
      COMMON/AREA3/
     1       ST(20,5),SL(20,5),SD(20,10,5),VS(20,10,5),NUMAT,
     2NCELP,CONFAC,NSTRN
      DIMENSION ROREAD( 5),EBREAD( 5),ESREAD( 5),ACOEF( 5),BCOEF( 5)
C
C
C  READ PROBLEM CONTROL CARDS
C
C
  150 READ(5,100)HEAD
      WRITE(6,99)
      WRITE(6,100)HEAD
```

```
      READ(5,1)NUMEL,NUREL,NUMNP,NURNP,NUMBC,NUMAT,NANLYS,IANLYS,IGEN
      WRITE(6,101)NUMEL
      WRITE(6,825)NUREL
      WRITE(6,102)NUMNP
      WRITE(6,824)NURNP
      WRITE(6,103)NUMBC
      WRITE(6,2000) NUMAT
C
C
C  READ ELEMENT DATA
C
C
      READ(5,9)(NUMER(N),NPIR(N),NPJR(N),NPKR(N),N=1,NUREL)


C  READ NODAL DATA
C
C
      READ(5,3)
     1           (NPNUR(M),XORDR(M),YORDR(M),XLDR(M),YLDR(M),
     2DSXR(M),DSYR(M),M=1,NURNP)
C
C     GENERATION OF NOT READ ELEMENTS
C
      DO 161 N=1,NUREL
      M=N+1
      IF(M-NUREL) 162,162,163
  162 I=NUMER(M)-NUMER(N)
      IF(I-1)163,163,164
  164 L=NUMER(N)
      NPA=NPIR(N)
      NPC=NPKR(N)
      K=0
      KO=2*K
      KE=1
      IO=I+1
      IF(IGEN.EQ.0) GO TO 3000
      DO 3166 JO=1,IO
      J=JO-1
      LJ=L+J
      NUME(LJ)=NUMER(N)+J
      IF(2-KE) 3168,3168,3167
 3167 NPI(LJ)=NPA+KO
      NPJ(LJ)=NPA-1+KO
      NPK(LJ)=NPC+KO
      GO TO 3174
 3168 NPI(LJ)=NPA+KO
      NPJ(LJ)=NPC+KO
      NPK(LJ)=NPC+1+KO
      K=K+1
      KO=K
      KE=0
 3174 ET(LJ)=ETR(N)
      RO(LJ)=ROR(N)
      XU(LJ)=XUR(N)
      COED(LJ)=COEDR(N)
      DT(LJ)=DTR(N)
      KE=KE+1
 3166 CONTINUE
      GO TO 161
```

```
 3000 DO 166 JO=1,IO
      J=JO-1
      LJ=L+J
      NUME(LJ)=NUMER(N)+J
      IF(2-KE)169,168,167
  167 NPI(LJ)=NPA+KO
      NPJ(LJ)=NPA-1+KO
      NPK(LJ)=NPC+KO
      GO TO 174
  168 NPI(LJ)=NPA+KO
      NPJ(LJ)=NPC+KO
      NPK(LJ)=NPC+1+KO
      GO TO 174
  169 IF(3-KE)172,171,166
  171 NPI(LJ)=NPA+KO
      NPJ(LJ)=NPC+1+KO
      NPK(LJ)=NPC+2+KO
      GO TO 174
  172 NPI(LJ)=NPA+KO
      NPJ(LJ)=NPC+2+KO
      NPK(LJ)=NPA+1+KO
      K=K+1
      KO=2*K
      KE=0
  174 ET(LJ)=ETR(N)
      RO(LJ)=ROR(N)
      XU(LJ)=XUR(N)
      COED(LJ)=COEDR(N)
      DT(LJ)=DTR(N)
      KE=KE+1
  166 CONTINUE
      GO TO 161
  163 L=NUMER(N)
      NUME(L)=NUMER(N)
      NPI(L)=NPIR(N)
      NPJ(L)=NPJR(N)
      NPK(L)=NPKR(N)
      ET(L)=ETR(N)
      RO(L)=ROR(N)
      XU(L)=XUR(N)
      COED(L)=COEDR(N)
      DT(L)=DTR(N)
  161 CONTINUE
C
C
C     GENERATION OF NOT READ NODAL POINTS
C
      DO 151 M=1,NURNP
      N=M+1
      IF(N-NURNP) 152,152,186
  152 I=NPNUR(N)-NPNUR(M)
      GO TO 154
  186 I=0
  154 L=NPNUR(M)
      IO=I+1
      DO 156 JO=1,IO
      J=JO-1
      LJ=L+J
      NPNUM(LJ)=NPNUR(M)+J
      IF(I-0) 188,188,189
```

```
  188 XORD(LJ)=XORDR(M)
      YORD(LJ)=YORDR(M)
      GO TO 191
  189 XORD(LJ)=XORDR(M)+((XORDR(N)-XORDR(M))/I)*J
      YORD(LJ)=YORDR(M)+((YORDR(N)-YORDR(M))/I)*J
  191 IF(J-0) 158,158,159
  159 IF(J-I) 157,153,156
  158 XLOAD(LJ)=XLDR(M)
      YLOAD(LJ)=YLDR(M)
      DSX(LJ)=DSXR(M)
      DSY(LJ)=DSYR(M)
      GO TO 156
  153 XLOAD(LJ)=XLDR(N)
      YLOAD(LJ)=YLDR(N)
      DSX(LJ)=DSXR(N)
      DSY(LJ)=DSYR(N)
      GO TO 156
  157 XLOAD(LJ)=0
      YLOAD(LJ)=0
      DSX(LJ)=0
      DSY(LJ)=0
  156 CONTINUE
  151 CONTINUE
C
C     INITIALIZE TOTAL DISPLACEMENTS AND STRESSES AND STRAINS
 606  DO 10 J=1,NUMNP
      DSXO(J)=0.0
      DSYO(J)=0.0
   10 CONTINUE
      DO 11 J=1,NUMEL
      XV(J)=0.
      YV(J)=0.
      XYV(J)=0.
      EPXV(J)=0.
      EPYV(J)=0.
   11 CONTINUE
      WRITE(6,111)
      WRITE(6,109) (NPNUM(M),XORD(M),YORD(M),XLOAD(M),YLOAD(M),
     1DSX(M),DSY(M),M=1,NUMNP)
C
C
C  READ BOUNDARY CONDITIONS.
C
C
      READ(5,4)(NPB(L),NFIX(L),SLOPE(L),          L=1,NUMBC)
C
C
      WRITE(6,112)
      WRITE(6,4)(NPB(L),NFIX(L),SLOPE(L),          L=1,NUMBC)
C  ASSIGN PROPER MATERIAL NUMBER IF NECESSARY
      DO 854 I=1,NUMEL
 854  MAT(I)=1
      READ(5,6) MATN
      IF(MATN.EQ.0) GO TO 56
      DO 55 I=1,MATN
 55   READ(5,20) M,MAT(M)
C
C ACOEF=2.C*COS(PHI)/(1.-SIN(PHI)),BCOEF=2.*SIN(PHI)/(1-SIN(PHI))
C
C
```

```
C  READ MATERIAL PROPERTIES.
C
C
 56   DO 850 I=1,NUMAT
      READ(5,2010) ROREAD(I),EBREAD(I),ESREAD(I),ACOEF(I),BCOEF(I)
      WRITE(6,2020)ROREAD(I),EBREAD(I),ESREAD(I),ACOEF(I),BCOEF(I)
 850  CONTINUE
      DO 57 N=1,NUMEL
      I=MAT(N)
      RO(N)=ROREAD(I)
      EBULK(N)=EBREAD(I)
      ESHEAR(N)=ESREAD(I)
      OBFAC(N)=1.0
  57  CONTINUE
C
C
C  READ OVERBURDEN FACTOR
C
C
      READ  (5,6) NOBSET
      IF(NOBSET.EQ.0) GO TO 48
      DO 771 I=1,NOBSET
      READ (5,753)  M,NSET,OBFAC(M)
      IF (NSET.EQ.0) GO TO 771
      DO 772 J=1,NSET
      M=M+1
 772  OBFAC(M)=OBFAC(M-1)
 771  CONTINUE
C
C
C  READ TRIAXIAL TEST DATA CONTROL CARD.
C
C
 48   READ(5,2021) NCELP,NSTRN,CONFAC
      IF(NCELP.EQ.0) GO TO 44
      CALL TESTD
C
C
C  INTERPOLATE INITIAL MODULI FOR ALL ELEMENTS
C
C
      DO 600 M=1,NUMEL
      IF(RO(M).LE.0.0) GO TO 600
      I=NPI(M)
      J=NPJ(M)
      K=NPK(M)
      Y1=ABS(YORD(I)-YORD(J))
      Y2=ABS(YORD(J)-YORD(K))
      Y3=ABS(YORD(K)-YORD(I))
      DEPTH=0.0
      IF(Y1.GT.DEPTH) DEPTH=Y1
      IF(Y2.GT.DEPTH) DEPTH=Y2
      IF(Y3.GT.DEPTH) DEPTH=Y3
      DEPTH=DEPTH/2.
      NCOUNT=0
      N=MAT(M)
      OBP=DEPTH*RO(M)*OBFAC(M)
      AVGSIG=OBP*0.5
 18   NCOUNT=NCOUNT+1
      SIGM1=OBP
```

```
      SIGM2=AVGSIG
      SIGM3=AVGSIG
      SIGOCT=(SIGM1+SIGM2+SIGM3)/3.
      SIGIN=SIGM1*SIGM2*SIGM3
      CONFS=SIGIN/(SIGOCT**2)
      DIVOCT=SQRT((SIGM1-SIGM2)**2+(SIGM2-SIGM3)**2+(SIGM3-SIGM1)**2)
      DIVOCT=DIVOCT/3.
      DO 720 J=1.NCELP
      JLS=J
      IF( CONFS-SL(J.N)) 721.720.720
  720 CONTINUE
  721 CONTINUE
      DO 790 K=1.NSTRN
      JS1=K
      IF(DIVOCT-SD(K.JLS-1.N)) 791.790.790
  790 CONTINUE
  791 CONTINUE
      DO 50 K=1.NSTRN
      JS2=K
      IF(DIVOCT-SD(K.JLS.N)) 51.50.50
   50 CONTINUE
   51 CONTINUE
      PR1=1.061*(VS(JS1.JLS-1.N)-VS(JS1-1.JLS-1.N))/(ST(JS1.N)-ST(JS1-1.
     1N))-1.0
      IF(PR1.GT.0.49) PR1=0.49
      PR2=1.061*(VS(JS2.JLS   .N)-VS(JS2-1.JLS   .N))/(ST(JS2.N)-ST(JS2-1.
     1N))-1.0
      IF(PR2.GT.0.49) PR2=0.49
      PR3=PR1+((PR2-PR1)*( CONFS-SL(JLS-1.N))/(SL(JLS.N)-SL(JLS-1.N)))
      IF(PR3.GT.0.49 ) PR3=0.49
      CONST=PR3/(1.-PR3)
      HPR=OBP*CONST
      HPR=(HPR+AVGSIG)/2.
      CSTRS=ABS(HPR-AVGSIG)
      IF(NCOUNT.GE.21) GO TO 52
      IF(ABS(HPR-AVGSIG).LT.0.01) GO TO 52
      AVGSIG=HPR
      GO TO 18
   52 WRITE(6.125) M.NCOUNT.HPR.CSTRS.PR3
      DIF1=SD(JS1.JLS-1.N)-SD(JS1-1.JLS-1.N)
      ETP1=DIF1/(ST(JS1.N)-ST(JS1-1.N))
      GTP1=ETP1/(0.9428*(1.+PR1))
      DIF2=SD(JS2.JLS.N)-SD(JS2-1.JLS.N)
      ETP2=DIF2/(ST(JS2.N)-ST(JS2-1.N))
      GTP2=ETP2/(0.9428*(1.+PR2))
      GTP=GTP1+ (GTP2-GTP1)*(CONFS -SL(JLS-1.N))/(SL(JLS.N)-SL(JLS-1.N))
      GTP=100.*GTP
      EBULK(M)=GTP*2.*(1.+PR3)/(3.*(1.-2.*PR3))
      ESHEAR(M)=GTP
  600 CONTINUE
      IF(NCELP.NE.0) GO TO 46
   44 IF(NANLYS.EQ.0) GO TO 46
   46 WRITE(6.110)
C
C
C  PRINT ELEMENT DATA
C
C
      WRITE(6.2055)(NUME(N).NPI(N).NPJ(N).NPK(N).EBULK(N).RO(N).ESHEAR(N
     1). MAT(N).      N=1.NUMEL)
```

```
C
C
C  READ PARTICULARS   OF CURRENT STEP.
C
C
      READ(5.6) KOPT
      READ(5.6) ITOPT
      READ(5.20) NSTEP.NTENS
      DO 500 JM = 1.NSTEP
      READ(5.13)NUMELS.NUMNPS.NUMBCS.NCPIN.NOPIN.NCYCM.TOLER.XFAC.LNUM
      NUMEL=NUMELS
      NUMNP=NUMNPS
      NUMBC=NUMBCS
      DO 761 N=1.NUMNP
      TAD(N)=0.0
      TAL(N)=0.0
  761 CONTINUE
C
C
C  READ BOUNDARY LOADS FOR CURRENT STEP
C
C
      READ(5.5) NLOAD
      IF(NLOAD.EQ.0) GO TO 4050
      DO 4051 I=1.NLOAD
      READ(5.602) N.YLOAD(N).XLOAD(N)
      IF(YLOAD(N).NE.0.0) TAL(N)=2.0
      IF(XLOAD(N).NE.0.0) TAL(N)=1.0
 4051 CONTINUE
C
C
C  READ BOUNDARY DISPLACEMENTS FOR CURRENT STEP
C
C
 4050 READ(5.6) NBOUN
      IF(NBOUN.EQ.0) GO TO 41
      DO 601 N=1.NBOUN
      READ(5.602) M.DSY(M).DSX(M)
      IF(DSY(M).NE.0.0) TAD(M)=2.0
      IF(DSX(M).NE.0.0) TAD(M)=1.0
  601 CONTINUE
   41 WRITE (6.101) NUMEL
      WRITE(6.102)NUMNP
      WRITE(6.103)NUMBC
      WRITE(6.104)NCPIN
      WRITE(6.105)NOPIN
      WRITE(6.106)NCYCM
      WRITE(6.107)TOLER
      WRITE(6.108)XFAC
      WRITE(6.117)LNUM
      NITER=0
      IF(NSTEP.EQ.1) GO TO 160
      IF(NCELP.EQ.0) GO TO 160
      WRITE(6.110)
      WRITE(6.2055)(NUME(N).NPI(N).NPJ(N).NPK(N).EBULK(N).RO(N).ESHEAR(N
     1). MAT(N).       N=1.NUMEL)
      WRITE(6.111)
      WRITE(6.109) (NPNUM(M).XORD(M).YORD(M).XLOAD(M).YLOAD(M).
     1DSX(M).DSY(M).M=1.NUMNP)
C
```

```
C        INITIALIZATION
C
  160 NCYCLE=0
      NITER=NITER+1
      NUMPT=NCPIN
      NUMOPT=NOPIN
      DO 175 L=1.NUMNP
      DO 170 M=1.9
      SXX(L.M)=0.0
      SXY(L.M)=0.0
      SYX(L.M)=0.0
      SYY(L.M)=0.0
  170 NP(L.M)=0
      NP(L.10)=0
  175 NP(L.1)=L
C
C        MODIFICATION OF LOADS AND ELEMENT DIMENSIONS
C
      NERROR=0
      DO 180 N=1.NUMEL
      ET(N)=0.0
      COED(N)=0.0
      DT(N)=0.0
      XU(N)=0.0
      I=NPI(N)
      J=NPJ(N)
      K=NPK(N)
      AJ(N)=XORD(J)-XORD(I)
      AK(N)=XORD(K)-XORD(I)
      BJ(N)=YORD(J)-YORD(I)
      BK(N)=YORD(K)-YORD(I)
  176 AREA=(AJ(N)*BK(N)-BJ(N)*AK(N))/2.
      IF(AREA) 701.701.177
  177 THERM(N)=ET(N)*COED(N)*DT(N)/(XU(N)-1.)
      DL=AREA*RO(N)/3.
      XLOAD(I)=THERM(N)*(BK(N)-BJ(N))/2.+XLOAD(I)
      XLOAD(J)=-THERM(N)*BK(N)/2.+XLOAD(J)
      XLOAD(K)=THERM(N)*BJ(N)/2.+XLOAD(K)
      YLOAD(I)=THERM(N)*(AJ(N)-AK(N))/2.+YLOAD(I)-DL
      YLOAD(J)=THERM(N)*AK(N)/2.+YLOAD(J)-DL
      YLOAD(K)=-THERM(N)*AJ(N)/2.+YLOAD(K)-DL
      IF(AREA.GT.0.0) GO TO 180
  701 WRITE(6.711)N
      NERROR=NERROR+1
  180 CONTINUE
      IF(NERROR.GT.0) GO TO 925
C
C        FORMATION OF STIFFNESS ARRAY
C
      DO 200 N=1.NUMEL
      AREA=(AJ(N)*BK(N)-AK(N)*BJ(N))*.5
      COMM=0.25/AREA
      A(1.1)=BJ(N)-BK(N)
      A(1.2)=0.0
      A(1.3)=BK(N)
      A(1.4)=0.0
      A(1.5)=-BJ(N)
      A(1.6)=0.0
      A(2.1)=0.0
      A(2.2)=AK(N)-AJ(N)
```

```
      A(2,3)=0.0
      A(2,4)=-AK(N)
      A(2,5)=0.0
      A(2,6)=AJ(N)
      A(3,1)=AK(N)-AJ(N)
      A(3,2)=BJ(N)-BK(N)
      A(3,3)=-AK(N)
      A(3,4)=BK(N)
      A(3,5)=AJ(N)
      A(3,6)=-BJ(N)
      IF(IANLYS.EQ.0) COM1=EBULK(N)+ESHEAR(N)*(4./3.)
      IF(IANLYS.EQ.0) COM2=EBULK(N)-ESHEAR(N)*(2./3.)
      IF(IANLYS.GT.0) COM1=4.*ESHEAR(N)*(EBULK(N)+ESHEAR(N)/3.)/(EBULK(N
     1)+(4./3.)*ESHEAR(N))
      IF(IANLYS.GT.0) COM2=2.*ESHEAR(N)*(EBULK(N)-(2./3.)*ESHEAR(N))/(EB
     1ULK(N)+(4./3.)*ESHEAR(N))
      B(1,1)=    COMM*COM1
      B(1,2)=COMM*COM2
      B(1,3)=0.0
      B(2,1)=COMM*COM2
      B(2,2)=COMM*COM1
      B(2,3)=0.0
      B(3,1)=0.0
      B(3,2)=0.0
      B(3,3)=COMM*ESHEAR(N)
C
      DO 182 J=1,6
      DO 182I=1,3
      S(I,J)=0.0
      DO 182 K=1,3
  182 S(I,J)=S(I,J)+B(I,K)*A(K,J)
      DO 183 J=1,6
      DO 183 I=1,3
  183 B(J,I)=S(I,J)
      DO 184 J=1,6
      DO 184 I=1,6
      S(I,J)=0.0
      DO 184 K=1,3
  184 S(I,J)=S(I,J)+B(I,K)*A(K,J)
C
      LM(1)=NPI(N)
      LM(2)=NPJ(N)
      LM(3)=NPK(N)
      DO 200 L=1,3
      DO 200 M=1,3
      LX=LM(L)
      MX=0
  185 MX=MX+1
      IF(NP(LX,MX)-LM(M)) 190,195,190
  190 IF(NP(LX,MX)) 185,195,185
  195 NP(LX,MX)=LM(M)
      IF(MX-10) 196,702,702
  196 SXX(LX,MX)=SXX(LX,MX)+S(2*L-1,2*M-1)
      SXY(LX,MX)=SXY(LX,MX)+S(2*L-1,2*M)
      SYX(LX,MX)=SYX(LX,MX)+S(2*L,2*M-1)
  200 SYY(LX,MX)=SYY(LX,MX)+S(2*L,2*M)
C
C     COUNT OF ACJACENT NODAL FCINTS
C
      DO 206 M=1,NUMNP
```

```
      MX=1
  205 MX=MX+1
      IF (NP(M,MX)) 206,206,205
  206 NAP(M)=MX-1
C
C     INVERSION OF NODAL POINT STIFFNESS
C
      DO 210 M=1,NUMNP
      COMM=SXX(M,1)*SYY(M,1)-SXY(M,1)*SYX(M,1)
      TEMP=SYY(M,1)/COMM
      SYY(M,1)=SXX(M,1)/COMM
      SXX(M,1)=TEMP
      SXY(M,1)=-SXY(M,1)/CCMM
      SYX(M,1)=-SYX(M,1)/CCMM
  210 CONTINUE
C
C     MODIFICATION OF BOUNDARY FLEXIBILITIES
C
      DO 240 L=1,NUMBC
      M=NPB(L)
      NP(M,1)=0
      IF(NFIX(L)-1) 225,220,215
  215 C=(SXX(M,1)*SLOPE(L)-SXY(M,1))/(SYX(M,1)*SLOPE(L)-SYY(M,1))
      R=1.-C*SLOPE(L)
      SXX(M,1)=(SXX(M,1)-C*SYX(M,1))/R
      SXY(M,1)=(SXY(M,1)-C*SYY(M,1))/R
      SYX(M,1)=SXX(M,1)*SLOPE(L)
      SYY(M,1)=SXY(M,1)*SLOPE(L)
      GO TO 240
  220 SYY(M,1)=SYY(M,1)-SYX(M,1)*SXY(M,1)/SXX(M,1)
      GO TO 230
  225 SYY(M,1)=0.0
  230 SXX(M,1)=0.0
  235 SXY(M,1)=0.0
      SYX(M,1)=0.0
  240 CONTINUE
C
C     ITERATION OF NODAL POINT DISPLACEMENTS
C
      KOUNT=0
  243 WRITE(6,119)
      KOUNT=KOUNT+1
  244 SUM=0.0
      DO 290 M=1,NUMNP
      NUM=NAP(M)
      IF (SXX(M,1)+SYY(M,1)) 275,290,275
  275 FRX=XLOAD(M)
      FRY=YLOAD(M)
      DO 280 L=2,NUM
      N=NP(M,L)
      FRX=FRX-SXX(M,L)*DSX(N)-SXY(M,L)*DSY(N)
  280 FRY=FRY-SYX(M,L)*DSX(N)-SYY(M,L)*DSY(N)
      DX=SXX(M,1)*FRX+SXY(M,1)*FRY-DSX(M)
      DY=SYX(M,1)*FRX+SYY(M,1)*FRY-DSY(M)
      DSX(M)=DSX(M)+XFAC*DX
      DSY(M)=DSY(M)+XFAC*DY
      IF(NP(M,1)) 285,290,285
  285 SUM=SUM+ABS(DX/SXX(M,1))+ABS(DY/SYY(M,1))
  290 CONTINUE
C
```

```
C       CYCLE COUNT AND PRINT CHECK
C
        NCYCLE=NCYCLE+1
        IF (NCYCLE-NUMPT) 305,300,300
    300 NUMPT=NUMPT+NCPIN
        WRITE(6,120)NCYCLE,SUM
    305 IF (SUM-TOLER) 400,400,310
    310 IF(NCYCM-NCYCLE) 400,400,315
    315 IF (NCYCLE-NUMOPT) 244,320,320
    320 NUMOPT=NUMOPT+NOPIN
C
C       PRINT OF DISPLACEMENTS AND STRESSES
C
  400   CONTINUE
        IF (SUM-TOLER) 440,440,430
    430 IF (NCYCM-NCYCLE) 440,440,243
    440 WRITE(6,975)SUM,TOLER
    975 FORMAT(5H0SUM=1E15.6,6HTOLER=1E15.6)
        DO 421 N=1,NUMEL
        I=NPI(N)
        J=NPJ(N)
        K=NPK(N)
        EPX=(BJ(N)-BK(N))*DSX(I)+BK(N)*DSX(J)-BJ(N)*DSX(K)
        EPY=(AK(N)-AJ(N))*DSY(I)-AK(N)*DSY(J)+AJ(N)*DSY(K)
        GAM=(AK(N)-AJ(N))*DSX(I)-AK(N)*DSX(J)+AJ(N)*DSX(K)
       1+(BJ(N)-BK(N))*DSY(I)+BK(N)*DSY(J)-BJ(N)*DSY(K)
        COMM=1./(AJ(N)*BK(N)-AK(N)*BJ(N))
        IF(IANLYS.EQ.0) COM1=EBULK(N)+ESHEAR(N)*(4./3.)
        IF(IANLYS.EQ.0) COM2=EBULK(N)-ESHEAR(N)*(2./3.)
        IF(IANLYS.GT.0) COM1=4.*ESHEAR(N)*(EBULK(N)+ESHEAR(N)/3.)/(EBULK(N
       1)+(4./3.)*ESHEAR(N))
        IF(IANLYS.GT.0) COM2=2.*ESHEAR(N)*(EBULK(N)-(2./3.)*ESHEAR(N))/(EB
       1ULK(N)+(4./3.)*ESHEAR(N))
        COM3=ESHEAR(N)
        X=COMM*(COM1*EPX+COM2*EPY)+THERM(N)
        Y=COMM*(COM2*EPX+COM1*EPY)+THERM(N)
        XY=COMM*COM3*GAM
        XV(N)=XV(N)+X
        YV(N)=YV(N)+Y
        XYV(N)=XYV(N)+XY
        EPXV(N)=EPXV(N)+(EPX*100.)/(AJ(N)*BK(N)-AK(N)*BJ(N))
        EPYV(N)=EPYV(N)+(EPY*100.)/(AJ(N)*BK(N)-AK(N)*BJ(N))
        GAMV(N)=GAMV(N)+GAM*100.*COMM
        C=(XV(N)+YV(N))/2.0
        R=SQRT(((YV(N)-XV(N))/2.0)**2+XYV(N)**2)
        XMAX(N)=C+R
        XMIN(N)=C-R
        PA(N)=0.5*57.29578*ATAN(2.*XYV(N)/(YV(N)-XV(N)))
        IF(2.*XV(N)-XMAX(N)-XMIN(N))405,420,420
    405 IF(PA(N)) 410,420,415
    410 PA(N)=PA(N)+90.0
        GO TO 420
    415 PA(N)=PA(N)-90.0
   420  ANG=PA(N)*11./630.
        CC=COS(ANG)**2
        SS=SIN(ANG)**2
        SC=COS(ANG)*SIN(ANG)
        EMAX(N)=EPXV(N)*CC+EPYV(N)*SS-SC*GAMV(N)
        EMIN(N)=EPXV(N)*SS+EPYV(N)*CC+SC*GAMV(N)
        IF(ITOPT.EQ.0) GO TO 421
```

```
      IF(NITER.EQ.2) GO TO 421
      WRITE(6,124) NUME(N),XV(N),YV(N),XYV(N),XMAX(N),XMIN(N),PA(N),
     1EPXV(N),EPYV(N),EMAX(N),EMIN(N)
      XV(N)=XV(N)-X
      YV(N)=YV(N)-Y
      XYV(N)=XYV(N)-XY
      EPXV(N)=EPXV(N)-(EPX*100.)/(AJ(N)*BK(N)-AK(N)*BJ(N))
      EPYV(N)=EPYV(N)-(EPY*100.)/(AJ(N)*BK(N)-AK(N)*BJ(N))
      GAMV(N)=GAMV(N)-GAM*100.*CGMM
  421 CONTINUE
C
C
C  FIND THE MAXIMUM AND MINIMUM PRINCIPAL STRESSES
      SIG1=0.0
      SIG2=0.0
      M1=0
      M2=0
      DO 630 M=1,NUMEL
      IF(XMAX(M).LT.SIG1) GO TO 631
      SIG1=XMAX(M)
      M1=M
  631 IF(XMIN(M).GT.SIG2)  GO TO 630
      SIG2=XMIN(M)
      M2=M
  630 CONTINUE
      WRITE(6,117) JM
      WRITE (6,633) (SIG1,M1,SIG2,M2)
C
      DO 650 J=1,NUMNP
      IF(ITOPT.EQ.1.AND.NITER.EQ.1) GO TO 770
      XLOAD(J)=0.0
      YLOAD(J)=0.0
      XORD(J)=XORD(J)+DSX(J)
      YORD(J)=YORD(J)+DSY(J)
      DSXQ(J)=DSX(J)+DSXQ(J)
      DSYQ(J)=DSY(J)+DSYQ(J)
      DSX(J)=0.0
      DSY(J)=0.0
      GO TO 650
  770 DSXQ(J)=DSX(J)+DSXQ(J)
      DSYQ(J)=DSY(J)+DSYQ(J)
      WRITE (6,122)  NPNUM(J),DSXQ(J),DSYQ(J)
      DSXQ(J)=DSXQ(J)-DSX(J)
      DSYQ(J)=DSYQ(J)-DSY(J)
      IF(TAD(J).EQ.1.0) DSY(J)=0.0
      IF(TAD(J).EQ.2.0) DSX(J)=0.0
      IF(TAD(J).NE.0.0) GO TO 5001
      DSX(J)=0.0
      DSY(J)=0.0
 5001 IF(TAL(J).EQ.1.0) YLOAD(J)=0.0
      IF(TAL(J).EQ.2.0) XLOAD(J)=0.0
      IF(TAL(J).NE.0.0) GO TO 650
      XLOAD(J)=0.0
      YLOAD(J)=0.0
  650 CONTINUE
      IF(KOPT.EQ.0) GO TO 664
      IF(ITOPT.GT.0.AND.NITER.EQ.1.AND.KOPT.GT.0) GO TO 664
      IF(KOUNT.GT.1) GO TO 681
      WRITE(6,121)
      WRITE(6,122)(NPNUM(M),DSXQ(M),DSYQ(M),M=1,NUMNP)
```

```
      WRITE(6.123)
      WRITE(6.124) (NUME(N).XV(N).YV(N).XYV(N).XMAX (N).XMIN (N).PA (N).
     1EPXV(N).EPYV(N).EMAX (N).EMIN (N).N=1.NUMEL)
  681 IF(NSTEP.EQ.1) GO TO 925
      IF(JM.EQ.NSTEP) GC TO 925
      IF(SIG1.LE.0.005) GO TO 664
C   TENSILE STRESS REMOVED
      DO 660 M=1.NUMEL
      IF(XMAX(M).LE.0.0) GO TO 660
      ANG=PA(M)*11./630.
      I=NPI(M)
      J=NPJ(M)
      K=NPK(M)
      AJ(M)=XORD(J)-XORC(I)
      AK(M)=XORD(K)-XORD(I)
      BJ(M)=YORD(J)-YCRD(I)
      BK(M)=YORD(K)-YORD(I)
      AJ1=AJ(M)*COS(ANG)+BJ(M)*SIN(ANG)
      BJ1=-AJ(M)*SIN(ANG)+BJ(M)*COS(ANG)
      AK1=AK(M)*COS(ANG)+BK(M)*SIN(ANG)
      BK1=-AK(M)*SIN(ANG)+BK(M)*COS(ANG)
      R1I=XMAX(M)*(BK1-EJ1)/2.
      R1I=-R1I
      R1J=-XMAX(M)*BK1/2.
      R1J=-R1J
      R1K=XMAX(M)*BJ1/2.
      R1K=-R1K
      XMAX(M)=0.0
      XV(M)=XMIN(M)*(SIN(ANG)**2)
      YV(M)=XMIN(M)*(COS(ANG)**2)
      XYV(M)=XMIN(M)*SIN(ANG)*COS(ANG)
      IF(XMIN(M).LE.0.0)  GO TO 661
      R2I=XMIN(M)*(AJ1-AK1)/2.
      R2I=-R2I
      R2J=XMIN(M)*AK1/2.
      R2J=-R2J
      R2K=-XMIN(M)*AJ1/2.
      R2K=-R2K
      XMIN(M)=0.0
      XV(M)=0.0
      YV(M)=0.0
      XYV(M)=0.0
      XLOAD(I)=COS(ANG)*R1I+XLOAD(I)-SIN(ANG)*R2I
      XLOAD(J)=COS(ANG)*R1J+XLOAD(J)-SIN(ANG)*R2J
      XLOAD(K)=COS(ANG)*R1K+XLOAD(K)-SIN(ANG)*R2K
      YLOAD(I)=SIN(ANG)*R1I+YLOAD(I)+COS(ANG)*R2I
      YLOAD(J)=SIN(ANG)*R1J+YLOAD(J)+COS(ANG)*R2J
      YLOAD(K)=SIN(ANG)*R1K+YLOAD(K)+COS(ANG)*R2K
      GO TO 660
  661 XLOAD(I)=COS(ANG)*R1I+XLOAC(I)
      XLOAD(J)=COS(ANG)*R1J+XLCAD(J)
      XLOAD(K)=COS(ANG)*R1K+XLOAD(K)
      YLOAD(I)=SIN(ANG)*R1I+YLOAD(I)
      YLOAD(J)=SIN(ANG)*R1J+YLCAC(J)
      YLOAD(K)=SIN(ANG)*P1K+YLOAD(K)
  660 CONTINUE
      WRITE(6.6)KOUNT
      GO TO 243
  664 IF(ITOPT.GT.0.AND.NITER.EQ.1) GO TO 764
      WRITE (6.121)
```

```
      WRITE(6,122)(NPNUM(M),DSXQ(M),DSYQ(M),M=1,NUMNP)
      WRITE(6,123)
      WRITE(6,124) (NUME(N),XV(N),YV(N),XYV(N),XMAX (N),XMIN (N),PA (N),
     1EPXV(N),EPYV(N),EMAX (N),EMIN (N),N=1,NUMEL)
C
C
C  INTERPOLATE MODULI
C
C
  764 DO 501 JJ=1,NUMEL
      NCOUN=0
      IF(ITOPT.EQ.0)  RO(JJ)=0.0
      IF(NITER.EQ.2)  RO(JJ)=0.0
      IF (NANLYS.EQ.0) GO TO 500
      IF(KOPT.GT.0.AND.ITOPT.EQ.1.AND.NITER.EQ.1.AND.XMAX(JJ).GE.0.0) GO
     1TO 501
      AVGSIG=ABS(XMAX(JJ))
      IF(XMAX(JJ).GE.0.0)AVGSIG=0.0
      DIVS=ABS(XMIN(JJ))-AVGSIG
      DIVS=ABS(DIVS)
      N=MAT(JJ)
      DIVSF=ACOEF(N)+BCOEF(N)*ABS(XMAX(JJ))
      IF(XMAX(JJ).GE.0.0) DIVSF=ACOEF(N)
      IF(NCELP.EQ.0) GO TO 852
      SIGM1=ABS(XMIN(JJ))
      SIGM2=(AVGSIG+SIGM1)/2.
      SIGM3=AVGSIG
      IF(IANLYS.GT.0) SIGM2=0.0
  950 NCOUN=NCOUN+1
      SIGOCT=(SIGM1+SIGM2+SIGM3)/3.
      SIGIN=SIGM1*SIGM2*SIGM3
      CONFS=SIGIN/(SIGOCT**2)
      DIVOCT=SQRT((SIGM1-SIGM2)**2+(SIGM2-SIGM3)**2+(SIGM3-SIGM1)**2)
      DIVOCT=DIVOCT/3.
      DO 26 J=1,NCELP
      JLS=J
      IF( CONFS-SL(J,N)) 27,26,26
   26 CONTINUE
   27 CONTINUE
      DO 28 K=1,NSTRN
      JS1=K
      IF(DIVOCT-SD(K,JLS-1,N)) 29,28,28
   28 CONTINUE
   29 CONTINUE
      DO 751 K=1,NSTRN
      JS2=K
      IF(DIVOCT-SD(K,JLS,N)) 752,751,751
  751 CONTINUE
  752 CONTINUE
      PR1=1.061*(VS(JS1,JLS-1,N)-VS(JS1-1,JLS-1,N))/(ST(JS1,N)-ST(JS1-1,
     1N))-1.0
      IF(PR1.GT.0.49) PR1=0.49
      PR2=1.061*(VS(JS2,JLS   ,N)-VS(JS2-1,JLS   ,N))/(ST(JS2,N)-ST(JS2-1,
     1N))-1.0
      IF(PR2.GT.0.49) PR2=0.49
      PR3=PR1+((PR2-PR1)*( CONFS-SL(JLS-1,N))/(SL(JLS,N)-SL(JLS-1,N)))
      IF(PR3.GT.0.49 ) PR3=0.49
      DIF1=SD(JS1,JLS-1,N)-SD(JS1-1,JLS-1,N)
      ETP1=DIF1/(ST(JS1,N)-ST(JS1-1,N))
      GTP1=ETP1/(0.9428*(1.+PR1))
```

```
      DIF2=SD(JS2.JLS.N)-SD(JS2-1.JLS.N)
      ETP2=DIF2/(ST(JS2.N)-ST(JS2-1.N))
      GTP2=ETP2/(0.9428*(1.+PR2))
      GTP=GTP1+ (GTP2-GTP1)*(CONFS -SL(JLS-1.N))/(SL(JLS.N)-SL(JLS-1.N))
      GTP=100.*GTP
      BULKM   =GTP*2.*(1.+PR3)/(3.*(1.-2.*PR3))
      SHEARM=GTP
      IF(IANLYS.GT.0) GO TO 852
      SIGMM2=PR3*(SIGM1+SIGM3)
      SIGMM2=(SIGMM2+SIGM2)/2.
      STRS=ABS(SIGMM2-SIGM2)
      IF(NCOUN.GE.11) GO TO 851
      IF(ABS(SIGMM2-SIGM2).LT.0.01) GO TO 851
      SIGM2=SIGMM2
      GO TO 950
  851 WRITE(6.125) JJ.NCOUN.SIGM2.STRS.PR3
  852 CONTINUE
      IF(NITER.EQ.1)TEBULK=BULKM
      IF(NITER.EQ.2)EBULK(JJ)=BULKM
      IF(ITOPT.GT.0.AND.NITER.EQ.1)EBULK(JJ)=(EBULK(JJ)+TEBULK)/2.
      IF(ITOPT.EQ.0.AND.NITER.EQ.1)EBULK(JJ)=TEBULK
      IF(NITER.EQ.1)TSHEAR=SHEARM
      IF(NITER.EQ.1.AND.DIVS.GE.DIVSF.AND.NTENS.GT.0) TSHEAR=EBULK(JJ)/5
     10.
      IF(NITER.EQ.2)ESHEAR(JJ)=SHEARM
      IF(NITER.EQ.2.AND.DIVS.GE.DIVSF.AND.NTENS.GT.0) ESHEAR(JJ)=EBULK(J
     1J)/50.
      IF(ITOPT.GT.0.AND.NITER.EQ.1)ESHEAR(JJ)=(ESHEAR(JJ)+TSHEAR)/2.
      IF(ITOPT.EQ.0.AND.NITER.EQ.1)ESHEAR(JJ)=TSHEAR
      IF(ESHEAR(JJ).GT.(1.45*EBULK(JJ)))ESHEAR(JJ)=1.45*EBULK(JJ)
      IF(ESHEAR(JJ).LT.(EBULK(JJ)/50.))ESHEAR(JJ)=EBULK(JJ)/50.
  501 CONTINUE
      WRITE(6.110)
      WRITE(6.2055)(NUME(N).NPI(N).NPJ(N).NPK(N). EBULK(N). RO(N).ESHEAR(N
     1). MAT(N).      N=1.NUMEL)
      IF(ITOPT.EQ.0) GO TO 500
      IF(NITER.EQ.1) GO TO 160
  500 CONTINUE
C
      GO TO 925
C
C     PRINT OF ERRORS IN INPUT DATA
C
  702 WRITE(6.712)LX
C
C
C     FORMAT STATEMENTS
C
C
    1 FORMAT (9I5)
    2 FORMAT(1I5.3I4.4E12.4.1F8.4)
    3 FORMAT(I5.4F10.0.2F12.8)
    4 FORMAT (2I5.1F8.3)
    5 FORMAT (3E15.8)
    6 FORMAT(1I5)
    7 FORMAT(I4.6F8.0)
    8 FORMAT(2I4.2F8.0)
    9 FORMAT(4I5)
   13 FORMAT(6I5.2F10.0.I5)
   20 FORMAT (2I5)
```

```
   21  FORMAT(7F5.0)
    23 FORMAT (1X,'LATSTRESS',6X, 6F8.3/)
    24 FORMAT (1X,'STRAIN',3X,1F6.2, 6F8.3/)
   40  FORMAT(12F6.0)
    99 FORMAT (1H1)
   100 FORMAT(18A4)
   101 FORMAT (30HONUMBER OF ELEMENTS            =1I4/)
   102 FORMAT (30H NUMBER OF NODAL POINTS        =1I4/)
   103 FORMAT (30H NUMBER OF BOUNDARY POINTS     =1I4/)
   104 FORMAT (30H CYCLE PRINT INTERVAL          =1I4/)
   105 FORMAT (30H OUTPUT INTERVAL OF RESULTS    =1I4/)
   106 FORMAT (30H CYCLE LIMIT                   =1I4/)
   107 FORMAT (30H TOLERANCE LIMIT               =1E12.4/)
   108 FORMAT (30H OVER RELAXATION FACTOR        =1F6.3)
   117 FORMAT (30H LIFT NUMBER                   =1I4/)
   109 FORMAT (1I8,4F12.6,2F12.8)
   110 FORMAT (74H1EL.    I     J  K        EBULK     DENSITY        ESHEAR
      1MAT NO.            )
   111 FORMAT(80H1          NP       X-ORD       Y-ORD      X-LOAD      Y-LOAD
      1     X-DISP      Y-DISP    )
   112 FORMAT(20H BOUNDARY CONDITIONS)
   119 FORMAT(34H0          CYCLE       FORCE UNBALANCE)
   120 FORMAT (1I12,1E20.6)
   121 FORMAT(42HONODAL POINT X-DISPLACEMENT Y-DISPLACEMENT)
   122 FORMAT (1I12,2E15.6)
   123 FORMAT(5H1ELNO 4X,8HX-STRESS 4X,8HY-STRESS 3X,9HXY-STRESS 2X,10HMA
      1X-STRESS 2X,10HMIN-STRESS 2X,9HDIRECTION 3X,8HX-STRAIN 3X,8HY-STRA
      2IN 1X,10HMAX-STRAIN 1X,10HMIN-STRAIN)
   124 FORMAT(1I5,5E12.5,5E11.4)
   125 FORMAT(2I5,3E12.5)
   126 FORMAT(1I4,2E12.5)
  602  FORMAT(I5,2F10.0)
  633  FORMAT ('0',
      1'MAX. PRINCIPAL STRESS=',F10.5,'AND OCCURS IN ELEM.',I6//
      2'MIN. PRINCIPAL STRESS=',F10.5,'AND OCCURS IN ELEM.',I6//)
   711 FORMAT(32HOZERO OR NEGATIVE AREA, EL.NO. =1I4)
   712 FORMAT(33HOOVER 8 N.P. ADJACENT TO N.P. NO.1I4)
  670  FORMAT(//4I5,6F12.6)
  753  FORMAT(2I5,F10.0)
   823 FORMAT(5H1NODE 4X,8HX-STRESS 4X,8HY-STRESS 3X,9HXY-STRESS)
   824 FORMAT (30H NUMBER OF REAC NODAL POINTS =1I4/)
   825 FORMAT (30H NUMBER OF REAC ELEMENTS      =1I4/)
  1010 FORMAT(I5,6F5.0)
  1020 FORMAT(I5,4F15.6)
  1030 FORMAT(3I5)
 2000  FORMAT('0','NUMBER OF THE MATERIAL=',I5/)
 2010  FORMAT(5F10.0)
 2020  FORMAT('0',10X,'DENSITY=',F15.6//,10X,'BULK MODULUS=',F15.6//,10X,
      1'SHEAR MODULUS=',F15.6//,10X,'ACOEF.='F15.6//,10X,'BCOEF.=',F15.6)
  2021 FORMAT(2I5,F10.0)
 2051  FORMAT(10F5.0)
 2052  FORMAT(11F5.0)
 2053  FORMAT('0',10X,'STRESS-STRAIN RELATIONSHIPS FOR MATERIAL='I5//)
  2055 FORMAT(I5,3I4,3E12.4,I5)
 C
 C
   925 STOP
 C
       END
 C
```

```
C
C
C
      SUBROUTINE TESTO
C
C
C
C CONVERSION OF TRIAXIAL TEST DATA FRCM CONVENTIONAL FORM TO STRESS
C  INVARIANT FORM AND  INTERPOLATION
C
C
C
      DIMENSION SL(10,5),SD(20,10,5),VS(20,10,5),SIGINV(20,10,5),
     1VSTN(20,10,5)
      COMMON/AREA3/
     1        ST(20,5),SIGINT(20,5),TOCTD(20,10,5),GOCT(20,10,5),NUMAT,
     1NCELP,CONFAC,NSTRN
C
C
C
C  READ CELL PRESSURE CATA FOR GIVEN MATERIALS
C
C
      DO 10 N=1,NUMAT
      READ(5,1010) (SL(J,N),J=1,NCELP)
      DO 15 J=1,NCELP
      SL(J,N)=SL(J,N)*CONFAC
      SIGINT(J,N)=SL(J,N)
   15 CONTINUE
C
C
C  READ DEVIATORIC STRESS DATA FOR GIVEN MATERIALS
C
C
      DO 20 K=1,NSTRN
      READ(5,1020) ST(K,N),(SD(K,J,N),J=1,NCELP)
      DO 25 J=1,NCELP
      SD(K,J,N)=SD(K,J,N)*CONFAC
   25 CONTINUE
   20 CONTINUE
      WRITE (6,1030) N
      WRITE(6,1040) (SL(J,N),J=1,NCELP)
C
C
C  READ VOLUMETRIC STRAIN CATA FOR GIVEN MATERIALS
C
C
      DO 30 K=1,NSTRN
      READ  (5,1020) ST(K,N),(VS(K,J,N),J=1,NCELP)
      WRITE(6,1050)  ST(K,N),(VS(K,J,N),J=1,NCELP)
   30 CONTINUE
      DO 35 K=1,NSTRN
      WRITE(6,1050)  ST(K,N),(SD(K,J,N),J=1,NCELP)
   35 CONTINUE
   10 CONTINUE
      DO 40 N=1,NUMAT
      DO 45 J=1,NCELP
      DO 50 K=1,NSTRN
      PROD= (SL(J,N)**2)*(SC(K,J,N)+SL(J,N))
      SIGOCT=SL(J,N)+(SD(K,J,N))/3.
```

```
      IF(J.EQ.1.AND.K.EQ.1) GO TO 51
      SIGINV(K,J,N)=PROD/(SIGOCT**2)
   51 IF(J.EQ.1.AND.K.EQ.1) SIGINV(K,J,N)=0.0
   50 CONTINUE
   45 CONTINUE
      DO 70 I=1,NCELP
      DO 55 K=1,NSTRN
      DO 60 J=1,NCELP
      JLS=J
      IF(SIGINT(I,N)-SIGINV(K,J,N))61,60,60
   60 CONTINUE
   61 CONTINUE
      TOCTD(K,I,N)=SD(K,JLS-1,N)+(SD(K,JLS,N)-SD(K,JLS-1,N))*(SIGINT(I,N
     1)-SIGINV(K,JLS-1,N))/(SIGINV(K,JLS,N)-SIGINV(K,JLS-1,N))
      TOCTD(K,I,N)=TOCTD(K,I,N)*0.4714
      VSTN(K,I,N)=VS(K,JLS-1,N)+(VS(K,JLS,N)-VS(K,JLS-1,N))*(SIGINT(I,N)
     1-SIGINV(K,JLS-1,N))/(SIGINV(K,JLS,N)-SIGINV(K,JLS-1,N))
      GOCT(K,I,N)=0.4714*(3.*ST(K,N) -VSTN(K,I,N))
   55 CONTINUE
   70 CONTINUE
      WRITE(6,1031) N
      WRITE (6,1041) (SIGINT(I,N),I=1,NCELP)
      DO 75 K=1,NSTRN
   75 WRITE(6,1050)ST(K,N),(TOCTD(K,I,N),I=1,NCELP)
      DO 80 K=1,NSTRN
   80 WRITE(6,1050) ST(K,N),(GOCT(K,J,N),J=1,NCELP)
   40 CONTINUE
 1000 FORMAT(3I5,F10.0)
 1010 FORMAT(10F5.0)
 1020 FORMAT(11F5.0)
 1030 FORMAT('0','DATA IN CONVENTIONAL FORM FOR MATERIAL NO.',I5/)
 1031 FORMAT('0',' DATA IN STRESS INVARIANT FORM FOR MATERIAL NO. ',I5/)
 1040 FORMAT(1X,'LATSTRESS',6X,10F8.3/)
 1041 FORMAT(1X,'J3/(SIGOCT)**2',1X,10F8.3/)
 1050 FORMAT(1X,'STRAIN',3X,F6.2,10F8.3/)
 1060 FORMAT(I5)
 1070 FORMAT(3F10.0)
 1071 FORMAT(3F8.3,4F12.4)
      RETURN
C
      END
C
END OF FILE
```

APPENDIX B

COMPUTER PROGRAM FOR THREE DIMENSIONAL FINITE ELEMENT ANALYSIS

B.1 Scope

This appendix contains a description of the computer program used for three dimensional finite element analysis and a listing of the program.

B.2 Language, Code and Limitations

Language: The computer program presented here was written in FORTRAN IV language and run on an IBM 360/67 computer with an MTS operating system at the University of Alberta, Edmonton.

Code: The title of the code is Finite Element Non-Linear Analysis for Three Dimensional Problems (FENA3D).

Limitations: The program as presented in this appendix is dependent on the MTS system subroutines and can handle a problem less than or equal to the following size:

Number of elements	=	350
Number of nodes	=	450
Number of materials	=	5
Number of cell pressures at which triaxial data is supplied	=	10
Number of axial strain points at which triaxial data is supplied	=	20

If the size of a problem exceeds the above limits the dimensions have to be increased accordingly. The minimum required dimension for each array is given in B.4.1.

One of the main limitations of a three dimensional analysis is the requirement of a large computer storage. In the present program the equation solver solves the equations in blocks using a core storage of (2*MBAND*(MBAND+1)) locations, MBAND being the half-band width. The core storage needed increases rapidly with the half-band width. On a computer with an available capacity of 1000K a maximum band width of about 320 can be handled with the use of the present program. Also it is to be noted that the computation time increases very rapidly with the half-band width. So it is normally preferable to limit the half-band width to about 250 while using the present program.

B.3 Development, The Main Features of Program and Computation Time

B.3.1 Development

The development of the present program was based on the ideas used by E.L. Wilson (University of California, 1966) in coding a two dimensional finite element program with a solver that solves the equations by Gaussian elimination in blocks. The program was developed by the author in the year 1971.

B.3.2 Main Features

The program consists of eight subroutines and a main program. Eight other system-dependent subroutines are referenced in this program. These are:

TIME,ADROF,RCALL,SETDSN,WRITE,READ,NOTE,POINT

the details of which can be obtained from the manual of the MTS system subroutines. Fig. B.1 shows the sequence of calling the different subroutines written for the present program. The function of the Main Program and each subroutine is described here in brief.

<u>Main Program</u>. Variables whose dimensions are prescribed depending on the half-band width computed for the current analysis, are passed to other subroutines. These variables change the dimensions of certain arrays appearing in certain DIMENSION statements of other subroutines.

<u>Subroutine MSUB</u>. This is the master subroutine which calls other subroutines necessary for the analysis. In this subroutine the coefficients needed for integration by Gaussian quadrature are computed, and the elastic parameters needed for each step in the non-linear analysis are calculated.

<u>Subroutine READIN</u>. This subroutine reads all the data pertaining to nodes, elements, materials, loads, and boundary conditions and interpolates the initial moduli needed in the non-linear analysis for all elements. It also calculates the half-band width for the current problem.

<u>Subroutine TESTD</u>. This subroutine reads the triaxial test data and converts it into the stress-invariant form.

<u>Subroutine ASTIF</u>. This subroutine assembles the load vector, and the total stiffness matrix from the element stiff-

ness obtained by calling the subroutine ELSTIF. It calls the subroutine MODIFY in order to modify the total stiffness matrix, and load vector to suit the given displacement boundary conditions. Formation and modification of the total stiffness matrix, and the load vector are done in blocks of size MBAND*(MBAND+1) and the information is written on a temporary sequential disc file.

Subroutine ELSTIF. This subroutine forms the element stiffness matrix for each element and returns to ASTIF. An isoparametric, eight-node hexahedral element has been used for the present program. The same element is specialized to represent triangular prisms or tetrahedra. The subroutine also forms the element stress matrix, computes the element stresses, and returns them to the subroutine STRESS.

Subroutine MODIFY. This subroutine modifies the total stiffness matrix, and the load vector according to the prescribed boundary displacement conditions and returns them to the subroutine ASTIF.

Subroutine BAND1. This is an equation solver which solves the equations by the direct method of Gaussian elimination. The equations are solved in single precision and in blocks by transferring parts of stiffness matrix, and load vector from sequential files to core and vice versa. Two temporary sequential disc files of sufficient size are used. The required size of sequential files in terms of the number of tracks (NTRACK) can be determined as follows:

Let each track of the file correspond to NBYTES (about 7000)

Let the number of equations to be solved be NEQ

Let the half-band width be MBAND

Number of blocks needed to write information into a file is obtained from NBLOCK=(NEQ/MBAND)+1

Number of tracks needed for the file can be obtained from NTRACK=(NBLOCK)*(MBAND)*(MBAND+1)/(NBYTES)+1.

File 2 is used to write the total stiffness matrix, and the load vector as formed in the subroutine ASTIF and File 1 is used to write information regarding the reduced equations obtained in the process of Gaussian elimination.

Subroutine STRESS. This subroutine computes the stresses and strains related to elements and nodes by calling the subroutine ELSTIF for the formation of the element stress matrix.

B.3.3 Computation Time

It has been observed that considerable savings on the cost of computation (even up to 50%) can be effected by introducing an efficient method of data transfer between core and sequential files. In the present program such transfers are effected by calling certain system-subroutines and by making suitable EQUIVALENCE statements. Table B.1 compares the computation time needed for solving 738 equations with a half-band width of 171 by using different methods of handling the transfer of data between core and files. The example considered here was concerned with a three dimensional finite element analysis of an earth dam. Total computation time for the complete analysis of the problem and the percent reductions in time have been presented in Table B.1. In the present program, Method 5 indicated in Table B.1, has been used as it effects the maximum reduction of the computation time.

B.3.3.1 Estimation of Computation (CPU) Time

It is generally useful to estimate before hand the approximate computation time spent in the assembly of the total stiffness matrix and the solution of equations for a given problem. The cost of computation sometimes dictates the size of the problem in terms of the number of nodes and elements. By knowing the number of nodes, the half-band width and the number of elements for a given problem the computation time needed for the solution of equations may be estimated by referring to Fig. B.2. This figure shows the relationship between the half-band width (MBAND) and the computation time for solution of equations equal to MBAND in number, in each block. This relationship has been obtained by solving problems of different sizes using the three dimensional program. The computation time needed for the solution of equations in a problem is obtained by multiplying the number of blocks with the computation time per block, read from Fig. B.2 at the given half-band width. The time needed for the assembly of the total stiffness matrix is estimated between 0.8 sec. and 1.2 sec. per element depending on whether a two-point or three-point integration formula is used for the formation of the element stiffness. This time multiplied by the number of elements gives the time for the formation of the total stiffness matrix.

Since the time required for solution of a given number of equations at a given half-band width depends on the number of displacement boundary conditions imposed, the time given by Fig. B.2 should be considered as approximate.

B.4 Nomenclature

In Section B.4.1 that follows, the variables that need a change in their dimension declaration according to the size of the problem are designated by parentheses after the variable name. The description and the minimum required size of the variable are also indicated. The variables defining the minimum sizes are given as input to the program.

B.4.1 Description and Size of Variables

Name	Description	Minimum Size When Applicable
ACOEF( )	Shear strength parameter associated with cohesion given by 2c cos ϕ/(1-sin ϕ)	(NUMAT)
BCOEF( )	Shear strength parameter associated with σ_3 given by 2 sin ϕ/(1-sin ϕ)	(NUMAT)
CONFAC	Conversion factor used to convert the triaxial test results to the units in which analysis is performed	
DISPX( )	Total displacement of a node in x-direction	(NUMNP)
DISPY( )	Total displacement of a node in y-direction	(NUMNP)
DISPZ( )	Total displacement of a node in z-direction	(NUMNP)
EBREAD( )	Bulk modulus read for each material type	(NUMAT)

Name	Description	Minimum Size When Applicable
EBULK( )	Bulk modulus assigned to each element	(NUMEL)
EDEV( )	Shear modulus assigned to each element	(NUMEL)
ESREAD( )	Shear modulus read for each material type	(NUMAT)
GOCT( )	Percent octahedral shear strain	(NSTRN, NCELP,NUMAT)
HED( )	Heading for the identification of the problem	(18)
ITOPT	Code to identify whether a step is to be analyzed once or twice	
KODE( )	Code for each node to identify the type of boundary displacement condition	(NUMNP)
KOEL( )	Code for each element to identify the type of integration formula to be used	(NUMEL)
KOUNT( )	Counter used for computing the nodal stresses	(NUMNP)
KTERMI	Code to identify whether the execution to be stopped after the generation of the element and nodal data	
M	Element or nodal number	
MAT( )	Material number assigned to each element	(NUMEL)
MATN	Number of elements to which material number has to be changed	
MBAND	Half-band width as calculated in program	
N	Element or nodal number	
NANLYS	Code to identify whether the analysis is linear or non-linear	

Name	Description	Minimum Size When Applicable
NBOUN	Number of nodes at which the boundary displacements or loads are specified in a particular step	
NCELP	Number of confining pressures at which triaxial test data is supplied as input	
NOBSET	Number of sets of elements for which the overburden factor is prescribed	
NP( )	Vector to store the eight nodes of each element	(8,NUMEL)
NSET	Number of elements (excluding the one read) for which the same overburden factor has to be assigned	
NSHEAR	Code to identify whether shear failure is to be considered or not	
NSTEP	Number of steps for the analysis	
NSTRN	Number of axial strain points at which the triaxial data is supplied	
NUM1	Number of sets of nodes for which codes other than zero are to be assigned	
NUM2	Number of nodes (excluding the one read) for which the same code has to be assigned	
NUMAT	Number of material types present in the given problem	
NUMCE	Number of sets of hexahedra and base triangular prisms to be generated	
NUMEL	Number of elements in the problem	
NUMELS	Number of elements in a particular step	
NUMJK	Number of hexahedra or base triangular prisms (excluding the one read) to be generated	

Name	Description	Minimum Size When Applicable
NUMNP	Number of nodes in the problem	
NUMTH	Number of tetrhedra in the problem	
NUMTP	Number of triangular prisms in the problem	
OBFAC( )	Overburden factor	(NUMEL)
RO( )	Density of the material in an element	(NUMEL)
ROREAD( )	Density of the material read for each material type	(NUMAT)
SD( )	Deviatoric stresses read from test data	(NSTRN, NCELP,NUMAT)
SGTEL	Total element stresses	(NUMEL,6)
SGTNP	Total nodal stresses	(NUMNP,6)
SGTPS( )	Principal stresses and strains in an element	(NUMEL,7)
SIGA( )	Nodal stresses in a particular step	(NUMNP,6)
SIGINT( )	A vector used in the conversion of data from triaxial form to stress invariant form	(NCELP, NUMAT)
SIGINV( )	A vector used in the coversion of data from triaxial form to stress invariant form	(NSTRN, NCELP,NUMAT)
SL( )	Number of triaxial cell pressure values at which data is supplied	(NCELP, NUMAT)
ST( )	Number of percent axial strain values at which triaxial data is supplied	(NSTRN, NUMAT)
STN( )	Percent nodal strains in a particular step	(NUMNP,3)
STNT( )	Percent total nodal strains	(NUMNP,3)
STRNT( )	Percent total element strains	(NUMEL,6)
TOCTD( )	Octahedral shear stress	(NSTRN, NCELP,NUMAT)

Name	Description	Minimum Size When Applicable
U( )	Force or displacement in x-direction given as input at a nodal point	(NUMNP)
V( )	Force or displacement in y-direction given as input at a nodal point	(NUMNP)
VS( )	Volumetric strain obtained from triaxial test	(NSTRN, NCELP,NUMAT)
VSTN( )	A vector used in the conversion of the triaxial test data to stress invariant form	(NSTRN, NCELP,NUMAT)
W( )	Force or displacement in z-direction given as input at a nodal point	(NUMNP)
X( )	x-coordinate of a nodal point	(NUMNP)
Y( )	y-coordinate of a nodal point	(NUMNP)
Z( )	z-coordinate of a nodal point	(NUMNP)

B.5 Input Data Procedure

B.3.4.1 has to be referred for the explanation of the name of variables used in this section.

(1) Problem Control Cards (2 cards)

(a) Problem Identification Card (1 card) (18A4)

1-72 HED

(b) Preliminary Information Card (1 card) (7I6)

1-6 NUMNP

7-12 NUMEL

13-18 NUMAT

19-24 NUMCE

25-30 NUMTP

31-36 NUMTH

37-42 NANLYS Zero for linear analysis and one for non-linear analysis

Figs. B.3 and B.4 show an example of a three dimensional idealization of a model dam representing different types of elements as given below:

Type of Elements	Element Numbers
Hexahedra	2,3,5,10
Base triangular prisms	7,8
Triangular prisms	1,4,9 (for element 9 back-face is inclined)
Tetrahedra	6

The preliminary information card for this problem would be as follows:

NUMNP = 23

NUMEL = 10

NUMAT = 1 (number of material types equal to one for this example)

NUMCE = 4

NUMTP = 3

NUMTH = 1

NANLYS = 0 (analysis is linear)

(2) Nodal Point Data Cards (Number of cards less than or equal to NUMNP) (2I5,6F5.0)

1-5 N

6-10 KODE( )

11-15 X( )

16-20 Y( )

21-25 Z( )

26-30 U( )

31-35 V( )

36-40 W( )

In an earth dam problem the nodes can seldom be arranged with equal spacing. However in problems where nodes can be spaced equally with the other two coordinate distances being constant only the extreme nodes need to be given as input. The intermediate nodes are generated with nodal displacements and loads equal to zero and nodal code equal to zero. The following nodal codes are used to represent the various boundary displacement conditions.

KODE(N)	X-Displacement Specified	Y-Displacement Specified	Z-Displacement Specified
0	NO	NO	NO
1	NO	NO	YES
2	NO	YES	NO
3	YES	NO	NO
4	YES	NO	YES
10	YES	YES	NO
11	NO	YES	YES
12	YES	YES	YES

(3) Nodal Code Change Control Card (1 card) (I5)

1-5 NUM1 (If no changes are needed NUM1 is equal to zero and (4) is omitted)

As mentioned before the intermediate nodes are generated with zero nodal codes. However if some of them happen to have codes other than zero it becomes necessary to assign the proper codes. NUM1 gives the number of sets of nodes to which the proper codes are to be assigned.

(4) Nodal Code Change Cards (2*NUM1 cards)

(a) Number of nodes in a set excluding the one read (I5)

1-5 NUM2

(b) Nodal Number and the Code (2I5)

1-5 N

6-10 KODE(N)

As an example for (3) let it be assumed that the nodal points shown in the sketch below are spaced equally in x and z directions for a particular value of y and have a code equal 2.

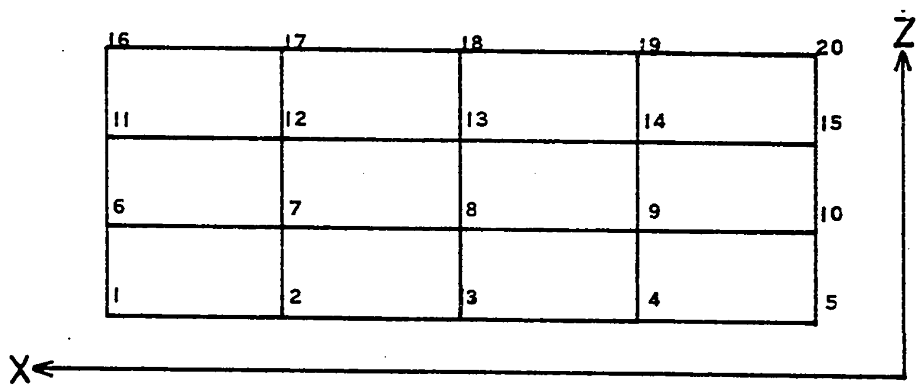

If the intermediate nodes namely 2,3,4,7,8,9,12,13, 14,17,18 and 19 are generated with the extreme nodes as input they will be generated with a code equal to zero. Since the proper code to be assigned to the intermediate nodes is 2, the following input cards are necessary.

4 (NUM1) (I5)

2		(NUM2) (I5)
2	2	(N,KODE(N)) (2I5)
2		(NUM2) (I5)
7	2	(N,KODE(N)) (2I5)
2		(NUM2) (I5)
12	2	(N,KODE(N)) (2I5)
2		(NUM2) (I5)
17	2	(N,KODE(N)) (2I5)

(5) Cards for Generation of Hexahedra and Base Triangular Prisms (2*NUMCE cards)

(a) Number of elements (excluding the one given as input) to be generated (I5)

1-5	NUMJK

(b) Element data card (11I5)

1-5	M
6-10	KOEL(M)
11-15	NP(1,M)
16-20	NP(2,M)
21-25	NP(3,M)
26-30	NP(4,M)
31-35	NP(5,M)
36-40	NP(6,M)
41-45	NP(7,M)
46-50	NP(8,M)
51-55	MAT(M)

Considering the example in Fig. B.3 the sets of base triangular prisms and hexahedra to be generated are 4 which is given by the number NUMCE. Each set is represented by two cards. The first card gives the value NUMJK and the second card gives the details of the element from which the other elements equal to NUMJK in numbers are generated in that particular set. The element code to be given as input indicates the type of integration formula (two or three point) to be used for that particular element. If the element is a regular body, e.g., a rectangular prism or a triangular prism, a two point integration formula is used and in the case of a skewed element a three point integration formula is used for better accuracy. In addition, the code indicates whether the given element is a hexahedron or not. If the element is not a hexahedron, the evaluation of stresses at the corners of the element (for the purpose of computing the nodal stresses) has to be done very close to the corner (but not at the corner) to avoid a division by zero. The following element codes are used in the present program:

Element Code	Integration Formula Used	Type of Element
0	Two point Gaussian quadrature	Regular hexahedron
1	Two point Gaussian quadrature	Regular element other than a hexahedron
2	Three point Gaussian quadrature	Skewed element other than a hexahedron
3	Three point Gaussian quadrature	Skewed hexahedron

The following gives the set-up of cards for the generation of the hexahedra and the base triangular prisms for the example given in Fig. B.3 and Fig. B.4.

1(NUMJK(I5)

2,0,12,3,2,11,15,6,5,14,1(M,KOEL(M),(NP(KK,M),KK=1,8), MAT(M))(11I5)

0(NUMJK(I5)

5,0,16,7,6,15,18,9,8,17,1(M,KOEL(M),(NP(KK,M), KK=1,8),MAT(M))(11I5)

1(NUMJK)(I5)

7,1,12,12,11,11,20,15,14,19,1(M,KOEL(M),(NP(KK,M), KK=1,8),MAT(M))(11I5)

0(NUMJK)(I5)

10,3,21,16,15,20,23,18,17,22,1(M,KOEL(M),(NP(KK,M), KK=1,8),MAT(M))(11I5)

The elements 3 and 8 will be generated accordingly with the same element code and material numbers given for elements 2 and 7 respectively.

(6) Cards for the Generation of Triangular Prisms (NUMTP cards) (11I5)

If NUMTP is zero (6) is to be omitted.

1-5	M
6-10	KOEL(M)
11-15	NP(1,M)
16-20	NP(2,M)
21-25	NP(3,M)
26-30	NP(4,M)
31-35	NP(5,M)
36-40	NP(6,M)
41-45	NP(7,M)

46-50 NP(8,M)

51-55 MAT(M)

In the example shown in Fig. B.2, NUMTP=3. The cards set up would be as follows:

1,1,11,2,1,10,14,5,5,14,1(M,KOEL(M),(NP(KK,M),KK=1,8), MAT(M))(11I5)

4,1,15,6,5,14,17,8,8,17,1(M,KOEL(M),(NP(KK,M),KK=1,8), MAT(M)(11I5)

9,2,20,15,14,19,22,17,17,22,1(M,KOEL(M),(NP(KK,M), KK=1,8),MAT(M))(11I5)

(7) Cards for the Generation of Tretrahedra (NUMTH cards) (11I5)

If NUMTH is zero (7) will be omitted.

1-5 M

6-10 KOEL(M)

11-15 NP(1,M)

16-20 NP(2,M)

21-25 NP(3,M)

26-30 NP(4,M)

31-35 NP(5,M)

36-40 NP(6,M)

41-45 NP(7,M)

46-50 NP(8,M)

51-55 MAT(M)

In the example shown in Fig. B.3 NUMTH=1. The card set up would be as follows:

6,2,11,11,10,10,19,14,14,19,1(M,KOEL(M),(NP(KK,M), KK=1,8),MAT(M))(11I5)

(8) Cards for Changing the Material Numbers for Certain Elements

(a) Control Card to Change Material Numbers (1 card) (I5)

1-5 MATN

(b) Cards to Change Material Numbers (MATN cards) (2I5)

1-5 M

6-10 MAT(M)

As the material number for the generated elements will be the same as that assigned to the element given as input, it would sometimes be necessary to alter the material number in some of the generated elements. When these changes are not necessary MATN is equal to zero and (b) is omitted.

(9) Overburden Factor Control Card (1 card) (I5)

1-5 NOBSET (If the analysis is linear NOBSET=0 and (10) is omitted)

(10) Overburden Factor Cards (Number of cards = NOBSET) (2I5,F10.0)

1-5	M	Element number
6-10	NSET	
11-20	OBFAC( )	To be given only if the value is not equal to one

The following example provides an explanation for (9) and (10)

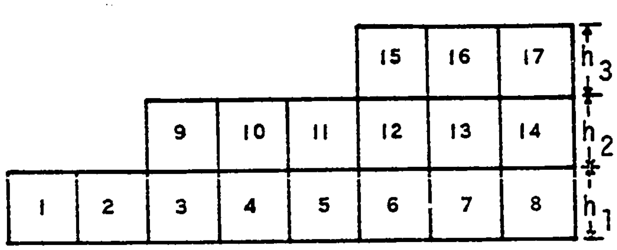

γ_3 is density of material for elements 15 to 17

γ_2 is density of material for elements 9 to 14

γ_1 is density of material for elements 1 to 8

When a non-linear analysis has to be performed for gravity loaded structures the initial moduli are computed for each element considering the overburden pressure at the mid height of the element. In the sketch shown above there are 17 elements to be considered in a particular step. The overburden pressure at the mid height of a certain element say 8 is $(\gamma_1 h_1/2 + \gamma_2 h_2 + \gamma_3 h_3)$ where γ_1, γ_2 and γ_3 are the densities of the materials and h_1, h_2 and h_3 are the heights as shown. Now the overburden factor can be defined for the element 8 as follows:

$$\text{OBFAC}(8) = (\gamma_1 h_1/2 + \gamma_2 h_2 + \gamma_3 h_3)/\gamma_1 h_1/2).$$

If for example $h_1 = h_2 = h_3 = h$ and $\gamma_1 = \gamma_2 = \gamma_3 = \gamma$, then the overburden factor control card and the overburden factor cards will be as given below:

NOBSET=3

M	NSET	OBFAC(M)
3	2	3.0
6	2	5.0
12	2	3.0

OBFAC(M)=1.0 is automatically set in the program and hence need not be supplied in the data. In the present example elements 1,2,9,10,11,15,16 and 17 will have an overburden factor equal to unity.

(11) Triaxial Test Data Control Card (1 card) (2I5,F10.0)

1-5 NCELP

6-10 NSTRN

11-20 CONFAC

If the analysis is linear a blank card for (11) to be supplied and (12), (13), (14) are omitted.

(12) Cell Pressure Card (1 card) (10F5.0)

If the test results are to be supplied say at 0,5,10,30 and 40 psi cell pressure values the input is as follows:

1-5	0.0
6-10	5.0
11-15	10.0
16-20	30.0
21-25	40.0

(13) Axial Strain and Deviatoric Stress Cards (Number of cards = NSTRN) (11F5.0)

Each card will have the axial strain punched in the first five columns and the deviatoric stresses corresponding to the various cell pressures (given in (12)) at that particular axial strain are punched in the subsequent columns.

(14) Axial Strain and Volumetric Strain Cards (Number of cards = NSTRN) (11F5.0)

Each card will have the axial strain punched in the first five columns and the volumetric strain corresponding to the various cell pressures (as given by (12)) at that particular axial strain are punched in the subsequent columns. Volume expansion is to be neglected while giving the volumetric strain input.

(15) Card for the Termination of Execution After the Generation of Element and Nodal Data (1 card) (I5)

1-5 KTERMI (KTERMI=1 terminates execution and KTERMI=0 does not terminate execution)

When the data is run for the first time it is preferable to terminate the execution after the generation of element and nodal data so that the correctness of generation can be verified. Also the correct value of MBAND computed during this first run can be utilized in setting the dimensions of certain vectors in MAIN PROGRAM as described in (21).

(16) Card to Control Iteration Option (1 card) (I5)

1-5 ITOPT (ITOPT=1 causes each step to be analyzed twice and ITOPT=0 causes each step to be analyzed only once. In the case of a linear analysis ITOPT=0)

(17) Card to Indicate the Number of Steps and the Option for the Consideration of Shear Failure (1 card) (2I5)

1-5 NSTEP

6-10 NSHEAR (NSHEAR=1 causes the shear failure to be considered and if NSHEAR=0 shear failure is not considered)

(18) Card to Read the Number of Elements Involved in a Particular Step (1 card) (I5)

1-5 NUMELS

(19) Card to Read the Number of Nodal Points at Which Incremental Loads or Displacements are Prescribed in a Given Step (1 card) (I5)

1-5 NBOUN

(20) Cards that Input Incremental Nodal Loads or Displacements (NBOUN cards) (I5,3F10.0)

1-5 N

6-15 U(N)

16-25 V(N)

26-35 W(N)

U( ), V( ) and W( ) could be either the prescribed forces or the prescribed displacements in x, y and z directions. In a particular coordinate direction if a displacement boundary condition is specified then the read quantity becomes a prescribed displacement in that direction; otherwise it is taken as a prescribed force in that direction. It is not possible to prescribe a force and a displacement simultaneously in a given direction at a given nodal point.

(21) Procedure to Set the Dimensions of the Arrays in the MAIN PROGRAM

The dimensions of these arrays are based on the half-band width and the number of equations which in turn depend on the problem. So it is necessary to know the value of the half-band width and the number of equations for the problem on hand to set the dimensions of arrays in MAIN PROGRAM. Because of the facility provided to terminate the execution of the program after the generation of the element and nodal data, and the calculation of the half-band width (MBAND) in subroutine READIN, it is not necessary to know the correct value of MBAND beforehand. An arbitrary value of say 100 can be assumed during the first run for setting the dimensions of arrays in MAIN PROGRAM. The dimension of these arrays do not effect the execution up to the generation of nodes and elements. After obtaining the correct value of MBAND the dimensions of the arrays in MAIN PROGRAM are reset for the final run. The number of equations (NE1) is given as three times the total number of nodes involved in the problem on hand. The dimensioning of arrays is as follows:

```
DIMENSION B(NE1),A(MBAND,2*MBAND),BL(MBAND),BR(MBAND),
AL(MBAND**2),AR(MBAND**2)

EQUIVALENCE (B(1),BL(1)),(B(MBAND+1),BR(1)),(A(1,1),
AL(1)),(A(1,MBAND+1),AR(1))

NE1=3*NUMNP

MB1=MBAND
```

The quantities that appear in MAIN PROGRAM of the listing given in Section B.8 correspond to the value of MBAND equal to 114 and NE1 equal to 405.

B.6 Control Cards to Create Sequential Files and to Run Data

The following control cards were used to create the sequential files and to run the data:

```
$CREATEβ-TβTYPE=SEQβSIZE=nT

$CREATEβ-TEMP2βTYPE=SEQβSIZE=nT

$RUNβ-LOAD#β1=-Tβ2=-TEMP2
```

The value n representing the number of tracks was obtained using the procedure given in Section B.3.2

B.7 Output of the Results

The following results are obtained as output:

(1) The complete nodal and element data with the initial values of the elastic parameters assigned to each element.

(2) Cumulative nodal displacements, stress and strains for elements and nodes for each step of the analysis.

(3) Element principal stress and strains for each step of the analysis.

(4) Elastic parameters assigned to each element in each step of the analysis.

B.8 Listing of Program

A listing of the computer program appears after the Fig. B.4.

TABLE B.1

COMPARISON OF THE COMPUTATION TIME WITH DIFFERENT METHODS OF DATA TRANSFERS

In all the following methods a three dimensional finite element analysis of an earth dam, consisting of 738 equations with a half-band width of 171 has been performed in single precision		Type of write and read statements used.	CPU time for solution of equations (sec.)	Total CPU time for the analysis (sec.)	Percent reduction of of total CPU time %
NO.	METHOD USED				
1	Two sequential files are created. Transfers between core and files are effected by FORTRAN read and write statements in subscripted form. For back substitution the file 1 is over-read every time from the beginning to the proper block.	File 1: WRITE(1)(NB1,B(N),(A(M,N),M=2,MBAND),N=1,MBAND) File 1: READ(1)(NB1,B(N),(A(M,N),M=2,MBAND),N=1,MBAND) File 2: WRITE(2)(B(I),(A(J,I),J=1,MBAND),I=1,MBAND) File 2: READ(2)(B(N),(A(M,N),M=1,MBAND),N=MBAND,2*MBAND)	99.00	173.44	
2	One sequential file for File 2 and a line file for File 1 are created. Direct access is made available for File 1. Transfers between core and files are effected as in (1) except that over-reading is eliminated by direct access read and write statements.	File 1: WRITE(1'IDx1000)(B(N),(A(M,N),M=2,MBAND),N=1,MBAND) File 1: READ(1'IDx1000)(B(N),(A(M,N),M=2,MBAND),N=1,MBAND) File 2: WRITE(2)(Same as in (1)) File 2: READ(2)(Same as in (1))	84.90	159.77	7.88
3	Two sequential files are created. Transfers between core and files are effected as in (1) and (2). Direct access with sequential file 1 is obtained by calling subroutines NOTE and POINT.	File 1: WRITE(1)(Same as in (1)) called NOTE File 1: READ(1) (Same as in (1)) called POINT File 2: WRITE(2)(Same as in (1)) File 2: READ(2)(Same as in (1))	72.86	147.30	15.00
4	Two sequential files are created. Transfers between core and file are effected by FORTRAN unsubscripted read and write statements made possible by equivalence statements. Direct access with sequential file 1 is same as in (3).	File 1: WRITE(1) AL,B1 File 1: READ(1) AL,BL File 2: WRITE(2) AL,BL File 2: READ(2) AR,BR Called NOTE and POINT, made EQUIVALENCE statements	39.61	101.53	41.40
5	Two sequential files are created. Transfers between core and file are effected by calling subroutines READ and WRITE with same equivalence statements as in (4). Direct access with sequential file 1 is made available as in (3) and (4).	File 1: CALL WRITE(AL (LL),LEN,0,1,FDUB, & 550) File 1: CALL READ(AL(LL),LEN,0,LZ,FDUB, & 550) File 2: CALL WRITE(AL(LL),LEN,0,1,2, & 550) File 2: CALL READ(AR(LL),LEN,0,LO,2, & 550) Similar statements for BL and BR Called NOTE and POINT and made EQUIVALENCE statements	21.48	77.00	55.50

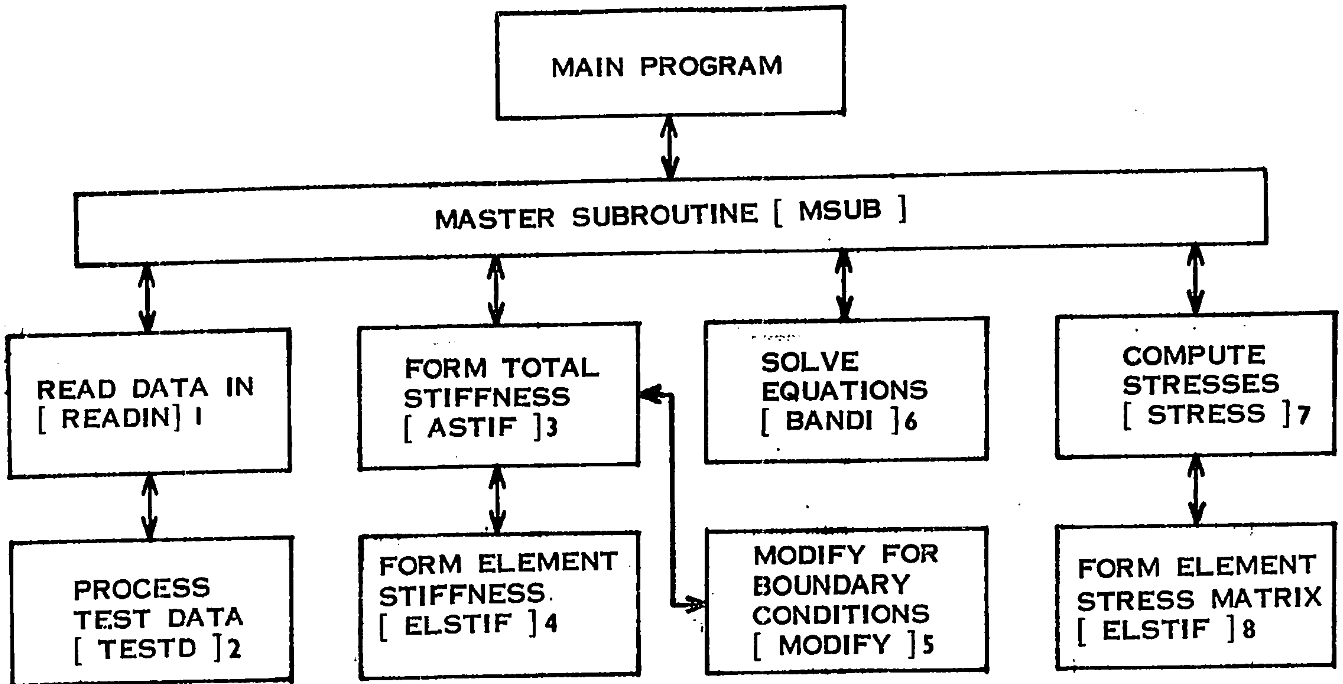

NUMBERS INDICATE THE ORDER OF CALLING DIFFERENT SUBROUTINES

NAME OF SUBROUTINE APPEARS WITHIN BRACKETS

3 TO 8 IS REPEATED FOR EVERY STEP OF THE INCREMENTAL ANALYSIS

FIG. B.1 SEQUENCE OF CALLING DIFFERENT SUBROUTINES

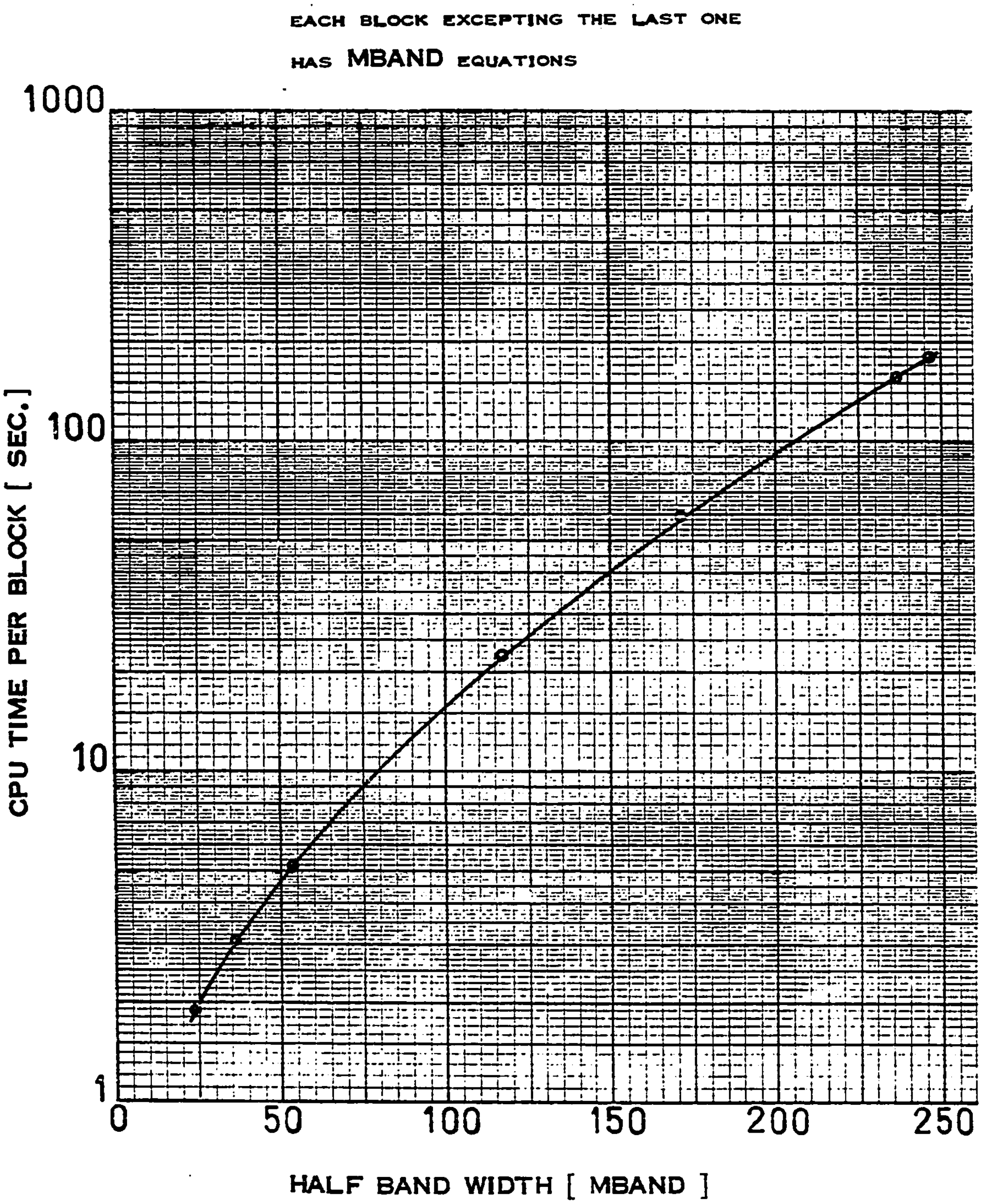

FIG. B.2 APPROXIMATE CPU TIME FOR SOLUTION OF EQUATIONS IN 3-D PROGRAM

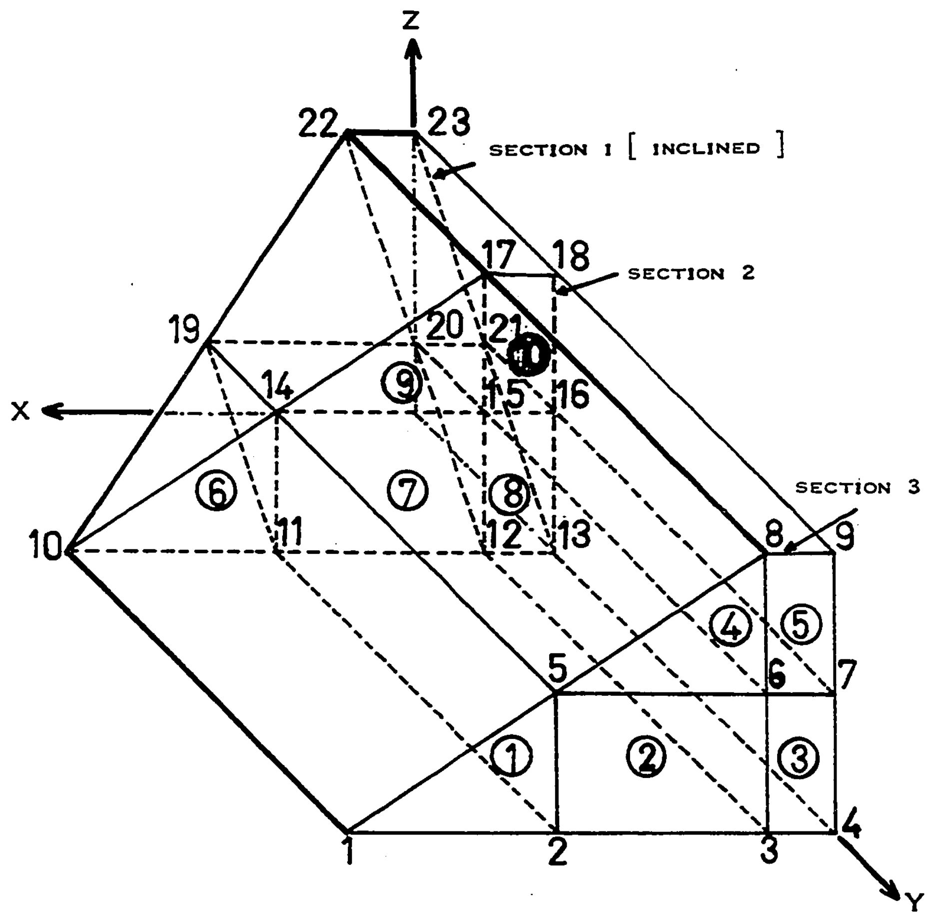

FIG. B.3 THREE DIMENSIONAL VIEW OF A MODEL DAM [ELEMENT NUMBERS ARE CIRCLED]

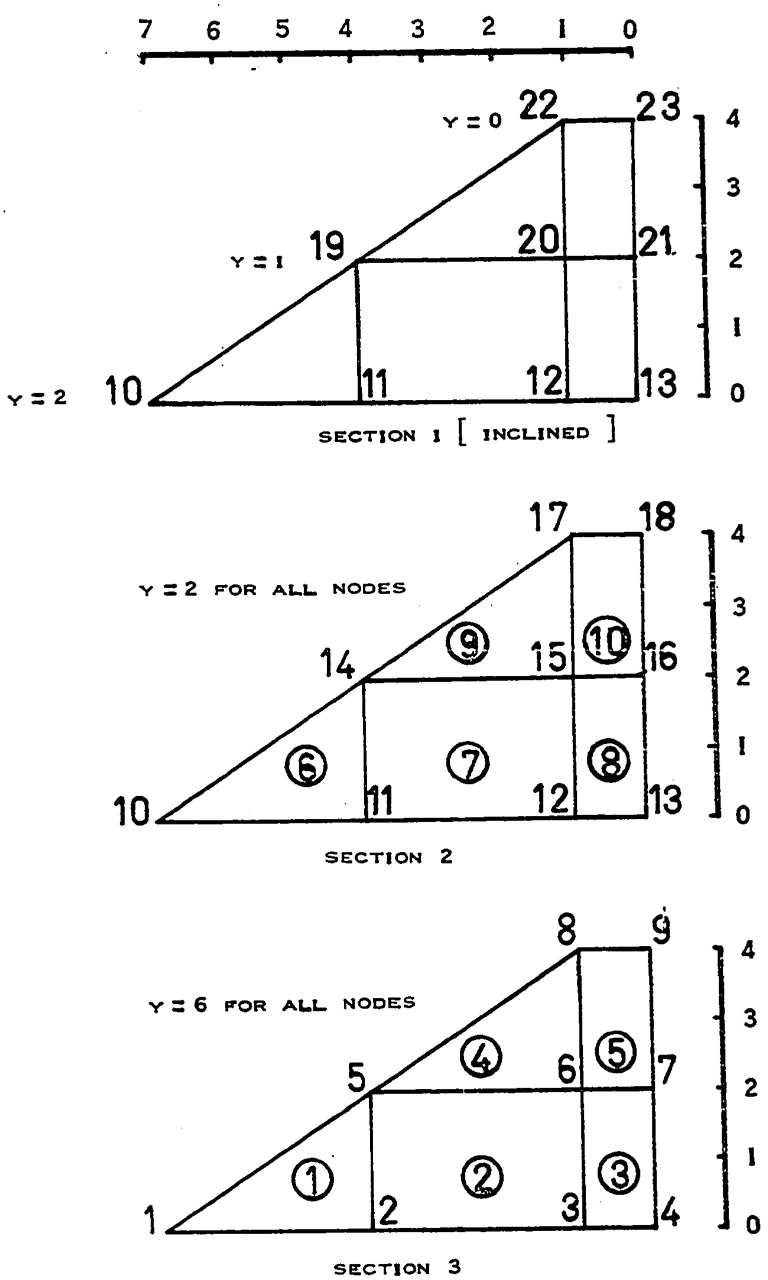

FIG. B.4 SECTIONAL VIEWS OF MODEL DAM
[ELEMENT NUMBERS ARE CIRCLED]

```
C THREE DIMENSIONAL FINITE ELEMENT PROGRAM USING ISOPARAMETRIC HEXAHEDRA
C WITH 24 DEGREES OF FREEDOM PER EACH ELEMENT. EQUATIONS ARE SOLVED BY
C GAUSSIAN ELIMINATION IN BLOCKS.
C
C
C
C DEVELOPED & CODED BY A.V.G.KRISHNAYYA. CIVIL ENG. DEPT.. U OF A.1971.
C
C
C  MAIN PROGRAM THAT CHANGES THE DIMENSIONS AND EQUIVALENCE STATEMENTS
C ACCORDING TO THE SIZE OF THE PROBLEM
C
      DIMENSION B(405). A(114.228).BL(114).BR(114).AL(12996).AR(12996)
      EQUIVALENCE (B(1).BL(1)).(B(115).BR(1)).(A(1.1).AL(1)).(A(1.115).
     1AR(1))
      NE1=405
      MB1=114
      MB2=2*MB1
      LA=MB1**2
      LA2=LA
      CALL MSUB(B.A.BL.BR.AL.AR.MB1.MB2.LA.LA2.NE1)
      STOP
      END
C
C
      SUBROUTINE MSUB(AP.STIF.APL.APR.STIFL.STIFR.MB1.MB2.LA.LA2.NE1)
C
C THIS IS THE MASTER SUBROUTINE WHICH CALLS OTHER SUBROUTINES REQUIRED
C FOR ANALYSIS. IT INTERPOLATES  THE ELASTIC PARAMETERS FOR EACH STEP.
C
      COMMON NANLYS.KSHIFT. RO(350).X(450).Y(450).Z(450).U(450).V(450).
     1W(450).SGTEL(350.6).SGTPS(350.7).STRNT(350.6).STNT(450.3).
     2  ECMI(3.3).STRN(6) .ESTIF(24.24).ECM(6.6).EBM(6.24).ESM(6.24).WT
      COMMON NUMNP.NUMEL. NE2. KODE( 450).SGTNP(450.6).
     1NP(8. 350).MAT( 350).MBAND.NEQ.M.LM(24).KOEL( 350).
     2PSY(52).ETA(52).ZTA(52).AQ(43).PP(24).ELDISP(24).
     3KOUNT( 450).SIGA( 450.6).STN( 450.3).SIGEL(6).SIGP(7).NUMBLK.
     4  DISPX(450).DISPY(450).DISPZ(450)
      COMMON EBULK(350).EDEV(350).NITER.ITOPT.ACOEF( 5).BCOEF( 5).STP(3)
      COMMON/AREA1/ST(20.5).SL(10.5).SD(20.10.5).VS(20.10.5).NUMAT.NCELP
     1.CONFAC.NSTRN
      DIMENSION AP(NE1).STIF(MB1.MB2).APL(MB1).APR(MB1).STIFL(LA2).
     1STIFR(LA)
C
C COORDINATES OF PARENT ELEMENT ARE STORED IN THREE VECTORS
      CALL TIME (0)
      EXTERNAL GETFD
      INTEGER ADROF.FDUB
      CALL RCALL(GETFD.2.0.ADROF('-T ').1.FDUB.&100)
      CALL SETDSN(1.'-T '.FDUB.&100)
      GO TO 101
  100 WRITE(6.600)
  600 FORMAT(' FILE ERROR')
      STOP
  101 CONTINUE
      NE2=NE1
```

```
      DO 88 I=1,5,4
      J1=I+1
      DO 89 K=I,J1
      PSY(K)=-1.
      PSY(K+2)=+1.
   89 CONTINUE
   88 CONTINUE
      DO 90 I=1,5,4
      ETA(I)=-1.
      ETA(I+1)=1.
      ETA(I+2)=1.
   90 ETA(I+3)=-1.
      DO 91 I=1,4
      ZTA(I)=-1.
   91 ZTA(I+4)= 1.
      DO 60 I= 45,49,4
      J1=I+1
      DO 61 K=I,J1
      PSY(K)=-0.99
      PSY(K+2)=0.99
 61   CONTINUE
 60   CONTINUE
      DO 62 I=45,49,4
      ETA(I)=-0.99
      ETA(I+1)=0.99
      ETA(I+2)=0.99
 62   ETA(I+3)=-0.99
      DO 63 I=45,48
      ZTA(I)=-0.99
 63   ZTA(I+4)=0.99
CARGUMENTS AND WEIGHTING FACTORS ARE STORED IN FOUR VECTORS
C TWO POINT FORMULA
      T1=-0.57735027
      T2=-(T1)
      DO 79 I=9,12
      PSY(I)=T1
   79 PSY(I+4)=T2
      DO 81 I=9,13,4
      ETA(I)=T1
      ETA(I+1)=T1
      ETA(I+2)=T2
   81 ETA(I+3)=T2
      DO 82 I=9,15,2
      ZTA(I)=T1
   82 ZTA(I+1)=T2
C THREE POINT FORMULA
      T3=-0.77459667
      T4=0.0
      T5=-(T3)
      A1=0.55555556
      A2=0.888888889
      DO 85 I=17,25
      PSY(I)=T3
      PSY(I+9)=T4
   85 PSY(I+18)=T5
      DO 86 I=17,35,9
      J1=I+2
      DO 87 K=I,J1
      ETA(K)=T3
      ETA(K+3)=T4
```

```
      ETA(K+5)=T5
   87 CONTINUE
   86 CONTINUE
      DO 92 I=17,41,3
      ZTA(I)=T3
      ZTA(I+1)=T4
      ZTA(I+2)=T5
   92 CONTINUE
      AQ(17)=(A1**3)
      AQ(19)=(A1**3)
      AQ(23)=(A1**3)
      AQ(25)=(A1**3)
      AQ(35)=(A1**3)
      AQ(37)=(A1**3)
      AQ(41)=(A1**3)
      AQ(43)=(A1**3)
      DO 95 I=18,28,2
   95 AQ(I)=(A1**2)*A2
      DO 96 I=32,42,2
   96 AQ(I)=(A1**2)*A2
      AQ(21)=(A2**2)*A1
      AQ(27)=(A2**2)*A1
      AQ(29)=(A2**2)*A1
      AQ(31)=(A2**2)*A1
      AQ(33)=(A2**2)*A1
      AQ(39)=(A2**2)*A1
      AQ(30)=(A2**3)
      CALL READIN(AP,STIF,APL,APR,STIFL,STIFR,ME1,MB2,LA,LA2)
      CALL TIME(1,1)
CKTERMI>0TERMINATES EXECUTION AFTER GENERATION OF NODAL & ELEMENT DATA
C******************** READ STATEMENT *******************************************
      READ(5,1015) KTERMI
      IF(KTERMI.GT.0) GO TO 28
C ITOPT=0 PAST STRESS SOLUTION
C ITOPT=1 AVERAGE STRESS SOLUTION
C******************** READ STATEMENT *******************************************
      READ(5,1015) ITOPT
C
C  INITIALIZE THE TOTAL ELEMENT AND NODAL STRESSES,STRAINS AND
C  NODAL DISPLACEMENTS
      DO 10 I=1,NUMNP
      DISPX(I)=0.0
      DISPY(I)=0.0
      DISPZ(I)=0.0
      DO 10 J=1,6
   10 SGTNP(I,J)=0.0
      DO 15 I=1,NUMNP
      DO 15 J=1,3
   15 STNT(I,J)=0.0
      DO 30 I=1,NUMEL
      DO 30 J=1,6
   30 SGTEL(I,J)=0.0
      DO 31 I=1,NUMEL
      DO 31 J=1,6
   31 STRNT(I,J)=0.0
      DO 35 I=1,NUMEL
      DO 35 J=1,7
   35 SGTPS(I,J)=0.0
C NSTEP=NUMBER OF INCREMENTS
C NSHEAR=0 SHEAR FAILURE NOT CONSIDERED
```

```
C NSHEAR=1 SHEAR FAILURE CONSIDERED
C******************** READ STATEMENT ********************************************
      READ (5,1000)  NSTEP,NSHEAR
      DO 20 IJK=1,NSTEP
C NUMEL= NUMBER OF ELEMENTS CONSIDERED IN CURRENT INCREMENT
C******************** READ STATEMENT ********************************************
      READ (5,1015) NUMELS
      WRITE(6,1015) IJK
      WRITE(6,1015) NUMELS
      NUMEL=NUMELS
C
C
C
C******************** READ STATEMENT ********************************************
      READ(5,1015) NBOUN
      IF(NBOUN.EQ.0) GO TO 222
      WRITE(6,2003)
      DO 206 J=1,NBOUN
C******************** READ STATEMENT ********************************************
      READ(5,2020) N,U(N),V(N),W(N)
      WRITE(6,2002) N,U(N),V(N),W(N)
  206 CONTINUE
  222 NITER=0
  205 NITER=NITER+1
      CALL  ASTIF(AP,STIF,APL,APR,STIFL,STIFR,MB1,MB2,LA,LA2)
      CALL  TIME(1,1)
C
      CALL  BAND1(AP,STIF,APL,APR,STIFL,STIFR,MB1,MB2,LA,LA2,FDUB)
      WRITE (6,2003)
      DO 25 N=1,NUMNP
      DISPX(N)=DISPX(N)+AP(3*N-2)
      DISPY(N)=DISPY(N)+AP(3*N-1)
      DISPZ(N)=DISPZ(N)+AP(3*N)
   25 WRITE (6,2002) N,DISPX(N),DISPY(N),DISPZ(N)
      CALL  TIME(1,1)
      IF(ITOPT.EQ.0) GO TO 255
      IF(NITER.EQ.2) GO TO 255
      DO 251 N=1,NUMNP
      DISPX(N)=DISPX(N)-AP(3*N-2)
      DISPY(N)=DISPY(N)-AP(3*N-1)
      DISPZ(N)=DISPZ(N)-AP(3*N)
  251 CONTINUE
C
  255 CALL  STRESS(AP,STIF,AFL,APR,STIFL,STIFR,MB1,MB2,LA,LA2)
      CALL  TIME(1,1)
      IF(NSTEP.EQ.1.AND.ITOPT.EQ.0) GO TO 28
      DO 26 M=1,NUMEL
      MTYPE=MAT(M)
      IF(ITOPT.EQ.0) RO(M)=0.0
      IF(NITER.EQ.2) RO(M)=0.0
      IF(NANLYS.EQ.0) GO TO 26
      AVGSIG=ABS(SGTPS(M,1))
      IF(SGTPS(M,1).GE.0.0)AVGSIG=0.0
      DIVS=ABS(SGTPS(M,3))-AVGSIG
      DIVS=ABS(DIVS)
      VSTR=ABS(SGTPS(M,3))
      N=MAT(M)
      DIVSF=ACOEF(N)+BCOEF(N)*ABS(SGTPS(M,1))
      IF(SGTPS(M,1).GE.0.0) DIVSF=ACOEF(N)
      IF(NCELP.EQ.0) GO TO 450
```

```
      SIGM1=ABS(SGTPS(M,3))
      SIGM2=ABS(SGTPS(M,2))
      IF(SGTPS(M,2).GE.0.0) SIGM2=0.0
      SIGM3=ABS(SGTPS(M,1))
      IF(SGTPS(M,1).GE.0.0) SIGM3=0.0
      SIGOCT=(SIGM1+SIGM2+SIGM3)/3.
      SIGIN=SIGM1*SIGM2*SIGM3
      CONFS=SIGIN/(SIGOCT**2)
      DIVOCT=SQRT((SIGM1-SIGM2)**2+(SIGM2-SIGM3)**2+(SIGM3-SIGM1)**2)
      DIVOCT=DIVOCT/3.
      DO 41 J=1,NCELP
      JLS=J
      IF(CONFS-SL(J,N)) 42,41,41
   41 CONTINUE
   42 CONTINUE
      DO 43 K=1,NSTRN
      JS1=K
      IF (DIVOCT-SD(K,JLS-1,N)) 44,43,43
   43 CONTINUE
   44 CONTINUE
      DO 300 K=1,NSTRN
      JS2=K
      IF(DIVOCT-SD(K,JLS,N)) 301,300,300
  300 CONTINUE
  301 CONTINUE
      PR1=1.061*(VS(JS1,JLS-1,N)-VS(JS1-1,JLS-1,N))/(ST(JS1,N)-ST(JS1-1,
     1N))-1.0
      IF(PR1.GT.0.49) PR1=0.49
      PR2=1.061*(VS(JS2,JLS   ,N)-VS(JS2-1,JLS   ,N))/(ST(JS2,N)-ST(JS2-1,
     1N))-1.0
      IF(PR2.GT.0.49) PR2=0.49
      PR3=PR1+((PR2-PR1)*( CONFS-SL(JLS-1,N))/(SL(JLS,N)-SL(JLS-1,N)))
      IF(PR3.GT.0.49 ) PR3=0.49
      DIF1=SD(JS1,JLS-1,N)-SD(JS1-1,JLS-1,N)
      ETP1=DIF1/(ST(JS1,N)-ST(JS1-1,N))
      GTP1=ETP1/(0.9428*(1.+PR1))
      DIF2=SD(JS2,JLS,N)-SD(JS2-1,JLS,N)
      ETP2=DIF2/(ST(JS2,N)-ST(JS2-1,N))
      GTP2=ETP2/(0.9428*(1.+PR2))
      GTP=GTP1+ (GTP2-GTP1)*(CONFS -SL(JLS-1,N))/(SL(JLS,N)-SL(JLS-1,N))
      GTP=100.*GTP
      BULKM   =GTP*2.*(1.+PR3)/(3.*(1.-2.*PR3))
      SHEARM=GTP
      IF(NCELP.NE.0) GO TO 455
  450 CONTINUE
C DETERMINE MODULI FROM OTHER THAN TRIAXIAL DATA
  455 CONTINUE
      IF(NITER.EQ.1) TEBULK=BULKM
      IF(NITER.EQ.2)EBULK(M)=BULKM
      IF(ITOPT.GT.0.AND.NITER.EQ.1)EBULK(M)=(TEBULK+EBULK(M))/2.
      IF(ITOPT.EQ.0.AND.NITER.EQ.1)EBULK(M)=TEBULK
      IF(NITER.EQ.1)TEDEV=SHEARM
      IF(NITER.EQ.1.AND.DIVS.GE.DIVSF.AND.NSHEAR.GT.0)TEDEV=EBULK(M)/50.
      IF(NITER.EQ.2)EDEV(M)=SHEARM
      IF(NITER.EQ.2.AND.DIVS.GE.DIVSF.AND.NSHEAR.GT.0)EDEV(M)=EBULK(M)/5
     10.
      IF(ITOPT.GT.0.AND.NITER.EQ.1) EDEV(M)=(TEDEV+EDEV(M))/2.
      IF(ITOPT.EQ.0.AND.NITER.EQ.1) EDEV(M)=TEDEV
      IF(EDEV(M).GT.(1.45*EBULK(M)))EDEV(M)=1.45*EBULK(M)
      IF(EDEV(M).LT.(EBULK(M)/50.)) EDEV(M)=EBULK(M)/50.
```

```
   26  CONTINUE
       WRITE(6,2010) (M,EBULK(M),EDEV(M),RO(M),M=1,NUMEL)
       IF(ITOPT.EQ.0) GO TO 20
       IF(NITER.EQ.1) GO TO 205
       CALL TIME(1,1)
   20  CONTINU=
C
 1000 FORMAT(2I5)
1015  FORMAT(I5)
 1050 FORMAT(2F15.6)
2002  FORMAT (I4,3E15.5)
 2003 FORMAT('1',10X,'NODAL DISPLACEMENTS'//,'NODE      X_DISP
     1Y-DISP              Z-DISP'//)
2005  FORMAT(///,1H ,10X, 21H  MATERIAL PROPERTIES //
     11X, 8HELE. NO.,4X, 9HBULK MOD.,4X,14HSHEAR  MODULUS,4X,11HUNIT WEI
     2GHT,//)
2010  FORMAT(1H ,I5,F17.4,F15.3,F17.4)
 2020 FORMAT(I5,3F10.0)
 28    RETURN
       END
C
C
      SUBROUTINE READIN(AP,STIF,APL,APR,STIFL,STIFR,MB1,MB2,LA,LA2)
C
C  THIS SUBROUTINE READS AND PRINTS MATERIAL DATA, NODAL DATA, ELEMENT CATA.
C  IT GENERATES COORDINATES OF INTERMEDIATE NODAL POINTS AND CALCULATES
C  THE BAND WIDTH AND NUMBER OF ECUATIONS
C
C
C
      COMMON NANLYS,KSHIFT, RO(350),X(450),Y(450),Z(450),U(450),V(450),
     1W(450),SGTEL(350,6),SGTPS(350,7),STRNT(350,6),STNT(450,3),
     2  ECMI(3,3),STRN(6) ,ESTIF(24,24),ECM(6,6),EBM(6,24),ESM(6,24),WT
      COMMON NUMNP,NUMEL, NE2, KODE( 450),SGTNF(450,6),
     1NP(8, 350),MAT( 350),MBAND,NEQ,M,LM(24),KOEL( 350),
     2PSY(52),ETA(52),ZTA(52),AQ(43),PP(24),ELDISP(24),
     3KOUNT( 450),SIGA( 450,6),STN( 450,3),SIGEL(6),SIGP(7),NUMBLK,
     4  DISPX(450),DISPY(450),DISPZ(450)
      COMMON EBULK(350),EDEV(350),NITER,ITOPT,ACOEF( 5),BCOEF( 5),STP(3)
      COMMON/AREA1/ST(20,5),SL(10,5),SD(20,10,5),VS(20,10,5),NUMAT,NCELP
     1,CONFAC,NSTRN
      DIMENSION AP(NE2),STIF(MB1,MB2),APL(MB1),APR(MB1),STIFL(LA2),
     1STIFR(LA)
C
      DIMENSION HED(18),OBFAC(350),ROREAD( 5),EBREAD( 5),ESREAD( 5)
C  READ PRELIMINARY INFORMATION
C NANLYS TO BE ZERO WHEN NUMAT=1 AND ANALYSIS IS LINEAR
C******************** READ STATEMENT ********************************************
      READ  (5,1000) HED,NUMNP,NUMEL,NUMAT,NUMCE,NUMTP,NUMTH,NANLYS
      WRITE (6,2000) HED,NUMNP,NUMEL,NUMAT,NUMCE,NUMTP,NUMTH
C
C  READ AND WRITE MATERIAL PROPERTIES
C
C  READ AND WRITE NODAL DATA AND GENERATE INTERMEDIATE NODAL DATA
C
   32  WRITE(6,2015)
       L=1
C******************** READ STATEMENT ********************************************
      READ(5,1020) N,KODE(N),X(N),Y(N),Z(N),U(N),V(N),W(N)
      GO TO 40
```

```
C
   20 READ(5,1020) N,KODE(N),X(N),Y(N),Z(N),U(N),V(N),W(N)
      DN = N-L
      DX =(X(N)-X(L))/DN
      DY =(Y(N)-Y(L))/DN
      DZ=(Z(N)-Z(L))/DN
25    L=L+1
C
      IF(N-L) 50,40,30
30    X(L) = X(L-1)+DX
      Y(L) = Y(L-1)+DY
      Z(L)=Z(L-1)+DZ
      KODE(L)= 0
      U(L) = 0
      V(L)= 0
      W(L)=0
      GO TO 25
C
   40 IF(NUMNP-N)750,60,20
  750 WRITE (6,2025) N
      CALL EXIT
C
C  ASSIGN PROPER CODE FOR NODES GENERATED BEFORE WITH KODE(N)=0
C
C******************** READ STATEMENT ******************************************
   60 READ (5,1037) NUM1
      IF(NUM1.EQ.0) GO TO 83
      DO 81 I=1,NUM1
C******************** READ STATEMENT ******************************************
      READ (5,1037) NUM2
C******************** READ STATEMENT ******************************************
      READ (5,1016) N,KODE(N)
      IF (NUM2.EQ.0) GO TO 81
      DO 82 J=1,NUM2
      N=N+1
      KODE(N)=KODE(N-1)
   82 CONTINUE
   81 CONTINUE
   83 WRITE(6,2020)(N,KODE(N),X(N),Y(N),Z(N),U(N),V(N),W(N),N=1,NUMNP)
C
C
C  READ AND WRITE ELEMENT DATA
C
C  GENERATE THE HEXAHEDRA AND BASE TRIANGULAR PRISMS IF ANY
      WRITE (6,2030)
      DO 70 IJ=1,NUMCE
C******************** READ STATEMENT ******************************************
      READ (5,1037) NUMJK
      WRITE(6,1037) NUMJK
C******************** READ STATEMENT ******************************************
      READ (5,1036) M,KOEL(M),(NP(KK,M),KK=1,8),MAT(M)
      WRITE(6,1036) M,KOEL(M),(NP(KK,M),KK=1,8),MAT(M)
      IF (NUMJK.EQ.0) GO TO 70
      DO 71 JK=1,NUMJK
      M=M+1
      KOEL(M)=KOEL(M-1)
      MAT(M)=MAT(M-1)
      NP(1,M)=NP(1,M-1)+1
      NP(2,M)=NP(2,M-1)+1
      NP(3,M)=NP(3,M-1)+1
```

```
      NP(4,M)=NP(4,M-1)+1
      NP(5,M)=NP(5,M-1)+1
      NP(6,M)=NP(6,M-1)+1
      NP(7,M)=NP(7,M-1)+1
      NP(8,M)=NP(8,M-1)+1
      WRITE(6,1036) M,KOEL(M),(NP(KK,M),KK=1,8),MAT(M)
   71 CONTINUE
   70 CONTINUE
      IF(NUMTP.EQ.0) GO TO 74
C  READ THE TRIANGULAR PRISMS
      DO 84 I=1,NUMTP
C******************** READ STATEMENT *********************************************
      READ (5,1036) M,KOEL(M),(NP(KK,M),KK=1,8),MAT(M)
      WRITE(6,1036) M,KOEL(M),(NP(KK,M),KK=1,8),MAT(M)
  84  CONTINUE
   74 IF (NUMTH.EQ.0) GO TO 75
C  READ THE TETRAHEDRA
      DO 73 I=1,NUMTH
C******************** READ STATEMENT *********************************************
      READ (5,1036) M,KOEL(M),(NP(KK,M),KK=1,8),MAT(M)
      WRITE(6,1036) M,KOEL(M),(NP(KK,M),KK=1,8),MAT(M)
  73  CONTINUE
  75  IF(NUMAT.EQ.1) GO TO 510
C ASSIGN PROPER MAT(M) FOR ELEMENTS WHOSE MAT(M).NE.1
C******************** READ STATEMENT *********************************************
      READ(5,1037) MATN
      IF(MATN.EQ.0) GO TO 510
C******************** READ STATEMENT *********************************************
      DO 2 I=1,MATN
  2   READ(5,1016) M,MAT(M)
  510 DO 200 I=1,NUMAT
C
C ACOEF=2.C*COS(PHI)/(1.-SIN(PHI)),BCOEF=2.*SIN(PHI)/(1-SIN(PHI))
C
C********************* READ STATEMENT *********************************************
      READ  (5,2057) ROREAD(I),EBREAD(I),ESREAD(I),ACOEF(I),BCOEF(I)
      WRITE(6,2059)  ROREAC(I),EBREAD(I),ESREAD(I),ACOEF(I),BCOEF(I)
 200  CONTINUE
      DO 140 N=1,NUMEL
      I=MAT(N)
      RO(N)=ROREAD(I)
      EBULK(N)=EEREAD(I)
      EDEV(N)=ESREAD(I)
      OBFAC(N)=1.0
 140  CONTINUE
C******************** READ STATEMENT *********************************************
      READ (5,1037) NOBSET
      IF(NOBSET.EQ.0) GO TO 150
      DO 145 I=1,NOBSET
C******************** READ STATEMENT *********************************************
      READ (5,1050) M,NSET,OBFAC(M)
      IF(NSET.EQ.0) GO TO 145
      DO 155 J=1,NSET
      M=M+1
 155  OBFAC(M)=OBFAC(M-1)
 145  CONTINUE
C******************** READ STATEMENT *********************************************
 150  READ(5,1050) NCELP,NSTRN,CONFAC
      IF(NCELP.EQ.0) GO TO 100
      CALL TESTD
```

```
      DO 600 M=1,NUMEL
      IF(RO(M).LE.0.0) GO TO 600
      N=MAT(M)
      NCOUNT=0
      DEPTH=(ABS(Z(NP(5,M))-Z(NP(1,M)))+ABS(Z(NP(6,M))-Z(NP(2,M)))
     1+ABS(Z(NP(7,M))-Z(NP(3,M)))+ABS(Z(NP(8,M))-Z(NP(4,M))))*0.125
      OBP=DEPTH*RO(M)*OBFAC(M)
      AVGSIG=OBP*0.5
   18 NCOUNT=NCOUNT+1
      SIGM1=OBP
      SIGM2=AVGSIG
      SIGM3=AVGSIG
      SIGOCT=(SIGM1+SIGM2+SIGM3)/3.
      SIGIN=SIGM1*SIGM2*SIGM3
      CONFS=SIGIN/(SIGOCT**2)
      DIVOCT=SQRT((SIGM1-SIGM2)**2+(SIGM2-SIGM3)**2+(SIGM3-SIGM1)**2)
      DIVOCT=DIVOCT/3.
      DO 720 J=1,NCELP
      JLS=J
      IF( CONFS-SL(J,N)) 721,720,720
  720 CONTINUE
  721 CONTINUE
      DO 790 K=1,NSTRN
      JS1=K
      IF(DIVOCT-SD(K,JLS-1,N)) 791,790,790
  790 CONTINUE
  791 CONTINUE
      DO 50 K=1,NSTRN
      JS2=K
      IF(DIVOCT-SD(K,JLS,N)) 51,50,50
   50 CONTINUE
   51 CONTINUE
      PR1=1.061*(VS(JS1,JLS-1,N)-VS(JS1-1,JLS-1,N))/(ST(JS1,N)-ST(JS1-1,
     1N))-1.0
      IF(PR1.GT.0.49) PR1=0.49
      PR2=1.061*(VS(JS2,JLS   ,N)-VS(JS2-1,JLS   ,N))/(ST(JS2,N)-ST(JS2-1,
     1N))-1.0
      IF(PR2.GT.0.49) PR2=0.49
      PR3=PR1+((PR2-PR1)*( CONFS-SL(JLS-1,N))/(SL(JLS,N)-SL(JLS-1,N)))
      IF(PR3.GT.0.49 ) PR3=0.49
      CONST=PR3/(1.-PR3)
      HPR=OBP*CONST
      HPR=(HPR+AVGSIG)/2.
      CSTRS=ABS(HPR-AVGSIG)
      IF(NCOUNT.GE.21) GO TO 52
      IF(ABS(HPR-AVGSIG).LT.0.01) GO TO 52
      AVGSIG=HPR
      GO TO 18
   52 WRITE(6,125) M,NCOUNT,HPR,CSTRS,PR3
      DIF1=SD(JS1,JLS-1,N)-SD(JS1-1,JLS-1,N)
      ETP1=DIF1/(ST(JS1,N)-ST(JS1-1,N))
      GTP1=ETP1/(0.9428*(1.+PR1))
      DIF2=SD(JS2,JLS,N)-SD(JS2-1,JLS,N)
      ETP2=DIF2/(ST(JS2,N)-ST(JS2-1,N))
      GTP2=ETP2/(0.9428*(1.+PR2))
      GTP=GTP1+ (GTP2-GTP1)*(CONFS -SL(JLS-1,N))/(SL(JLS,N)-SL(JLS-1,N))
      GTP=100.*GTP
      EBULK(M)=GTP*2.*(1.+PR3)/(3.*(1.-2.*PR3))
      EDEV(M)=GTP
  600 CONTINUE
```

```
      IF(NCELP.NE.0) GO TO 310
  100 IF(NANLYS.EQ.0) GO TO 310
C ASSIGN MODULI FROM OTHER THAN TRIAXIAL DATA
  310 DO 76 M=1,NUMEL
   76 WRITE(6,1036) M,KCEL(M),(NP(KN,M),KN=1,8),MAT(M)
      WRITE(6,2005)
      WRITE(6,2010) (M,EBULK(M),EDEV(M),RO(M),M=1,NUMEL)
C
C     DETERMINE BAND WIDTH AND NUMBER OF EQUATIONS
C
      L=0
      DO 80 M=1,NUMEL
      DO 80 I=1,7
      II=I+1
      DO 80 J=II,8
      K= IABS(NP(I,M)-NP(J,M))
      IF (K.GT.L)   L=K
80    CONTINUE
      WRITE(6,3000)
C
      MBAND=3*(L+1)
      NEQ1=3*NUMNP
C
      WRITE(6,2040)MBAND,NEQ1
      IF(MBAND.LE.300)GO TO 90
      CALL EXIT
C
3000  FORMAT(  '  READIN COMPLETED ' ///)
90    RETURN
C
C  FORMAT STATEMENTS
  125 FORMAT(2I5,2E15.6,F8.5)
 1000 FORMAT(18A4/ 7I6)
 1016 FORMAT(2I5)
 1036 FORMAT(11I5)
 1037 FORMAT(I5)
 2000 FORMAT(1H1,10X,18A4,////
     1 1H ,     26H NUMBER OF NODAL POINTS = ,I6/
     2 1H ,     26H NUMBER OF ELEMENTS     = ,I6/
     3 1H ,     26H NUMBER OF MATERIALS    = ,I6/
     4 1H ,     26H NUMBER OF HEXA. READ   = ,I6/
     5 1H ,     26H NUMBER OF PRISMS       = ,I6/
     6 1H ,     26H NUMBER OF TETRAHEDRA   = ,I6)
 2005 FORMAT(///,1H ,10X, 21H  MATERIAL PROPERTIES //
     11X, 8HELE. NO.,4X, 9HBULK MOD.,4X,14HSHEAR  MODULUS,4X,11HUNIT WEI
     2GHT,//)
 1010 FORMAT(6X,F12.0,2F6.0)
 2010 FORMAT(1H ,I5,F17.4,F15.3,F17.4)
 2012 FORMAT (F17.4,F15.3,F17.4)
 2015 FORMAT('1',10X,'NODAL POINT INPUT'//,'NODE  KODE    XCOORD       Y
     1 COORD       Z COORD       X FORCE       Y FORCE       Z FORCE'//)
 1020 FORMAT(2I5,6F5.0)
 2020 FORMAT(I4,I6,6F12.3)
 2025 FORMAT(1H0,28H ERROR IN NODAL DATA,NODE = ,I4)
 2030 FORMAT('1',10X,'ELEMENT DATA'///,'ELEM EL.CODE N1    N2    N3    N4
     1 N5    N6    N7    N8 MAT.NUM.'//)
 1035 FORMAT (6I6,F6.0)
 2040 FORMAT(///10X,' BAND WIDTH          =',I6/
     1          10X,'NUMBER OF EQUATIONS =',I6)
 2050 FORMAT(///10X, 33H PROBLEM EXCEEDS SPECIFIED LIMITS )
```

```
 2051 FORMAT(5F5.0)
 2052 FORMAT(6F5.0)
 2053 FORMAT('0',10X,'STRESS - STRAIN RELATIONSHIPS FOR MATERIAL',I6//)
 2055 FORMAT(1X,'LATSTRESS',6X,5F8.3/)
 2056 FORMAT(1X,'STRN.=',3X,F6.2,5F8.3/)
 2057 FORMAT(5F10.0)
 2059 FORMAT(5F15.6)
 1050 FORMAT(2I5,F10.0)
 2060 FORMAT(5F10.2)
C
      END
C
      SUBROUTINE TESTD
C
C THIS SUBROUTINE CONVERTS TRIAXIAL TEST DATA FROM CONVENTIONAL FORM
C TO INVARIANT FORM.
C
C
      DIMENSION SL(10,5),SD(20,10,5),VS(20,10,5),SIGINV(20,10,5),
     1VSTN(20,10,5)
      COMMON/AREA1/
     1          ST(20,5),SIGINT(10,5),TOCTD(20,10,5),GOCT(20,10,5),NUMAT,
     1NCELP,CONFAC,NSTRN
      DO 10 N=1,NUMAT
C****************************READ STATEMENT ***************************************
      READ(5,1010) (SL(J,N),J=1,NCELP)
      DO 15 J=1,NCELP
      SL(J,N)=SL(J,N)*CONFAC
      SIGINT(J,N)=SL(J,N)
   15 CONTINUE
      DO 20 K=1,NSTRN
C********************** READ STATEMENT ********************************************
      READ(5,1020) ST(K,N),(SD(K,J,N),J=1,NCELP)
      DO 25 J=1,NCELP
      SD(K,J,N)=SD(K,J,N)*CONFAC
   25 CONTINUE
   20 CONTINUE
      WRITE (6,1030) N
      WRITE(6,1040) (SL(J,N),J=1,NCELP)
      DO 30 K=1,NSTRN
C********************** READ STATEMENT ********************************************
      READ  (5,1020) ST(K,N),(VS(K,J,N),J=1,NCELP)
      WRITE(6,1050)  ST(K,N),(VS(K,J,N),J=1,NCELP)
   30 CONTINUE
      DO 35 K=1,NSTRN
      WRITE(6,1050)  ST(K,N),(SD(K,J,N),J=1,NCELP)
   35 CONTINUE
   10 CONTINUE
      DO 40 N=1,NUMAT
      DO 45 J=1,NCELP
      DO 50 K=1,NSTRN
      PROD= (SL(J,N)**2)*(SD(K,J,N)+SL(J,N))
      SIGOCT=SL(J,N)+(SD(K,J,N))/3.
      IF(J.EQ.1.AND.K.EQ.1) GO TO 51
      SIGINV(K,J,N)=PROD/(SIGOCT**2)
   51 IF(J.EQ.1.AND.K.EQ.1) SIGINV(K,J,N)=0.0
   50 CONTINUE
   45 CONTINUE
      DO 70 I=1,NCELP
      DO 55 K=1,NSTRN
```

```
      DO 60 J=1,NCELP
      JLS=J
      IF(SIGINT(I,N)-SIGINV(K,J,N))61,60,60
   60 CONTINUE
   61 CONTINUE
      TOCTD(K,I,N)=SD(K,JLS-1,N)+(SD(K,JLS,N)-SD(K,JLS-1,N))*(SIGINT(I,N
     1)-SIGINV(K,JLS-1,N))/(SIGINV(K,JLS,N)-SIGINV(K,JLS-1,N))
      TOCTD(K,I,N)=TOCTD(K,I,N)*0.4714
      VSTN(K,I,N)=VS(K,JLS-1,N)+(VS(K,JLS,N)-VS(K,JLS-1,N))*(SIGINT(I,N)
     1-SIGINV(K,JLS-1,N))/(SIGINV(K,JLS,N)-SIGINV(K,JLS-1,N))
      GOCT(K,I,N)=0.4714*(3.*ST(K,N) -VSTN(K,I,N))
   55 CONTINUE
   70 CONTINUE
      WRITE(6,1031) N
      WRITE (6,1041) (SIGINT(I,N),I=1,NCELP)
      DO 75 K=1,NSTRN
   75 WRITE(6,1050)ST(K,N),(TOCTD(K,I,N),I=1,NCELP)
      DO 80 K=1,NSTRN
   80 WRITE(6,1050) ST(K,N),(GOCT(K,J,N),J=1,NCELP)
   40 CONTINUE
 1000 FORMAT(3I5,F10.0)
 1010 FORMAT(10F5.0)
 1020 FORMAT(11F5.0)
 1030 FORMAT('0','DATA IN CONVENTIONAL FORM FOR MATERIAL NO.',I5/)
 1031 FORMAT('0',' DATA IN STRESS INVARIANT FORM FOR MATERIAL NO. ',I5/)
 1040 FORMAT(1X,'LATSTRESS',6X,10F8.3/)
 1041 FORMAT(1X,'J3/(SIGOCT)**2',1X,10F8.3/)
 1050 FORMAT(1X,'STRAIN',3X,F6.2,10F8.3/)
 1060 FORMAT(I5)
 1070 FORMAT(3F10.0)
 1071 FORMAT(3F8.3,4F12.4)
      RETURN
      END
C
      SUBROUTINE ASTIF(AP,STIF,APL,APR,STIFL,STIFR,MB1,MB2,LA,LA2)
C
C THIS SUBROUTINE TAKES EACH ELEMENT IN TURN AND FORMS THE ELEMENT STIFFNESS
C MATRIX (BY CALLING ELSTIF).IT ASSEMBLES THE ELEMENT STIFFNESSES INTO
C TOTAL STIFFNESS MATRIX . ASSEMBLES THE APPLIED LOAD VECTOR & MODIFIES
C THE ASSEMBLAGES FOR DISPLACEMENT BOUNDARY CONDITIONS ( BY CALLING
C MODIFY).
C
      COMMON NANLYS,KSHIFT, RO(350),X(450),Y(450),Z(450),U(450),V(450),
     1W(450),SGTEL(350,6),SGTPS(350,7),STRNT(350,6),STNT(450,3),
     2  ECMI(3,3),STRN(6) ,ESTIF(24,24),ECM(6,6),EBM(6,24),ESM(6,24),WT
      COMMON NUMNP,NUMEL, NE2, KODE( 450),SGTNP(450,6),
     1NP(8, 350),MAT( 350),MBAND,NEQ,M,LM(24),KOEL( 350),
     2PSY(52),ETA(52),ZTA(52),AQ(43),PP(24),ELDISP(24),
     3KOUNT( 450),SIGA( 450,6),STN( 450,3),SIGEL(6),SIGP(7),NUMBLK,
     4  DISPX(450),DISPY(450),DISPZ(450)
      COMMON EBULK(350),EDEV(350),NITER,ITOPT,ACOEF( 5),BCOEF( 5),STP(3)
      COMMON/AREA1/ST(20,5),SL(10,5),SD(20,10,5),VS(20,10,5),NUMAT,NCELP
     1,CONFAC,NSTRN
      DIMENSION AP(NE2),STIF(MB1,MB2),APL(MB1),APR(MB1),STIFL(LA2),
     1STIFR(LA)
C
      INTEGER*2 LEN
      NBYTES=MBAND*MBAND*4
      FNUMRC=FLOAT(NBYTES)/32000
      NUMREC=NBYTES/32000
```

```
      IF((FNUMRC-NUMREC).GT.0.0) NUMREC=NUMREC+1
  600 FORMAT( 'FILE ERROR IN ASTIF')
C
C     INITIALIZATION
C
      REWIND 2
      NB=MBAND/3
      ND=3*NB
      NEQ=2*ND
      NUMBLK=0
C
      DO 10 I=1.NEQ
      AP(I)=0.0
      DO 10 J=1.ND
   10 STIF(J.I)=0.0
      DO 21 I=1.6
      DO 21 J=1.6
      ECM(I.J)=0.0
   21 CONTINUE
C
C   FORM ELEMENT CONSTITUTIVE MATRIX (ECM) IF NUMAT=1)
      IF(NUMAT.NE.1) GO TO 20
      IF(NANLYS.NE.0) GO TO 20
C
      COM1=EBULK(1)+1.33333*EDEV(1)
      COM2=EBULK(1)-0.666667*EDEV(1)
      COM3=EDEV(1)
      ECM(1.1)=COM1
      ECM(2.2)=COM1
      ECM(3.3)=COM1
      ECM(4.4)=COM3
      ECM(5.5)=COM3
      ECM(6.6)=COM3
      ECM(1.2)=COM2
      ECM(1.3)=COM2
      ECM(2.1)=COM2
      ECM(2.3)=COM2
      ECM(3.1)=COM2
      ECM(3.2)=COM2
      DET=COM1**3+2.*COM2**3-3.*COM1*COM2**2
      COM4=(COM1**2-COM2**2)/DET
      COM5=(COM2**2-COM1*COM2)/DET
      ECMI(1.1)=COM4
      ECMI(2.2)=CCM4
      ECMI(3.3)=COM4
      ECMI(1.2)=COM5
      ECMI(1.3)=COM5
      ECMI(2.1)=COM5
      ECMI(2.3)=COM5
      ECMI(3.1)=COM5
      ECMI(3.2)=CCM5
C
C     FORM STIFNESS MATRIX IN BLOCKS
   20 NUMBLK=NUMBLK+1
      NH=NB*(NUMBLK+1)
      NM=NH-NB
      NL=NM-NB+1
      WRITE(6.1001) NUMBLK.NL.NM
      KSHIFT=3*NL-3
      DO 110 M=1.NUMEL
```

```
      IF(MAT(M))110,110,25
   25 DO 35 I=1,8
      IF(NP(I,M)-NL)35,20,30
   30 IF(NP(I,M)-NM)40,40,35
   35 CONTINUE
      GO TO 110
C
   40 CALL ELSTIF(AP,STIF,AFL,APR,STIFL,STIFR,MB1,MB2,LA,LA2,1)
      MAT(M)=-MAT(M)
C     ASSEMBLE ESTIF  INTO TOTAL STIFFNESS MATRIX
      DO 75 I=1,8
      I2=3*I
      LM(I2)=3*NP(I,M)
      LM(I2-1)=LM(I2)-1
   75 LM(I2-2)=LM(I2)-2
C
      DO 100 I=1,24
      II=LM(I)-KSHIFT
      DO 100 J=1,24
      JJ=LM(J)-II+1-KSHIFT
      IF(JJ.LE.0) GO TO 100
      STIF(JJ,II)=STIF(JJ,II)+ESTIF(I,J)
  100 CONTINUE
C     ADD GRAVITY LOADS IN TO AP VECTOR
      DO 46 I=3,24,3
      II=LM(I)-KSHIFT
   46 AP(II)=AP(II)-WT
  110 CONTINUE
      WRITE(6,1000)
      WRITE(6,1002) (M,MAT(M),M=1,NUMEL)
C     ADD NODAL LOADS INTO AP VECTOR
      DO 51 N=NL,NM
      N2=3*N-KSHIFT
      AP(N2)=AP(N2)+W(N)
      AP(N2-1)=AP(N2-1)+V(N)
   51 AP(N2-2)=AP(N2-2)+U(N)
C     MODIFY STIFFNESS AND LOAD VECTOR FOR DISPLACEMENTS
      DO 102 N=NL,NM
      IF(N-NUMNP) 111,111,102
  111 N2=3*N-KSHIFT
      IF (KODE(N)-10)82,72,62
   62 IF(KODE(N).EQ.12)GO TO 61
      IK=N2-1
      CALL MODIFY(AP,STIF,APL,APR,STIFL,STIFR,MB1,MB2,LA,LA2,IK,N)
      CALL MODIFY(AP,STIF,APL,APR,STIFL,STIFR,MB1,MB2,LA,LA2,N2,N)
      GO TO 102
   61 II=N2-2
      IK=N2-1
      CALL MODIFY(AP,STIF,APL,APR,STIFL,STIFR,MB1,MB2,LA,LA2,IK,N)
      CALL MODIFY(AP,STIF,APL,APR,STIFL,STIFR,MB1,MB2,LA,LA2,N2,N)
      CALL MODIFY(AP,STIF,APL,APR,STIFL,STIFR,MB1,MB2,LA,LA2,II,N)
      GO TO 102
   72 II=N2-2
      IK=N2-1
      CALL MODIFY(AP,STIF,APL,APR,STIFL,STIFR,MB1,MB2,LA,LA2,II,N)
      CALL MODIFY(AP,STIF,APL,APR,STIFL,STIFR,MB1,MB2,LA,LA2,IK,N)
      GO TO 102
   82 IF(KODE(N)-1)102,78,101
   78 CALL MODIFY(AP,STIF,APL,APR,STIFL,STIFR,MB1,MB2,LA,LA2,N2,N)
      GO TO 102
```

```
  101  IF(KODE(N)-3) 105,106,107
  106  II=N2-2
       CALL MODIFY(AP,STIF,AFL,APR,STIFL,STIFR,MB1,MB2,LA,LA2,II,N)
       GO TO 102
   105 IK=N2-1
       CALL MODIFY(AP,STIF,AFL,APR,STIFL,STIFR,MB1,MB2,LA,LA2,IK,N)
       GO TO 102
  107  II=N2-2
       CALL MODIFY(AP,STIF,APL,APR,STIFL,STIFR,MB1,MB2,LA,LA2,II,N)
       CALL MODIFY(AP,STIF,APL,APR,STIFL,STIFR,MB1,MB2,LA,LA2,N2,N)
  102  CONTINUE
C
C      WRITE BLOCK OF EQUATIONS ON DISC AND SHIFT UP LOWER BLOCK
       LEN=32000
       LL=1
       DO 400 L=1,NUMREC
       IF(L.EQ.NUMREC)LEN=NBYTES-((NUMREC-1)*32000)
       CALL WRITE(STIFL(LL),LEN,0,1,2,&401)
       WRITE(6,1005) LL,LEN,STIFL(LL)
       LL=LL+8000
       GO TO 400
  401  WRITE(6,600)
       STOP
  400  CONTINUE
       LEN=MBAND*4
       CALL WRITE(APL,LEN,0,1,2,&401)
       WRITE(6,1005) MBAND,LEN,APL(1)
 1005  FORMAT(2I10,E20.7)
       DO 270 I=1,ND
       K=I+ND
       AP(I)=AP(K)
       AP(K)=0.0
       DO 270 J=1,ND
       STIF(J,I)=STIF(J,K)
  270  STIF(J,K)=0.0
C
C      CHECK FOR LAST BLOCK
C
       IF(NM-NUMNP)20,280,280
  280  CONTINUE
       RETURN
 1000  FORMAT( /10X,'ELEMENT STIFFNESS FORMED FOR ELEMENTS WITH -VE MAT(M
      1)IN THE FOLLOWING:'/)
 1001  FORMAT(  /10X,'BLOCK NUMBER=',I5/10X,'LOWEST NODE NUMBER=',I5/10X,
      1'HIGHEST NODE NUMBER=',I5/)
 1002  FORMAT (26I5)
       END
C
       SUBROUTINE ELSTIF(AP,STIF,APL,APR,STIFL,STIFR,MB1,MB2,LA,LA2,KOP)
C  THIS SUBROUTINE FORMS THE ELEMENT STIFFNESS MATRIX (ESTIF) OR
C  ELEMENT STRESS MATRIX (ESM)
C
       COMMON NANLYS,KSHIFT, RO(350),X(450),Y(450),Z(450),U(450),V(450),
      1W(450),SGTEL(350,6),SGTPS(350,7),STRNT(350,6),STNT(450,3),
      2  ECMI(3,3),STRN(6) ,ESTIF(24,24),ECM(6,6),EBM(6,24),ESM(6,24),WT
       COMMON NUMNP,NUMEL, NE2, KODE( 450),SGTNP(450,6),
      1NP(8, 350),MAT( 350),MBAND,NEQ,M,LM(24),KOEL( 350),
      2PSY(52),ETA(52),ZTA(52),AQ(43),PP(24),ELDISP(24),
      3KOUNT( 450),SIGA( 450,6),STN( 450,3),SIGEL(6),SIGP(7),NUMBLK,
      4  DISPX(450),DISPY(450),DISPZ(450)
```

```
      COMMON EBULK(350).EDEV(350).NITER.ITOPT.ACOEF( 5).BCOEF( 5).STP(3)
      COMMON/AREA1/ST(20.5).SL(10.5).SD(20.10.5).VS(20.10.5).NUMAT.NCELP
     1.CONFAC.NSTRN
      DIMENSION AP(NE2).STIF(MB1.MB2).APL(MB1).APR(MB1).STIFL(LA2).
     1STIFR(LA)
      DO 70 I=1.24
      DO 70 J=1.24
   70 ESTIF(I.J)=0.0
      VOL=0.0
      L1=NP(1.M)
      L2=NP(2.M)
      L3=NP(3.M)
      L4=NP(4.M)
      L5=NP(5.M)
      L6=NP(6.M)
      L7=NP(7.M)
      L8=NP(8.M)
C FORM CONSTITUTIVE MATRIX
      IF(NANLYS.NE.0) GO TO 2
      IF(NUMAT.EQ.1) GO TO 17
    2 COM1=EBULK(M)+1.33333*EDEV(M)
      COM2=EBULK(M)-0.6666667*EDEV(M)
      COM3=EDEV(M)
      ECM(1.1)=COM1
      ECM(2.2)=COM1
      ECM(3.3)=COM1
      ECM(4.4)=COM3
      ECM(5.5)=COM3
      ECM(6.6)=COM3
      ECM(1.2)=COM2
      ECM(1.3)=COM2
      ECM(2.1)=COM2
      ECM(2.3)=COM2
      ECM(3.1)=COM2
      ECM(3.2)=COM2
      DET=COM1**3+2.*COM2**3-3.*COM1*COM2**2
      COM4=(COM1**2-COM2**2)/DET
      COM5=(COM2**2-COM1*COM2)/DET
      ECMI(1.1)=COM4
      ECMI(2.2)=COM4
      ECMI(3.3)=COM4
      ECMI(1.2)=COM5
      ECMI(1.3)=COM5
      ECMI(2.1)=COM5
      ECMI(2.3)=COM5
      ECMI(3.1)=COM5
      ECMI(3.2)=COM5
C
   17 IF(KOP.EQ.2) GO TC 14
      IF(KOEL(M).LE.1) GO TC 11
      IF(KOEL(M).GE.2) GO TO 12
   11 DO 21 LN1=9.16
      L=LN1
      GO TO 13
   12 DO 22 LN2=17.43
      L=LN2
      GO TO 13
   14 IF(KOEL(M).EQ.1) GO TO 81
      IF(KOEL(M).EQ.2) GO TO 81
      DO 20 LN3=1.8
```

```
      L=LN3
      GO TO 13
   81 DO 25 LN4=45,52
      L=LN4
      GO TO 13
   15 L=44
      PSY(44)=0.0
      ETA(44)=0.0
      ZTA(44)=0.0
C FORMULATE DERIVATIVE MATRIX
   13 PEP1=-(1./8.)*(1.-ETA(L))*(1.-ZTA(L))
      PEP2=-(1./8.)*(1.+ETA(L))*(1.-ZTA(L))
      PEP3= (1./8.)*(1.+ETA(L))*(1.-ZTA(L))
      PEP4= (1./8.)*(1.-ETA(L))*(1.-ZTA(L))
      PEP5=-(1./8.)*(1.-ETA(L))*(1.+ZTA(L))
      PEP6=-(1./8.)*(1.+ETA(L))*(1.+ZTA(L))
      PEP7=+(1./8.)*(1.+ETA(L))*(1.+ZTA(L))
      PEP8=+(1./8.)*(1.-ETA(L))*(1.+ZTA(L))
      PET1=-(1./8.)*(1.-PSY(L))*(1.-ZTA(L))
      PET2=+(1./8.)*(1.-PSY(L))*(1.-ZTA(L))
      PET3=+(1./8.)*(1.+PSY(L))*(1.-ZTA(L))
      PET4=-(1./8.)*(1.+PSY(L))*(1.-ZTA(L))
      PET5=-(1./8.)*(1.-PSY(L))*(1.+ZTA(L))
      PET6=+(1./8.)*(1.-PSY(L))*(1.+ZTA(L))
      PET7=+(1./8.)*(1.+PSY(L))*(1.+ZTA(L))
      PET8=-(1./8.)*(1.+PSY(L))*(1.+ZTA(L))
      PZT1=-(1./8.)*(1.-PSY(L))*(1.-ETA(L))
      PZT2=-(1./8.)*(1.-PSY(L))*(1.+ETA(L))
      PZT3=-(1./8.)*(1.+PSY(L))*(1.+ETA(L))
      PZT4=-(1./8.)*(1.+PSY(L))*(1.-ETA(L))
      PZT5=+(1./8.)*(1.-PSY(L))*(1.-ETA(L))
      PZT6=+(1./8.)*(1.-PSY(L))*(1.+ETA(L))
      PZT7=+(1./8.)*(1.+PSY(L))*(1.+ETA(L))
      PZT8=+(1./8.)*(1.+PSY(L))*(1.-ETA(L))
C FORM THE JACOBIAN MATRIX
      X1J=PEP1*X(L1)+PEP2*X(L2)+PEP3*X(L3)+PEP4*X(L4)+PEP5*X(L5)+
     1PEP6*X(L6)+PEP7*X(L7)+PEP8*X(L8)
      X2J=PET1*X(L1)+PET2*X(L2)+PET3*X(L3)+PET4*X(L4)+PET5*X(L5)+
     1PET6*X(L6)+PET7*X(L7)+PET8*X(L8)
      X3J=PZT1*X(L1)+PZT2*X(L2)+PZT3*X(L3)+PZT4*X(L4)+PZT5*X(L5)+
     1PZT6*X(L6)+PZT7*X(L7)+PZT8*X(L8)
      Y1J=PEP1*Y(L1)+PEP2*Y(L2)+PEP3*Y(L3)+PEP4*Y(L4)+PEP5*Y(L5)+
     1PEP6*Y(L6)+PEP7*Y(L7)+PEP8*Y(L8)
      Y2J=PET1*Y(L1)+PET2*Y(L2)+PET3*Y(L3)+PET4*Y(L4)+PET5*Y(L5)+
     1PET6*Y(L6)+PET7*Y(L7)+PET8*Y(L8)
      Y3J=PZT1*Y(L1)+PZT2*Y(L2)+PZT3*Y(L3)+PZT4*Y(L4)+PZT5*Y(L5)+
     1PZT6*Y(L6)+PZT7*Y(L7)+PZT8*Y(L8)
      Z1J=PEP1*Z(L1)+PEP2*Z(L2)+PEP3*Z(L3)+PEP4*Z(L4)+PEP5*Z(L5)+
     1PEP6*Z(L6)+PEP7*Z(L7)+PEP8*Z(L8)
      Z2J=PET1*Z(L1)+PET2*Z(L2)+PET3*Z(L3)+PET4*Z(L4)+PET5*Z(L5)+
     1PET6*Z(L6)+PET7*Z(L7)+PET8*Z(L8)
      Z3J=PZT1*Z(L1)+PZT2*Z(L2)+PZT3*Z(L3)+PZT4*Z(L4)+PZT5*Z(L5)+
     1PZT6*Z(L6)+PZT7*Z(L7)+PZT8*Z(L8)
C INVERT THE JACOBIAN MATRIX
      DETJ=X1J*(Y2J*Z3J-Z2J*Y3J)-Y1J*(X2J*Z3J-Z2J*X3J)+Z1J*(X2J*Y3J-Y2J*
     1X3J)
      IF(DETJ.LE.0.0) GO TO 75
      X1I=(1./DETJ)*(Y2J*Z3J-Z2J*Y3J)
      X2I=(1./DETJ)*(Y3J*Z1J-Z3J*Y1J)
      X3I=(1./DETJ)*(Y1J*Z2J-Z1J*Y2J)
```

```
      Y1I=(1./DETJ)*(Z2J*X3J-X2J*Z3J)
      Y2I=(1./DETJ)*(Z3J*X1J-X3J*Z1J)
      Y3I=(1./DETJ)*(Z1J*X2J-X1J*Z2J)
      Z1I=(1./DETJ)*(X2J*Y3J-Y2J*X3J)
      Z2I=(1./DETJ)*(X3J*Y1J-Y3J*X1J)
      Z3I=(1./DETJ)*(X1J*Y2J-Y1J*X2J)
      PP(1 )=X1I*PEP1+X2I*PET1+X3I*PZT1
      PP(2 )=Y1I*PEP1+Y2I*PET1+Y3I*PZT1
      PP(3 )=Z1I*PEP1+Z2I*PET1+Z3I*PZT1
      PP(4 )=X1I*PEP2+X2I*PET2+X3I*PZT2
      PP(5 )=Y1I*PEP2+Y2I*PET2+Y3I*PZT2
      PP(6 )=Z1I*PEP2+Z2I*PET2+Z3I*PZT2
      PP(7 )=X1I*PEP3+X2I*PET3+X3I*PZT3
      PP(8 )=Y1I*PEP3+Y2I*PET3+Y3I*PZT3
      PP(9 )=Z1I*PEP3+Z2I*PET3+Z3I*PZT3
      PP(10)=X1I*PEP4+X2I*PET4+X3I*PZT4
      PP(11)=Y1I*PEP4+Y2I*PET4+Y3I*PZT4
      PP(12)=Z1I*PEP4+Z2I*PET4+Z3I*PZT4
      PP(13)=X1I*PEP5+X2I*PET5+X3I*PZT5
      PP(14)=Y1I*PEP5+Y2I*PET5+Y3I*PZT5
      PP(15)=Z1I*PEP5+Z2I*PET5+Z3I*PZT5
      PP(16)=X1I*PEP6+X2I*PET6+X3I*PZT6
      PP(17)=Y1I*PEP6+Y2I*PET6+Y3I*PZT6
      PP(18)=Z1I*PEP6+Z2I*PET6+Z3I*PZT6
      PP(19)=X1I*PEP7+X2I*PET7+X3I*PZT7
      PP(20)=Y1I*PEP7+Y2I*PET7+Y3I*PZT7
      PP(21)=Z1I*PEP7+Z2I*PET7+Z3I*PZT7
      PP(22)=X1I*PEP8+X2I*PET8+X3I*PZT8
      PP(23)=Y1I*PEP8+Y2I*PET8+Y3I*PZT8
      PP(24)=Z1I*PEP8+Z2I*PET8+Z3I*PZT8
C FORM ELEMENT B MATRIX
      DO 10 I=1,6
      DO 10 J=1,24
   10 EBM(I,J)=0.0
      DO 30 J=1,22,3
      EBM(4,J)=PP(J+1)
      EBM(6,J)=PP(J+2)
   30 EBM(1,J)=PP(J)
      DO 31 J=2,23,3
      EBM(4,J)=PP(J-1)
      EBM(5,J)=PP(J+1)
   31 EBM(2,J)=PP(J)
      DO 32 J=3,24,3
      EBM(5,J)=PP(J-1)
      EBM(6,J)=PP(J-2)
   32 EBM(3,J)=PP(J)
C FORM ELEMENT STRESS MATRIX
      DO 50 I=1,6
      DO 50 J=1,24
      ESM(I,J)=0.0
      DO 50 K=1,6
   50 ESM(I,J)=ESM(I,J)+ECM(I,K)*EBM(K,J)
      IF (KOP.EQ.1) GO TO 51
      IF(L.NE.44) GO TO 16
      DO 52 I=1,6
      SIGEL(I)=0.0
      DO 52 J=1,24
   52 SIGEL(I)=SIGEL(I)+ESM(I,J)*ELDISP(J)
      DO 510 I=1,6
      STRN(I)=0.0
```

```
      DO 500 J=1,24
500   STRN(I)=STRN(I)+EBM(I,J)*ELDISP(J)
      STRN(I)=STRN(I)*100.
510   CONTINUE
      GO TO 80
 16   IF(KOEL(M).EQ.0) GO TO 82
      IF(KOEL(M).EQ.3) GO TO 82
      N=NP(L-44,M)
      KOUNT(N)=KOUNT(N)+1
      DO 83 I=1,6
      DO 83 J=1,24
 83   SIGA(N,I)=SIGA(N,I)+ESM(I,J)*ELDISP(J)
      DO 84 I=1,3
      DO 84 J=1,24
 84   STN(N,I)=STN(N,I)+EBM(I,J)*ELDISP(J)
 25   CONTINUE
      GO TO 15
 82   N=NP(L,M)
      KOUNT(N)=KOUNT(N)+1
      DO 35 I=1,6
      DO 35 J=1,24
 35   SIGA(N,I)=SIGA(N,I)+ESM(I,J)*ELDISP(J)
      DO 36 I=1,3
      DO 36 J=1,24
 36   STN(N,I)=STN(N,I)+EBM(I,J)*ELDISP(J)
 20   CONTINUE
      GO TO 15
 51   IF(KOEL(M).LE.1) GO TO 55
C FORM ELEMENT STIFNESS MATRIX THREE POINT INTEGRATION
      DO 61 I=1,24
      DO 61 J=1,24
      DO 61 K=1,6
 61   ESTIF(I,J)=ESTIF(I,J)+AQ(L)*EBM(K,I)*ESM(K,J)*DETJ
      VOL=VOL+AQ(L)*DETJ
      WT=VOL*RO( M)/8.
 22   CONTINUE
      GO TO 80
C FORM ELEMENT STIFFNESS MATRIX TWO POINT INTEGRATION
 55   DO 60 I=1,24
      DO 60 J=1,24
      DO 60 K=1,6
 60   ESTIF(I,J)=ESTIF(I,J)+EBM(K,I)*ESM(K,J)*DETJ
      VOL=VOL+DETJ
      WT=VOL*RO( M)/8.
 21   CONTINUE
      GO TO 80
 75   WRITE(6,1000)M
      CALL EXIT
 80   RETURN
C
C
1000  FORMAT (1H1, 18H VOLUME OF ELEMENT ,I4, 18H IS LESS THAN ZERO)
      END
C
      SUBROUTINE STRESS(AP,STIF,APL,APR,STIFL,STIFR,MB1,MB2,LA1,LA2)
C
C THIS SUBROUTINE FORMS THE ELEMENT STRESS MATRIX (ESM),MULTIPLIES BY
C THE ELEMENT DISPLACEMENT VECTOR (ELDISP)AND RECORDS THE STRESSES IN
C SIGEL (BY CALLING ELSTIF). IT THEN COMPUTES PRINCIPAL STRESSES AND
C STRAINS FOR ELEMENTS AND NODAL STRESSES.
```

```
C
      COMMON NANLYS.KSHIFT. RO(350).X(450).Y(450).Z(450).U(450).V(450).
     1W(450).SGTEL( 350.6).SGTPS(350.7).STRNT(350.6).STNT(450.3).
     2  ECMI(3.3).STRN(6) .ESTIF(24.24).ECM(6.6).EBM(6.24).ESM(6.24).WT
      COMMON NUMNP.NUMEL. NE2. KODE( 450).SGTNP(450.6).
     1NP(8. 350).MAT( 350).MBAND.NEQ.M.LM(24).KOEL( 350).
     2PSY(52).ETA(52).ZTA(52).AQ(43).PP(24).ELDISP(24).
     3KOUNT( 450).SIGA( 450.6).STN( 450.3).SIGEL(6).SIGP(7).NUMBLK.
     4  DISPX(450).DISPY(450).DISPZ(450)
      COMMON EBULK(350).EDEV(350).NITER.ITOPT.ACOEF( 5).BCOEF( 5).STP(3)
      COMMON/AREA1/ST(20.5).SL(10.5).SD(20.10.5).VS(20.10.5).NUMAT.NCELP
     1.CONFAC.NSTRN
      DIMENSION AP(NE2).STIF(MB1.MB2).APL(MB1).APR(MB1).STIFL(LA2).
     1STIFR(LA)
C
      DO 5 N=1.NUMNP
      KOUNT(N)=0
      DO 5 J=1.6
    5 SIGA(N.J)=0.0
      DO 6 N=1.NUMNP
      DO 6 J=1.3
    6 STN(N.J)=0.0
C
      SIG1=0.0
      SIG2=0.0
      SIG3=0.0
      M1=0
      M2=0
      M3=0
C
      WRITE(6.2000)
      DO 100 M=1.NUMEL
C   COMPUTE ELEMENT DISPLACEMENTS
C
      DO 10 I=1.8
      I2=3*I
      LMI2=3*NP(I.M)
      ELDISP(I2)=AP(LMI2)
      ELDISP(I2-1)=AP(LMI2-1)
   10 ELDISP(I2-2)=AP(LMI2-2)
C
C COMPUTE  ELEMENT STRESSES
C
      MAT(M)=IABS(MAT(M))
      CALL ELSTIF(AP.STIF.AFL.APR.STIFL.STIFR.MB1.MB2.LA.LA2.2)
      DO 15 I=1.6
   15 SGTEL(M.I)=SGTEL(M.I)+SIGEL(I)
C
      DO 500 I=1.6
  500 STRNT(M.I)=STRNT(M.I)+STRN(I)
      WRITE (6.2010)M.(SGTEL(M.I).I=1.6).  (STRNT(M.I).
     1I=1.3)
C
C COMPUTE ELEMENT PRINCIPAL STRESSES  AND PRINCIPAL STRAINS
C
      T1=SGTEL(M.1)+SGTEL(M.2)+SGTEL(M.3)
      T2=SGTEL(M.1)*SGTEL(M.2)+SGTEL(M.2)*SGTEL(M.3)+SGTEL(M.3)*SGTEL(M.
     11)-SGTEL(M.4)**2-SGTEL(M.5)**2-SGTEL(M.6)**2
      T3=SGTEL(M.1)*SGTEL(M.2)*SGTEL(M.3)+2.*SGTEL(M.4)*SGTEL(M.5)*
     1SGTEL(M.6)-SGTEL(M.1)*(SGTEL(M.5)**2)-SGTEL(M.2)*(SGTEL(M.6)**2)
```

```
     2-SGTEL(M,3)*(SGTEL(M,4)**2)
CSOLUTION OF CUBIC EQUATION BY NEWTON METHOD
      IF(ABS(T3).LE.1.E-50)  GO TO 36
      S=0.0
      DO 31 I=1,20
      FS=S**3-T1*(S**2)+T2*S-T3
      FPR=3.*(S**2)-2.*T1*S+T2
      IF(ABS(FPR).LE.1.E-30) GO TO 12
      GO TO 11
   12 WRITE(6,2060) FPR
      FPR=1.0
   11 X1=S-FS/FPR
      IF(ABS(X1-S ).LT.1.E-6) GO TO 32
   31 S=X1
   32 T4=(T1-X1)/2.
      T5=SQRT(((T1-X1)**2)/4.-T3/X1)
   36 IF(ABS(T3).LE.1.E-50)  T4=T1/2.
      IF(ABS(T3).LE.1.E-50)  T5=SQRT((T1**2)/4.-T2)
      IF(ABS(T3).LE.1.E-50)  X1=0.0
      X2=T4+T5
      X3=T4-T5
      SIGP(1)=X1
      SIGP(2)=X2
      SIGP(3)=X3
C PRINCIPAL STRESSES ARRANGED IN ORDER
      DO 33 I=1,2
      JJ=3-I
      DO 34 J=1,JJ
      IF(SIGP(J).LT.SIGP(J+1))GO TO 35
      GO TO 34
   35 X4=SIGP(J)
      X5=SIGP(J+1)
      SIGP(J+1)=X4
      SIGP(J)=X5
   34 CONTINUE
   33 CONTINUE
CCOMPUTE MAXIM. SHEAR STRESS
      SIGP(4)=(SIGP(1)-SIGP(3))/2.
      DO 20 I=1,4
   20 SGTPS(M,I)=SIGP(I)
      T1=STRNT(M,1)+STRNT(M,2)+STRNT(M,3)
      T2=STRNT(M,1)*STRNT(M,2)+STRNT(M,2)*STRNT(M,3)+STRNT(M,3)*STRNT(M,
     11)-0.25*(STRNT(M,4)**2+STRNT(M,5)**2+STRNT(M,6)**2)
      T3=STRNT(M,1)*STRNT(M,2)*STRNT(M,3)+0.25*(STRNT(M,4)*STRNT(M,5)*ST
     1RNT(M,6)-STRNT(M,1)*(STRNT(M,5)**2)-STRNT(M,2)*(STRNT(M,6)**2)-
     2STRNT(M,3)*(STRNT(M,4)**2))
      IF(ABS(T3).LE.1.E-50)  GO TO 536
      S=0.0
      DO531 I=1,20
      FS=S**3-T1*(S**2)+T2*S-T3
      FPR=3.*(S**2)-2.*T1*S+T2
      IF(ABS(FPR).LE.1.E-30) GO TO512
      GO TO511
  512 WRITE(6,2060) FPR
      FPR=1.0
  511 X1=S-FS/FPR
      IF(ABS(X1-S ).LT.1.E-6) GO TO532
  531 S=X1
  532 T4=(T1-X1)/2.
      T5=SQRT(((T1-X1)**2)/4.-T3/X1)
```

```
  536 IF(ABS(T3).LE.1.E-50)  T4=T1/2.
      IF(ABS(T3).LE.1.E-50)  T5=SQRT((T1**2)/4.-T2)
      IF(ABS(T3).LE.1.E-50)  X1=0.0
      X2=T4+T5
      X3=T4-T5
      STP(1)=X1
      STP(2)=X2
      STP(3)=X3
C PRINCIPAL STRAINS ARRANGED IN ORDER
      DO 533 I=1.2
      JJ=3-I
      DO 534 J=1.JJ
      IF(STP(J).LT.STP(J+1)) GO TO 535
      GO TO 534
  535 X4=STP(J)
      X5=STP(J+1)
      STP(J+1)=X4
      STP(J)=X5
  534 CONTINUE
  533 CONTINUE
      DO 520 I=1.3
      J=I+4
  520 SGTPS(M.J)=STP(I)
      IF(ITOPT.EQ.0) GO TO 350
      IF(NITER.EQ.2) GO TO 350
      DO 200 I=1.6
  200 SGTEL(M.I)=SGTEL(M.I)-SIGEL(I)
      DO 201 I=1.6
  201 STRNT(M.I)=STRNT(M.I)-STRN(I)
C
C   FIND  MAXIMUM  ELEMENT STRESSES
  350 IF(SGTPS(M.1).LT.SIG1) GO TO 115
      SIG1=SGTPS(M.1)
      M1=M
  115 IF(SGTPS(M.3).GT.SIG2) GO TO 120
      SIG2=SGTPS(M.3)
      M2=M
  120 IF(SGTPS(M.4).LT.SIG3) GO TO 100
      SIG3=SGTPS(M.4)
      M3=M
  100 CONTINUE
      WRITE(6.2040) SIG1.M1.SIG2.M2.SIG3.M3
      WRITE(6.2001)
      WRITE(6.2002) (M.(SGTPS(M.I).I=1.7).M=1.NUMEL)
C
C  FIND AVERAGE NODAL STRESSES AND STRAINS (X)
      DO 110 N=1.NUMNP
      RK=KOUNT(N)
      IF(RK.EQ.0.0) GO TO 110
      DO 116 I=1.6
      SIGA(N.I)= SIGA(N.I)/RK
  116 CONTINUE
  110 CONTINUE
      DO 111 N=1.NUMNP
      RP=KOUNT(N)
      IF(RP.EQ.0.0) GO TO 111
      DO 117 I=1.3
      STN(N.I)=100.*STN(N.I)/RP
  117 CONTINUE
  111 CONTINUE
```

```
      WRITE(6,2050)
      DO 27 N=1,NUMNP
      IF(KOUNT(N).EQ.0) GO TO 27
      DO 25 I=1,6
   25 SGTNP(N,I)=SGTNP(N,I)+SIGA(N,I)
      DO 26 J=1,3
   26 STNT(N,J)=STNT(N,J)+STN(N,J)
      WRITE(6,2055) N,SGTNP(N,1),SGTNP(N,2),SGTNP(N,3),SGTNP(N,4),SGTNP(
     1N,5),SGTNP(N,6),STNT(N,1),STNT(N,2),STNT(N,3)
      IF(ITOPT.EQ.0) GO TO 27
      IF(NITER.EQ.2) GO TO 27
      DO 250 I=1,6
  250 SGTNP(N,I)=SGTNP(N,I)-SIGA(N,I)
      DO 251 J=1,3
  251 STNT(N,J)=STNT(N,J)-STN(N,J)
   27 CONTINUE
      RETURN
C
 2000 FORMAT('1',10X,'ELEMENT STRESSES'///,'ELEM   SIGMA X     SIGMA Y
     1   SIGMA Z     SIGMAXY     SIGMAYZ     SIGMAZX     STRAINXX     ST
     2RAINYY    STRAINZZ'//)
 2010 FORMAT(I4, 9E12.5)
 2001 FORMAT('1',10X,'PRINCIPAL STRESSES'///,'ELEM   SIGMA 3     SIGMA 2
     1     SIGMA 1     MAXSHEAR     STRAIN3    1 STRAIN2     STRAIN1'//)
 2002 FORMAT(I4,7E12.5)
 2040 FORMAT(1H1,
     1 27H MAXIMUM PRINCIPAL STRESS = ,E15.5,19H AND OCCURS IN ELEM,I6//
     2 27H MINIMUM PRINCIPAL STRESS = ,E15.5,19H AND OCCURS IN ELEM,I6//
     3 27H MAXIMUM SHEAR  STRESS    = ,E15.5,19H AND OCCURS IN ELEM,I6)
 2050 FORMAT('1',10X,'AVERAGE NODAL STRESS'///,'NODE    SIGMA X    SIGMA
     1Y     SIGMA Z     SIGMA XY     SIGMA YZ     SIGMA ZX     STRAINX
     2    STRAINY     STRAINZ'///)
 2055 FORMAT(I4,9E12.5)
 2060 FORMAT(E12.5)
C
      END
C
C
      SUBROUTINE MODIFY (AP,STIF,APL,APR,STIFL,STIFR,MB1,MB2,LA,LA2,I,N)
C
C THIS SUBROUTINE MODIFIES THE TOTAL STIFFNESS MATRIX AND LOAD VECTOR
C FOR DIPLACEMENT BOUNDARY CONDITIONS.
C
      COMMON NANLYS,KSHIFT, RO(350),X(450),Y(450),Z(450),U(450),V(450),
     1W(450),SGTEL(350,6),SGTPS(350,7),STRNT(350,6),STNT(450,3),
     2  ECNI(3,3),STRN(6) ,ESTIF(24,24),ECM(6,6),EBM(6,24),ESM(6,24),WT
      COMMON NUMNP,NUMEL, NE2, KODE( 450),SGTNP(450,6),
     1NP(8, 350),MAT( 350),MBAND,NEQ,M,LM(24),KOEL( 350),
     2PSY(52),ETA(52),ZTA(52),AQ(43),PP(24),ELDISP(24),
     3KOUNT( 450),SIGA( 450,6),STN( 450,3),SIGEL(6),SIGP(7),NUMBLK,
     4  DISPX(450),DISPY(450),DISPZ(450)
      COMMON EBULK(350),EDEV(350),NITER,ITOPT,ACOEF( 5),BCOEF( 5),STP(3)
      COMMON/AREA1/ST(20,5),SL(10,5),SD(20,10,5),VS(20,10,5),NUMAT,NCELP
     1,CONFAC,NSTRN
      DIMENSION AP(NE2),STIF(MB1,MB2),APL(MB1),APR(MB1),STIFL(LA2),
     1STIFR(LA)
C
      DISP=U(N)
      IF((I-3*N+1+KSHIFT).EQ.0) DISP=V(N)
      IF((I-3*N+KSHIFT).EQ.0) DISP=W(N)
```

```
C
      DO 50 J=2,MBAND
      IL=I+J-1
      IU=I-J+1
      IF(IU.LE.0)GO TO 10
      AP(IU)=AP(IU)-STIF(J,IU)*DISP
      STIF(J,IU)=0.0
10    IF(IL.GT.NEQ) GO TO 50
      AP(IL)=AP(IL)-STIF(J,I)*DISP
      STIF(J,I)=0.0
50    CONTINUE
      AP(I)=DISP
      STIF(1,I)=1.0
      RETURN
C
      END
C
C
      SUBROUTINE BAND1(E,A,BL,BR,AL,AR,MB1,MB2,LA,LA2,FDUB)
C
C THIS SUBROUTINE SOLVES EQUATIONS IN BLOCKS USING GAUSSIAN ELIMINATION.
C SYSTEM SUBROUTINES READ AND WRITE ARE CALLED FOR DATA TRANSFERS BETWEEN
C CORE AND FILES. SYSTEM SUBROUTINES NOTE AND POINT ARE CALLED FOR BACK
C SPACEING DATA IN FILE 1 DURING BACK SUBSTITUTION.
C
      COMMON NANLYS,KSHIFT, RO(350),X(450),Y(450),Z(450),U(450),V(450),
     1W(450),SGTEL(350,6),SGTPS(350,7),STRNT(350,6),STNT(450,3),
     2  ECMI(3,3),STRN(6) ,ESTIF(24,24),ECM(6,6),EBM(6,24),ESM(6,24),WT
      COMMON NUMNP,NUMEL, NE2, KODE( 450),SGTNP(450,6),
     1NP(8, 350),MAT( 350),MM   ,NEQ,M,LM(24),KOEL( 350),
     2PSY(52),ETA(52),ZTA(52),AQ(43),PP(24),ELDISP(24),
     3KOUNT( 450),SIGA( 450,6),STN( 450,3),SIGEL(6),SIGP(7),NUMBLK,
     4  DISPX(450),DISPY(450),DISPZ(450)
      COMMON EBULK(350),EDEV(350),NITER,ITOPT,ACOEF( 5),BCOEF( 5),STP(3)
      COMMON/AREA1/ST(20,5),SL(10,5),SD(20,10,5),VS(20,10,5),NUMAT,NCELP
     1,CONFAC,NSTRN
      DIMENSION INFO(4),INDEX(20)
      DIMENSION B(NE2),A(MB1,MB2),BL(MB1),BR(MB1),AL(LA2),AR(LA)
      INTEGER*2 LEN
      NBYTES=MM*MM*4
      FNUMRC=FLOAT(NBYTES)/32000
      NUMREC=NBYTES/32000
      IF((FNUMRC-NUMREC).GT.0.0) NUMREC=NUMREC+1
600   FORMAT( 'ERROR FILE IN BAND1')
      NN=NEQ/2
C
C
      REWIND 1
      REWIND 2
      NB=0
      WRITE(6,1002 )MM, NUMREC
1002  FORMAT(2I10,E20.7)
      GO TO 50
C
C     SHIFT BLOCK OF EQUATIONS
C
10    NB=NB+1
      DO 20 N=1,NN
      NM=NN+N
      B(N)=B(NM)
```

```
      B(NM)=0.0
      DO 20 M=1,MM
      A(M,N)= A(M,NM)
   20 A(M,NM)=0.0
C
C     READ EQUATIONS IN TO CORE
C
      IF(NUMBLK-NB)50,60,50
   50 LL=1
      DO 500 L=1,NUMREC
      CALL READ(AR(LL),LEN,0,LD,2,&550)
      WRITE(6,1003) LEN,LL,MM,NUMREC,AR(LL)
      LL=LL+8000
      GO TO 500
  550 WRITE(6,600)
      STOP
  500 CONTINUE
      CALL READ (BR,LEN,0,LD,2,&550)
      WRITE(6,1002) LEN,NN,BR(1)
 1003 FORMAT(4I10,E20.7)
      IF(NE)60,10,60
C
C     REDUCE BLOCK OF EQUATIONS
C
   60 DO 100 N=1,NN
      IF(A(1,N))65,100,65
   65 B(N)=B(N)/A(1,N)
      DO 90 L=2,MM
      IF(A(L,N))70,90,70
   70 C=A(L,N)/A(1,N)
      I=N+L-1
      J=0
      DO 80 K=L,MM
      J=J+1
   80 A(J,I)=A(J,I)-C*A(K,N)
      B(I)=B(I)-A(L,N)*B(N)
      A(L,N)=C
   90 CONTINUE
  100 CONTINUE
      WRITE(6,1000) NB
      CALL TIME(1,1)
C
C     WRITE BLOCK OF RECUCED EQUATIONS
C
      IF(NUMBLK-NB)110,120,110
  110 CONTINUE
      CALL NOTE(FDUB,INFO)
      INDEX(NB)=INFO(2)
      LEN=32000
      LL=1
      DO 700 L=1,NUMREC
      IF(L.EQ.NUMREC)LEN=NBYTES-((NUMREC-1)*32000)
      CALL WRITE(AL(LL),LEN,0,1,FDUB,&550)
      WRITE(6,1002) LL,LEN,AL(LL)
      LL=LL+8000
  700 CONTINUE
      LEN=MM*4
      CALL WRITE(BL,LEN,0,1,FDUB,&550)
      WRITE(6,1002) LL,LEN,BL(1)
      GO TO 10
```

```
C
C        BACK SUBSTITUTION
C
  120    DO 140 M=1,NN
         N=NN+1-M
         DO 130 K=2,MM
         L=N+K-1
  130    B(N)=B(N)-A(K,N)*B(L)
         NM=N+NN
         B(NM)=B(N)
  140    A(NB,NM)=B(N)
         WRITE(6,1001) NB
         CALL TIME(1,1)
         NB=NB-1
         IF(NB)150,160,150
  150    CONTINUE
         INFO(1)=INDEX(NB)
         CALL POINT(FDUB,INFO,1)
         LL=1
         DO 800 L=1,NUMREC
         CALL READ(AL(LL),LEN,0,LZ,FDUB,&550)
         WRITE(6,1002) LL,LEN,AL(LL)
         LL=LL+8000
  800    CONTINUE
         CALL READ(BL,LEN,0,LZ,FDUB,&550)
         WRITE(6,1002) LL,LEN,BL(1)
         GO TO 120
C
C        ORDER UNKNOWNS IN B ARRAY
C
  160    K=0
         NUMEQ=3*NUMNP
         DO 180 NB=1,NUMBLK
         DO 180 N=1,NN
         NM=N+NN
         K=K+1
         IF(K.GT.NUMEQ) GO TO 190
  180    B(K)=A(NB,NM)
  190    RETURN
C
 1000    FORMAT(//10X,'EQUATICNS FECUCED IN BLOCK NUMBER=',I5//)
 1001    FORMAT(//10X,'BACK SUBSTITUTICN CCMPLETED IN BLOCK NUMBER=',I5//)
         END
END OF FILE
```

APPENDIX C

ELEMENT STIFFNESS FORMULATION FOR ISOPARAMETRIC HEXAHEDRON

C.1 Scope

This appendix contains the element stiffness formulation for an isoparametric, eight-node hexahedral element with 24 degrees of freedom. The formulation given here is essentially based on the one described by Clough (1969).

C.2 Interpolation Functions

An isoparametric element is the one in which the displacements and the geometry of the element are described by the same interpolation functions. It can be shown that such an element with a proper choice of the interpolation functions, satisfies the necessary requirements for the convergence of the finite element solution to the correct answer (Zienkiewicz et al., 1969). For the eight node hexhedron shown in Fig. C.1 the relationship between the local coordinates (ξ,η,ζ) of the parent element and the global cartisian coordinates (x,y,z) of the element is provided by a set of linear interpolation functions as:

$$\begin{Bmatrix} x \\ y \\ z \end{Bmatrix} = \begin{bmatrix} N & 0 & 0 \\ 0 & N & 0 \\ 0 & 0 & N \end{bmatrix} \begin{Bmatrix} \bar{x} \\ \bar{y} \\ \bar{z} \end{Bmatrix} \qquad \text{(C.1)}$$

in which $\overline{x}$, $\overline{y}$, and $\overline{z}$ are the coordinates of the eight nodes of the element (Fig. C.1(b)) expressed in Cartesian global coordinate system as:

$$\overline{x}^T = \langle x_1 x_2 \quad \ldots \quad x_i \quad \ldots \quad x_8 \rangle$$

$$\overline{y}^T = \langle y_1 y_2 \quad \ldots \quad y_i \quad \ldots \quad y_8 \rangle$$

$$\overline{z}^T = \langle z_1 z_2 \quad \ldots \quad z_i \quad \ldots \quad z_8 \rangle \quad ,$$

and

$$N = \langle N_1 N_2 \quad \ldots \quad N_i \quad \ldots \quad N_8 \rangle \quad .$$

The linear interpolation functions are expressed in terms of the local coordinates of the parent element as:

$$N_i = 1/8(1 + \xi\xi_i)(1 + \eta\eta_i)(1 + \zeta\zeta_i) \quad , \qquad \text{(C.2)}$$

in which ξ_i, η_i and ζ_i are the coordinates of the eight nodes of the parent element as shown in Fig. C.1(a). According to the definition of an isoparametric element the displacements (u,v,w,) of the element should be expressed by the same interpolation functions used to describe the geometry. By analogy with Eq. C.1 the displacements are expressed as:

$$\begin{Bmatrix} u \\ v \\ w \end{Bmatrix} = \begin{bmatrix} N & 0 & 0 \\ 0 & N & 0 \\ 0 & 0 & N \end{bmatrix} \begin{Bmatrix} \overline{u} \\ \overline{v} \\ \overline{w} \end{Bmatrix} \qquad \text{(C.3)}$$

where $\overline{u}$, $\overline{v}$, $\overline{w}$ are the nodal displacement vectors expressed as:

$$\overline{u}^T = \langle u_1 u_2 \quad \ldots \quad u_i \quad \ldots \quad u_8 \rangle$$

$$\overline{v}^T = \langle v_1 v_2 \quad \ldots \quad v_i \quad \ldots \quad v_8 \rangle$$

$$\overline{w}^T = \langle w_1 w_2 \quad \ldots \quad w_i \quad \ldots \quad w_8 \rangle \quad .$$

C.3 Element Stiffness Evaluation

The element strains are expressed in terms of the nodal displacements by performing the appropriate differentiation on Eq. C.3. The resulting expression is:

$$\begin{Bmatrix} \varepsilon_{xx} \\ \varepsilon_{yy} \\ \varepsilon_{zz} \\ \gamma_{xy} \\ \gamma_{yz} \\ \gamma_{zx} \end{Bmatrix} = \begin{bmatrix} \frac{\partial N}{\partial x} & 0 & 0 \\ 0 & \frac{\partial N}{\partial y} & 0 \\ 0 & 0 & \frac{\partial N}{\partial z} \\ \frac{\partial N}{\partial y} & \frac{\partial N}{\partial x} & 0 \\ 0 & \frac{\partial N}{\partial z} & \frac{\partial N}{\partial y} \\ \frac{\partial N}{\partial z} & 0 & \frac{\partial N}{\partial x} \end{bmatrix} \begin{Bmatrix} \overline{u} \\ \overline{v} \\ \overline{w} \end{Bmatrix} \quad . \tag{C.4}$$

Eq. C.4 can be expressed in the abbreviated form as:

$$\{\varepsilon\} = [B] \, \{\overline{r}\} \quad . \tag{C.5}$$

The derivatives needed in the strain matrix of Eq. C.4 are obtained from:

$$\begin{Bmatrix} \dfrac{\partial N}{\partial x} \\ \\ \dfrac{\partial N}{\partial y} \\ \\ \dfrac{\partial N}{\partial z} \end{Bmatrix} = [J]^{-1} \begin{Bmatrix} \dfrac{\partial N}{\partial \xi} \\ \\ \dfrac{\partial N}{\partial \eta} \\ \\ \dfrac{\partial N}{\partial \zeta} \end{Bmatrix} \qquad (C.6)$$

where [J] is the Jacobian matrix which can in turn be obtained from:

$$[J] = \begin{bmatrix} \dfrac{\partial x}{\partial \xi} & \dfrac{\partial y}{\partial \xi} & \dfrac{\partial z}{\partial \xi} \\ \\ \dfrac{\partial x}{\partial \eta} & \dfrac{\partial y}{\partial \eta} & \dfrac{\partial z}{\partial \eta} \\ \\ \dfrac{\partial x}{\partial \zeta} & \dfrac{\partial y}{\partial \zeta} & \dfrac{\partial z}{\partial \zeta} \end{bmatrix} = \begin{Bmatrix} \dfrac{\partial N}{\partial \xi} \\ \\ \dfrac{\partial N}{\partial \eta} \\ \\ \dfrac{\partial N}{\partial \zeta} \end{Bmatrix} [\bar{x} \ \bar{y} \ \bar{z}] \qquad (C.7)$$

By inverting [J] obtained from Eq. C.7 and using Eq. C.6 and Eq. C.4 the strain matrix [B] is evaluated. As the strain matrix is expressed in local coordinates, the integration necessary to evaluate the element stiffness has to be performed in the same local coordinates using the relationship for the elemental volume:

$$dv = dx\ dy\ dz = \det[J]\ d\xi\ d\eta\ d\zeta \qquad (C.8)$$

The element stiffness can now be evaluated from:

$$[K] = \int_V [B]^T [C][B]dv = \int_{-1}^{1}\int_{-1}^{1}\int_{-1}^{1} [B]^T[C][B]\det[J]d\xi\, d\eta\, d\zeta \qquad (C.9)$$

where [C] the constitutive matrix given by:

$$[C] = \frac{E}{(1+\nu)(1-2\nu)} \begin{bmatrix} 1-\nu & \nu & \nu & 0 & 0 & 0 \\ \nu & 1-\nu & \nu & 0 & 0 & 0 \\ \nu & \nu & 1-\nu & 0 & 0 & 0 \\ 0 & 0 & 0 & \frac{1-2\nu}{2} & 0 & 0 \\ 0 & 0 & 0 & 0 & \frac{1-2\nu}{2} & 0 \\ 0 & 0 & 0 & 0 & 0 & \frac{1-2\nu}{2} \end{bmatrix} \qquad (C.10)$$

The integrations are performed numerically using Gaussian quadrature formulae.

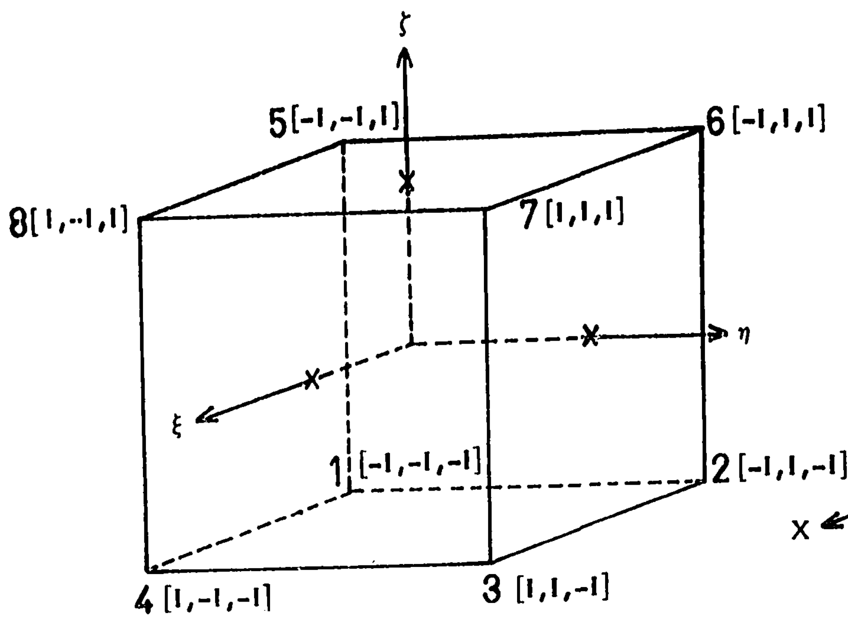

(a) LOCAL CO-ORDINATES

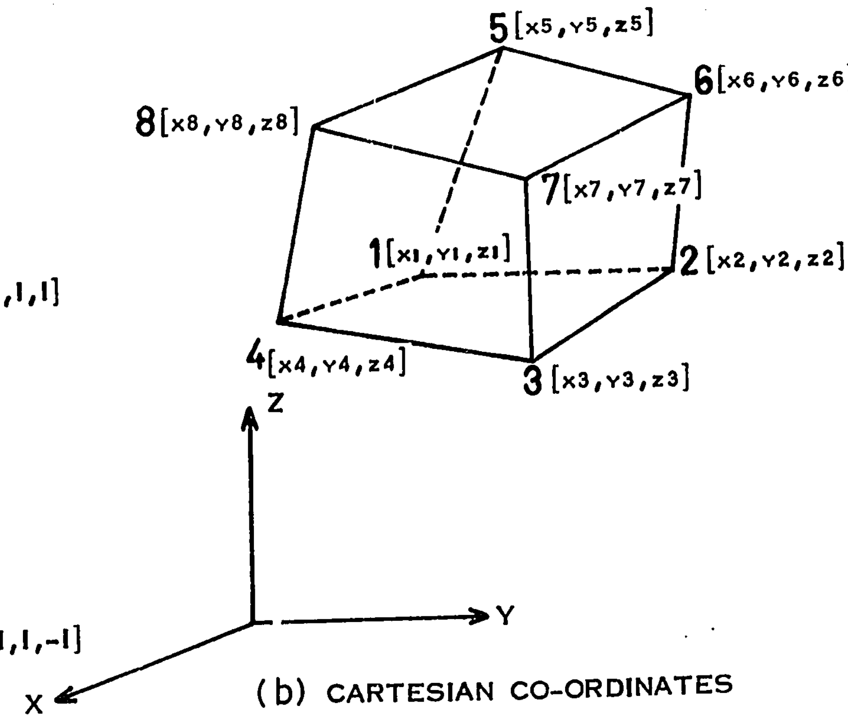

(b) CARTESIAN CO-ORDINATES

FIG. C.1 EIGHT NODE HEXAHEDRON REPRESENTATION IN LOCAL AND CARTESIAN CO-ORDINATES

APPENDIX D

FINITE ELEMENT METHOD FOR THE ANALYSIS OF INDIRECT TENSION TEST

D.1 Scope

This appendix describes the main features of a two dimensional finite element method used for the analysis of an indirect tension test when the material is assumed to be bilinear, having different moduli in compression and tension.

D.2 Basic Considerations for a Bilinear Material

A finite element method for solving two dimensional problems involving a bilinear material was suggested by Wilson (1963). The method that uses a successive approximation technique can be handled very conveniently by the two dimensional finite element program that uses an iterative equation solver (Wilson, 1963). The program given in Appendix A was modified by the author, following the procedure suggested by Wilson (1963), to consider the bilinear property of material.

A bilinear material has the following three possible stress-strain relationships depending on the stress state:

Type I - Both principal stresses are compressive

Type II - Both principal stresses are tensile

Type III - One principal stress is compressive while the other is tensile.

For Type I and Type II the stress-strain relationship in x-y coordinate system is of the normal form. For Type III the stress-strain relationship is a function of the angle of inclination of the major principal stress with the x-axis. In terms of the principal coordinate system the stress-strain relationship is written as:

$$\{\bar{\sigma}\} = [\bar{C}]\ \{\bar{\varepsilon}\} \tag{D.1}$$

where $[\bar{C}]$ is given by Eq. 2.7 of Chapter II. If $\{\sigma\}$ and $\{\varepsilon\}$ represent stresses and strains in x-y coordinate system then

$$\{\bar{\varepsilon}\} = [T]^T\ \{\varepsilon\} \tag{D.2}$$

$$\{\sigma\} = [T]\ \{\bar{\sigma}\} \tag{D.3}$$

with [T], the transformation matrix, given by:

$$[T] = \begin{bmatrix} \cos^2\theta & \sin^2\theta & 2\sin\theta\cos\theta \\ \sin^2\theta & \cos^2\theta & -2\sin\theta\cos\theta \\ -\sin\theta\cos\theta & \sin\theta\cos\theta & \cos^2\theta - \sin^2\theta \end{bmatrix} \tag{D.4}$$

Since $\{\sigma\} = [c]\ \{\varepsilon\}$ the constitutive matrix in x-y coorindate system for a bilinear material is given as:

$$[C] = [T]\ [\bar{C}]\ [T]^T \tag{D.5}$$

In the finite element program the constitutive matrix for

Type III as given by Eq. D.5 is computed for an element considering the angle θ obtained from the previous solution.

D.3 Analysis of Indirect Tension Test

The finite element idealization of a quadrant of the circular section analyzed is shown in Fig. D.1. To start with the solution was obtained for $E_c/E_t = 1$ and for the assigned value of G/E_c. Before the next solution was attempted each element was assigned the appropriate constitutive matrix depending on the type to which it belongs. For Type III the constitutive matrix was obtained from Eq. D.5. The solution thus obtained for $E_c/E_t = 1$ was used to perform the necessary modifications for obtaining the next solution. The solution procedure was repeated until the stresses and displacements obtained in two successive solutions closely agree with each other. For the analyses performed the final solution could be obtained after 10 to 15 repetitions.

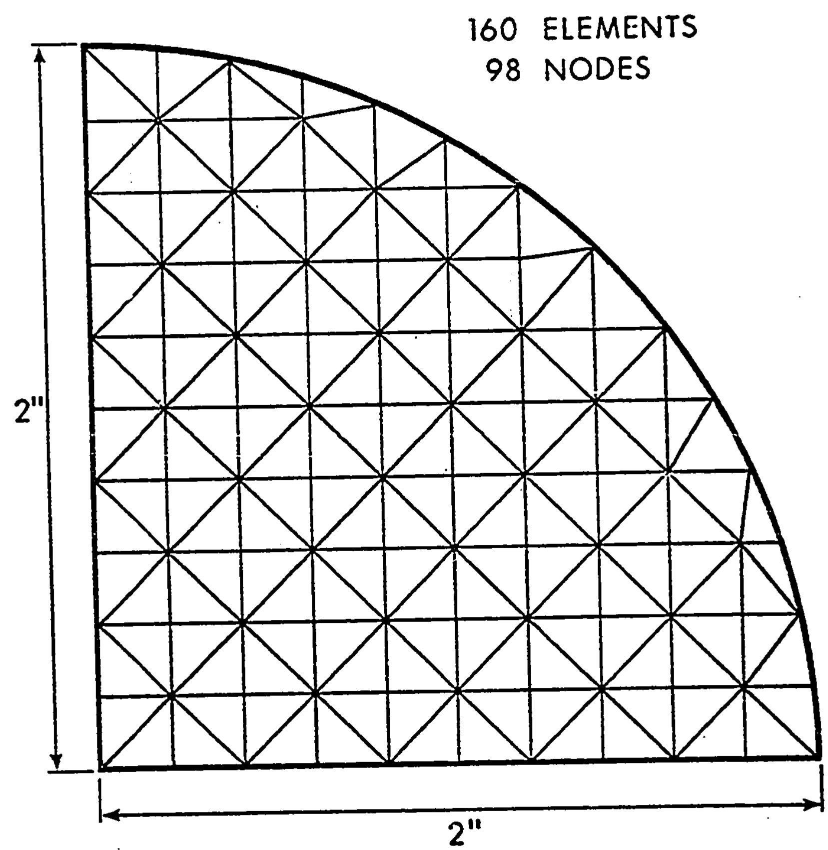

FIG. D.I FINITE ELEMENT IDEALIZATION OF A QUADRANT OF THE CIRCULAR SECTION ANALYSED